



KIT SCIENTIFIC REPORTS 7632

# **Exergy-based Planning and Thermography-based Monitoring for energy efficient buildings**

Progress Report

Peter Kohlhepp, Jens Buchgeister



Peter Kohlhepp, Jens Buchgeister

**Exergy-based Planning and Thermography-based Monitoring  
for energy efficient buildings**

Progress Report

**Karlsruhe Institute of Technology**  
**KIT SCIENTIFIC REPORTS 7632**



# **Exergy-based Planning and Thermography-based Monitoring for energy efficient buildings**

Progress Report

by

Peter Kohlhepp (IAI)

Jens Buchgeister (ITAS)

Report-Nr. KIT-SR 7632

### Impressum

Karlsruher Institut für Technologie (KIT)  
KIT Scientific Publishing  
Straße am Forum 2  
D-76131 Karlsruhe  
[www.ksp.kit.edu](http://www.ksp.kit.edu)

KIT – Universität des Landes Baden-Württemberg und  
nationales Forschungszentrum in der Helmholtz-Gemeinschaft



Diese Veröffentlichung ist im Internet unter folgender Creative Commons-Lizenz  
publiziert: <http://creativecommons.org/licenses/by-nc-nd/3.0/de/>

KIT Scientific Publishing 2012  
Print on Demand

## Zusammenfassung

Dieser Bericht konkretisiert die Forschungsarbeiten zum Subtopic 2-5-5 „Technologien für Energieeffizienz im Bausektor“ des HGF Forschungsprogramms Technik, Innovation und Gesellschaft (Laufzeit 2010 bis 2014).

Der Bausektor, welcher in den OECD Ländern für ungefähr ein Drittel des gesamten Endenergiebedarfs verantwortlich ist, birgt bekanntlich große Potenziale zur Energieeinsparung. Aus technischer Sicht wird die Bedarfsreduktion über den Einsatz hocheffizienter Wärmedämmung und effizienter Heiz-, Lüftungs- und Klimaanlage erreicht. Jedoch benötigt die Bewertung und Optimierung der Energieeffizienz eines Gebäudes in der Praxis einen ganzheitlichen Ansatz, der die vollständige Lebensweganalyse abdeckt und die Wechselwirkungen innerhalb des Gebäudes und mit seiner natürlichen und urbanen Umgebung erfasst. Der Entwurf eines neuen Gebäudes oder die Erneuerung im Bestand unterscheiden sich grundsätzlich von der Vorgehensweise bei industriellen Produkten und Prozessen, weil jedes Gebäude einzigartig durch seine Lage und Umgebung ist und somit auch die Randbedingungen jedes Projekts. Die Definition der Leistungsmerkmale von Gebäuden schließt unterschiedliche soziale und kulturelle Perspektiven genauso wie komplexe funktionale und technische Eigenschaften mit ein. Infolge der langen Lebensdauer eines Gebäudes besitzt jedes Leistungskriterium einen nachhaltigen Einfluss. Ein integraler Planungs- und Monitoring-Prozess erfordert unterstützende Informationstechnik, deren Kern ein semantisches Gebäudemodell bildet, das die geometrischen und semantischen Modelleigenschaften einschließlich der Kosten- und Sachbilanzdaten der Materialien über deren gesamte Lebenswege abbildet, um lebenswegbasierte Modellsimulationen des Gebäudes nach vorgegebenen Leistungsanforderungen vornehmen zu können.

Die Diskussion von Energieeffizienz fußt auf dem 1. fundamentalen Gesetz der Thermodynamik der Energieerhaltung, das die Qualität der Umwandlung einer Energieform, die immer mit irreversiblen Verlusten verbunden ist, außer Acht lässt. So besteht ein großer Qualitätsunterschied, ob eine thermische Energiemenge hoher Temperatur oder eine gleichgroße Menge niedriger Temperatur umgewandelt wird. Nur eine Exergieanalyse (nach dem 2. thermodynamischen Gesetz) kann den Wirkungsgrad eines Umwandlungsprozesses bewerten. Tatsächlich ist die thermodynamische Ineffizienz begleitet von Exergievernichtung, die zu erhöhtem Bedarf an Brennstoff, Kosten und Umweltbelastungen führt. Andererseits kann die Minimierung von thermodynamischen Ineffizienzen einen höheren stofflichen und energetischen Aufwand zur Herstellung von Anlagenkomponenten wie z.B. Wärmeaustauschern erfordern. Mit Hilfe lebenswegbasierter Systemanalyse und Optimierungsrechnung werden diese gegenläufigen Effekte gegeneinander abgewogen. Als ein Teil der Methodenentwicklung werden die exergoökonomische und exergoökologische Analyse, die zur kosteneffizienten und umweltfreundlichen Gestaltung von Energieumwandlungsprozessen schon seit langem praktisch Anwendung finden, zusammengeführt und auf den Gebäudebereich übertragen.

Bei der Betrachtung existierender Gebäude stehen die vergleichende Verifizierung des tatsächlichen stofflichen und energetischen Aufwands im Gebäudebetrieb an den Vorgaben zur Gebäudeplanung im Fokus, ferner eine Verbesserung der zustandsabhängigen Instandhaltung und des Monitoring von Gebäuden. Hier würde sich eine Fortführung der Gebäudesimulation im Betrieb anbieten, wobei die gleichen Zielvariablen der Energiekennwerte wie in der Planungsphase berechnet werden. Jedoch ist die schritthaltende Kalibrierung des Modells zur Identifizierung des tatsächlichen Gebäudestands bekanntermaßen schwierig, aufwendig und unterbestimmt. Als Technologieoptionen eröffnet die Infrarotthermografie, in 6 Freiheitsgraden in Bezug auf das 3D-Gebäudemodell lokalisiert und zugleich gekoppelt mit der thermodynamischen Gebäudesimulation, neue Möglichkeiten zur Identifizierung von Bauwerksparametern. Umgekehrt würde die Simulation die quantitative Auswertung der Wärmebilder liefern und die Energieauswirkungen im Vergleich zu thermischen Referenzbildern abschätzen. Dies ist zurzeit eine Lücke in der Gebäudethermografie. Dieses neuartige Konzept unter dem Namen Quantitative Georeferenzierte Thermografie (QGT) wird im Detail spezifiziert.

Diese Konzeptstudie umfasst vier Kapitel. Der rechtliche Hintergrund in der Europäischen Union und in Deutschland zur Reduktion von CO<sub>2</sub> Emissionen, dem Ausbau der erneuerbaren Energien sowie den aktuellen Energiestandards im Gebäudebereich ist Gegenstand des ersten Kapitels. Das

zweite Kapitel führt die Definition von Exergie und die Methoden der exergoökonomischen und exergoökologischen Analyse ein und gibt eine Übersicht über den Status quo von Software-Tools im Gebäudebereich unter Verwendung des Exergiekonzepts. Zudem werden Anlagenkomponenten im Gebäude und unterschiedliche Gebäudetypen klassifiziert, das erforderliche Forschungsprogramm zur Anwendung des Exergiekonzepts bei der integralen Gebäudeplanung ausgearbeitet und die Gesamtarchitektur der Softwarekomponenten präsentiert. Das Kapitel 3 untersucht wichtige verwandte Themenfelder wie die laufende Betriebsoptimierung von Gebäuden, Thermografie zur Gebäude-diagnostik, semantische Gebäudemodelle (BIM) und ihre Verknüpfung zu Energiesimulationen, Identifizierung von Gebäudeparametern, radiometrische Kameramodelle sowie Wärmebildanalyse. Das Kapitel 4 definiert die quantitative georeferenzierte Thermografie (QGT) als Erweiterung eines diskreten dynamischen Systems durch mobile Sensoren zur Identifizierung von Gebäudeparametern. Technische Kernfragen wie die mobile Messgleichung und die Objektlokalisierung bei Wärmebildkameras werden im Detail diskutiert. Erforderliche Erweiterungen zum Datenaustauschformat des Gebäudemodells zur Unterstützung der kontinuierlichen Überwachung werden ebenfalls spezifiziert. Die adressierten Forschungsfragen werden in einem detaillierten Arbeitsprogramm unteretzt.

## Abstract

This report substantiates the research objectives of subtopic 2-5-5 "Technologies for energy efficiency in the Building Sector" of the Helmholtz Research Program Technology, Innovation, and Society (funding period 2010-2014).

The building sector, accounting for roughly one third of total energy use in OECD countries, provides huge and well-known potentials for energy savings. Technically, they may be reached by highly efficient insulation systems and efficient active HVAC systems. However, assessing and optimizing the energy performance in practice needs a holistic approach covering the entire life cycle and focusing on the interactions within the building and between its natural and urban environment. The design of new buildings or the renovation of existing ones differ greatly from industrial processes because each building is unique by its site and environment, and so are the initial conditions of each project. Defining performance criteria involves different social and cultural perspectives as well as complex functional and technical properties. Due to the long lifetime of buildings, any performance criterion has a long-lasting impact. An integral planning and monitoring process needs information technology support at the core of which reside the building information model (BIM) and building performance simulation models that integrate life cycle information and life cycle costing.

The discussion of energy efficiency roots in the fundamental first law of thermodynamics which disregards the irreversible loss of energy quality when, for example, converting thermal energy from a higher to a lower temperature. Only exergy (or thermodynamic second law) analysis can assess the performance of energy conversion processes. In fact, the thermodynamic inefficiency attending the destruction of exergy leads to higher consumption of fuel and increased environmental impacts and costs. On the other hand, minimization of inefficiencies could increase the materials and energy needed for the fabrication of components such as heat exchangers. These life cycle effects are balanced by systems analysis for design optimization. As part of the method development, the exergoeconomic and exergoenvironmental analysis methods, well known practices in designing cost-effective and environmentally friendly energy conversion systems, are joined and transferred to the building sector.

Looking at existing buildings, research focuses on verifying the actual building performance against the design model, and on improved condition-based maintenance and monitoring. This may be done by carrying on the design simulation through the use phase, calculating the same goal variables of energy performance. However, the model calibration to identify and keep track of the actual building condition is admittedly difficult, laborious and under-determined. As to technology options, infrared thermography localized in six degrees of freedom with respect to the 3-D BIM and co-running the thermodynamic simulation model opens up new possibilities for its parameter identification. Vice versa, simulation may provide for the quantitative interpretation of thermal images by their energy impact when compared to reference images, which is lacking in building thermography today. This novel concept denoted quantitative geo-referenced thermography (QGT) is specified in detail.

This concept study comprises four chapters. The legislative background in the European Union and in Germany as to reduction of carbon dioxide emission, promotion of renewable energy, and energy performance in the building sector is reviewed in chapter 1. Chapter 2 introduces the definition of exergy and the methodology of exergoeconomic and exergoenvironmental analysis and reviews the status quo including software tools. The building components and types are classified, the work program of research needed is fleshed out, and the software architecture is presented. Chapter 3 surveys essential and closely related areas such as continuous commissioning, thermography for building diagnostics, semantically attributed geometry models of buildings (BIM) and their links to energy simulation, parameter identification, radiometric camera models, and thermal image analysis. Chapter 4 defines QGT as the extension of a discrete dynamic system by mobile sensors for parameter identification. Core technical issues such as the mobile measurement equation and the IR camera localization are discussed in depth. Extensions of a BIM exchange format required to support continuous monitoring are also specified. The research questions to be addressed are developed in a detailed work program.

## **Keywords**

Exergo-economic-environmental analysis, life cycle assessment, building performance simulation, parameter identification, quantitative thermography

## List of symbols / Nomenclature

$A$	Surface area	$[m^2]$
$af(t)$	Aging function of lifetime $t$ of a building or component	
$\dot{B}_j$	Environmental impact rate of the $j$ -th material stream (Eco-indicator 99)	$[\text{Points/s}]$
$b_j$	Specific environmental impact with the production of the $j$ -th material stream per exergy unit of the same stream (Eco-indicator 99)	$[\text{Points/GJ}]$
$c, c_p$	Specific heat capacity at constant pressure	$[\text{MJ}/(\text{kg K})]$
$D$	layer thickness	$[m]$
$E, J, G$	radiosity, i.e. emissive power density per unit surface area	$[\text{W}/m^2]$
$E_b$	blackbody radiosity	$[\text{W}/m^2]$
$\dot{E}$	Exergy rate	$[\text{MW}]$
$e$	specific exergy	$[\text{MJ}/(\text{kg K})]$
$f_b$	Exergoenvironmental factor expressing the relative contribution of component-related environmental impact to the sum of environmental impacts associated with the component	
$f(x)$	Probability density function (pdf) of a random variable $x$	
$f_R(x, \omega, \omega_v)$	Bidirectional reflectance distribution function (BRDF) indicating the fraction of directional radiance entering a facet at position $x$ from direction (angle) $\omega$ and re- reflected in direction (angle) $\omega_v$ .	
$F$	Geometric view factor of radiation transfer	
$h$	specific enthalpy	$[\text{MJ}/\text{kg}]$
$H, H^{cond}, H^{conv}, H^{rad}$	Heat transfer coefficient (conductive, convective, radiative)	$[\text{W}/(\text{m}^2\text{K})]$
$L, L_b$	Radiance, i.e. radiosity per solid angle $sr$ ; blackbody radiance	$[\text{W}/(\text{m}^2 \text{sr})]$
$m$	mass	$[\text{kg}]$
$\dot{m}$	Mass flow rate	$[\text{kg}/\text{s}]$
$\dot{n}$	Mole flow rate	$[\text{mole}/\text{s}]$
$p$	pressure	$[\text{N}/\text{m}^2]$
$Q, Q_s, Q_{dif}$	Heat flux per volume due to source/sink terms or diffusion	$[\text{W}/\text{m}^3]$
$\dot{Q}$	Heat rate	$[\text{MW}]$
$r_b$	Relative difference of exergy-related environmental impacts	
$R$	Specific gas constant	$[\text{J}/(\text{mole K})]$
$R$	Thermal resistance	$[\text{m}^2\text{K}/\text{W}]$
$R(\lambda)$	Spectral sensitivity of an IR detector; Spectral response function $R: [\lambda_0, \lambda_1] \rightarrow [0, 1]$	
$s$	Specific entropy	$[\text{J}/(\text{kg K})]$
$t$	Time	$[\text{s}]$
$T$	Temperature	$[\text{K}]$
$T(x, y, z, t)$	Temperature field of space coordinates $x, y, z$ , and time $t$	
$\nabla T = (\partial T/\partial x, \partial T/\partial y, \partial T/\partial z)^T$	Spatial temperature gradient	
$\nabla^2 T := \nabla \cdot (\nabla T) = \partial^2 T/\partial x^2 + \partial^2 T/\partial y^2 + \partial^2 T/\partial z^2$	Divergence of temperature field	
$Tr$	Rigid motion transformation (translation, rotation) in $\mathbb{R}^3$	
$v$	Wind speed	$[\text{m}/\text{s}]$
$v_{ij}$	Visibility of a facet $j$ from facet $i$ (0 or 1)	

$\Delta V, V$	(Differential) volume	$[m^3]$
$w$	Weighting factor	
$\dot{W}$	Work rate	$[MW]$
$\dot{Y}$	Component-related environmental impact rate associated with the life cycle of the component (Eco-indicator 99)	$[Points/s]$
$y_D^*$	Exergy destruction ratio, which compares the exergy destruction within a component with the exergy destruction within the overall system	$[\%]$

### Greek letters

$\alpha_i$	Linear factor by which the $i$ -th object surface contributes to the radiance received by an IR detector	
$\varepsilon$	Exergetic efficiency (chapter 2)	
$\varepsilon$	Emissivity $[0...1]$ (chapters 3, 4, Appendices)	
$\kappa$	Thermal conductivity	$[W/mK]$
$\tau$	Transmittance $[0...1]$	
$\lambda$	Wavelength	$[m]$
$\rho$	Specific density	$[kg/m^3]$
$\theta_{i,j}$	Angle of the normal of the $i$ -th planar facet included with the line of sight to another facet $j$	$[rad]$
$\omega$	Frequency	$[s^{-1}]$

### Vectors, matrices, and time functions in dynamic systems

$\mathbf{A} \in \mathbb{R}^{n,n}$	System matrix of a continuous building model described by linear ODE, or of a linearized discrete system
$\mathbf{B} \in \mathbb{R}^{n,m}$	Input matrix of a building system model
$C: \mathbb{R}^n \rightarrow \mathbb{R}^m$	Measurement function (thermography, non-linear function)
$\mathbf{g}$	Vector of geometric quantities (positions, orientations, lengths,...)
$\mathbf{g}^{mob}$	Mobile camera pose, i.e. rigid motion transformation with six degrees of freedom, e.g. $(x, y, z, \alpha, \beta, \gamma)$
$\mathbf{p}$	Parameter vector $(p_1, \dots, p_m)^T$ of a building model
$\mathbf{p}_i$	Parameter variable consisting of identifier $id_i$ , value $p_i$ , value range $\mathbf{P}_i$
$\mathcal{P}$	set of parameter names (identifiers)
$\mathbf{s}$	Sensitivity vector $(\partial y / \partial p_1, \dots, \partial y / \partial p_m)^T$ of a scalar measurement $y$ with respect to a parameter vector $\mathbf{p} = (p_1, \dots, p_m)^T$
$\mathbf{T}$	State vector trajectory of temperatures
$\mathbf{u}$	Control / Input vector; building load (weather, occupancy data)
$\mathbf{U}$	Time function / Trajectory / Schedule of building load
$\mathbf{U}_{[k]}$	discrete load sequence comprising $k$ time steps
$\mathbf{U}_{[t_0, t_1]}$	continuous load schedule over time interval $[t_0, t_1]$
$\hat{\mathbf{U}}$	Simulated / Estimated load schedule
$\bar{\mathbf{U}}$	Normalized / Scaled load schedule
$\mathbf{y}, \hat{\mathbf{y}}$	Measurement vector or array; measurement prediction
$e, \mathbf{E}$	Prediction error (scalar residual, error trajectory)
$\xi$	Measurement noise vector (disturbances)
$\mathbf{z}$	Performance vector; simulation goal variables



### Subscripts (chapter 2)

<i>aux</i>	auxiliary
<i>ch</i>	chemical
<i>D</i>	destruction
<i>dc</i>	dissipative component
<i>dif</i>	difference
<i>el</i>	electric
<i>F</i>	fuel
<i>ideal_gas</i>	ideal gas
<i>in</i>	input
<i>j</i>	<i>j</i> -th stream or material stream of the energy conversion system
<i>k</i>	<i>k</i> -th component of the energy conversion system
<i>kin</i>	kinetic
<i>out</i>	output
<i>q</i>	heat
<i>P</i>	product
<i>ph</i>	physical
<i>pot</i>	potential
<i>TOT</i>	total (with reference to the component)
<i>total</i>	total (with reference to the system)
<i>w</i>	work
<i>0</i>	reference environment

### Superscripts (chapter 2)

<i>AV</i>	available
<i>CH</i>	chemical
<i>CI</i>	investment costs
<i>CO</i>	construction
<i>DI</i>	disposal
<i>EN</i>	endogenous
<i>EX</i>	exogenous
<i>HX</i>	heat exchanger
<i>OM</i>	operation, maintenance
<i>PH</i>	physical
<i>UN</i>	unavailable

## List of Acronyms

AD	<b>A</b> utomatic <b>d</b> ifferentiation
AHU	<b>A</b> ir <b>h</b> andling <b>u</b> nit (→HVAC)
API	<b>A</b> pplication <b>p</b> rogrammer's <b>i</b> nterface
AR	<b>A</b> sset <b>r</b> ating of a building (energy certification)
ARMAX	<b>A</b> uto- <b>R</b> egressive- <b>M</b> oving <b>A</b> verage, <b>e</b> xogenous
ASHRAE	<b>A</b> merican <b>S</b> ociety of <b>H</b> eating, <b>R</b> efrigeration and <b>A</b> ir- <b>C</b> onditioning <b>E</b> ngineers
ASTM	<b>A</b> merican Society for <b>T</b> esting and <b>M</b> aterials
AT	<b>A</b> ctive <b>t</b> hermography
BAS	<b>B</b> uilding <b>a</b> utomation <b>s</b> ystem
BES	<b>B</b> uilding <b>e</b> nergy <b>s</b> imulation program / model
BESTEST	Test and Validation project for Energy Simulation, conducted by the Model Evaluation and Improvement Experts Group of the →IEA
BHKS	<b>B</b> undesindustrieverband <b>H</b> eizungs-, <b>K</b> lima-, <b>S</b> anitärtechnik (German industry association of heating, climate and sanitary technique)
BIM	<b>B</b> uilding <b>i</b> nformation <b>m</b> odel
BMV, BMVBS	<b>B</b> undes <b>m</b> inisterium für <b>V</b> erkehr, <b>B</b> auwesen, <b>S</b> tädtebau und <b>R</b> aumordnung (German Ministry of Transportation, Construction, Urban and Regional Development)
BMWi	<b>B</b> undes <b>m</b> inisterium für <b>W</b> irtschaft (German Ministry of Economics)
BPS	<b>B</b> uilding <b>p</b> erformance <b>s</b> imulation program / model
BRDF	<b>B</b> idirectional <b>r</b> eflectance <b>d</b> istribution <b>f</b> unction
Building EQ	Project in the Intelligent Energy Europe Programme of the European Commission
CC	<b>C</b> ontinuous <b>c</b> ommissioning
CCICED	<b>C</b> hina <b>C</b> ouncil for <b>I</b> nternational <b>C</b> ooperation on <b>E</b> nvironment and <b>D</b> evelopment
CD	<b>C</b> onceptual <b>d</b> esign of a building
CExC	<b>C</b> umulative <b>E</b> xergy <b>C</b> onsumption
CFD	<b>C</b> omputational <b>F</b> luid <b>D</b> ynamic
CHTC	<b>C</b> onvective <b>h</b> eat <b>t</b> ransfer <b>c</b> oefficient
CIBSE	<b>C</b> hartered <b>I</b> nstitution of <b>B</b> uilding <b>S</b> ervices <b>E</b> ngineers (British standardization organization)
CIFE	<b>C</b> enter for <b>I</b> ntegrated <b>F</b> acility <b>E</b> ngineering (Stanford University)
DAI	<b>D</b> esign <b>A</b> nalysis <b>I</b> nterface <b>I</b> nitiative
DC	<b>D</b> issipative <b>C</b> omponent
DOE	1) US Department of Energy, 2) A building energy simulation program developed by the DOE

EC	<b>E</b> uropean <b>C</b> ommission
ECBCS	<b>E</b> nergy <b>C</b> onservation in <b>B</b> uildings and <b>C</b> ommunity <b>S</b> ystems Programme of the → IEA
EE	<b>E</b> nergy <b>e</b> fficiency
EEG	<b>E</b> rneuerbare- <b>E</b> nergie- <b>G</b> esetz (legislation by the German federal government)
EnEG	<b>E</b> nergie- <b>E</b> inspar <b>e</b> sgesetz (German Energy Conservation Act)
EnEV	<b>E</b> nergie- <b>E</b> inspar- <b>V</b> erordnung (German Energy Conservation Ordinance)
EPBD	<b>E</b> uropean <b>E</b> nergy <b>P</b> erformance of <b>B</b> uildings <b>D</b> irective
ESP-r	<b>E</b> nvironmental <b>S</b> ystem <b>P</b> erformance - research: a British building energy simulation program (→BES)
FD	<b>F</b> inal <b>d</b> esign
FEMP	<b>F</b> ederal <b>E</b> nergy <b>M</b> anagement <b>P</b> rogram of the US Department of Energy
FIM	<b>F</b> isher <b>I</b> nformation <b>M</b> atrix
gbXML	<b>G</b> reen <b>B</b> uilding <b>X</b> ML open schema and exchange standard (→BIM)
GIS	<b>G</b> eographic <b>i</b> nformation <b>s</b> ystem
GPS	<b>G</b> lobal <b>p</b> ositioning <b>s</b> ystem
GSA	<b>G</b> eneral <b>S</b> ervice <b>A</b> dministration of the United States
HAM	<b>H</b> eat, <b>a</b> ir, and <b>m</b> oisture transfer in buildings
HTC	<b>H</b> eat <b>t</b> ransfer <b>c</b> oefficient
HVAC	<b>H</b> eating, <b>v</b> entilation, and <b>a</b> ir- <b>c</b> onditioning
IAI	<b>I</b> nternational <b>A</b> lliance for <b>I</b> nteroperability
IEA	<b>I</b> nternational <b>E</b> nergy <b>A</b> gency
IEKP	" <b>I</b> ntegriertes <b>E</b> nergie- und <b>K</b> lima- <b>P</b> rogramm" (Energy and Climate Package of the German federal government, "Meseberger Beschlüsse" 2007)
IES	<b>I</b> ntegrated <b>E</b> nvironmental <b>S</b> olutions, an energy simulation program (→BES)
IFC	<b>I</b> ndustry <b>F</b> oundation <b>C</b> lasses (→BIM)
IMU	<b>I</b> nertial <b>M</b> easurement <b>U</b> nit
IR	<b>I</b> nfrared
IRT	<b>I</b> nfrared <b>t</b> hermography
ISO	<b>I</b> nternational <b>s</b> tandardization <b>o</b> rganization
KWK	<b>K</b> raft- <b>W</b> ärme- <b>K</b> opplung (cogeneration of heat and electricity)
LBNL	<b>L</b> awrence <b>B</b> erkeley <b>N</b> ational <b>L</b> aboratory (US public research institution)
LCA	<b>L</b> ife <b>c</b> ycle <b>a</b> ssessment
LCI	<b>L</b> ife <b>c</b> ycle <b>i</b> nventory
LCIA	<b>L</b> ife <b>c</b> ycle <b>i</b> mpact <b>a</b> ssessment

LEED	<b>L</b> eadership in <b>E</b> nergy and <b>E</b> nvironmental <b>D</b> esign, a certification system for the design, construction and operation of high performance green buildings introduced by the U.S. Green Building Council (USGBC) in 1998.
LHMC	<b>L</b> atin <b>H</b> ypercube <b>M</b> onte <b>C</b> arlo sampling (simulation)
LowEX	<b>L</b> ow <b>E</b> xergy, German alliance project (...)
NDE	<b>N</b> ondestructive <b>e</b> valuation/examination
NDT	<b>N</b> ondestructive <b>t</b> esting
NIST	<b>N</b> ational institute of <b>s</b> tandards and <b>t</b> echnology in the USA
NRCC	<b>N</b> ational <b>R</b> esearch <b>C</b> ouncil of <b>C</b> anada
NREL	<b>N</b> ational <b>R</b> enewable <b>E</b> nergy <b>L</b> aboratory (US public research institution)
OC	<b>O</b> ngoing <b>c</b> ommissioning
OGC	<b>O</b> pen <b>G</b> eospatial <b>C</b> onsortium
OR	<b>O</b> perational <b>r</b> ating of a building (energy benchmarking)
PD	<b>P</b> reliminary <b>d</b> esign
pdf, PDF	<b>P</b> robability <b>d</b> ensity <b>f</b> unction
QGT	<b>Q</b> uantitative <b>g</b> eo-referenced <b>t</b> hermography
QIRT	<b>Q</b> uantitative <b>i</b> nfrared <b>t</b> hermography
REEB	European <b>R</b> oadmap for <b>e</b> nergy- <b>e</b> fficient <b>b</b> uildings
RESNET	<b>R</b> esidential <b>E</b> nergy <b>S</b> ervices <b>N</b> etwork
RHTC	<b>R</b> adiative <b>h</b> eat <b>t</b> ransfer <b>c</b> oefficient
SI	Dynamic <b>S</b> ystems <b>I</b> dentification
SMSG	US <b>S</b> ignature <b>M</b> easurement <b>S</b> tandards <b>G</b> roup
STEP	<b>S</b> tandard for the <b>E</b> xchange of <b>P</b> roduct <b>M</b> odel <b>D</b> ata (→ ISO, precursor of →BIM)
TABS	<b>T</b> hermally <b>A</b> ctivated <b>B</b> uilding <b>S</b> tructure
TIG	<b>T</b> echnologie, <b>I</b> nnovation, <b>G</b> esellschaft (name of a Helmholtz research program)
TRNSYS	<b>T</b> ransient <b>S</b> ystem <b>S</b> imulation <b>P</b> rogram (→ BES / BPS)
TRR	<b>T</b> otal <b>R</b> evenue <b>R</b> equirements
UV	<b>U</b> ltraviolet
VIP	<b>V</b> acuum <b>i</b> nsulated <b>p</b> anel
WBCSD	<b>W</b> orld <b>B</b> usiness <b>C</b> ouncil for <b>S</b> ustainable <b>D</b> evelopment
WH	<b>W</b> orking <b>h</b> ypothesis

# Table of Contents

1	Systems analysis of the building sector - background .....	1
1.1	General Legislation in the European Union .....	1
1.2	Specific Legislation in Germany .....	2
1.2.1	Energy Conservation Act EnEG, Energy Conservation Ordinance EnEV, and Heating Costs Ordinance HeizkostenV .....	2
1.2.2	Renewable Energies Act EEG .....	3
1.2.3	Act on Renewable Energies and Heat EEWärmeG .....	3
1.2.4	Act on Co-Generation KWKG .....	3
1.2.5	Energy Concept 2010 of the Federal Government .....	4
1.2.6	Further Legal Steps .....	4
1.3	Problem analysis of the building sector .....	4
1.4	Life cycle aware planning process .....	5
1.4.1	Integral planning of buildings .....	5
1.4.2	Life cycle model for energy efficient buildings .....	6
1.4.3	Exergy - a measure of energy efficiency .....	8
1.4.4	Intermediate findings .....	9
2	Methodology .....	11
2.1	Review of Exergy Concept .....	11
2.1.1	Exergy Analysis .....	13
2.1.2	Exergoenvironmental Analysis .....	14
2.1.3	Exergoenvironmental Variables and Evaluation .....	15
2.1.4	Exergoeconomic Analysis .....	20
2.1.5	Exergo-economic-environmental Analysis .....	23
2.2	State of the art of exergy analysis in the building sector .....	24
2.2.1	Application of exergy analysis in the building sector .....	27
2.2.2	Tools for exergy analysis of buildings .....	27
2.2.3	Interim findings .....	30
2.3	Research working plan for an application of exergo-economic-environmental analysis .....	31
2.4	Energy performance assessment .....	33
2.4.1	Design Phase .....	33
2.4.2	Operational Phase .....	38
2.4.3	Systems architecture for performance assessment .....	44
3	Fundamentals and related work .....	47
3.1	Ongoing commissioning .....	47
3.1.1	Definition .....	47
3.1.2	CC/OC implementation in the Building EQ program .....	48
3.1.3	Linking CC/OC with monitoring data .....	49
3.2	Thermography for Building Diagnostics .....	52
3.2.1	Non-destructive testing .....	52
3.2.2	Application examples .....	55

3.3	Building Information Modeling (BIM) .....	63
3.3.1	Definition .....	63
3.3.2	BIM exchange standards.....	64
3.4	Energy Performance Simulation .....	65
3.4.1	EnergyPlus.....	66
3.4.2	ESP-r.....	66
3.4.3	Ecotect .....	67
3.4.4	TRNSYS .....	68
3.4.5	Modelica .....	68
3.4.6	Matlab based platforms (HamLab).....	69
3.4.7	IES .....	69
3.4.8	Discussion and conclusion .....	70
3.5	Validation and Calibration of Building Simulators .....	70
3.5.1	General Methodology.....	71
3.5.2	Case studies, sensors, and measurements .....	74
3.5.3	Discussion and conclusion .....	76
3.6	Thermographic Analysis .....	76
3.6.1	Radiometric camera models.....	77
3.6.2	Estimates of emissivity and reflectivity .....	78
3.6.3	Model validation and calibration.....	80
3.6.4	Quantitative thermal image analysis.....	80
3.7	Allinson's Aerial Thermography .....	82
3.7.1	Scope of survey.....	83
3.7.2	Sensitivity analysis .....	84
3.7.3	Problems and limitations .....	87
4	Quantitative Geo-referenced Thermography .....	89
4.1	Thermodynamic building model .....	89
4.1.1	Thermal coefficients .....	90
4.1.2	Numerical solution.....	92
4.1.3	Simulation model.....	92
4.1.4	Heat, air, and moisture transfer .....	95
4.2	Measurement and identification framework.....	96
4.2.1	Mobile camera model.....	97
4.2.2	Parameter identification.....	99
4.2.3	Residual Analysis.....	101
4.2.4	Simulating non-measured load.....	104
4.2.5	Input design problem.....	106
4.2.6	Representative load schedules .....	107
4.3	New application scenarios .....	109
4.3.1	Spatially focused calibration.....	109
4.3.2	Learning individual aging functions .....	110
4.3.3	Mobile measurement design.....	111
4.3.4	Thermography-guided geometry refinement .....	113
4.3.5	QGT applications in the life cycle.....	114
4.4	BIM-integrated thermography.....	116

4.4.1	Mobile observer in detail .....	117
4.4.2	Localizing the infrared camera .....	120
4.5	BIM for design, analysis, and monitoring .....	124
4.5.1	Linking design and thermal analysis .....	124
4.5.2	Lifelong performance monitoring .....	128
4.6	Research questions and agenda .....	131
4.6.1	Energy system model .....	133
4.6.2	BIM integration.....	135
4.6.3	Experimental investigation and field testing.....	137
4.6.4	Impact analysis .....	138
5	Conclusion and Outlook.....	139
A	Radiometric camera models .....	143
A.1	Summary of aerial thermography model after Allinson .....	143
A.2	A note on view factor calculation .....	149
A.3	Bi-directional reflectance distribution function (BRDF).....	151
A.4	Radiation networks.....	152
B	List of Figures .....	156
C	List of Tables.....	159
D	References.....	160





## **1 Systems analysis of the building sector - background**

One of the greatest challenges of the 21<sup>st</sup> Century is the safety of a dependable energy supply, which in expectation of the climate change only a less amount of greenhouse gas emissions are emitted and economic and social aspects are taken into account. The building sector is of high importance regarding the demand of energy, because in Germany and the EU, approximately 40% of final energy consumption stems due to this sector (BMVBS 2007; BMWi 2011; BMWi, BMU 28.09.10; Garcia-Casals 2006). Due to the application of fossil fuels to cover the energy demand of buildings in the building sector is responsible for 15 and more % of direct greenhouse gas emissions in Germany but also in countries of the European Union (BMVBS 2007; BMWi 2011; BMWi, BMU 28.09.10). The high energy consumption and the high amount of greenhouse gas emissions are the main reasons for the EU commission and parliament to pass new laws and directives in order to improve the energy efficiency of the building sector.

In the following, the important laws of the EU parliament and German government for the energy and building sector are described (Schickel 2010).

### **1.1 General Legislation in the European Union**

The legal basis for the adoption of national funding programs is the directive 93/76/EEC to limit carbon dioxide emissions by a more efficient use of energy. This directive, known briefly as SAVE, was intended to stabilize until 2000 CO<sub>2</sub> emissions in the European Union on the level of 1990 or below. The measures listed in this directive, such as an energy performance certificate for buildings, the inspection of heating systems, or funding of energy counseling for enterprises consuming a high amount of energy, were incorporated and updated in various following directives.

The next important directive to support the use of renewable energies was the directive to support electricity production from renewable energy sources on the EU electricity market, the RES 2001/77/EC. This directive was amended by the directive 2006/108/EC when Bulgaria and Romania joined the European Union. It authorizes the EU member states to financially support electricity production from renewable energies without violating competition law. The directive is aimed at increasing the share of electricity produced from renewable energies from 14% in 2001 to 22% in 2010 and at doubling the share of renewable energies in gross energy consumption to 12%, where gross energy consumption is obtained from all domestic primary energy carriers applied and the difference between imports and exports of primary energy carriers.

In the buildings sector, adoption of the EPBD, Energy Performance of Buildings Directive, by the EU Commission represented a major milestone. This directive 2002/91/EC obliges Europeans to issue energy certificates and to fulfill stricter, for some member states first, requirements on the efficiency of the building shell, heating, ventilation, cooling, and illumination (the latter in non-residential buildings only) (EU Parliament and EU Council 2002). To update the EPBD with stricter requirements, a draft has already been coordinated largely by politics. Without modifying basic provisions of the valid EPBD, clarity shall be enhanced and the scope of validity shall be extended. It is envisaged to strengthen the leading role of the public sector in the field of "energy-efficient buildings".

## 1.2 Specific Legislation in Germany

Political requirements relating to an efficient use of energy in Germany are the result of extensive laws and ordinances and instructions for their implementation. They contain requirements and information on the efficient use of energy, which were adopted as early as in the 1970s as a response to the first oil crisis. The Heat Insulation Ordinance became effective in 1977. The first Heating Systems Ordinance entered into force in 1978.

Other major steps were taken recently after the climate conferences and the Kyoto protocol only. An important position paper to complement and tighten energy legislation was the “Integrated Energy and Climate Package” (IEKP) formulated in August 2007. It was announced to reduce CO<sub>2</sub> emission until 2020 by 40% compared to the level of 1990. In total, 29 measures to reduce greenhouse gas emissions and increase the efficiency of energy use are listed in the IEKP. They explicitly include the reduction of primary energy consumption. Based on this “Integrated Energy and Climate Package”, a large number of laws and ordinances were amended or newly adopted. Legal regulations and ordinances relevant to the buildings sector are listed below.

### 1.2.1 Energy Conservation Act EnEG, Energy Conservation Ordinance EnEV, and Heating Costs Ordinance HeizkostenV

The Energy Conservation Act (EnEG) and the Energy Conservation Ordinance (EnEV) are of highest importance. In Germany, these national laws were adopted to implement the Energy Performance of Buildings Directive (EPBD) of the European Commission. In the Energy Conservation Ordinance, the building and its technical equipment are considered an entity for joint energy assessment for the first time. First calculation principles were developed for non-residential buildings. Mathematical formulations are made in DIN V 18599, parts 1 to 10, on the “Energetic Assessment of Buildings”. In analogy to the calculation of the energetic quality of a really planned building and the technical installations contained therein, a fictitious building is considered as reference building. The primary energy need determined for the real building to be built must not exceed the demand of the fictitious reference building in order to be given a permit for the construction of a new building. The results of the mathematical calculation according to DIN are documented in the energy certificate for the administration, the builder, or the tenant. For existing buildings, an energy certificate is needed, if a major reconstruction is made or the building is re-let or re-financed. For public buildings with public access, the legislative authority has adopted a special requirement to be fulfilled by the energy certificate. Since October 2009, this certificate has to be displayed “at a prominent point” in these buildings, such that it can be seen easily by all persons.

The requirements outlined in the EnEV 2009 are much tighter than the EnEV 2007. It is aimed at reducing primary energy consumption by 30%. This ordinance applies to new or largely modified buildings irrespective of their use. To reach this reduction of energy consumption, the maximum permissible primary energy demands of the fictitious reference building were lowered. In addition, energy requirements on heat recovery of ventilation and air conditioning systems or thermal insulations of pipelines were increased. Moreover, chimney sweepers have been assigned supervisory tasks when inspecting heat-producing appliances.

In addition to the EnEV, the “Ordinance on Consumption-dependent Accounting of Heating and Warm Water Costs”, HeizkostenV, is supposed to support the careful use of energy. Within a period of one month, the tenant or user of the building is to be informed about the meter reading result. With this, the legislative authority wishes to give an economic incentive for the efficient use of energy.

### **1.2.2 Renewable Energies Act EEG**

To ensure sustainable development of energy supply and to reduce its costs, the government adopted a new version of the “Act on the Amendment of the Legislation on Renewable Energies in the Electricity Sector and on the Modification of Associated Regulations”. This new EEG became effective at the beginning of 2009 and applies to hydropower, gases from landfills, sewage treatment, and mines, biomass, geothermal energy, and wind energy as well as to solar radiation as renewable sources. It is envisaged to save fossil energy carriers and to improve technologies for the production of electricity from renewable energies. It is aimed at increasing the share of renewable energies in electricity production to at least 30% until 2020. Consequently, the Act contains regulations for grid operators regarding the connection and reimbursement of system operators generating electricity from renewable energies exclusively. Since the adoption of the EEG, secured income for system operators has resulted in a massive push of private investments in the new construction of photovoltaic systems for electricity production.

### **1.2.3 Act on Renewable Energies and Heat EEWärmeG**

The Act on Promotion of Renewable Energies in the Heat Sector also became effective on January 01, 2009. It obliges builders of buildings to be newly constructed to at least partly use renewable energies for heating and the preparation of warm water in order to increase the share of renewable energies on the heat market to 14% until 2020. The renewable energies that can be used for this purpose are solar energy, biomass, such as wood pellets, or geothermal heat. Moreover, alternative measures to increase the energy efficiency of a building are considered. Such measures, for instance, include an improved thermal insulation exceeding the requirements of EnEV, connection to a district heating network of appropriate quality, and the use of a co-generation scheme or of exhaust heat by heat recovery systems. This legal provision also applies to existing buildings, if extensions covering a surface area of more than 50 m<sup>2</sup> are built or if major reconstruction measures are to take place. If an extension building or modifications of installations or reconstruction measures are subject to the EnEV 2009, the Thermal Insulation Act has to be observed as well. In addition, existing buildings, even if no modifications are made, may be subject to separate state regulations irrespective of the EEWärmeG, for instance, in Baden-Württemberg.

### **1.2.4 Act on Co-Generation KWKG**

The newly amended Act on the Promotion of Co-generation (KWKG) of 2002, amended in 2006, also became effective at the beginning of 2009. This Act also dates back to the Integrated Energy and Climate Package (IEKP) mentioned in Section 1.2. It aims at increasing electricity production by co-generation in Germany to 25% until 2020. For support, the legislative authority funds the modernization and new construction of co-generation systems, the commercialization of the fuel cell, and the new construction and extension of heat networks based on heat from co-generation systems.

For systems to be newly constructed, bonuses shall be granted for the total amount of electricity generated, not only for the electricity fed into the public grid, but also for electricity used for own consumption. Payment for feeding electricity into the grid and for own electricity supply is subject to a total annual efficiency of the co-generation unit of least 70%. Remuneration for feeding electricity into the grid is 5.11 cents/kWh for systems of up to 50 kWel, 2.1 cents/kWh for systems of up to 2 MWel, and 1.5 cents/kWh for systems above 2 MWel. Support will be continued for systems commissioned between January 2009 and December 2016. This support of large co-generation systems

and the bonus granted for electricity fed into the grid and used for own consumption represent an incentive for using both electricity and heat to ensure an efficient use of energy.

### 1.2.5 Energy Concept 2010 of the Federal Government

The energy concept of the federal government (BMWi, BMU 28.09.10) was adopted by German parliament in September 2010. It envisages transition into an era of renewable energies. Until 2050, emission of greenhouse gases in Germany shall be reduced by at least 80% compared to 1990. Germany is to become one of the most efficient and environmentally most compatible economies with competitive energy costs and a high and wide level of prosperity.

As one of nine important fields of action, the concept explicitly mentions the “Energetic Restoration of Buildings and Energy-efficient Construction” ((BMWi, BMU 28.09.10), p. 22). Large potentials are supposed to result from the fact that three quarters of existing old buildings were constructed prior to the first Thermal Insulation Ordinance of 1979 and most of the heating systems do not yet correspond to the state of the art.

It is therefore the central objective to reduce in the long term the heat consumption of existing buildings and to have a nearly climate-neutral building inventory until 2050. Climate-neutral means that the buildings have very low energy consumption and that the remaining energy demand is covered mainly by renewable energies. For this purpose, the energetic restoration rate has to be doubled from about 1% annually to 2%. Until 2020, the demand for heat is to be reduced by 20%. Until 2050, primary energy demand is to be reduced by 80%. In 2020, the objectives and measures will be evaluated based on the successes reached until then.

### 1.2.6 Further Legal Steps

According to the coalition agreement, the present coalition intends to check the measures taken under the integrated energy and climate program for their efficiency in 2011 and to provide for further legal guidance and development, if objectives are not fulfilled.

## 1.3 Problem analysis of the building sector

It has been known since the seventies that the energy demand for heating and warm water supply for a building has a high amount. Therefore, the legislative body has begun to pass laws to reduce the energy demand in the building sector (Schickel 2010). Nevertheless, buildings hold great potential to improve their energy efficiency because of their long lifetime and the slow progress in renovating existing buildings. In Germany the federal industry association of heating, climate and sanitary technique (BHKS) estimated that after nearly seventy years all existing private buildings are renovated to the energy conservation ordinance standard 2009 (EnEV 2009) (EnEV 2009). Furthermore the German federal government has taken into account this knowledge in their energy concept 2050 and carried out an intelligent renovation roadmap and comprehensive support to double the renovation rate for the next decade (BMWi, BMU 28.09.10).

A simple way to improve energy efficiency (EE) is remodeling of components by the well-known best available technology. This is supported by legislation but it needs too much time especially when we are looking at the past forty years.

These facts lead to the first (trivial) insight but with far-reaching consequences:

The high relevance of the use phase, due to the long lifetime of a building, leads to the high demand of heating energy and hot water supply. It is a key factor in the high energy consumption in the building sector.

Designing a new building or retrofitting an existing one greatly differs from industrial products because each building is unique by its site and environment. Defining building performance is a complex task of its own, involving different social and cultural perspectives as well as functional and technical properties. Due to the long lifetime (use phase) of buildings, any performance criterion such as energy efficiency has a long-lasting impact. Maintenance and renovation of existing buildings exhibit a unique character, too, because the initial conditions for each project are different. Furthermore, many actors from different companies are involved in construction, use, maintenance and disposal of buildings. Therefore, designing or retrofitting need an integral planning process with information technology support in order to find the ideal path for optimizing building performance, especially energy efficiency.

A typical process of building planning, construction, and operation can be separated into four distinct phases: basics, design, construction, and operation, as illustrated in figure 1-1 (Kotaji et al. 2003). The phase of basics serves both client and architect for a declared framework of building performance such as reduced energy demand. Key choices as to building orientation, structure of the envelope, daylight design (fenestration) or provision of energy sources are made early in the design, often by architects. These decisions have a large impact on future energy efficiency but may still be changed at minimal costs (Klinge 1994) (figure 1-1). Therefore, an early starting point for the design and assessment of the energy concept, involving all experts with specific key qualifications, is a crucial step towards an energy-efficient building: later amendments or revisions will produce comparatively marginal performance gains but cause increasing cost, disruption, and environmental impact.

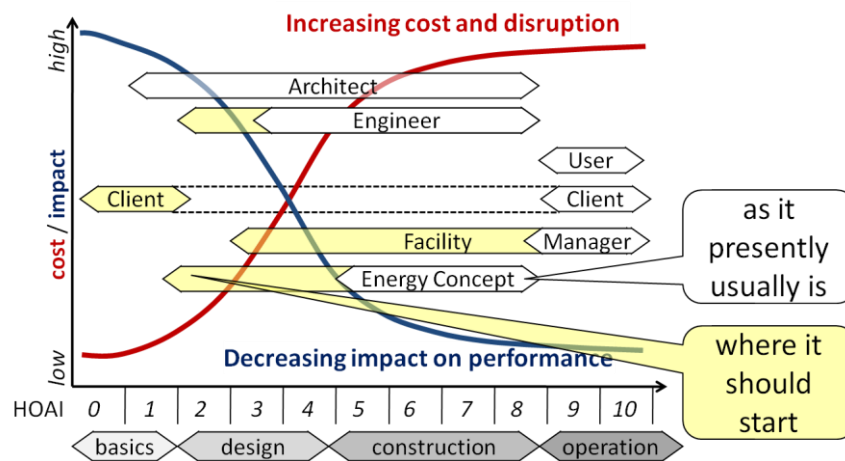


Figure 1-1: Building design process and stakeholders. Source: (Klinge 1994)

## 1.4 Life cycle aware planning process

### 1.4.1 Integral planning of buildings

Quite often, the term “integral planning” is used in an inflationary manner. Solving complex construction jobs requires an aggregation of interdisciplinary expert knowledge and its punctual goal-

oriented application (Voss et al. 2005). The building performance presents a multi-objective function taking into account behavioral patterns of users with respect to thermal comfort, indoor air quality, acoustics and more, as well as such criteria as daylight, energy consumption, and architectural design of a building. It is understandable that an effort to meet each objective will face a conflict of goals. Although the procedure for the process of integral planning is not harmonized, it focuses on the identification of these conflicts.

According to (Voss et al. 2005), the integral planning process can be characterized by the following conceptual properties:

- An iterative process of cognition is performed, including all experts with specific key qualifications.
- The interdisciplinary teamwork and the assignment of tasks are actively coordinated.
- The design options are analyzed, assessed, and optimized by planning tools based on information technology.
- The examination of life cycle costing and life cycle impact assessment leads to high transparency of the planning process.

These characteristic traits warrant the quality, consistency and goal-oriented result of integral planning process.

To design energy efficient buildings with complex (multi-dimensional) performance criteria, an integrated building performance simulation (BPS) should be used for transparent and objective decision making. BPS and thermal behavior predictions are to be elucidated further as crucial technologies for design, construction and operation of so called Green buildings, and will also play a vital role in performance monitoring in the operational phase (section 2-4).

Experience shows that BPS can indeed result in a significant reduction of the emission of greenhouse gases and give substantial improvements in comfort levels (Hensen et al. 2004). But an optimum of energy saving can only be accurately calculated based on a life cycle approach which covers the full life cycle of construction, operation, demolition, and disposal phases of building materials, as illustrated in figure 1-2.

### **1.4.2 Life cycle model for energy efficient buildings**

Traditionally, the methodology of life cycle assessment (LCA) has been suitably applied to increase the environmental performance of industrial products, but much less so for buildings because the main impacts are related to the use phase (Kotaji et al. 2003). The application of LCA starts to develop eco-label criteria for hard floor coverings (Baldo et al. 2002), compare building insulation products (Schmidt et al. 2004a, 2004b), assess the potential environmental impacts that might result from meeting energy demands in buildings (Osman, Ries 2007), and assess the reduction of CO<sub>2</sub> emissions in the construction field through the selection of materials for houses of low environmental impact (Abeysondra et al. 2007).

Authors have also employed LCA as a tool to analyze energy consumption of processing construction components. It started with a comparison of building materials, for example, concrete versus steel building frames (Jönsson et al. 1998). Another relevant object of investigation was floor coverings which were analyzed in several studies at different European locations<sup>1</sup>. Previous LCAs have general-

---

<sup>1</sup> The reader is referred to Günther, Langowski 1997; Jönsson et al. 1997; Potting, Blok 1995; Paulsen 2003; Rivala et al. 2006; Nebel et al. 2006.

ly focused on areas such as building materials, energy, water, and material use; only very few studies of complete buildings have been published<sup>2</sup>.

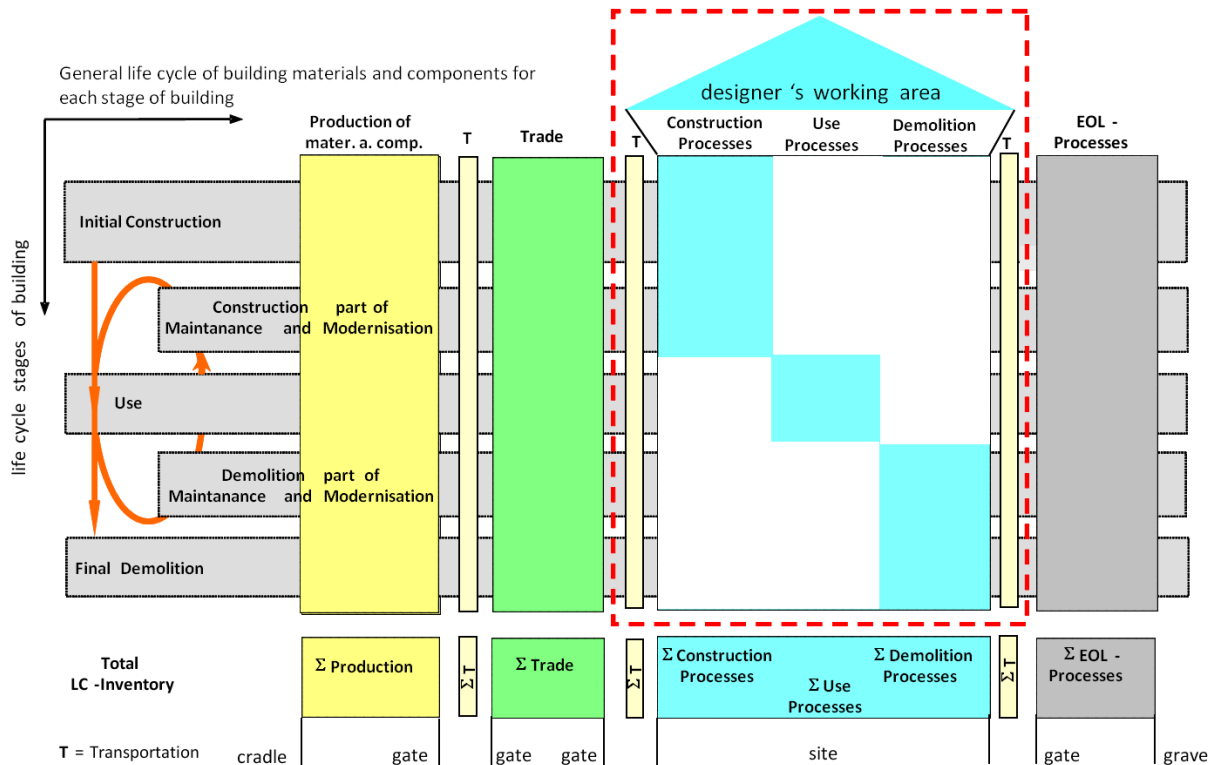


**Figure 1-2:** Matrix over life cycle stages of a building and the life cycle supply chain of each building material and component for each stage of a building (Buchgeister et al. 27/08/2007)

The life cycle analysis of a complete building is a very complex task, which is shown in figure 1-2 as a matrix of considered system boundaries. The left side presents the life cycle stages of a building which are generally considered if the performance and environmental impacts of a complete building are analyzed. In the following, the temporal sequence of the building life cycle stages is described. It starts with the initial construction phase which includes the full life cycle (value added chain) of all building materials and components in the horizontal line. The life cycle comprises extraction, production, trade, transportation, installation, on-site processes, and end-of-life processes for all incurred waste materials. After the initial construction of the building the use phase begins. A life time between 80 and 100 years for residential buildings, in general, is quoted in the literature (Klocke 1988; Winter 2002, revised 2008).

Eventually, the aging of building materials and components of heating, ventilation and air conditioning (HVAC) plants makes a renovation necessary. The renovation starts with a partial demolition, for example, a window and its frame. The production of a new window and its installation on site follow. The interior cycle of use phase, demolition and construction part of maintenance and modernization runs through the life time of the building. Following the final demolition phase the built-up area can be used for other services again.

<sup>2</sup> Examples are found in Thormark 2002; Kofoworola, Gheewala 2008; Mithraratne, Vale 2004; Citherlet, De-faux 2007; Thiers, Peuportier 2012.

Many assumptions, for example of the lifetime of each facility, have been made in life cycle inventory analysis regarding goal and scope definition by LCA practitioners. Especially for the future demolition, recycling and disposal processes in consideration of the long building use phase it has to handle the uncertainty for these made assumptions. Furthermore, appropriate to ISO 14040 cut-off criteria are determined to fix the system boundaries of the modeled building. Nonetheless, the modeling of the entire building life cycle is an obvious advantage of the holistic and integral approach which includes all life cycle phases in a transparent and comprehensible way. The life cycle modeling involved in an integral planning process is the basic prerequisite to optimize the energy efficiency of buildings.

### 1.4.3 Exergy - a measure of energy efficiency

For the building sector the energy conservation ordinance (EnEV) has foreseen the primary energy demand as yardstick of energy efficiency. This regulation is mandatory for the calculation of the primary energy demand of new and existing buildings in Germany. The simple energy model is shown in figure 1-3. The energy calculation includes all input and output heat flows such as transmission of window, roof and wall, and ventilation heat losses of the building envelope as well as the energy gains by solar radiation.

However, the discussion of energy efficiency in general is based on the fundamental first law of thermodynamics. It formulates that energy cannot be consumed and destroyed. Consequently, energy can only be converted from one form to another and only losses through the considered system boundaries influence energy efficiency. Experience shows that not all energy forms can be completely converted into other forms because thermodynamic inefficiencies occur. Based on this experience the second law of thermodynamics has been formulated. As a consequence, in thermodynamic theory some forms of energy are considered to be more useful than others. Therefore, apart from the quantitative aspects, energy transfers can also be associated with a quality aspect. This is easy to understand as it summarizes in a simply communicable way the fact that not all forms of energy are equivalent. Therefore, an efficiency analysis of energy conversion systems takes into account the second law of thermodynamics in order to identify the thermodynamic efficiency of process components. In other words, the source of thermodynamic inefficiency in an energy conversion system is quantified and identified by a second law thermodynamic analysis. Such a thermodynamic analysis is also known as exergy analysis.

In order to design a cost-effective energy conversion system, exergy analysis is combined with life cycle cost analysis resulting in so-called exergoeconomic analysis (in earlier literature thermo-economic analysis) (Tsatsaronis 1984; Tsatsaronis, Winhold 1985a, 1985b). In the case of an environmentally friendly design, an exergy analysis is combined with life cycle assessment, called exergoenvironmental analysis (Meyer et al. 2009).

A critical and analytical account of the development of the concept of exergy and its applications from the beginnings to the year 2004 was written by Sciubba and Wall (Sciubba, Wall 2007). The fundamental statement of the authors is that today practically each process analysis includes exergy considerations. Many references of reviewed scientific papers are cited to underpin the argument. It seems that the exergy approach is on the way of being regarded as a standard procedure in industrial analysis. Consequently, heating, ventilation and air conditioning (HVAC) plants are applications of exergy analysis to individual components. Still, there is no holistic analysis and optimization procedure of a building as a large complex energy conversion system including all HVAC components. A further challenge is integration into an integral planning process of a building.



The accurate definition and derivation of the exergy concept and the state of the art of exergy based analysis are described in chapter 2.

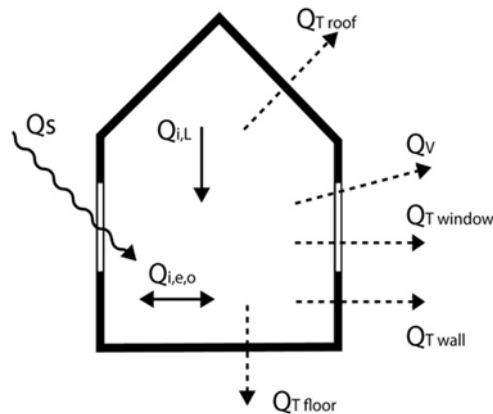


Figure 1-3: Simple integrated energy model of a building within German EnEV (Schlüter, Thesseling 2009)

#### 1.4.4 Intermediate findings

As part of the method development for energy efficient building design different working hypothesis are stated.

(WH1-1) The well-known practice of exergoeconomic and exergoenvironmental analysis for cost-effective and environmentally-friendly design of energy conversion systems (like power plants) should be transferred and applied as a yardstick to the building design process which is defined by the term “Exergy+”.

Presently, an obstacle is posed by the immense computational resources required for complete optimization of a building design including a high number of relevant parameters. But this is not seen as a fundamental limitation on the way of constant advances and refinements of both theoretical and application-oriented exergy-based analyses.

Regarding tools for building performance simulation (BPS), the full building life cycle is not taken into account today because the BPS tools have not embedded any life cycle inventory (LCI) database. In general an interface between BPS and LCI database is possible, but currently not implemented. Another important point is that the performance of a building depends on a lot of different parameters, especially on user behavior and thermal comfort. The definition of building performance requires goal variables which can be defined in a flexible way taking into account different comfort wishes. The state of the art of building performance simulation systems and their possibilities are described in detail in chapters 2.2 and 3.4.

Additionally, the building performance simulation system has to integrate an interface for monitoring which allows the identification of thermophysical building parameters by measurements, e.g. infrared thermography measurements in a long-term perspective. Parameter changes detected by these measurements during the building use phase indicate energy losses due to aging of the building envelope and the system components. By long-term monitoring, a critical evaluation of the energy calculations in the building planning process is possible. Therefore, an integrated system architecture including the approaches of Exergy+ and Thermography+ is proposed and shown in the following figure 1-4.

This theoretical system architecture concept organizes the information technology to optimize, measure, monitor, and diagnose energy efficiency during the building life cycle in order to find the ideal path for the highest energy efficiency in future.

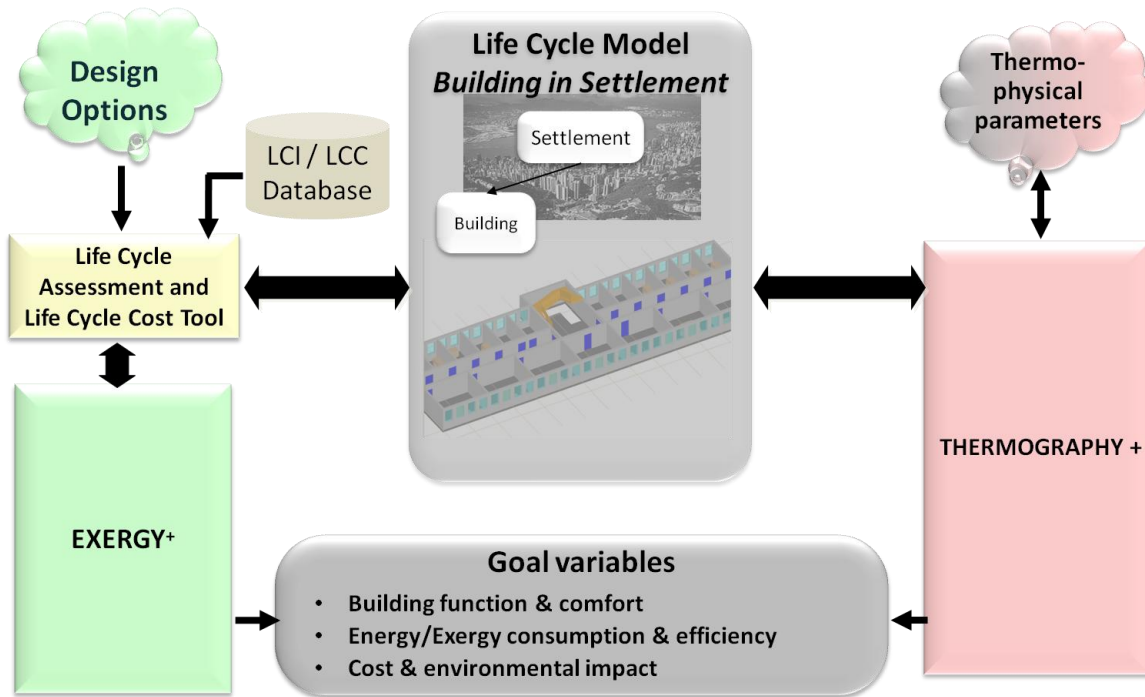


Figure 1-4: Simplified system architecture (block diagram) of the exergy and the thermography (QGT) tool

## 2 Methodology

This chapter describes in detail the different exergy-based methods and their application in the building sector. Based on the presented status quo a working program of the needed research is derived.

### 2.1 Review of Exergy Concept

The material and energy flow analysis based on the first law of thermodynamic disregards energy quality. Specifically, the irreversible loss in quality of thermal energy incurred by conversion from a higher to a lower temperature can only be shown by exergy (or thermodynamic second law) analysis. The definition of “exergy” for a thermodynamic second law analysis was made by Rant in the fifties (Rant 1956). The awareness of the advantages of exergy analysis has transferred practically into textbooks on thermodynamics (Szargut et al. 1988; Fratzscher et al. 1986; Bejan et al. 1996). In fact, the increase in inefficiencies always leads to a higher consumption of fuel, resulting in increasing environmental impacts but also costs. On the other hand, minimization of inefficiencies could increase the materials and energy needed for the construction of a component, for example, the area of a heat exchanger. These life cycle-related effects of components and the resulting impact on the environment (and costs) should be taken into account by systems analysis for design optimization. Therefore, exergy analysis is strictly required to provide the guidance needed in the design of energy conversion or chemical processes.

Szargut was first considering these life cycle-related effects in methodological work for environmentally friendly design. He suggested the cumulative exergy consumption (CExC) as an environmental indicator to reduce the consumption of natural resources (Szargut 1978). The CExC presents the calculation of exergy of energy carriers and raw materials (or non-renewable resources) along the life cycle.

Based on this approach, further methodological extensions were carried out; however, none of these published methods, takes into account either the complete life cycle of components<sup>3</sup> or all released emissions<sup>4</sup> as required for a product life cycle assessment (LCA).

The LCA is an internationally standardized method for the analysis of the consumption and emission of material and energy flows from all process steps within the product life cycle which leads to a life cycle inventory (LCI) result (DIN EN ISO 14040). Ideally, the system should be modelled in such a manner that inputs and outputs at its boundary (the environment) are calculated.

However, using the methodological framework of LCA to determine the environmental impact of a system it is impossible to point out the thermodynamic inefficiencies in the system, because the material and energy flow analysis is based on the first thermodynamic law.

The mentioned problems are solved by an exergoeconomic analysis published for example in (Bejan et al. 1996; Tsatsaronis, Cziesla 2002; Valero 2006). A similar problem to that discussed here arises during the economic assessment of energy conversion processes: in general, improving the thermodynamic efficiency of a component reduces the fuel costs. On the other hand, changes in the design

---

<sup>3</sup> E.g. Szargut et al. 2002; Szargut 2004; Szargut, Stanek 2005; Valero et al. 1986; Valero 1998; Sciubba 1999, 2002; Frangopoulos 1992; Frangopoulos, Caralis 1997.

<sup>4</sup> E.g. Cornelissen 1997; Gong, Wall 1997; Ayres et al. 1998; Dewulf et al. 2000; Dewulf, van Langenhove 2002.

of a component may result in higher costs of construction or maintenance. To find an optimum, fuel costs must be allocated to the respective component. The application of exergoeconomic analysis helps in understanding the cost-formation process and the flow of costs in an energy conversion system, and therefore in the design of a cost-effective system.

The combination of exergy analysis with LCA transforms the exergoeconomic analysis (a combination of exergy analysis and life cycle costing analysis) into the exergoenvironmental analysis (Meyer et al. 2009; Buchgeister 2010a). It has been developed in order to reveal to which extent each component of an energy conversion system is responsible for the overall environmental impact, and to identify the sources of that impact. A general structure and the analogy between exergoeconomic and exergoenvironmental analysis are shown in figure 2-1.

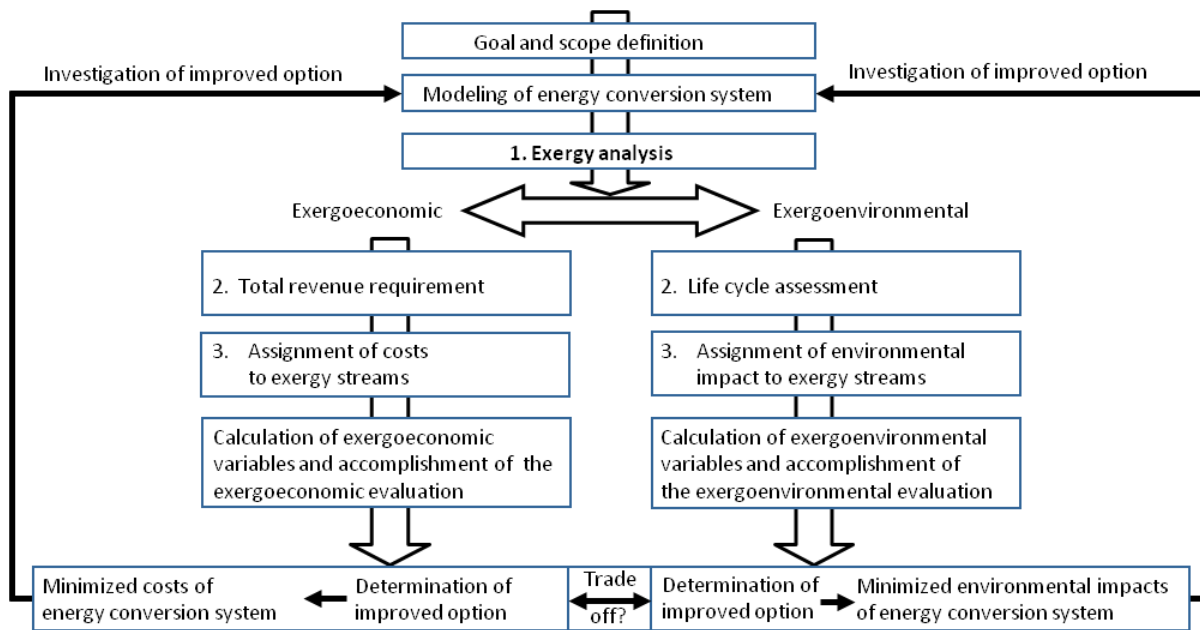


**Figure 2-1:** General structure, steps and analogy of the exergoeconomic and exergoenvironmental analysis

As shown in figure 2-1, the concept of exergoeconomic and exergoenvironmental analysis consists mainly of the following three steps:

- Exergy analysis of the investigated system;
- Total revenue requirement cost analysis and life cycle assessment of each system component and system input flow;
- Assignment of costs and environmental impact to each exergy flow.

Subsequently, exergoeconomic and exergoenvironmental variables are calculated and a corresponding evaluation is carried out. With the aid of a system evaluation, the components causing the highest costs or highest environmental impacts can be identified. By applying both methods to the same process it may be expected that in many cases the same process components are identified for improvement, but the results are not equivalent in general. The reason is the methodical difference between both methods in the calculation of the construction-related effort (and investment, respectively).

In the following, the exergoeconomic and exergoenvironmental method is described as a common rational basis for assigning cost and environmental impact to the energy carriers.

### 2.1.1 Exergy Analysis

A topical definition of the term exergy of a system is the maximum theoretical useful work obtainable as the system is brought into complete thermodynamic equilibrium with the thermodynamic environment while the system interacts only with this environment (Szargut et al. 1988; Fratzscher et al. 1986). This means that energy with a high convertibility potential is said to contain a high share of exergy. In other words, exergy is characterized as a property describing the quality of energy, which can be used for a competitive analysis of different forms of energy.

For exergy analysis, first, the boundaries of the system to be analyzed and the components involved must be defined. All relevant system sub-units that have a productive purpose should be regarded as separate components (Bejan et al. 1996; Lazzaretto, Tsatsaronis 2006). Next, the exergy values of all material and energy flows within the system must be determined. The exergy of the material flows can be calculated as the sum of their physical, chemical, kinetic, and potential exergy values, see equation (2-1). In many applications of energy conversion processes kinetic and potential exergy can be neglected (Bejan et al. 1996). The calculation of exergy values is discussed in detail in (Tsatsaronis, Czesla 2004-2007).

$$\dot{E}_{total} = \dot{E}_{ph} + \dot{E}_{ch} + \dot{E}_{kin} + \dot{E}_{pot} \quad eq. (2-1)$$

In exergy analysis, each component  $k$  is characterized by the definition of its exergy of product,  $\dot{E}_{P,k}$  and exergy of fuel  $\dot{E}_{F,k}$  shown in Fig. 2-2. Calculation of fuel and product is carried out according to the exergetic and economic purposes of the  $k$ -th component and is based on the SPEC0 approach (Lazzaretto, Tsatsaronis 2006).

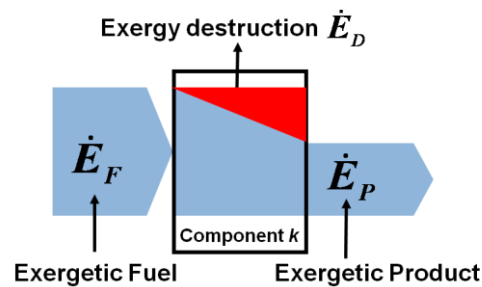


Figure 2-2: Basic exergy balance of component  $k$ .

The exergetic efficiency of the  $k$ -th component is defined as the ratio between the exergies of product and fuel. It was introduced by Grassmann in the nineteen-fifties (Grassmann 1950).

$$\varepsilon_k = \frac{\dot{E}_{P,k}}{\dot{E}_{F,k}} \quad eq. (2-2)$$

Exergy destruction  $\dot{E}_{D,k}$  in the  $k$ -th component is a direct measure of thermodynamic inefficiency. It is calculated as:

$$\dot{E}_{D,k} = \dot{E}_{F,k} - \dot{E}_{P,k} \quad eq. (2-3)$$

Exergy analysis gives answers to where thermodynamic inefficiencies occur in the system. In addition, it reveals their rates and causes. Moreover, exergy analysis puts all process components on the same physical basis to determine the functional interrelationship between components.

### 2.1.2 Exergoenvironmental Analysis

After the exergy analysis of the system an environmental analysis is carried out in the second step to determine the environmental impacts. For the exergoenvironmental analysis the method of life cycle assessment (LCA) is applied, which is standardized in ISO 14040 and 14044 (DIN EN ISO 14040; DIN EN ISO 14044).

LCA of the total system must include the supply of input flows, especially fuel, and cover the full life cycle of components. It is necessary to extend the exergy process model with the upstream chain of each input flow and the full life cycle of each component. Ideally, the system should be modeled in such a manner that inputs and outputs (the life cycle inventory) at its boundary (the environment) are calculated.

The inventory result calculated for the life cycle processes investigated is based on the general physical laws of conservation of energy and mass. Then, based on the LCI result, the environmental impacts are calculated for various impact categories applying a quantitative method of impact assessment. An impact category describes the impact pathway between the LCI results and their environmental areas of protection or so-called endpoint(s), i.e. the receptors that are damaged. It includes a cause-effect chain (environmental mechanism) by using indicators for quantitative characterization based on an environmental model. For the methodological development of exergoenvironmental analysis, a single-score life cycle impact assessment (LCIA) method, Eco-indicator 99, has been chosen (Goedkoop, Spriensma 2000). It is an LCIA method to support decision-making in a design for environment. The structure and environmental aspects considered are displayed in Fig. 2-3.

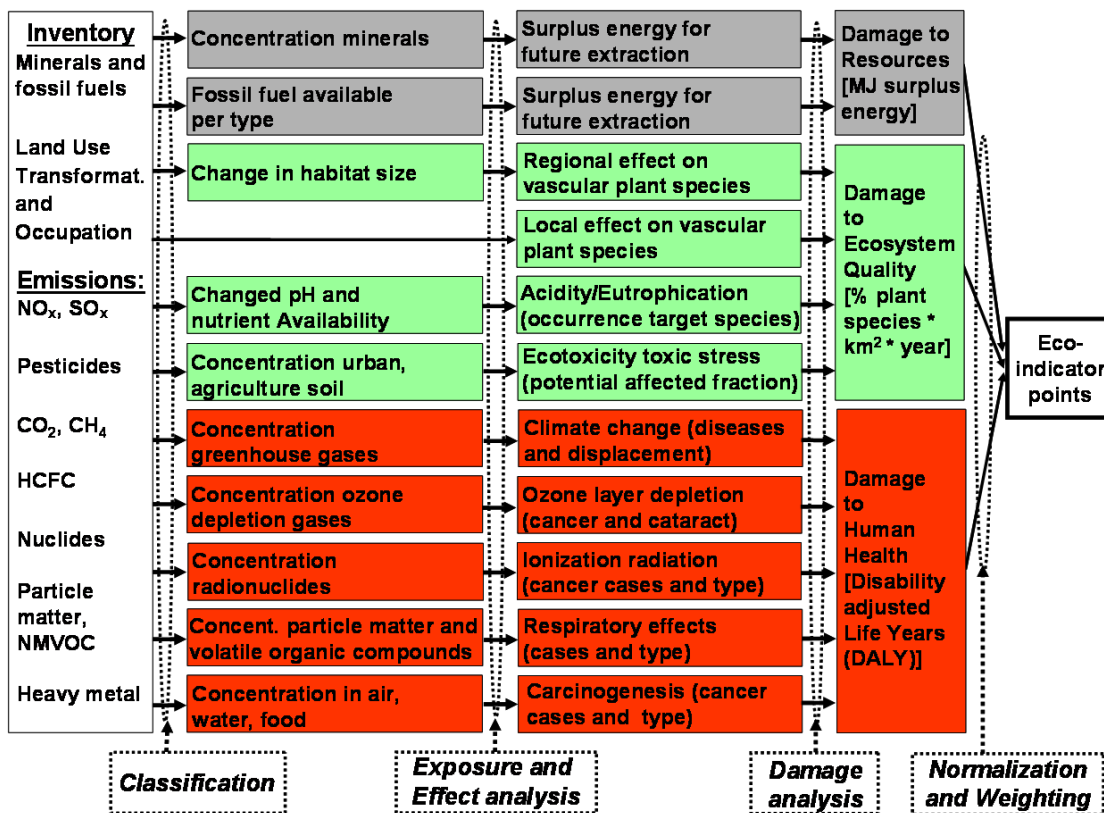


Figure 2-3: General structure and model of the life cycle impact assessment method – Eco-Indicator 99

The impact categories cover the range of environmental aspects and model environmental damage of three damage categories: Human health, ecosystem quality, and natural resources. The characterization model for each impact category is determined in detail in (Goedkoop, Spriensma 2000). In a last step, the three damage categories are normalized and weighted, with the result being expressed as Eco-indicator points, where higher damage is reflected by a higher Eco-indicator value.

Besides the selected Eco-indicator 99, other LCIA methods exist, which are discussed in literature (Udo de Haes, et al 2002; Jolliet, et al 2004).

A comparative investigation of exergoenvironmental analysis using Eco-indicator 99, CML 2001 and IMPACT 2002 as LCIA methods is presented by the authors in (Buchgeister 2009, 2010b). The conclusion of the comparison is that the application of the two LCIA methods used, CML 2001 and Impact 2002, instead of the Eco-indicator 99 has a small influence on the calculated exergoenvironmental variables (figure 2-4). For all applied methods the same components cause the highest impact.

However, in general the exergoenvironmental analysis requires the best yardstick for the assessment of environmental impacts which can be developed during further improvements within the field of life cycle impact assessment in future. The integration of these further developments in the exergoenvironmental analysis was foreseen in the structure.

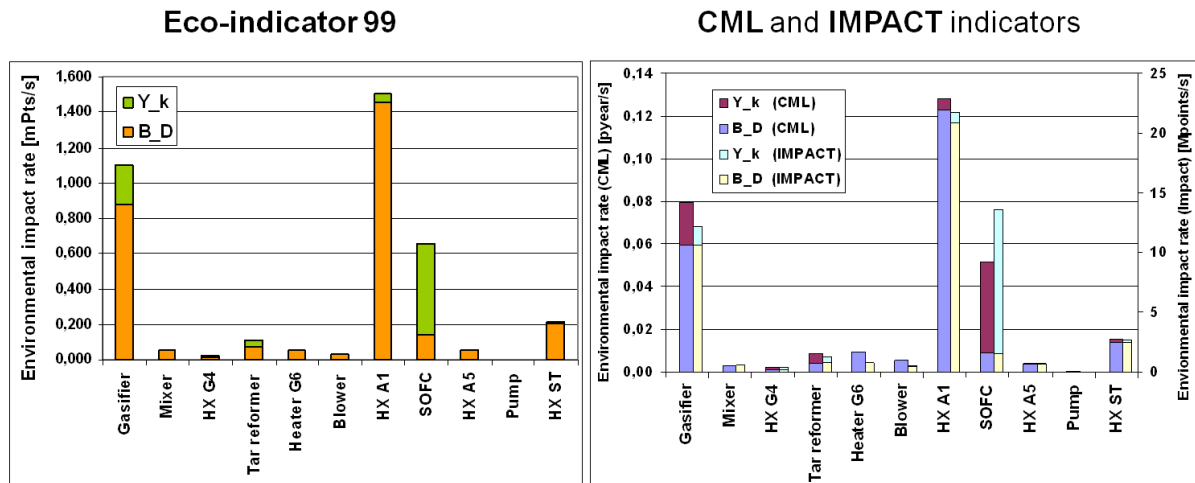


Figure 2-4: Summary of environmental impact rate of Eco-Indicator 99, CML 2001 and IMPACT 2002 LCIA methods

### 2.1.3 Exergoenvironmental Variables and Evaluation

In the third step, the LCA results (expressed in Eco-indicator points) are assigned to the corresponding exergy flows.

#### Definitions

The environmental impact rate  $\dot{B}_j$  is the environmental impact expressed in Eco-indicator points per time unit (Points/s or mPoints/s). The specific (exergy-based) environmental impact  $b_j$  is the average environmental impact associated with the production of the  $j$ -th flow per exergy unit of the same flow (Points/GJ or mPoints/GJ exergy). The environmental impact rate  $\dot{B}_j$  of the  $j$ -th material flow is the product of its exergy rate  $\dot{E}_j$  and the specific environmental impact  $b_j$ :

$$\dot{B}_j = \dot{E}_j b_j \quad \text{eq. (2-4)}$$

The environmental impact rate  $\dot{B}_j$  can also be calculated using the specific exergy  $b_j$  and the mass flow rate  $\dot{m}_j$ :

$$\dot{B}_j = \dot{m}_j e_j b_j \quad \text{eq. (2-5)}$$

Depending on the system or component being analyzed, it may be useful to distinguish between physical and chemical exergy. In this case, a specific environmental impact for each exergy component must be known in order to calculate the environmental impact rate  $\dot{B}_j$  or the average specific environmental impact  $b_j$ :

$$\dot{B}_j = \dot{B}_j^{PH} + \dot{B}_j^{CH} = b_j^{PH} \dot{E}_j^{PH} + b_j^{CH} \dot{E}_j^{CH} = b_j \dot{E}_j \quad \text{eq. (2-6a)}$$

Where

$$\dot{E}_j = \dot{E}_j^{PH} + \dot{E}_j^{CH} \text{ and } b_j = b_j^{CH} \frac{\dot{E}_j^{CH}}{\dot{E}_j} + b_j^{PH} \frac{\dot{E}_j^{PH}}{\dot{E}_j}. \quad \text{eq. (2-6b)}$$

The environmental impact rate  $\dot{B}_j$  is a weighted mean of the specific environmental impact rates.

Environmental impact rates associated with heat  $\dot{Q}$  and work  $\dot{W}$  are calculated as follows:

$$\dot{B}_q = b_q \dot{E}_q \quad \text{eq. (2-7)}$$

$$\dot{B}_w = b_w \dot{W} \quad \text{eq. (2-8)}$$

Where the exergy rate  $\dot{E}_q$  associated with a heat transfer is calculated using the following equation:

$$\dot{E}_q = \left(1 - \frac{T_0}{T_j}\right) \dot{Q}. \quad \text{eq. (2-9)}$$

Here  $T_0$  is the surrounding ambient temperature and  $T_j$  [K] the temperature at which the heat transfer crosses the boundary of the system. For the exergy analysis of the case study (Buchgeister 2010b), it was assumed that all heat transfers to the environment take place at  $T_0 = T_j$ . Otherwise, the temperature  $T_j$  is calculated by simulation software. It could also be the thermodynamic average temperature.

### Environmental impact balances and auxiliary equations

From the results of the exergetic analysis and LCA, the specific environmental impact  $b_j$  can be calculated directly for input flows (i.e. fuel flows) entering the overall system. Applying equation (2-4), where  $\dot{B}_j$  is the result of LCA for the fuel ( $j$ -th flow) and  $\dot{E}_j$  is the exergy rate of the  $j$ -th input flow,  $b_j$  is calculated as follows:

$$b_{j,in} = \frac{\dot{B}_{j,in}}{\dot{E}_{j,in}}. \quad \text{eq. (2-10)}$$

The values for internal and output flows can only be obtained by considering the functional relations among system components. This is done by formulating environmental impact balances and auxiliary equations.

The environmental impact balance for the  $k$ -th component states that the sum of environmental impact rates associated with all input flows plus the component environmental impact rate is equal



to the sum of the environmental impact rates associated with all output flows shown in Fig. 2-5. The equation is

$$\sum_{j=1}^n \dot{B}_{j,k,in} + \dot{Y}_k = \sum_{j=1}^m \dot{B}_{j,k,out} \quad eq. (2-11)$$

or

$$\sum_{j=1}^n (b_j \dot{E}_j)_{k,in} + \dot{Y}_k = \sum_{j=1}^m (b_j \dot{E}_j)_{k,out} \quad eq. (2-12)$$

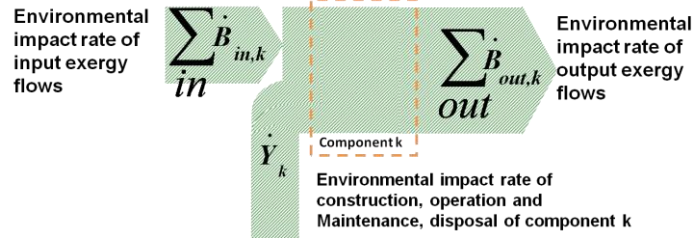


Figure 2-5: Environmental impact balance of component  $k$ .

LCA provides the environmental impact for each component comprising the three life cycle phases of construction ( $CO$ ), operation and maintenance ( $OM$ ), and disposal ( $DI$ ). The sum of all component-related environmental impacts is  $\dot{Y}_k$  as shown in equation (2-13):

$$\dot{Y}_k = \dot{Y}_k^{CO} + \dot{Y}_k^{OM} + \dot{Y}_k^{DI} \quad eq. (2-13)$$

Within the analyzed system, the direct emissions from a component are assigned to the operation and maintenance phase. The construction phase includes manufacturing, transport, and installation of components. Equations (2-11) or (2-12) of the environmental impact balance of a component cannot be solved if the number of output flows, and therefore the number of unknown variables, is greater than one.

Considering the heat exchanger HX shown in Fig. 2-6 as an example, the following equations for the environmental impact balance are obtained:

$$\dot{B}_1 + \dot{B}_3 + \dot{Y}_{HX} = \dot{B}_2 + \dot{B}_4 \quad eq. (2-14)$$

$$b_1 \dot{E}_1 + b_3 \dot{E}_3 + \dot{Y}_{HX} = b_2 \dot{E}_2 + b_4 \dot{E}_4 \quad eq. (2-15)$$

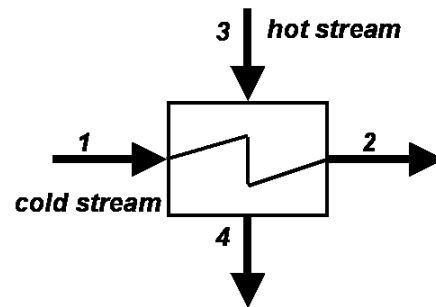


Figure 2-6: Schematic structure of a heat exchanger HX.

To solve this problem, additional auxiliary equations are required by exergy analysis. In general, the number of necessary auxiliary equations is equal to the number of exiting flows minus one. In exergoenvironmental analysis, auxiliary equations are developed in analogy to exergoeconomics by using environmental impact rates instead of cost rates and applying the following  $F$  and  $P$  principles, which refer to the definitions of the exergy of fuel and product for a component (Lazzaretto, Tsatsaronis 2006; Tsatsaronis, Czesla 2004-2007).

$F$  equations: To formulate these equations, the exergy flows supplying a component with exergy are considered. The decrease of exergy in these flows within a component is

part of the exergetic fuel of a component. The specific environmental impact of these flows remains constant between input and output.

*P* equations: To formulate a *P* equation, exergy flows are taken into consideration, the exergy content of which increases within a component. This increase is part of the exergy of the product of the component. Each exergy unit is supplied to all these exergy flows with the same average specific environmental impact,  $b_{P,k}$ .

The *F* principle can be applied to the heat exchanger example shown in Fig. 2-6, which operates above the surrounding temperature. Exergy from the hot stream is transferred to the cold stream. The decrease in the exergy of the hot stream is the exergy of the fuel of the component. According to the *F* principle, the specific environmental impact of the hot stream remains constant:

$$b_4 = b_3. \quad \text{eq. (2-16)}$$

Because of this equation and the decreased exergy rate of the hot stream, its environmental impact rate decreases ( $\dot{B}_4 < \dot{B}_3$ ). The difference ( $\dot{B}_3 - \dot{B}_4$ ) is assigned to the exiting cold stream through the environmental impact balance.

When the environmental impact rates of each exergy flow in a complex energy conversion system have to be calculated, it is advisable to formulate a system of linear equations comprising the environmental impact balances and the auxiliary equations. The solution of this system of equations reveals the unknown environmental impact rates and the corresponding specific environmental impacts.

### Treatment of dissipative components

Often components without a productive or exergetic purpose are part of a system. Examples for this type of components, which are called dissipative components (DC), are coolers, gas cleaning units, or throttling valves operating entirely or partially above surrounding temperature. These components decrease the exergy content of a flow without generating an immediately useful effect. A product from the thermodynamic viewpoint cannot be defined for these components, which serve either other so-called productive components or the overall system directly (Bejan et al. 1996). The environmental impact due to thermodynamic inefficiencies within a DC and the component-related environmental impact should be charged to the productive components or to the product of the overall system, if this system is served directly by the DC. This approach is similar to the one used in exergoeconomics for DC (Lazzaretto, Tsatsaronis 2006). In each DC there is a decrease of exergy between input and output:

$$\Delta \dot{E} = \dot{E}_{in} - \dot{E}_{out} \quad \text{eq. (2-17)}$$

For a DC the environmental impact balance reads as follows:

$$\dot{B}_{out} + \dot{B}_{dif,dc} = \dot{B}_{in} + \dot{B}_{aux} + \dot{Y}_{dc} \quad \text{eq. (2-18)}$$

The environmental impact rates associated with the input and output flows are  $\dot{B}_{in}$ , and  $\dot{B}_{out}$ , respectively.  $\dot{B}_{dif,dc}$  represents the net environmental impact associated with the DC that needs to be assigned to other components.  $\dot{B}_{aux}$  is the net environmental impact associated with the use of auxiliary fluids within the DC being considered.  $\dot{Y}_{dc}$  denotes the component-related environmental impact of the DC. Application of the *F* principle to the specific environmental impacts  $b_{in}$  and  $b_{out}$  leads to:

$$b_{out} = b_{in}. \quad eq. (2-19)$$

With the equations (2-17)-(2-19) the result for  $\dot{B}_{dif,dc}$  is:

$$\dot{B}_{dif,dc} = b_{in} \Delta \dot{E} + \dot{B}_{aux} + \dot{Y}_{dc} \quad eq. (2-20)$$

The environmental impact rate associated with the DC can now be assigned to productive component  $n$  served by the DC. This is achieved by extending the component-related environmental impact of the  $n$ -th productive component, according to equation (2-13):

$$\dot{Y}_n = \dot{Y}_n^{CO} + \dot{Y}_n^{OM} + \dot{Y}_n^{DI} + \dot{B}_{dif,dc} \quad eq. (2-21)$$

### Calculation of Exergoenvironmental Variables

Exergoenvironmental variables can be calculated for every process component, based on the exergy, the environmental impact rates and the specific environmental impact of each exergy flow in the process. Only two exergoenvironmental variables will be discussed here.

Within exergy analysis, the exergy destruction of each component is calculated. The exergoenvironmental analysis allows calculating the environmental impact rate  $\dot{B}_{D,k}$  associated with the exergy destruction  $\dot{E}_{D,k}$  in the  $k$ -th component by applying the following equation:

$$\dot{B}_{D,k} = b_{F,k} \dot{E}_{D,k} \quad eq. (2-22)$$

The rate of exergy destruction is multiplied by average specific environmental impacts of the exergetic fuel of the  $k$ -th component  $b_{F,k}$ . This value is calculated based on the definition of exergetic fuel and product within exergy analysis.

The sum of the environmental impacts  $\dot{B}_{TOT,k}$  of the  $k$ -th component is calculated by adding the environmental impacts of exergy destruction  $\dot{B}_{D,k}$  and the component-related environmental impacts  $\dot{Y}_k$ :

$$\dot{B}_{TOT,k} = \dot{B}_{D,k} + \dot{Y}_k \quad eq. (2-23)$$

This exergoenvironmental variable reveals the environmental relevance of each component. The exergoenvironmental evaluation is carried out by applying the exergoenvironmental variables. Based on the evaluation of the process and its components, possibilities for an improvement with respect to the environmental performance can be developed.

The relative difference  $r_{b,k}$  between the average specific environmental impact of the product  $b_{P,k}$  and the fuel  $b_{F,k}$  is given by:

$$r_{b,k} = \frac{b_{P,k} - b_{F,k}}{b_{F,k}}. \quad eq. (2-24)$$

This exergoenvironmental variable is an indicator of the potential for reducing the environmental impact associated with a component. A relatively high value of  $r_{b,k}$  indicates, in general, that the environmental impact of the corresponding component can be reduced with a smaller effort than the environmental impact of a component with lower value. Independently of the absolute value of

environmental impact, the relative difference of specific environmental impacts represents the environmental quality of a component.

The sources for the formation of environmental impact in a component are compared with the aid of the exergoenvironmental factor  $f_{b,k}$ , which expresses the relative contribution of the component-related environmental impact  $\dot{Y}_k$  to all environmental impacts associated with the  $k$ -th component:

$$f_{b,k} = \frac{\dot{Y}_k}{\dot{Y}_k + \dot{B}_{D,k}} = \frac{\dot{Y}_k}{\dot{B}_{TOT,k}} \quad eq. (2-25)$$

The component-related environmental impact  $\dot{Y}_k$  is dominant when the value of  $f_{b,k}$  is higher than approximately 0.7, whereas exergy destruction is the dominant source of environmental impact when the value of  $f_{b,k}$  is lower than approximately 0.3.

### Exergoenvironmental Evaluation

The formation of environmental impact at the system component level of energy conversion systems can be studied with the aid of the exergoenvironmental analysis presented here. The objective is to generate information that serves as a basis for the development of improved design options, enabling the environmental impact of the overall system to be reduced. A systematic evaluation should employ the following steps:

First, the environmentally relevant system components are identified through the sum of environmental impacts  $\dot{B}_{TOT,k}$ . From these components, we select those with the highest improvement potential, which is indicated by the relative difference of the specific environmental impacts  $r_{b,k}$ . The exergoenvironmental factor  $f_{b,k}$  reveals the main source of environmental impact associated with these components. Finally, suggestions for improvement can be developed based on the results of the LCA, if component-related impacts dominate the impact, or with the aid of exergy analysis, if thermodynamic inefficiencies are the dominant source of environmental impact for the component being considered.

#### 2.1.4 Exergoeconomic Analysis

In analogy to the exergoenvironmental analysis, an exergoeconomic analysis is also based on the exergy analysis of the energy conversion system be studied. It is followed by an economic analysis based on the method of total revenue requirements (TRR) which considers the entire life cycle of the energy conversion system in the same way as the LCA method (Bejan et al. 1996; Tsatsaronis, Czielsa 2004-2007).

The method of total revenue requirements consists of the following steps:

- Estimation of the total capital investment;
- Calculation of total revenue requirement (operation, maintenance, and disposal);
- Calculation of leveled product costs.

The investment costs are treated differently from fuel and operation and maintenance (O&M) expenses, because they are non-recurring costs.

The total capital investment (TCI) is defined as the sum of the fixed-capital investment (FCI) and other outlays. Here, the FCI includes the capital needed to purchase land, build all facilities, and install all machinery and equipment for an energy conversion system. The FCI represents the total system costs, assuming that no time is required for design and construction as so-called overnight construc-

tion. The estimation of FCI is differentiated according to two cost elements: direct and indirect costs. Direct costs are the costs of all permanent materials, equipment, labor, and other resources involved in the fabrication, erection, and installation of the permanent facilities. The indirect costs are defined as non-permanent parts of the facilities. They are required for the proper completion of the project.

Other outlays consist of the working capital, start-up costs, costs of licensing, research, and development, and allowance for funds used during construction. More detailed information is provided in (Bejan et al. 1996; Tsatsaronis, Czesla 2004-2007; Peters, Timmerhaus 1991).

After the estimation of the TCI, the annual total revenue requirement or total product costs are calculated. It is defined as the revenue that has to be collected in a given year through the sale of all products to compensate the operating company for all expenditures incurred in the same year and to ensure sound economic plant operation. The major cost categories included for the calculation of the TRR are shown in figure 2-7.

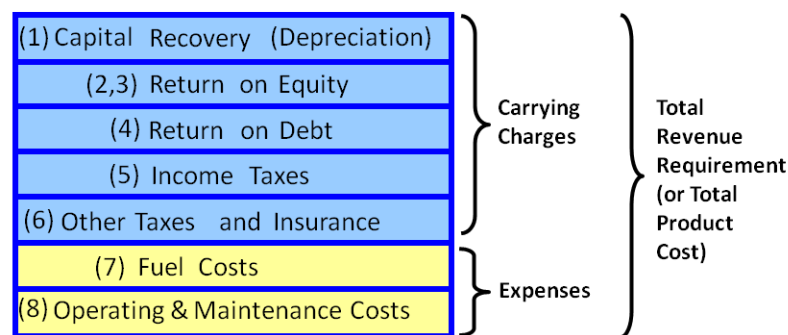


**Figure 2-7.** Revenue cost categories for the total revenue requirement (TRR) method (Bejan et al. 1996).

The expenses are defined as the sum of fuel costs and operating and maintenance costs. Expenses include goods and services that are used in a short period of time. In contrast to carrying charges, expenses are paid directly from revenue. Hence, they are not capitalized. The carrying charges illustrate the liabilities associated with an investment. The liability remains until the energy conversion system is taken out of operation at the end of its estimated economic life. For the calculation of carrying charges, a lot of economic parameters are needed, while for the accounting of expenses, specific technical parameters are necessary.

Afterwards, the revenue requirements (product costs) are leveled for all cost categories, because fuel and O&M costs generally increase, while carrying charges decrease with increasing years of operation. Leveled means that variable product costs are transformed into an equivalent series of constant payments, called annuities.

In the next step, the costs are assigned to the exergy streams in the process. It is also called exergy costing. In the end, the exergoeconomic evaluation is carried out.

On the basis of the evaluation of the process and its components, possibilities for an improvement with respect to the cost effectiveness can be developed.

As the exergoeconomic analysis is well-known, the needed formulas are presented in table 2-1 in comparison to the exergoenvironmental analysis.

From various exergoeconomic analyses of components, the relationship between investment costs and exergy destruction per unit of product exergy is known for the  $k$ -th component of an energy conversion system (Tsatsaronis 2007). A hyperbola curve as single line is presented in figure 2-8 on

the left side. The hyperbola is limited by two asymptotic lines, the specific unavoidable exergy destruction  $\left[\frac{\dot{E}_D}{\dot{E}_P}\right]_k^{UN}$ , and the specific unavoidable investment costs  $\left[\frac{\dot{Z}^{CI}}{\dot{E}_P}\right]_k^{UN}$ .

Both terms are evident, because the production of a component always leads to a minimum economic effort and each component has inefficiencies incurring a minimum of exergy destruction.

<b>Exergoeconomic Analysis</b>	<b>Exergoenvironmental Analysis</b>
<b>Exergy cost rate:</b> $\dot{C}_j = c_j \cdot \dot{E}_j$	<b>Exergoenvironmental impact rate:</b> $\dot{B}_j = b_j \cdot \dot{E}_j$
<b>Cost balance:</b> $\sum \dot{C}_{j,k,in} + \dot{Z}_k = \sum \dot{C}_{j,k,out}$	<b>Environmental impact balance:</b> $\sum \dot{B}_{j,k,in} + \dot{Y}_k = \sum \dot{B}_{j,k,out}$
<b>Component-related cost rate:</b> $\dot{Z}_k = \dot{Z}_k^{CI} + \dot{Z}_k^{OM}$	<b>Component-related environmental impact rate:</b> $\dot{Y}_k = \dot{Y}_k^{CO} + \dot{Y}_k^{OM} + \dot{Y}_k^{DI}$
<b>Relative cost difference:</b> $r_k = \frac{c_{P,k} + c_{F,k}}{c_{F,k}}$	<b>Relative environmental impact difference:</b> $r_{b,k} = \frac{b_{P,k} - b_{F,k}}{b_{F,k}}$
<b>Exergoeconomic factor:</b> $f_k = \frac{\dot{Z}_k}{\dot{Z}_k + \dot{C}_{D,k}}$	<b>Exergoenvironmental factor:</b> $f_{b,k} = \frac{\dot{Y}_k}{\dot{Y}_k + \dot{B}_{D,k}}$

**Table 2-1:** Variables used by exergoeconomic and exergoenvironmental analyses

A similar hyperbola is expected for the construction-related environmental impacts versus exergy destruction shown in figure 2-8 on the right side. Due to the same approach, the asymptotic lines of specific unavoidable exergy destruction are the same. The other asymptotic line declared as specific unavoidable construction-related environmental impacts evidently is associated with a production of a component, because a minimum of material and energy is needed for each component. These results have been analyzed in a case of electricity production by means of high temperature solid oxide fuel cell and biomass gasification process (Meyer et al. 2009). Of particular interest is the relationship between capital investment costs and construction-related environmental impacts of a component for the area of possible working points marked by a question mark. Hence, more comparable exergoeconomic and exergoenvironmental analyses of different components are needed.

Different approaches are applied to determine environmental impacts and costs, and the variables are not completely analogous. For example, direct emissions of the process are considered in the environmental analysis, while they do not have any influence on the economic side. These environmental costs might be internalized by an emissions trading system in the future. Another example is environmental impacts that are caused by the disposal or recycling of components. These impacts are not considered as detailed as in the economic analysis.

The internalization of all external environmental costs is a very challenging task that might be realized in the far future but is not yet reality. Therefore, at the moment a reliable improvement of a

process with respect to environmental and economic aspects can only be achieved by applying both methods. During an improvement process, it is important to keep both aspects in mind. An environmental optimization should not lead to a process that is not economic anymore and vice versa. Future analysis will have to show under which circumstances a relationship can be determined between the capital investment costs and construction-related environmental impacts of a component for the area of possible working points.

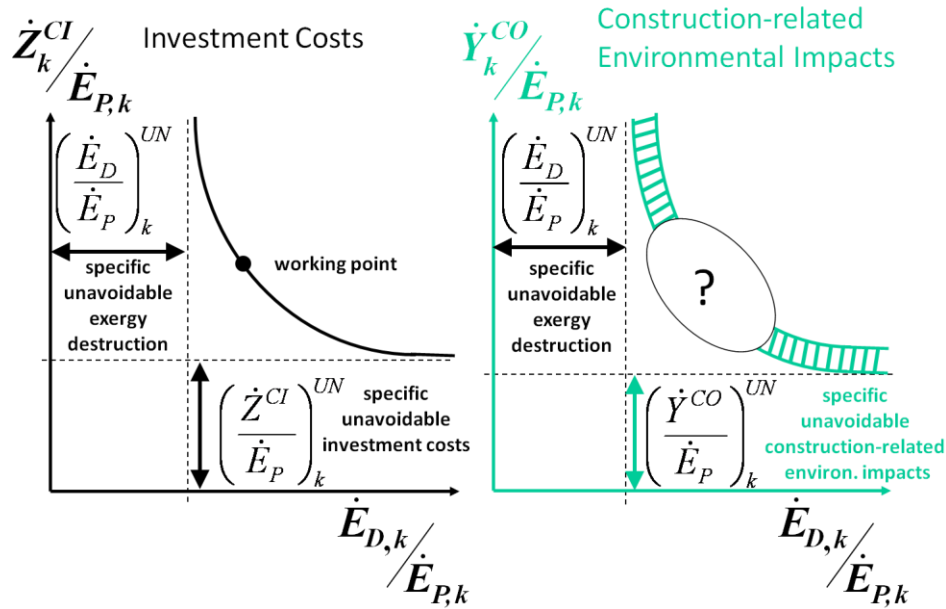


**Figure 2-8:** Expected relationship between investment costs and environmental impact of construction as a function of exergy destruction for the  $k$ -th component of an energy conversion system (Meyer et al. 2009).

### 2.1.5 Exergo-economic-environmental Analysis

A combination of exergoeconomic and exergoenvironmental analysis leads to the outcome of the so-called exergo-economic-environmental analysis whose rational basis is defined by exergy. For the application of both methodological analyses the best possible optimization (minimal environmental impacts as well as costs) of the energy conversion process is the goal. The optimization is controlled by means of raising efficiency of each component or reduced demand of the entire life cycle of each component. Here it is taken into account that the same component may interact differently with other components in an energy conversion process. Knowledge of the interrelationship between components and of the potential for improving each important component in optimizing the overall energy conversion system can be found in following literature (Tsatsaronis 1999). For this reason the fraction of exergy destruction in a single component is calculated which is thermodynamically avoidable and has no influence on any other component (ideal operating point). To determine this part of exergy destruction within a component, a linkage between two approaches is used for the mathematical description of the exergy destruction. This means that the exergy destruction within a component is split into avoidable and unavoidable parts and into endogenous and exogenous parts. The mathematical description of both separated exergy destruction approaches is shown in equations (2-26) and (2-27).

$$\dot{E}_{D,k} = \dot{E}_{D,k}^{UN} + \dot{E}_{D,k}^{AV} \quad \text{eq. (2-26)}$$

$$\dot{E}_{D,k} = \dot{E}_{D,k}^{EN} + \dot{E}_{D,k}^{EX} \quad \text{eq. (2-27)}$$

Unavoidable exergy destruction  $\dot{E}_{D,k}^{UN}$  is the part of exergy destruction within one component that cannot be eliminated even if the best available technology in the near future would be applied. The avoidable exergy destruction  $\dot{E}_{D,k}^{AV}$  is the difference between total and unavoidable exergy destruction and represents the real potential for improving the component.

The endogenous part of exergy destruction  $\dot{E}_{D,k}^{EN}$  is associated only with the irreversibility occurring in the  $k$ -th component when all other components operate in an ideal way and the component being considered operates with its current efficiency.

The exogenous part of exergy destruction  $\dot{E}_{D,k}^{EX}$  appearing in the  $k$ -th component is caused by the irreversibility occurring in the remaining components.

Past publications observed the separation of exergy destruction into avoidable and unavoidable parts (Tsatsaronis 1999; Tsatsaronis, Park 2002) as well as into endogenous and exogenous parts (Morosuk, Tsatsaronis 2006, 2007) with the objective to identify the contributions to exergy destruction by other components. Such an approach, which expands the conventional exergy analysis, is called advanced exergy analysis by Tsatsaronis and Morosuk (Tsatsaronis, Morosuk 2007). The mathematical result of combining the two approaches of splitting the exergy destruction is shown in equation (2-28).

$$\dot{E}_{D,k} = \dot{E}_{D,k}^{UN,EN} + \dot{E}_{D,k}^{UN,EX} + \dot{E}_{D,k}^{AV,EN} + \dot{E}_{D,k}^{AV,EX} \quad \text{eq. (2-28)}$$

The variables to be optimized are denoted by  $\dot{E}_{D,k}^{AV,EN}$  in equation (2-28); i.e. the avoidable endogenous investment costs or environmental impacts, respectively, of exergy destruction within a component should be minimized.

The combination of the advanced exergoeconomic and exergoenvironmental analysis leads to the integrated exergo-economical-environmental analysis which is a new sophisticated optimization approach for energy conversion processes.

## 2.2 State of the art of exergy analysis in the building sector

In this chapter is described the state of the art of exergy analysis in the building sector and important specific projects within the EU (IEA-ECBCS 2000 - 2003, 2006 - 2010; Torio, Schmidt 2011).

For the first time, the program on Energy Conservation in Buildings and Community Systems (ECBCS) of the International Energy Agency (IEA) finances the project Annex 37: "Low exergy systems for cooling and heating of buildings", which seeks low exergy system solutions in buildings. The work was started in the beginning of 2000 and completed by the end of 2003 (IEA-ECBCS 2000 - 2003).

During an expert meeting in September 2003, the decision was made to form a network on the issues of new energy systems in buildings and to continue the work of the ECBCS Annex 37. This was the starting point for a proposal of the research project of Annex 49, called "Low Exergy Systems for High-Performance Building and Communities" (IEA-ECBCS 2006 - 2010; Torio, Schmidt 2011).

The ECBCS Annex 49 was a three-year international research project. The project began in November 2006 and ran until November 2009. The main objective of this project was to develop concepts



for reducing exergy demand in the built environment, thus reducing the CO<sub>2</sub>-emissions of the building stock and supporting structures for setting up sustainable and secure energy structures for this sector.

Specific objectives of the project were:

- To use exergy analysis to develop tools, guidelines, recommendations, best-practice examples and background material for designers and decision makers in the fields of building, energy production and politics;
- To promote possible energy/exergy/cost-efficient measures for retrofit and new buildings, such as dwellings and commercial/public buildings;
- To promote exergy-related performance analysis of buildings, viewed from a community level.

The work within Annex 49 is based on an integral approach which includes not only the analysis and optimization of the exergy demand in heating and cooling systems, but also all other processes where energy/exergy is used within the building stock. In order to achieve this, the project worked with the underlying exergy analysis methodologies. The work items aimed at the development, assessment and analysis methodologies, and the development of a tool for the design and performance analysis of the regarded systems (IEA-ECBCS 2006 - 2010).

With this basis, the work on exergy efficient community supply systems focused on the development of exergy distribution, generation and storage system concepts, and served as a framework providing a collection of case studies. For the course of the project, both the generation and supply of and the use of energy/exergy were important issues. As a result, the development of exergy efficient building technology depends on the reduction of exergy demand for heating, cooling and ventilation of buildings. Knowledge transfer and dissemination activities of the project are focused on the collection and spreading of information on ongoing and finished work (IEA-ECBCS 2006 - 2010).

The report at the end of the Annex 49 project is addressed to building planners, architects and decision makers and tries to bring them closer to the exergy concept by giving an overview of the main features and benefits from this analysis. The technical details behind the exergy concept are explained in a simplified and applied manner, focusing on the outcomes of exergy analysis and its importance for building systems design. In addition, the main features of several building and community case studies highlight the importance and main benefits of this analysis approach.

In this way the thermodynamic theory is however neglected and a lack of knowledge is left because the addressed actors of building planners and architects get no guideline how to carry out an exergy analysis of a concrete building system.

### **Reference state**

For the calculation of exergy, the environmental state of reference plays a substantial role in general and especially of chemically reacting systems. Therefore a few papers examine the necessary conditions imposed on any definition of reference states by thermodynamic theory, and stresses the requirement of the reference system (Baehr, Schmidt 1963; Ahrendts 1974, 1980; Szargut et al. 1988), (Bisio, Rubatto 2000; Rosen, Dincer 2004).

To include the chemical contribution in a consistent way, Ahrendts proposes an equilibrium system formed by the atmosphere, the oceans, and a layer of the solid crust of the earth to define a reference state (Ahrendts 1980). The calculations included 17 chemical elements and 692 chemical compounds.

Accordingly, when the state of the system is significantly different from that of the chosen equilibrium system, exergy flows are not very sensitive to the definition of the reference environment. This is the case, for instance, in the energy and exergy analysis of power plants. In turn, when the properties of the system are close to those of the reference environment, results from exergy analysis undergo strong variations depending on the definition of the reference environment chosen. This is the case of exergy analysis of space heating and cooling in buildings.

For these processes Szargut recommends that when a merely physical conversion process is studied involving no chemical reactions, an individual reference level can be assumed for each constituent involved in the process. For example, if a cyclic closed process like the HVAC facilities involving humid air is being analyzed, it is sufficient to determine separately the reference level for water and for dry air, because the composition of dry air remains constant (Szargut et al. 1988).

The PhD thesis of Sakulpipatsin evaluated the influence of including the air humidity in the definition of both the building system and its reference environment on the exergy flows through the building envelope (Sakulpipatsin 2008). Two different climatic conditions were investigated: Bangkok (Thailand) as hot and humid climate and De Bilt (Netherlands) as cold and dry climate. In both cases regarding dynamic variations in the indoor and outdoor air humidity leads to the most accurate estimation of the exergy flows. In turn, neglecting ambient air humidity (i.e. regarded as zero or equal to indoor air humidity), leads to under estimations in the exergy flows arising differences of up to 86% in the total annual exergy flows for the hot and humid climate and around 3% in the cold dry climatic conditions.

In hot and humid climatic conditions buildings are usually equipped with cooling systems managing the temperature and indoor air humidity to be within comfort levels. Therefore, indoor and outdoor air humidity might differ significantly. In this case, it is of great importance to include the humidity in the definition of the system and its environment. In turn, in cold drier climates where the differences between indoor and outdoor air humidity is significantly lower, humidity can be obviated from the definition of both the system and its environment without significant losses in the accuracy of the exergy flows.

A critical view on the most recent studies on exergy analysis of renewable energy-based air conditioning systems is carried out in a recently published paper by Torio et al (Torio et al. 2009). Special attention is dedicated to the reference state, the steady state or dynamic approach and the performance indicators. The aim is to highlight specificities of the exergy approach applied to both air conditioning systems and renewable sources.

The results from exergy analyses of air conditioning systems have shown to be more sensitive to the reference environment than for other energy conversion systems, especially when and where the indoor conditions are near to the reference states. Nevertheless, no general agreement on the proper choice of the reference state has been found in the reviewed literature. Most of the analyzed papers perform exergy analysis as a steady-state approach. Moreover, some of them assume default values for the reference temperature, others adopt a local design value, still others assume local values representative of the period covered by the analysis. It has been found that a careful choice of the properties defining the reference environment under steady state analysis would lead to small differences in the results compared with dynamic approach, avoiding thus the necessity to face time consuming analyses.

However, it is not known which statistical parameters (e.g. mean, mode, median, etc.) describing the properties of the reference would lead to the best agreement with dynamic analysis over the same

period of time. Regarding the humidity content of the reference state, it is found that most papers disregard the chemical exergy of the outdoor air. This assumption may lead to relevant inaccuracies in warm and humid climates. In those studies where chemical exergy of the air is taken into account (e.g. studies on evaporative cooling processes), two opposite approaches have been highlighted: assuming a reference humidity ratio equal to the actual outdoor humidity value or equal to saturated air.

### 2.2.1 Application of exergy analysis in the building sector

The presented equations for an exergy analysis of an energy conversion process in chapter 2.1 can be also applied in the building sector, especially the equations (2-1)–(2-3). Furthermore, the specific additional equations of an exergy analysis for the building sector are listed. The physical exergy of a mass flow  $j$  is calculated as follows:

$$\dot{e}_{ph,j} = (h - h_0) - T_0(s - s_0). \quad \text{eq. (2-29)}$$

For the mass flow of an ideal gas the physical exergy calculation is described in equation (2-30):

$$\dot{e}_{ph,ideal\_gas} = c_p(T - T_0) - T_0 \left( c_p \ln \frac{T}{T_0} - R \ln \frac{p}{p_0} \right) \quad \text{eq. (2-30)}$$

Accordingly, when the state of the system is significantly different from that of the chosen dead-state, exergy flows are not very sensitive to the definition of the reference environment. This is the case, for instance, in the energy and exergy analysis of power plants. In turn, when the properties of the system are close to those of the reference environment, results from exergy analysis undergo strong variations depending on the definition of the reference environment chosen. This is the case of exergy analysis of space heating and cooling in buildings.

Subsequently, for this application some authors propose a reference environment defined as the variable outdoor environment surrounding the building (Torio et al. 2009; Alpuche et al. 2005; Chow et al. 2009; Angelotti, Caputo 2007).

This definition of the reference environment requires the use of dynamic energy and exergy analysis, therefore representing a more detailed and complex analysis than just steady-state assessment.

### 2.2.2 Tools for exergy analysis of buildings

During the Annex 49 project different tools for calculations of the exergy are developed which are published in (IEA-ECBCS 2009). In the following a short description of the tools are carried out.

#### Pre-design Tool for Excel

The excel-based pre-design tool aims at increasing the understanding of the exergy flows within the built environment and at facilitating further improvements on the energy use in this sector. It is a simple and transparent tool for architects and construction engineers.

The requirements for the user are to define the building details (e.g. building envelope, air tightness, etc.). Energy calculations are based on the German energy saving Standard (EnEV-2006) and follow a steady-state approach (DIN V 18599).

Based on the energy flows obtained, and depending on the temperature levels chosen for the building systems, an estimation of the exergy flows is carried out on a steady-state basis.

### Cascadia tool for exergy analysis of community systems (IEA-ECBCS 2009)

The Cascadia tool is an Excel-based software tool. It represents the building model as a simple thermal load and emphasizes mainly the energy supply and its distribution network. The model of the neighborhood consists of a centralized energy plant supplying a district heating piping network. In the implemented district energy concept, a variety of energy supplies for different supply conditions is taken into account. On the other side the thermal loads include high rise apartment buildings, low-rise or detached residential homes and a retail sector comprising strip malls or single-storey retail buildings.

Individual buildings are connected to the district energy system in a parallel configuration with the supply and return lines although three categories of buildings (high rise, residential, and retail) are connected sequentially.

Depending on the capabilities of the supply technology the district energy supply temperature is selected. In the district energy loop, the supply temperature is considered to be 90°C and reduced to 54°C for the heat pump and solar panel options. The Cascadia tool implements five supply technologies within the model:

- a medium-efficiency gas fired boiler,
- a high-efficiency condensing gas fired boiler,
- a reciprocating gas fired engine based cogeneration system,
- an electrically driven ground source heat pump,
- a flat plate solar thermal collector.

The results of the analysis are presented in terms of the primary energy requirements, i.e. the fossil based energy required for the creation of all thermal and electrical needs of the system. Since the intent of the tool is to demonstrate the impact of both technology and reduced demand on fossil fuel consumption, information is provided on the following issues:

- Energy efficiency of the system – heating and electrical generation as the percentage of primary input energy: this illustrates the amount of energy usefully deployed as space heating or as available electricity.
- Exergy efficiency of the overall system – the total exergy consumed in the process of space heating and power generation as the percentage of the overall exergy available: this illustrates the exergy losses in the delivery system.

The results are pointed out graphically in terms of the exergy flow through the district heating network and the temperature level of each use within the supply structure.

The model can be used only to examine a few different energy supply technologies, urban formats and heating techniques. Additionally, the temperature level of the components is fixed.

### SEPE: Software for exergy performing evaluation of system components (IEA-ECBCS 2009)

SEPE is an Excel-based software tool developed by the Royal Institute of Technology in Stockholm that utilizes the iteration features of Excel to perform a steady state exergy evaluation and optimization of different cooling and heating systems.

By copy-and-paste, different existing components could be combined to create and simulate heating or cooling systems. Connecting different systems is easy as it is only necessary to couple the absolute temperature and pressure of each system to the following one. To perform loops, once the required components have been placed and connected in the excel sheet, the input variables (absolute temperature and pressure) are connected to the output variables of the loop. Once the iteration options of Excel have been enabled, the program automatically updates the values until convergence.

Basically, all systems share the same structure. Each model is divided into three areas: an input area on the right, an output area on the left and the central part. All the defining equations are included in this central area: they define the transfer function of the model, the relation between input and output signals, i.e. how the values are to be processed. The user is requested to insert sizing and characteristic parameters to define the model: for example, a heat exchanger is modeled by the type and the mass flow of the energy carriers in the first and the second loop (air or water), the exchange surface, and the type of heat exchanger (i.e. parallel or counter flow).

The calculation of the exergy flows is performed by evaluating inlet and outlet pressures and temperatures at the nodes, given the reference temperature: by this, specific thermal and pressure exergy are calculated in two different ways according to whether the medium is water or air. The computation of the exergy flows and exergy losses is then made possible by multiplying them by the mass flow passing through the system.

By this tool wide possibilities of analysis and optimization are made available, covering the whole chain from generation to room system, through primary and secondary loops heat exchange, distribution, and emission systems. But no guideline is given as to how add the technical data and environment reference to the tool.

### Design Performance Viewer (DPV)

In the paper (Schlüter, Thesseling 2009), a critical review of exergy analysis of heating and ventilation systems is given, and a prototypical tool for exergy-based performance evaluation of buildings is presented. All geometry data such as areas and volumes are automatically taken from the building model. For the energy and exergy calculations, nine additional parameters have to be added to the object properties of rooms, walls and windows. These parameters have to be added once at the beginning of the modeling process. During the design only the parameter values have to be adapted, all geometry data is updated automatically.

The input parameters for the energy and exergy calculations of the heating chain are automatically set by choosing the preferred heating chain components in the interface. These system specific parameters are directly embedded into the program code and not as variables in the building model. Through this the design process of a building is restricted and the advantages of exergy analysis to improve the design of components are not fully exploited.

The tool interface addresses the architect and building designer. The amount of necessary input parameters was kept as small as possible. Many parameters are directly read out of the building information model. The design performance tool contains the following five different tabstrips:

- Building Data
- Performance
- Systems
- En./Ex. Balance
- Data.

For the tabstrip “Systems” user input is required to describe the subsystems of the heating chain. The heating chain is divided into four processes: generation of heat, storage, distribution, and emission. The selections for generation of heat are labeled such as “boiler” or “radiator”. Additionally, the design temperatures of the heating system as well as outside and inside temperatures defining the environmental conditions can be altered. The resulting input parameters are automatically set according to the combination of subsystems as some parameters influence parameters of other subsystems.

The building data shows extraction from the geometry model and provides information such as opening surface ratio or orientation ratio of the windows. This information is graphically represented by a bar chart. The building data table also displays the calculated average U- and g-values of walls and windows.

The “Performance” tabstrip displays selected energy performance indices and visualizes the calculated results in a Kivi diagram. The values of the performance indices are plotted onto their individual axes. Connecting the nodes creates a distinct shape, the “building performance footprint”. Thereby, fast visual feedback for a quick interpretation of the results is obtained.

### 2.2.3 Interim findings

It is clear that all different applied reference states and methodologies have an influence on the results achieved and tend to complicate the possibility to compare them and to derive shared assessments on systems and components. More investigations are then necessary to further clarify the limits of the reference state approach and the benefits of dynamic calculations, as well as the more suitable choice of the reference environment (from a temperature and humidity point of view) in both cases.

The prototypical tool DPV allows balancing the effects of possible measures to increase overall building performance. The results from the calculations of the simplified energy model implemented in DPV were compared to the results of a commercial and certified software (Weka Architektur, <http://www.weka-enev.de>), which is used to verify the conforming of the EnEV regulation. The results show variations below 5%, proving the sufficiency for the proposed early stage performance assessment. In contrast to the software used for comparison, the performance analysis of a single building takes only a few seconds using the DPV. In addition to the calculation of total energy and exergy demands, the building designer can decide which optimization measure is most suitable for the concept and context of the building. Most importantly, striking a balance between form, materialization and technical systems is possible from the beginning. If, for example, the façade cannot be altered, a better heating system using a different energy source can be chosen. If, as another example, a slab heating is desired, a certain setup of the heating system is necessary: Due to the smaller heat exchange rate of the slab heating, low heat losses are required. These can be achieved by choosing good envelope insulation and/or a mechanical ventilation. Also, solar gains can be used to heat up the rooms. In order to increase solar gains, the opening surfaces should be increased and the g-values of the glass should be adapted.

## 2.3 Research working plan for an application of exergo-economic-environmental analysis

Based on the problem analysis in chapter 1 and the evaluation of stated hypothesis a working plan is deduced to apply the exergoenvironmental and exergoeconomic analysis for cost-effective and environmentally-friendly design and as a yardstick to the integral planning process. One goal is to find an answer under which conditions could exergy serve as a useful concept for the building sector. At this juncture the work packages tasks are defined.

- To illustrate the energy and exergy flows of heat transmission and ventilation, a simple model for a building envelope of a family house including a heating system as shown in fig. 1-3 is applied.
- For this simple model life cycle assessment and costing are carried out in order to prepare the exergoenvironmental and exergoeconomic analysis.
- Exergoenvironmental and exergoeconomic variables are calculated for every process component, based on the exergy, the environmental impact and cost rates and the specific environmental impact and costs of each exergy flow in the process. The aim is to identify the environmentally and cost relevant system components. From these components the ones with the highest improvement potential are selected, which is indicated by the relative difference of the specific environmental impacts and costs,. The exergoenvironmental and exergoeconomic factor reveals the main source of environmental impact associated with these components.

Graphical methods will be investigated as to their appropriateness supporting decision-making, e.g. striking a balance between high costs and high environmental impact of components.

- A dynamic method is carried out for exergy analysis of building envelope and building services to distinguish the heating from the non-heating period.
- The simple model will be extended to cover various alternative design choices, e.g. different HVAC components:
  - a) Heating installation and hot water supply, including their insulation characteristics
  - b) Air-conditioning installation, ventilation
  - c) Indoor climatic conditions, including the designed indoor climate
  - d) Position and orientation of buildings, including outdoor climate.

Necessary specifications of these building components will be developed in order to apply exergo-economic-environmental analysis.

- For the purpose of this calculation buildings should be adequately classified into categories such as
  - a) Single-family houses of different types
  - b) Apartment blocks
  - c) Offices
  - d) Education buildings
  - e) Hospitals
  - f) Hotels and restaurants
  - g) Sports facilities

- h) Wholesale and retail trade services buildings.
- Guidelines for architects
  - a) Catalogue of classified buildings and building components as best practice
  - b) Default exergoeconomic, exergoenvironmental and exergo-economic-environmental values of defined buildings and building components.



## 2.4 Energy performance assessment

This chapter contains the main premises, viewpoints, and objectives driving the **thermography part** of our research project. They are stated as **working hypotheses** (WH2-1,..., WH2-7). Some hypotheses and viewpoints are backed by references to the relevant literature while others need to be specified and refined in the course of developing the technical concepts in chapter 4 below. Several claims lead to research problems which will be proved or disproved empirically by project work to be carried out in the remaining period of time (2012-14). Our outline of discussion presents a synopsis of the entire thermography part. Section 2.1 covers decisions made in the design phase and their impact on energy performance, while section 2.2 focuses on the operational phase. Section 2.3 summarizes our software architecture for integrated design and assessment of energy performance.

### 2.4.1 Design Phase

The terms 'Design Phase', or 'Design Process', are used generically in the building sector to include the prior 'Basics Phase' mentioned in section 1.3, which sometimes also appears under the name of 'Feasibility Study'. The design work proper can be further divided into Conceptual Design (CD), Preliminary Design (PD), and Final Design (FD) (de Wilde 2004).

(WH2-1) The contribution by the building sector to energy efficiency (EE) is not only the result of designers picking energy-saving *components* from a catalogue and summing up independent scores. Advanced information technology is required to balance design decisions for optimum results, and to estimate, measure, monitor, and diagnose *system-level* energy efficiency throughout the building life cycle.

As usual, measuring denotes the short-term capturing of sensor data while monitoring deals with long-term (spatial and temporal) trend analysis. In other words, (WH2-1) states: the *actual* EE is not simply architectural design assisted by spreadsheet calculation and, of course, waiting for materials research to invent ever more energy-efficient components. To begin with, the EE of *components* is understood as their *contribution to overall efficiency*, each functioning as part of a building system. These contributions are not abstract and generic but context dependent and, therefore, *individual*. For instance, the performance of a façade or window is a function of its *location* in a building and the *stress* due to specific influences of the climate or weather, while the contribution of an air handling unit depends on its particular *purpose* and *function*, i.e. on how the building is operated.

As early as in the design phase, *decisions* made at component level are *interdependent* and often *conflicting*. A globally optimum combination of decisions, therefore, is difficult to achieve and certainly not by simple summations and multiplications of costs. Early architectural design choices have the greatest impact on the overall EE, curtailing the options available later<sup>5</sup> (Gratia, de Herde 2003).

In the operational phase, discrepancies may arise between design or engineering intent and details of the actual building construction (Peper et al. 2003), between statistical and actual occupancy schedules or specific modes of operation, and between a climate profile and prevailing weather conditions (Neumann, Jacob 2010; Maile et al. 2007). In the course of a long building life, the condi-

---

<sup>5</sup> For example, the rough shape of the building envelope and the roof, building orientation, composition of façade and glazing, room shapes and sizes, principal air flows and paths of daylight. These decisions are long-lasting, hardly change and, as they shape the building character and its visual appearance, are made by **architects** and, therefore, referred to as architectural design choices.

tion of the envelope degrades and diverges from specifications (Platzer 2006)<sup>6</sup>. Inadvertent fiddling with HVAC control settings as well as undetected failure of mechanical or control components jeopardize the persistence of energy saving measures or commissioning benefits achieved at one time (Cho 2002; Frank et al. 2007).

As mentioned in section 1.3, the *building stock* anyway will not benefit from future major design efforts but will still contribute much to the actual energy performance in the building sector.

At this point, the authors are unable to quantify how much the aforementioned problems contribute to energy inefficiency in the building sector today, or how much improvement could be achieved by better tool support. Therefore, some subjective judgment remains with (WH2-1).

(WH2-2) **Building performance simulation** and **energy simulation** (BPS/BES) programs are the ideal tools, in principle, for design and analysis, i.e. for assessing, optimizing, and diagnosing energy performance together with other functional performance goals, throughout the building life cycle, not only during the design and engineering phases.

Experience shows that BPS can indeed result in a significant reduction of the emission of greenhouse gases and give substantial improvements in comfort levels (Hensen et al. 2004). Features and trends of some major BES programs and simulation frameworks are summarized briefly in section 3.4.

From the dynamic systems or control theory viewpoint, a BES describes the flows of mass and energy in time and space by solving the transport equations numerically, on the basis of conservation laws. Its **state vector** holds the values of the energy and mass flow rates and of temperatures at discrete points in space, i.e. on surfaces (envelope or interior) as well as in enclosed air zones. The term **control input** or **load** subsumes all external influences constituting or altering the heat flux acting upon the building state variables, such as weather impact, user occupancy, user-commanded HVAC control or thermostat set points. Any **output** values of interest, including energy performance metrics or indices (Hitchcock R.J. 2002; Perez-Lombard et al. 2009), can be calculated from the state variables. Basically, input, state, and output data evolve as time series or trajectories, modeling transient behavior, while simplified models calculating steady-state values of energy demand are a special case.

Working hypothesis (WH2-2) tacitly assumes that any aspect contributing to energy efficiency or functional performance can be quantified, measured or calculated by suitable algorithms. Primary requirements as to energy performance in Germany and its calculation are determined by the Energy Conservation Act, EnEG; the Heating Costs Ordinance; and the Energy Conservation Ordinance, EnEV (EnEV 2009) (section 1.2.1). The latter specifies the maximum heating energy demand per gross storey area and year [kWh/(m<sup>2</sup>a)], but neither describes the demand side completely including cooling energy, hot water, ventilation, electricity, nor relates the energy input directly to the *benefit* or *purpose* of the building. We therefore draw on a refined notion of energy efficiency (EE) which means *delivered building function per unit of energy input* (figure 2-9).

**Building performance – a case for simulation:** The energy input [kWh] from various sources can be metered and also simulated if the actual heating and cooling loads and the efficiency of energy conversion equipment (HVAC) are known. The *building function* or *service* is not so easy to quantify. Ultimately, it reflects the degree of productivity and utility the building imparts to its *occupants* or *users*, and therefore should be integrated over the actual number of *occupant hours*, not multiplied

---

<sup>6</sup> Numerous less-known examples of degradation, e.g. heat-structure interactions, or UV fading of absorptive coatings, are mentioned in Platzer 2006, apart from obvious patterns of damage, e.g. reduced envelope airtightness, water leakage / moisture, or compaction of insulation material.

by the occupied / heated area. *Utility or quality of service* can be calculated as a weighted average of sub-criteria, i.e. basic requirements of providing a protected, secure, and healthy (e.g. mould-free) environment. The main criteria such as *thermal comfort*, *day-lighting comfort*, and *acoustic performance*, are functions of time dependent physical quantities. Thermal comfort is a function of *air temperature* and *radiant temperature*, *air humidity* and *air flow velocity*. Visual comfort depends on the *brightness*, absence of direct *glare* and, possibly, *spectral composition* of light. To derive normalized quality measures, correlations are sought between measurable physical quantities and abstract criteria of utility and comfort. Complex performance models of this kind need to be calibrated by performing physiological measurements of electrical skin resistance, and by statistical surveying, asking building occupants about their degree of dissatisfaction or discomfort (Predicted Percentage Dissatisfied (PPD) metric (Fanger 1982, c1970; Wagner et al. 2007; Wienold 2009)). In any case, complex criteria of building performance cannot be easily captured on the spot, neither by simple sensor measurement nor by questioning the tenants, but must be simulated, i.e. calculated from calibrated models. Furthermore, detailed performance measures are essential in the design phase because energy consumption is not *determined* by the climate imposing the heating and cooling load, but will *depend* on the occupants via the *thermal comfort* they will experience.

Actual *development* of performance measures to assess the quality of building service is essential for BPS/BES, but lies outside our scope of research. It is therefore accepted and assumed that any goal variable, in principle, can be calculated by state-of-the-art BPS. In fact, the conceivable and computable goal variables vastly exceed the quantities directly *measurable* in any existing building today or in the foreseeable future. Design alternatives, construction details, different HVAC control strategies or ways of retrofitting an existing building can be *compared* quickly and *objectively* under *identical conditions* by simulation, and their consequences can be assessed in what-if scenarios. Sensitivity analyses are performed to study the quantitative impact of particular design parameters on goal variables, and to identify the most influential ones. An integrated building design might provide the specification of sensor points and measurements to be conducted later, so as to match and compare with corresponding simulation performance variables.

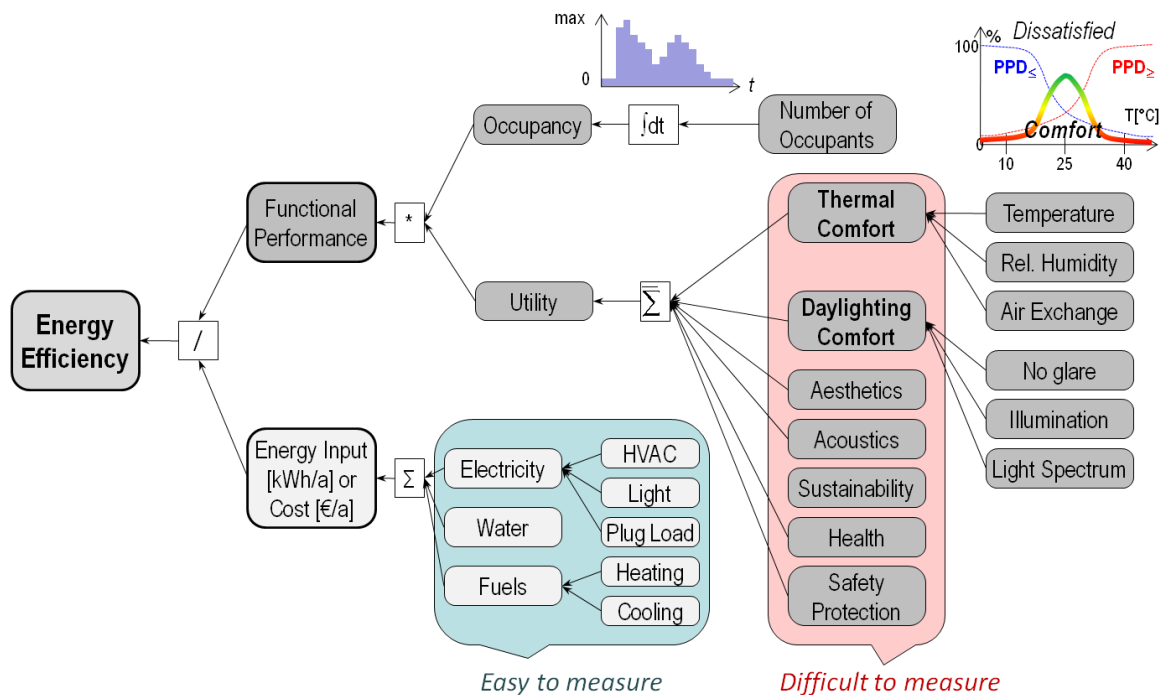


Figure 2-9: Example of a building performance measure

(WH2-2) treats a formal building design document and a simulation model as synonymous concepts, taking an idealized, rather 'purist' view: *Every architectural or civil engineering design can be simulated and, vice versa, any simulation model is just an executable building design with added measurements.*

Technically, the equivalence of a design document to an executable simulation model does not hold, as will be discussed under *data interoperability* issues. And from the viewpoint of business processes, there are barriers and discrepancies as to how architectural design proceeds today and how BES is actually applied, as explained in the following hypothesis (WH2-3).

(WH2-3) Energy simulation has a rather marginal impact on the actual performance of buildings in today's practice. BES is not heavily used for EE optimization and for decision-making in the design phase and even less so in the operational phases.

This statement is supported by extensive literature on building design, e.g. (Augenbroe 2002), (Ozel, Kohler 2004), (de Wilde 2004), (Gane, Haymaker 2008). For the planning phase, it follows basically from two observations. Firstly, decisions with the greatest impact on energy efficiency are made **early** in the design phase (Klinge 1994; Klinge, Lützkendorf 2007; GSA 2008). Referring to figure 1-1 in section 1.3, the energy concept should be optimized at an earlier stage than is the case now in order to avoid later and costly amendments that produce only marginal gains in energy performance. Secondly, the essential results that simulation tools provide rarely materialize until **late** design phases, and even then tool use does not strictly ensure energy optimization of the design, but compliance with certain minimum requirements (de Wilde 2004).

Better integration of building performance analysis into building design has been in the focus of major research projects, such as the *Design Analysis Interface* Initiative (DAI Augenbroe et al. 2003) or the *Building Energy Monitoring, Analyzing and Controlling* framework, BEMAC (O'Sullivan et al. 2004). De Wilde (de Wilde 2004) analyzes key research issues in his Ph.D. thesis such as how energy-saving building components are selected in current building projects, by whom, and in which phase. Which options are available, and what are the selection criteria? To what extent and what purposes are BES tools applied for in the selection process?

The focus was on public housing, i.e. large prestigious and energy-efficient office buildings of approximately 10.000 m<sup>2</sup> floor area. De Wilde (de Wilde 2004) divides the design process into a Feasibility Study (FS), Conceptual Design (CD), Preliminary Design (PD), Final Design (FD), and preparation of building specifications and construction drawings. Results of his case studies, interviews and surveys show that crucial choices are made in early phases (FS or CD) supported by little use of analysis tools; tools are applied mostly in later (PD or FD) phases. The motive in selecting components or making specific design choices is typically the designer's *personal experience* from earlier buildings or knowledge of reference projects; often, no alternatives are considered. Energy performance tools are used to *verify* that certain baseline requirements are met, not to *compare* options under multiple assessment criteria, and even less to optimize energy performance at a whole-building-level.

Several reasons may explain *why* BES programs have a limited impact on energy efficiency of buildings even in their design phase:

- *Traditional roles of stakeholders* in the design process: most decisions with a great impact on EE are made by *architects* who use BES infrequently for various reasons, such as alleged lack of economic incentives, lack of trust and confidence in the results, lack of time, or problems in preparing the necessary input data and interpreting the analysis results (de Wilde 2004). A collaborative approach of architects and design engineers or consultants, the latter being more inclined to continue using BES through the final design phases, may help lower these barriers (Hirsig 2010).

- Building energy simulation sometimes is considered an unimportant activity and a wasteful effort because it does not immediately benefit *building certification*, as mentioned in experience reports summarizing the Building EQ project (Neumann, Jacob 2008; Neumann, Jacob 2010).
- Due to the fragmented development of BPS tools and the rapid innovations in building and component technologies, state-of-the-art BPS tools are often not comprehensive enough to model and simulate the relevant physical phenomena and the controls of modern mechanical systems (Hensen et al. 2004). The designer options and needs for performance assessment when selecting energy-saving building components do not necessarily match the *option spaces* or *performance metrics* offered by the prevailing analysis tools. Development of new BES tools shows a continuous increase in capabilities and complexity which, however, adds to the *dependence on adequate modeling expertise*. In this way, new BES tools can increase the barriers to integrating simulation into the design process (de Wilde 2004).
- BES tools rarely adequately *map* the typical design tradeoffs and scenarios found *early* when information is necessarily *incomplete*. The simulation models lack flexibility in their *level of detail*, i.e. functional decomposition, resolution of the numerical solution in space and time (zoning or gridding, time steps). They may ask for specification details or input parameters that are simply not available yet. Most BES programs are geared towards accurate estimates of absolute performance figures rather than quick comparisons of different design variants (Hensen 2004; Attia 2011).
- *Data interoperability*, specifically data exchange among CAD tools for building design and simulation or analysis tools, is still limited. Data interoperability means that the same building information model (BIM) is shared by different applications, such as architectural CAD systems, facility management software, and thermal or acoustical analysis programs. Each agent extracts relevant information via suitable interfaces. This goal has been addressed by developing open standards, such as [IFC](#), [CityGML](#), or [gbXML](#); see section 3.3 (GSA 2008). Export filters are being developed for automatic geometry export from a BIM document to specific simulation programs. For example, export facilities have been implemented from IFC to the ETU Energy Advisor (Geiger et al. 2008) and to EnergyPlus (O’Sullivan et al. 2004; Maile et al. 2010b).

Nevertheless, *automatic* transformation between representations for different analysis purposes remains non-trivial. Geometry elements, such as free-standing walls or columns, are vital for shading analysis but are ignored in heat transfer analysis. On the other hand, a single spatial element such as a room enclosed by walls often corresponds to several distinct BES 'zones' and 'space boundaries', respectively (Maile et al. 2007; Maile et al. 2010b), and vice versa. Zones refer to spaces adopting a uniform temperature level and serviced by a single HVAC unit.

Furthermore, no BIM standard requires that actual instance documents exchanged be *complete* and *consistent* as to *simulation needs*; many attributes and features are optional. Missing ones must be detected and calculated<sup>7</sup> or surveyed manually from separate data sources, e.g. unknown thermo-physical coefficients or materials parameters. The authors are not aware of a truly general BES tool interpreting a neutral BIM *directly*, extracting or calculating *all* 3D geometry, material parameters,

---

<sup>7</sup> This holds even for the core part, the geometry specification. For instance, an IFC building model exchanged for illustration purposes possibly lacks an *explicit* and *contiguous* representation of the entire outer space boundary (*building envelope*) which is essential to most BES programs. This bounding surface must then be extracted automatically by analyzing the hierarchical structure of the building model (Geiger et al. 2008).

topological and functional information on the service systems (HVAC) from the document, and querying *only* weather and occupant data from the simulation operator<sup>8</sup>.

### 2.4.2 Operational Phase

As mentioned above, continuing assessment of a building by *simulation* under the uniform goal variables defined in the planning phase *could* give the operator an edge in diagnosis and verification, not obtainable by just *measuring* energy consumption (figure 2-10). The truth, however, is that once the real building exists, energy simulations probably are regarded even more as a waste of time, perhaps because the model is now separated from its target and no longer stands a chance of *becoming*, i.e. developing into, the actual construction. The closest possible approximation to a building existing and in use is a **validated simulation model** whose internal structure and parameters (thermal coefficients, in particular) are chosen to accurately reproduce any observable and relevant behavioral aspect of the real building.

(WH2-4) Keeping a sequence of behavioral images closely matching the real building over its life cycle, while greatly reducing the effort in modeling and validation required with current technology, is a key challenge to enhance the utility of BPS/BES and to maximize its impact on actual energy performance.

Even a validated model may furnish accurate performance predictions only within a narrow range of input conditions, e.g. weather patterns, close to the ones prevailing during the validation experiments. The parameter calibration process is tedious, requiring a high level of skill and knowledge both in simulation and in practical operation of a building. Although positive examples exist in the literature advocating the use of calibrated simulation models for commissioning (Claridge D.E. 2004; Visier J.C. 2005; Carling, Isakson 2004; Burhenne et al. 26/10/2010), this effort is rarely invested except for buildings in dedicated research or demonstration projects and for large public or commercial buildings (Reddy, Maor 2006; Torcellini et al. 2006). Monitoring the building performance over an extended period would require a corresponding history of models progressively refined, updated and validated as suggested by figure 2-10 (Fischer et al. 2006; Maile 2010; Maile et al. 2010a).

Indeed, there are strong links between the lifecycle of a real building and the versions a building simulation model undergoing transitions (figure 2-10):

- Certain events and processes in the building life entail changes or deviations in actual energy performance.
- These events and processes are mirrored by certain parameters (changes) in the simulation models; even structural modifications of the model may be needed to accommodate behavioral changes.
- Careful validation and recalibration of the model and its parameters to existing measurements reveals the true impact of life cycle events on energy performance, assuming that the model is run and compared under uniform performance criteria and load conditions.

---

<sup>8</sup> However, BIM-integrated design and performance analysis has been clearly addressed recently in the dissertation Schlüter 2010 presenting the Design Performance Viewer (DPV) for demand stage simulation.

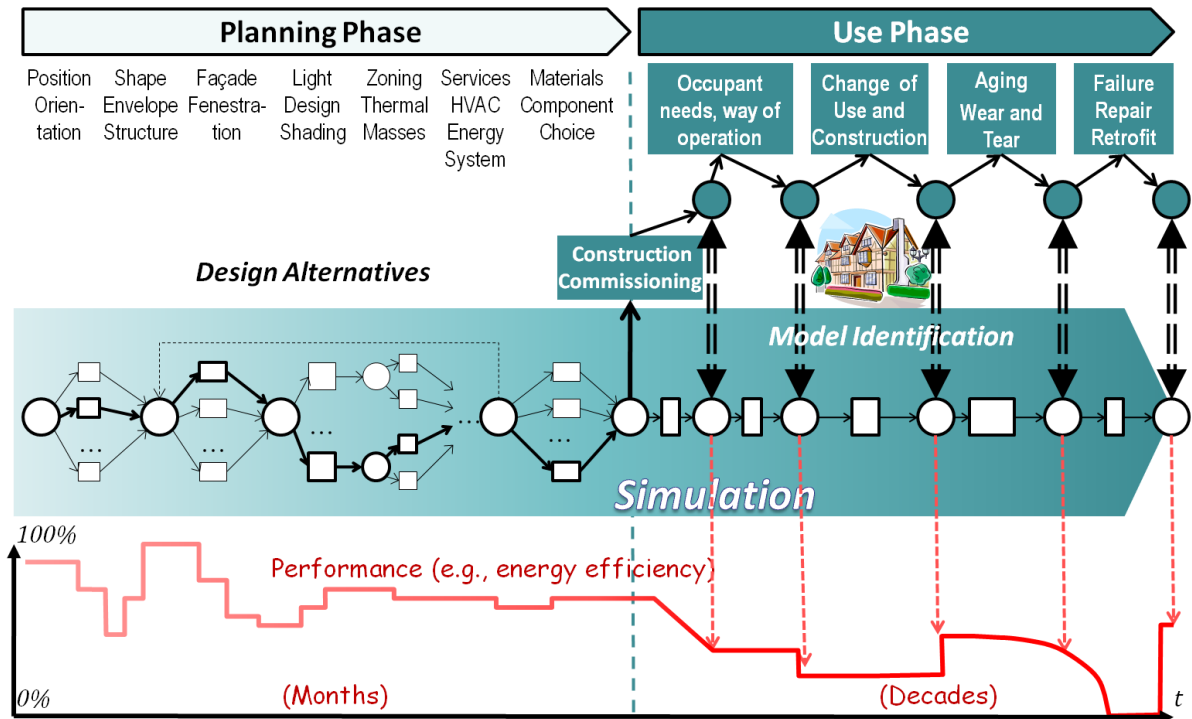


Figure 2-10: Towards lifelong performance simulation of buildings

Our focus will be on major processes and incidents in the building life cycle falling into three classes:

- i. The design materializes as built ( $\rightarrow$  initial commissioning). Performance promises by the simulation model are now examined and revised by assessing the actual building construction. This comparison initiates a process of mutual approximation: as construction of the building is tested against the design baseline implemented in the BPS, model realism is tested as well, and the model structure, behavior, and parameters are refined. Examples in construction include details of the building envelope such as glass curtain walls, vapor barriers, connections, junctions, and thermal bridges (Peper et al. 2003; Zalewski et al. 2010). On the model side, heat capacitance, thermal resistance, convective or radiative heat transfer coefficients describing a compound system or a single layer of material often deviate from their specifications, and their true values may be unknown (Heidt et al. 2003; Dong 2010).
- ii. Specific weather patterns, user habits or reactions of occupants to the building behavior experienced often compromise the HVAC control strategies intended for standard schedules and loads ( $\rightarrow$  ongoing commissioning). The induced workload passes through the thermal building mass and affects both energy usage and comfort. Sensible parameters include building time constants, air exchange rates due to infiltration, equipment gains, and load-dependent performance parameters of HVAC equipment. Parameter values proper may not even change, but modeling their uncertainty becomes more important when, e.g. set temperatures differ among building zones or when transient phenomena become dominant (Peper et al. 2003). The sensitivity of the output values to parameter uncertainty and, therefore, the accuracy requirements increase when operating conditions change, e.g. due to climate change (de Wilde, Tian 2009).
- iii. Building components age or suffer damage, and their properties change compared to those of new ones. Examples include moisture damage, weathering of façades, reflective proper-

ties of glazing or coating under sunlight, joints with reduced airtightness, poorly serviced boilers, changed operating points of HVAC controls, unnoticed drifting or faults of sensors (Cho 2002; Platzer 2006). The parameters affected are similar to those mentioned above under (i). Of course, repair, refurbishment, or retrofitting are complementary events in the lifecycle to be modeled as well. Changes in building structure with impacts on energy performance or thermal comfort are important as well, such as dividing large rooms into smaller ones or, vice versa, removing partition walls, or fitting suspended ceilings which change storey height and convective airflow.

We emphasize the *diagnostic* value obtainable only by calibrated simulation models. High energy consumption levels or poor thermal comfort may be obvious while the *reasons* (faults) are not. Conversely, specialized sensors detect many kinds of local problems, e.g. spots of air infiltration or humidity or thermal bridges, the potential impact of which on system performance is unknown. A BES model with thermophysical parameters recalibrated from sensor measurements, especially thermal images, could predict and quantify that impact and, for instance, trade off the cost of retrofitting against the gain in energy performance. This is the decisive advantage of simulation over purely measurement-based monitoring.

In this research, **quantitative georeferenced thermography** (QGT) is proposed as a new mobile sensor technology for calibrating building models. An infrared (IR) camera surveys a building so as to always *know* its *view pose* with respect to the coordinate frame of the building (it is *georeferenced*). The view pose provides an entry into a dynamic *building model* whose initial state values and *load trajectories* are set to mimic conditions prevailing during the survey. Identification or calibration of the model parameters requires a *radiometric camera model* predicting camera images for the given view pose, i.e. for any arbitrary measurement geometry. This camera model accompanies and extends the proper building model.

As a main research goal, the following claim remains to be proved or disproved empirically:

(WH2-5) Quantitative georeferenced thermography (QGT) can improve validation and parameter calibration of thermal building models, thus supporting better integration of BES into the building life cycle, and provide the quantitative interpretation of building thermography often missing today.

The underlying assumptions and technical developments to implement QGT will be explained in chapter 4. QGT draws on techniques and experience known from *active thermography* (AT) in non-destructive testing of materials, including the building sector<sup>9</sup>. For active thermography, the interested reader is referred to the QIRT conference proceedings (**Quantitative InfraRed Thermography**). AT characterizes materials properties, especially defects, by estimating quantitatively the changes induced in their thermophysical parameters. For this purpose, a test specimen is exposed to an artificial heating pattern and observed by an IR camera in a fixed setup with a known viewing geometry, e.g. a thermal test chamber or test cell.

QGT applies quantitative thermography not to parts controlled in dedicated test cells but to entire occupied buildings surveyed from arbitrary view points and under natural, solar or HVAC-induced heating patterns. We attempt to offset the loss of control due to the casual surveying by providing more advanced functions: the ability to localize the camera in 3D and to couple a mobile measurement model to a detailed building model. It remains to be seen whether parameter identification still works accurately and reliably enough to be useful under relaxed assumptions.

---

<sup>9</sup> For example, Grinzato et al. 1998; Wu, Busse 1998; Meola, Carlomagno 2004; Chiang et al. 2006; Bison et al. 2007; Sham 2008; Saboktakin et al. 2010.



Generally, different sensor measurements and corresponding model predictions can be employed for parameter estimation and identification of BES models (figure 2-11). Comparing a few methods will help to illustrate the situation envisaged in (WH2-5):

1. **Energy consumption** data and utility bills broken down into the main energy carriers (gas, district heat, and electricity) are always available and mostly electronically readable<sup>10</sup>, often on an hourly basis. This is why they are used most widely in model validation / calibration studies, e.g. (Reddy, Maor 2006; Torcellini et al. 2006). The corresponding predictions of energy consumption can be derived from the state variables of a BES model (Westphal, Lamberts 2005; Wang, Xu 2006). Since energy performance is calculated from energy input, model parameters should be calibrated to enable accurate prediction of the latter, which requires months of record data covering several different weather conditions. Simple building models (so called 2R2C or 3R2C<sup>11</sup>) with a few parameters only have been identified from energy consumption alone. Many different parameters *distributed spatially* across a complex building envelope can hardly be estimated *independently* from a *single time series* of energy consumption; the estimation problem is strongly underdetermined, and there is danger of compensation errors (Reddy, Maor 2006). Only parameters describing the HVAC components proper are readily accessible in this way. Energy consumption providing no added diagnostic value and a low degree of sensitivity to the parameters are further drawbacks: the building load, i.e. weather profiles and occupancy schedules are the factors influencing energy consumption most, far more so than any internal parameter such as the actual return temperature of a heating loop or the efficiency factor of a heat exchanger.
2. Sensors built into the HVAC plant providing short-term measurements of supply and return temperatures, air flow or water flow or pressure, play a similar role and have similar advantages and drawbacks. They are mostly installed and measurements from these sensors are often available, servicing e.g. a building automation system (BAS).
3. **Temperature spot measurements** corresponding directly to components of the model state vector (**zone air** or **surface** temperatures) require no measurement model proper for prediction, which is a big advantage. Their values can be determined by attaching a sensor to each part with internal parameters to identify (Heidt et al. 2003), (Lundin et al. 2004). Thermal properties are closely related to the goal variables (thermal comfort) and should therefore be measured and also predicted accurately, i.e. be part of calibration. Temperature spot measurements have been employed more often to *verify* simulation software packages in general than to validate individual building models against a real building. Thermocouples and (contact) thermometers are fairly slow and invasive in installation and data capturing, which is not a problem in demonstration buildings. They provide little data redundancy in estimating materials parameters with high certainty. Local faults or anomalies are hard to detect unless their position is already known.
4. **Mobile infrared cameras capturing images** (temperature fields) from a distance have a number of potential **advantages**:
  - Measurement is fast, contactless, and non-intrusive.
  - Camera images provide a comparatively high spatial resolution (typically 320x240-images) which means redundant data available to estimate the parameter values, achieving high certainty and low covariance.

---

<sup>10</sup> On-line measurements are available on the energy provider's side but not always on the consumer side for each heating or cooling loop.

<sup>11</sup> Notations Wang, Xu 2006 borrowed from the electrical circuit analogy: 'R' symbolizes thermal resistance, 'C' heat capacitance.

- Temperature fields permit localizing spatial variations and thereby assessing structural model uncertainties, i.e. they not only help to estimate parameters under the assumption of thermally homogeneous zones but allow their validity as such to be examined.
- Thermography is a proven qualitative method in building diagnostics used to detect and localize many kinds of anomalies and degradations of building materials with impact on thermal energy flow. Examples are discussed in section 3.2. When, in addition, a whole-building simulation model describes the thermal process observed, the impact of visible symptoms and features on goal variables can be quantified and, in that sense, a quantitative interpretation of infrared images can be obtained.
- Thermography is able to support a spatially focused, incremental way of estimating and calibrating large parameter sets in building models and, generally, in distributed-parameter systems, which constitutes a high-dimensional and highly non-linear optimization problem.
- Mobile cameras can be placed optimally in space and in time to observe transient heat transfer processes in order to capture the 'best' information. A case where spatial and directional dependency comes into play is recording the reflectance properties of glazing systems or coatings with anisotropic reflectance distribution.

On the other hand, IR cameras are still expensive items. For parameter estimation, mobile infrared cameras also have a severe drawback or, stated positively, their integration poses a major challenge to signal processing algorithms:

- Infrared cameras **do not sense temperatures directly** but thermal radiation intensity which is affected by disturbing background radiation from many different objects in the scene, including sky radiation. Nuisance parameters of emissivity, reflectivity, and transmissivity need to be identified *together* with the goal parameters proper. Modeling the infrared camera function faithfully, including the spectral response of the IR detector, is non-trivial, but essential (Allinson 2007).

Numerous IR camera applications are found in the literature for parameter identification and defect characterization in the building domain<sup>12</sup>. Analytical studies have been conducted mostly in test chambers and rely on known and fixed measurement geometry; in this case, no algorithm for localizing the camera pose is needed. IR cameras are rarely coupled with whole-building simulations, and detailed camera models are rare except for aerial surveys (Snyder 2004; Allinson 2007).

In fact, different sensors and measurements of types 1 to 3 may be combined for parameter estimation. Energy consumption, for instance, has been supplemented by spot temperature measurements in several studies (Heidt et al. 2003; Chantrasrisalai et al. 2003).

Finally, we briefly examine the relationship between identification and *development* of building simulation models. Our desire is to keep these aspects as orthogonal and independent as possible:

(WH2-6) This research project is not geared to a specific language, package, or platform available for developing building simulation models, nor does it attempt to advance the state of BPS modeling as such. Its purpose is to provide new and generic measurement interfaces for improved model validation and calibration, advancing in a direction orthogonal to the modeling and simulation features.

---

<sup>12</sup> For example, Grinzato et al. 1998; Griffith, Arasteh 1999; Cehlin et al. 2002; Wawrzynek, Bartoszek 2002; Datcu et al. 2005; Chiang et al. 2006; Krenzing, de Andrade 2007; Zalewski et al. 2010.

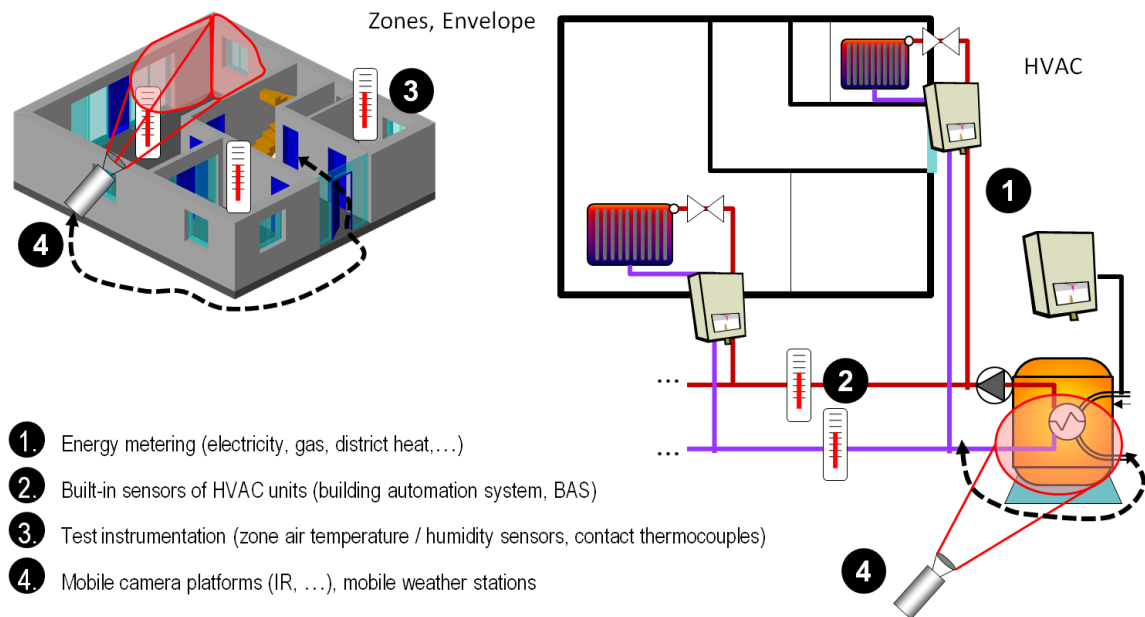


**Figure 2-11:** Sensors and measurements applicable for the identification of building simulation models

A vast body of knowledge in computational building physics has been accumulated in the past thirty years and is embodied in numerous specialized component libraries, e.g. for innovative HVAC systems or façades. Our small project budget does not allow us to make development efforts of our own in the BPS/BES field. Limiting our efforts to one particular simulator software could diminish its potential impact and, for testing purposes, would require implementing data conversion from a 'neutral' BIM into the BPS native input file format. The camera localization and camera modeling parts of our work will be largely *independent* of any specific BPS, anyway. Parameter identification as the technical core will benefit more from a (nonlinear, discrete-time) *dynamic system framework* describing the model rather than from a particular modeling 'philosophy' or language or the features implemented in a specific building component library.

On the other hand, each BPS/BES package makes assumptions, approximations, and simplifications of its own (AAS Maile 2010) in representing buildings, which in part explain the differences between simulated and measured performance variables. A 'generic' parameter identification method ignorant of the simulator and its specific AAS therefore may fail in practice.

In any case, prototype implementation for a specific simulation package or language will need access to its internal parameters, state variables, and possibly even the simulation code. Novel simulator interfaces are needed to communicate information, such as the functional correlation between a parameter and an output value, executable at run-time. The detailed requirements of these interfaces depend on the particular form of the state and measurement equations materializing and on the requirements of the parameter estimation (regression) algorithms. To study and analyze demands on the simulation framework in depth seems to indicate that we should develop a small BPS kernel as proof of concept, although this is definitely not intended. The kernel could serve as a reference to which simulation packages on the market would be compared later. Interfacing efforts encountered eventually could lead to new insight into the design of future BPS data models and provide ideas as to how design interfaces to optimally support remote observation and model identification.

### 2.4.3 Systems architecture for performance assessment

Following our problem analysis, a block diagram is presented in figure 2-12, summarizing the software architecture envisaged and refining figure 1-4:

- The **building information model (BIM)** at the core provides a hierarchical part-structured geometry model associating functional, semantic, and material attributes with each component and at each layer. The decomposition of buildings into floors, spaces (rooms) and sub-components follows design criteria determined by architects and civil engineers.

In the future, the BIM should implement extensions to support ongoing monitoring during the life cycle which, as a rule, do not exist today. In particular, there should be interfaces to load, store, and query *histories of inspection events*. An event holds inspection results, such as parameter values after identification as well as the surveying conditions under which they were obtained. Similarly, *operational events* document the exchange or repair of parts and describe major changes or adjustments made in the building or its operation, such as changed HVAC control algorithms.

The BIM acts as the central data repository or data warehouse for building simulation and provides interfaces to extract all the geometry features as well as functional properties and attributes related to building physics. Those are required to populate the simulation model, to generate a complete input description for the simulator, and to perform experiments.

- The building energy **simulation software (BPS/BES)** defines different metrics of functional performance as goal variables, including energy performance, and provides algorithms to calculate them. It provides for a user interface to define, run, compare and analyze experimental scenarios in terms of their goal variables. A scenario denotes simply a path of design decisions taken, i.e. alternatives picked from an option space, for instance, different components or even different parameter values characterizing the same component at different phases in the life cycle.

The BPS uses (imports, possibly transforms) the geometric and semantic entities from the BIM, but its spatial decomposition into thermal zones follows HVAC engineering criteria and, in general, differs from the architectural (BIM) space hierarchy.

In the future, the BPS will provide interfaces to the genuinely new components, Exergy+ on the left and Thermography+ on the right-hand side in figure 2-12.

- **Exergy+**, or exergo-economic-environmental analysis and design, converts the *energy* flows underlying the energy simulation model (BPS) into *exergy* flows explaining the consumption of exergy, by relating the flow of energy to the working and ambient temperature levels at the system boundary, respectively, cf. equation 2-9. Exergy+ implements specialized functions for exergo-economic-environmental assessment and comparison and accesses the BIM as a repository of information about the building design and the different options of energy supply available at the building or the urban levels. One feature distinguishing it from building simulation is *life cycle assessment* of all building parts and materials, including fuels and other consumables. Their life cycle, including fabrication, recycling, and disposal, is independent of the building life as shown in figure 1-2 above. Therefore, Exergy+ needs interfaces to dedicated data bases for LC inventory and cost (figure 2-12 on the upper left), which are not yet provided by most BIM exchange standards or by BPS tools.
- **Thermography+**, or quantitative geo-referenced thermography (QGT), captures IR images from viewpoints of estimated position and orientation, queries the model component(s) in

the visual focus, and accesses their parameters by means of new BES/BPS interfaces. The BES and the camera model collaborate in predicting thermal radiation images, which are represented as executable functions of the parameters. Parameter values minimizing an error function of the predicted and the captured images are estimated by means of an inverse model. When prior values of the same parameter are known, the BPS program processes both versions under identical load conditions, and the resulting differences in the goal variables will indicate the impact of parameter changes on energy performance. In this sense, QGT furnishes a quantitative interpretation of the IR image. Details will follow in chapter 4.

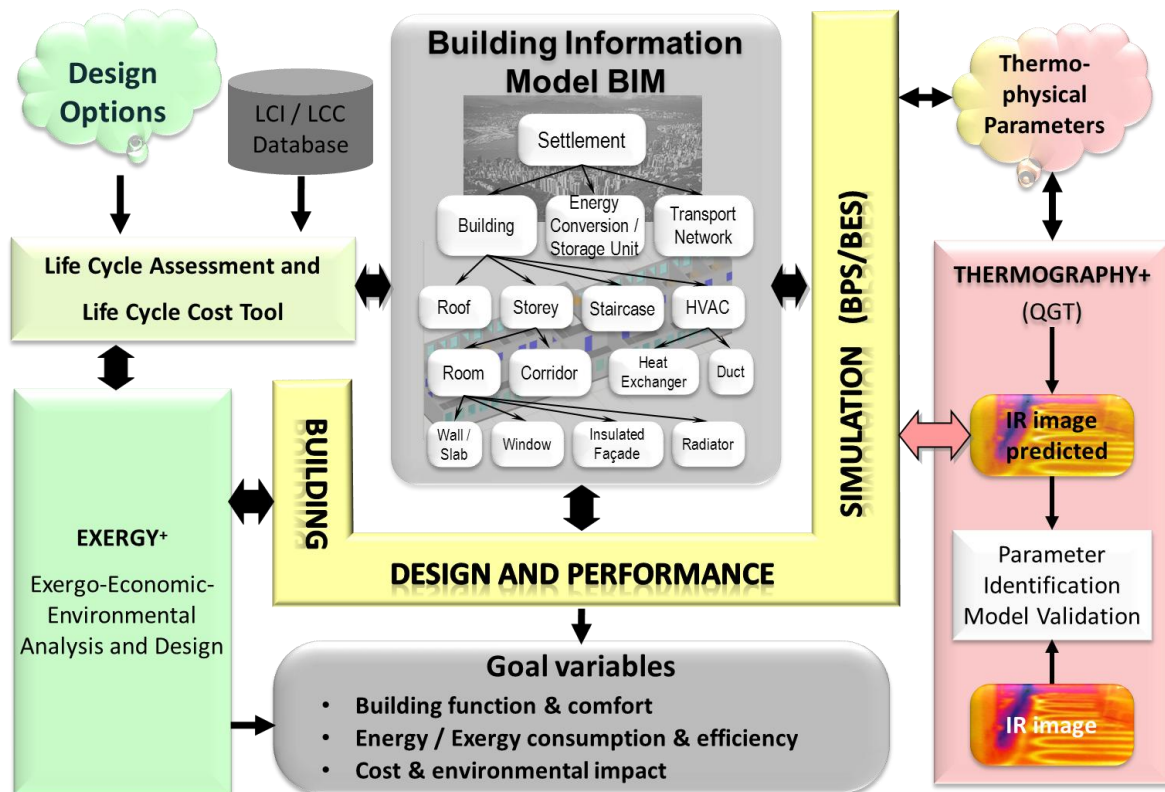


Figure 2-12: Proposed systems architecture (block diagram) of the Exergy+ and the Thermography+ (QGT) tools

From the Thermography+ point of view, Exergy+ is just another analysis tool calculating different *goal variables*, i.e. economic and ecological costs associated with exergy consumption. From the Exergy+ point of view, thermography could help in model validation by estimating *internal parameters* from remote thermal measurements, such as supply and return temperatures of the hot and the cold streams which affect the endogenous exergy destruction in a heat exchanger. This might be useful for transient Exergy+ analyses; however, the main focus lies on stationary analysis (e.g. according to DIN V 18599 DIN V 18599 or EN 13970 or DIN 4701-10) for early design comparisons.

We realize that our unified IT architecture in figure 2-12 presents an *idealized picture of reality* in the building sector. For residential homes, not even maintaining a life cycle BIM initially created from a 3D architectural CAD design is commonplace. Interoperability between building models and energy simulators remains difficult, mainly regarding compatibility and automatic transformation of data models. Existing tools for *exergy analysis* are not rooted in *energy simulators*, nor do they work by ‘transforming existing energy flows into exergy flows’; they are more like spreadsheet calculators

interfaced to LCI/LCC data bases and, optionally, directly to a BIM document (Schlüter, Thesseling 2009). Finally, today's building simulators have been designed to provide answers to building practitioners, not to provide interfaces to mobile cameras with variable measurement geometry (IR cameras) allowing them to query their internal variables, parameters, and functional equations. These limitations and constraints imposed by existing BIM and BPS tools, to be discussed in greater detail in chapter 3, will take effect as soon as new features are prototyped and tested within or on top of tools and frameworks *existing* on the market today. At that point, our uniform architecture will fall apart.

### 3 Fundamentals and related work

This chapter is about earlier research and relevant development and standardization efforts in several closely related areas. Section 3.1 briefly deals with *continuous commissioning* seeking to achieve lifelong energy efficient operation of buildings by monitoring. Thermography is one monitoring tool long applied in building diagnostics to detect various defects and types of degradation. Examples and the detection principle are illustrated in section 3.2. Quantitative geo-referenced thermography (QGT) should preserve this potential and extend it by quantitative assessment. Sections 3.3 – 3.6 are devoted to the information technology needed to support monitoring. Semantic building information models (BIM, 3.3) constitute the core and central repository in which energy simulators root. Languages and platforms for simulating building performance are discussed and compared in section 3.4. Model validation and parameter calibration are reviewed in sections 3.5 in general and in 3.6 for thermographic measurements. Measurement models, in particular infrared camera models ('IR simulators') are covered as well. Quantitative image analysis in the thermal spectrum by means of a thermodynamic model explaining the environment 'behind the image' is discussed in the building context. Section 3.7 concludes by reviewing Allinson's aerial thermographic survey from which much can be learned about the pitfalls of thermographic evaluation and the importance of accurate sensitivity and error analysis.

#### 3.1 Ongoing commissioning

Our main research goal is the development and analysis of new tools for monitoring the energy efficiency of buildings. These tools are based mainly on energy performance simulation the role of which will be strengthened and enhanced. Above all, they should assist the post-design and post-construction phases, help check whether EE targets are met once a building is operated, and track life cycle performance. Wherever their potential and contribution may lie, the new tools fall into the category known as **commissioning** (differentiated by attributes like *initial*, *continuous*, *ongoing* or *retro*) and therefore should fit into this framework. In this section the definition of commissioning is recalled and key goals, procedures and processes as well as research programs are summarized, emphasizing mainly conditions and regulations applying in Europe.

##### 3.1.1 Definition

*Continuous Commissioning* is a term invented by the Federal Energy Management Program (FEMP) of the U.S. Department of Energy. To quote the FEMP "Continuous Commissioning Guidebook" (Claridge D.E. 2002):

Continuous Commissioning (CC) is an ongoing process to resolve operating problems, improve comfort, optimize energy use and identify retrofits for existing commercial and institutional buildings and central plant facilities.

Accordingly, CC serves similar purposes in buildings as *Condition Based Maintenance* does for industrial plants. CC comprises two major phases, a *project development* phase followed by the *implementation and verification* phase (Claridge D.E. 2002; Schmidt et al. 2009). The CC project scope is clearly defined in the project development phase; this phase typically involves a CC audit followed by a proposal and a contract; it will not be discussed here any further. In the *implementation and verification* phase, six main steps are defined to implement the CC project:

1. Develop the CC plan and form the project team.
2. Develop performance baselines (document existing conditions).
3. Conduct system measurements and develop CC measures.
4. Implement CC measures.
5. Document comfort improvement and energy savings.
6. Keep commissioning continuous.

Initial commissioning of a building is covered in CC steps 1 and 2. Retro-commissioning is a CC process conducted in the building stock to make up for missing or incomplete initial commissioning.

CC focusing on energy performance of buildings has been a major research topic of the International Energy Agency (IEA ECBCS Annex 40 - Energy Conservation in Buildings and Community Systems Programme, Building Commissioning to Improve Energy Performance Visier J.C. 2005). The goals and measures of CC projects have been adjusted to the strategic goals of the European Union as stated in the European Energy Performance of Buildings Directive (EPBD), notably in two research programs and under the slightly modified title of Ongoing Commissioning (OC):

- **REEB** - European Roadmap for Energy-Efficient Buildings (Scherer et al. 2010).
- **Building EQ** - Intelligent Energy Europe Programme of the European Commission (Neumann, Jacob 2010).

Within the Building EQ program, CC/OC concepts have been developed, applied and tested in case studies covering public buildings in different climate zones, such as Finland, Sweden, Germany, and Italy. The program reported energy savings between 5% and up to 30% achieved or at least identified, payback times between 0.5 and 3 years (Neumann, Jacob 2010). OC applied to the test buildings showed certain measures mainly in the HVAC operation to improve energy performance. Roughly, these measures can be classified as follows:

- **HVAC Schedule:** Adapt *operating hours* of the main HVAC equipment precisely to the actual *demand profile* (day or night, weekday or weekend, heating or cooling period), and carry on with the ancillary equipment, especially air handling units (AHU) and ventilation.
- **HVAC Circuit control:** Adjust inlet water and supply air *temperatures*, modify set points and set-back points of heating and cooling circuits to optimize operating performance.
- Avoid inefficient *part load* operation of HVAC equipment (AHU).
- Install *heat recovery* in ventilation and AHU.
- Replace *oversized electrical equipment* (mainly pumps), or reduce power, speed, or temperature.

#### 3.1.2 CC/OC implementation in the Building EQ program

Building EQ developed a scheme of its own as to how to perform CC/OC projects, and proposed a four-step procedure plotted on a schematic flowchart. Each step was specified by the required and recorded input data, decisions, actions, and criteria to be met in order to proceed to the next step. Those steps were defined as follows.

- |              |   |
|--------------|---|
| BEQ Step 1 - | Benchmarking ( <b>Operational rating</b> ).   |
| BEQ Step 2 - | Certification ( <b>Asset rating</b> ).  |
| BEQ Step 3 - | Optimization (introduction of energy saving measures, fault detection and diagnosis, calculation, and documentation of energy savings). |
| BEQ Step 4 - | Regular Inspection (ongoing monitoring).  |



BEQ Steps 1 and 2 together define a performance baseline serving as a reference for subsequent improvements. The first of these, *operational rating*, provides a baseline of actual building performance called *benchmark*. The second, *asset rating*, supplies a theoretical target energy performance of a building. BEQ steps 1 and 2 roughly correspond to (part of) steps 3 and 2, respectively, in the FEMP definition above. The subsequent optimization BEQ step 3 refines the performance baseline and covers steps 4 and 5 in the FEMP framework. BEQ step 4 serves to maintain efficient operation, i.e. keep commissioning continuous (step 6 according to FEMP).

The definitions given below of **operational rating** and **asset rating**, and their principal differences, are crucial for understanding the scheme (ASHRAE 2009).

### **Operational Rating (OR)**

- Rates **building operation** by **measured** energy consumption per source of energy and per unit floor area; it requires a record of at least one year of operation.
- **Normalizes effects of the weather** by correction factors where the degree days of a *standard* year are divided by the *actual* degree days in the measurement period at the same location.
- Takes into account building occupancy and management, i.e. the **specific use pattern**.
- Provides a first classification and baseline for annual energy consumption, and is useful to energy managers and potential users of the building.

### **Asset Rating (AR)**

- Rates a **building** by **calculating**, i.e. predicting, its energy consumption per source of energy and unit floor area.
- Is based on **standard climate conditions** and **standard building use**.
- Uses detailed information about the building envelope and utility systems, including set points and hours of operation, and energy supply systems.
- Helps in comparing two buildings irrespective of their users, provides a baseline for building energy performance, and provides information about the main contributors to energy use and their major functional dependencies.

The difference between certification (asset rating) and operational rating is analogous to the car fuel consumption in a norm test compared to a real driver. Asset rating follows after operational rating in the Building EQ procedure which is the opposite of what we would expect from the energy simulation perspective exposed in chapter 2: AR corresponds to a detailed energy simulation model (BES) in the final design phase which comes before we can validate the BES by data from the first operating period, which would correlate with, or accompany, operational rating.

### **3.1.3 Linking CC/OC with monitoring data**

Optimization of the building operation with respect to energy performance requires *continuous monitoring*. To this end, the Building EQ program defined a *minimum dataset* which must be available, recorded and evaluated regularly. The definition of the minimum dataset is reproduced in table 3-1, comprising energy consumption data, weather conditions, indoor conditions, and system signals to be recorded hourly. The choice of data effectively supports fault detection, monitoring and optimization of the HVAC system as mentioned in section 3.1.1. A rationale for recording these data in particular is cost minimization by employing inexpensive sensors available in most buildings equipped with building automation systems (BAS). There is a substantial overlap with the monitoring

data recorded for QGT, mainly weather conditions. Other data, in particular 2D/3D *temperature fields* and estimated parameters, such as air infiltration rates, may not be essential for this kind of HVAC optimization, but are for monitoring the building envelope, for example.

The Building EQ project also is an attempt to reconcile and integrate the OC concept with the European Building Performance Directive (EPBD), at least to establish a strong link with the EPBD. This goal was achieved only in part. Some major conclusions and recommendations are summarized below from (Neumann, Jacob 2010) with some comments:

- Link between EPBD and CC: *While the EPBD sets requirements for the quality of the building envelope and the HVAC equipment, ongoing commissioning deals with their proper and efficient operation. EPBD can be a starting point but only if an asset rating is done in a comprehensive way, including existing buildings... The link is highly dependent on the national (EPBD) implementations in the different Member States. That is especially true of existing buildings which, in turn, represent the biggest savings potential... The diversity of different national implementations in the Member States complicates all attempts of a reasonable linkage. **Generally, the operating phase of a building has too little impact on the certification process to assure energy efficient operation of buildings certified.***
- Asset ratings: *These may be required for new buildings and major renovations, but the calculation methods are not really integrated into the normal planning process; their results cannot be directly used for the design calculations an engineer has to do anyway. Therefore, planners regard the certification as a burden, an extra effort.*

[Authors' note: we regard asset rating as a process closely related to 'building energy simulation'. This statement confirms what has been discussed under working hypothesis (WH2-2) in section 2.1].

- Energy calculation methods: *Should be able to deliver both a performance certificate (derived from standard boundary conditions) and the typical design values e.g. for heating and cooling power, or a study on indoor climate (derived from individual boundary conditions)...The Building EQ team therefore proposes to provide a common simulation kernel at a European level.*

[Authors' note: At the time of writing of this report it is not known whether such a European simulation kernel exists or has been decided upon already, or whether its development would start from scratch or use an existing framework. A European simulator kernel would be highly relevant as a potential development platform for quantitative thermography.]

- Monitoring requirements: *Ongoing monitoring based on hourly or sub-hourly measurements is crucial, but the results will be highly individual and not allow different buildings to be compared ... Measuring equipment is installed only if necessary for further analysis.*

[Authors' note: Mobile distance sensors like IR cameras or daylight cameras and even mobile weather stations could be deployed where needed and help capture the information relatively efficiently, routinely and non-intrusively, but are not suited to collect hourly readings permanently.]

- Data recording and data exchange: *Stringent systematization and standardization for the exchange of measured data is missing... Acquisition and exchange of the minimum dataset (measured data) was a significant hurdle... Generally, Building Automation Systems (BAS) are not designed for analyses of building performance and for recording and exchanging measured data in an efficient and standardized way...*

[Authors' note: As to data recording and exchange, having a well-documented event history is recognized as a core requirement. Both the temporal ordering (historical database) and the cause-and-effect relations between events should be captured. Events include energy-related measures or actions taken such as replacement or changed control settings, and milestones in monitoring and diag-

nosis, such as QGT surveys. For comparability and transferability of results it is vital that for each QGT event the input conditions are accurately documented, as will be outlined in section 4.5 below. Whether the information should reside inside the BIM (and possibly overload it) or in the building management / maintenance system (BMS) is an open question. In any case, the BIM as the central lifecycle document should provide a link to this information.]

- **Interoperability:** *Still a major hurdle in seamless exchanges of information and measured data ... BIM are available but seldom used...*

[Authors' note: Semantic rules seem to be missing to check whether a concrete BIM input document provides complete and consistent data to meet the needs of particular analysis software, be it energy analysis, daylight, or acoustic analysis.]

- **Fostering OC/CC:** *... More automation is needed in order to integrate ongoing monitoring in the daily routine of the operating staff, e.g. by providing rule-based analysis routines for fault detection and diagnosis. Moreover, all countries state that automation of the tools and thereby a reduction of labor cost connected to CC is crucial for wider application ... Cost-benefit of the application of CC-tools is still not documented satisfyingly.*

[Authors' note: For QGT, tool automation and cost-benefit analysis are assignments addressed under Research Agenda in section 4.6, but first the new concept must have demonstrated some degree of technical soundness and maturity.]

Item	Measured value	Unit	Min. time resolution	Remarks
<b>Consumption</b>				
	Total consumption of fuels	kWh	h	e.g. gas, oil, biomass
	Total consumption of district heat	kWh	h	
	Total consumption of district cold	kWh	h	
	Total consumption of electricity	kWh	h	
	Total consumption of water	m <sup>3</sup>	h	
<b>Weather</b>				
	Outdoor air temperature	°C	h	Private weather station or from weather data provider
	Outdoor relative humidity	%	h	See above
	Global insolation	W/m <sup>2</sup>	h	See above
<b>Indoor conditions</b>				
	Indoor temperature	°C	h	Choose one or more reference zones for measurement
	Indoor relative humidity	°C	h	See above
<b>System</b>				
	Flow / return temperatures of main water circuits	°C	h	Main heat/cold distribution in the <b>building</b> , not primary distribution, such as a district heating system.
	Supply and exhaust air temperature of main AHUs	°C	h	
	Supply and exhaust air relative humidity of main AHUs	%	h	
	Control signals of drives (pumps, fans)	0/1 or 0-100%		

**Table 3-1:** Minimum dataset for continuous commissioning from (Neumann, Jacob 2010)

## 3.2 Thermography for Building Diagnostics

This section discusses infrared thermography (IRT) applications to non-destructive testing (NDT) of building components and materials. Structural defects and types of degradation affecting energy efficiency can be detected from thermal symptoms. First, the basic principle behind NDT is illustrated following work of Wu and Busse (Wu, Busse 1998), Carino (Carino 1998) and others; for simplicity, only one space dimension is considered. Important application areas and examples of building thermography are discussed afterwards.

### 3.2.1 Non-destructive testing

Different building materials, even the same material under different ambient conditions, have different *heat transfer* properties expressed by *coefficients* such as thermal conductivity, heat capacity, radiometric emissivity, reflectivity, and transmittance. For example, conductivity determines the *rate* (speed) of heat flowing through a material in space and in time.

Figure 3-1 illustrates different samples of material heated from a temperature level  $T_0$  to  $T_1$  using the same heating power: for low heat capacity  $c$  and high thermal conductivity  $\kappa$  of material, respectively, the corresponding temperature function  $T(\kappa\rho^{-1}c^{-1}, t)$  rises steeply whereas, in the opposite case, it has a shallow slope. All samples start at temperatures  $T_0$  and eventually arrive at  $T_1$ ; at intermediate points,  $t_0$  and  $t_1$  in figure 3-1 (left), some samples are ahead while others lag behind and thus become *discernible*. Imagine a wall under uniform solar heating, the wall consisting of different materials arranged horizontally in the direction  $x$  and forming a longitudinal section, and let the thermal timelines or *heating profiles* at various points be stacked accordingly (figure 3-1 on the right).

With the temperature seen as a spatial distribution and a function of time  $T(x, y, z, t)$  (**thermal field**), the direction of the steepest rise or thermal gradient<sup>13</sup> is *normal* to a *homogeneous* wall (the normal direction  $z$  is not shown in fig. 3-1) but will deviate locally if the wall contains different materials. Spatial variations, including cracks, internal voids, and similar defects, can be observed by *infrared thermography* (IRT) simply because

- materials and material conditions often differ in their *heat coefficients*, causing different heating profiles or, in a snapshot, *spatially uneven thermal distributions*,
- a *spatial distribution* of temperature<sup>14</sup> can be captured and displayed instantaneously.

Local maxima or minima indicate the positions of material variations, and their amplitude  $\Delta T$  reveals something about the kind and extent of an irregularity. Even *sub-surface* defects leave an attenuated thermal fingerprint. One problem apparent from figure 3-1 is hitting the right moment,  $t_0$  or  $t_1$ , to observe a good thermal contrast,  $\Delta T(t)$ . To circumvent the decision, one may run the IR camera in the continuous (video) mode recording temperature profiles at frame rate and calculating *difference images* to approximate the temperature derivatives. Notwithstanding the noise amplification incurred by the difference operator, the material variations will be indicated by maxima in the derivative image, as has been shown in applications to historical buildings (Sham 2008).

<sup>13</sup>  $\nabla T := (\partial T/\partial x, \partial T/\partial y, \partial T/\partial z)^T = (0, 0, a)^T, a > 0$ .

<sup>14</sup> Distribution in one or two space dimensions  $T(x)$  or  $T(x, y)$ , such as the temperature of the wall surface. An IRT detector actually senses the radiative power  $L$  within a spectral band which is converted to temperature.

Figure 3-1 illustrates the detection principle but not the methods actually used for detection and quantification of material defects. In *active thermography* and *lock-in thermography* (Wu, Busse 1998), a *sinusoidal* heating pattern or thermal wave is imposed on a test specimen and its spatial and temporal response is observed by an infrared camera. The *amplitude* and the *phase shift* of the sinusoidal thermal response reveal quantitative properties such as the size or depth of a defect (Almond, Patel 1996, fig. 2.3), but depend as well on the excitation frequency in relation to the speed of heat propagation. The right choice of frequency greatly influences the quality of results.

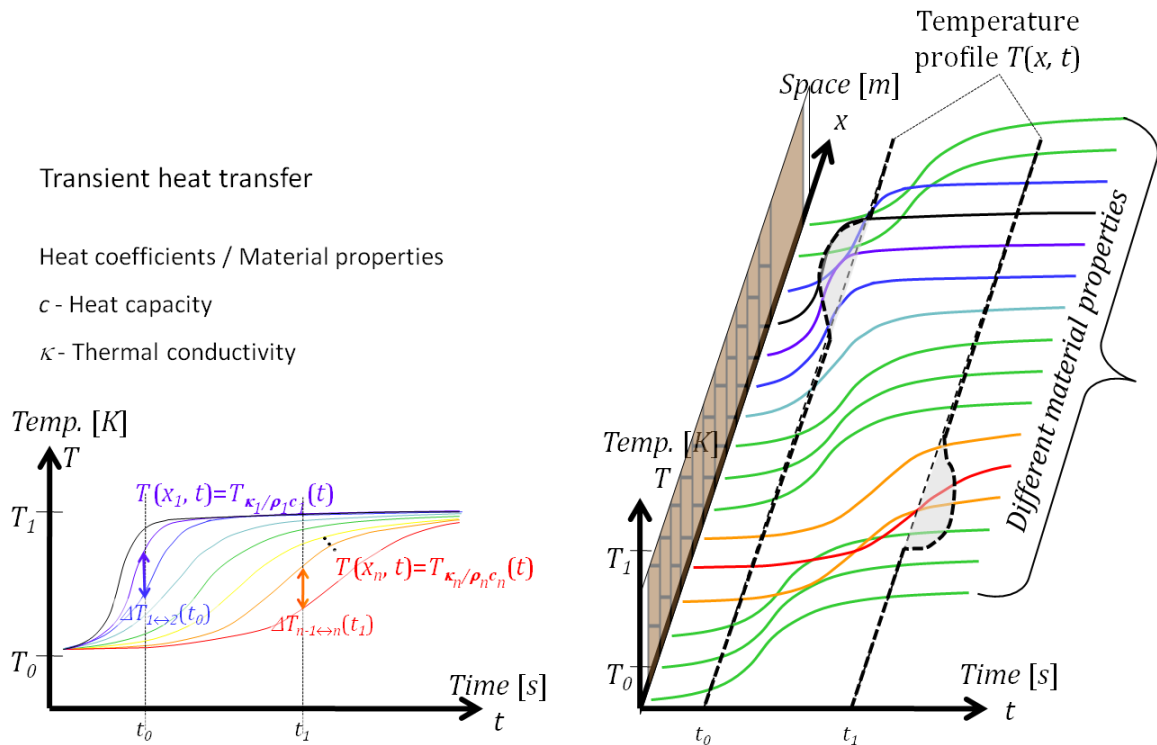


**Figure 3-1:** Principle of IRT detecting material properties by observing *transient* heat transfer. Spatially varying thermal coefficients produce a thermal contrast at each instant; the time of maximum thermal contrast  $\Delta T$  depends on the material as well. Heating may be imposed artificially (active thermography) or induced 'naturally', like solar or HVAC-controlled heating. (Qualitative sketch showing no true solutions of the heat diffusion equation, see e.g. Çengel 2003).

Lock-in thermography has been applied to diagnose voids or detachment in layered building structures (Grinzato et al. 1998). Another widespread technique is *pulsed or flash thermography* where a single and rather short but powerful energy pulse of visible light is applied. *Ultrasonic thermography* or *vibrothermography* is an NDT method which makes cracks in an object visible through *frictional* heating caused by high frequency ultrasounds. In this technique, the heat is generated through the dissipation of mechanical energy at the crack surfaces by ultrasonic waves (Saboktakin et al. 2010).

This discussion raises the following questions and problems:

1. **'Active' or 'passive'?** Detecting irregularities in material properties so far seems to rely on *transient* thermal phenomena, i.e. temperatures changing *in time* due to *artificial heating*. 'Natural' solar heating or HVAC heating can be exploited, too, and the response can be observed. However, under *steady-state* conditions, no changes over time are observable though a *spatial* temperature gradient may persist. Building thermography in a steady state, also called *passive* IRT, has been shown capable of detecting, for example, spots of moisture on a wall as long as there is a *permanent heat flow*. Figure 3-2 illustrates in principle why this

suffices. An open question still remains as to precisely which phenomena demand the use of *active* thermography.

2. **Diagnosis:** Infrared thermography alone is *not distinctive* enough to pinpoint the cause of a defect because different causes often produce the same symptoms. In the example in figure 3-1, *decreasing* the heat *capacity* would produce a similar effect as *increasing* the thermal *conductivity*, or reducing the material thickness. Imprecise knowledge or lacking awareness of ambient conditions quickly lead to rash conclusions. Coming up with a correct diagnosis requires human expertise in how an inspected piece of equipment works and why it appears warm or cool. This expertise should be supplemented and assisted by formalized *contextual knowledge* (in the BIM) and by making available an *anamnesis* of the *same* part under well-documented conditions.

IRT is potentially useful in characterizing any change in a component's life cycle that affects its thermal parameters. This could be a discrepancy between 'as-designed' and 'as-built', not necessarily a degradation or defect of a part already used. Comparing a real part to a design requires a new feature: *thermography simulation* and estimates of parameter *values* from images.

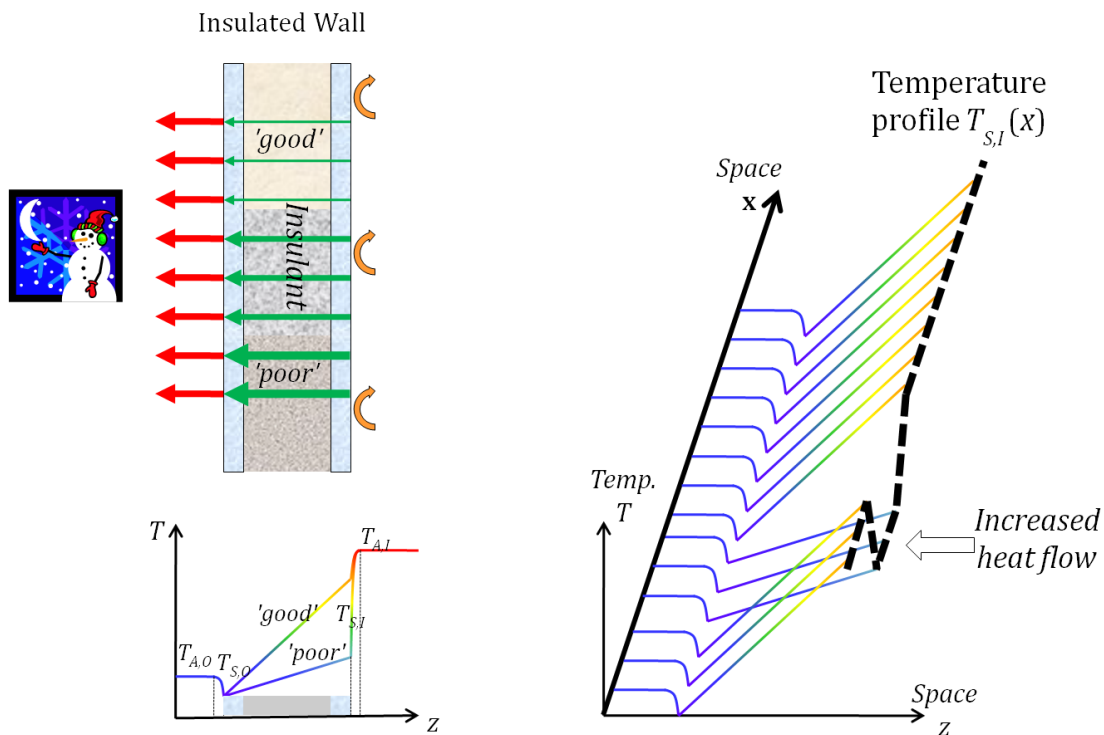


**Figure 3-2:** Principle of *passive* IRT observing an insulated wall under *stationary* conditions. **Left:** Thermal response of different materials to cooling at night; red arrows symbolize radiation, green arrows of different intensity indicate conduction, and circular arcs show convective gains by indoor heating.  $T_{S,O}$ ,  $T_{A,O}$ ,  $T_{S,I}$ ,  $T_{A,I}$  denote surface and air temperatures at the outer and inner wall positions, respectively ( $T_{S,O} < T_{A,O}$  because heat loss by radiation into the sky cools the outer surface below air temperature). High and low thermal resistances, respectively, correlate with steep and shallow thermal slopes inside the wall; the difference  $|T_{A,I} - T_{S,I}|$  in a way indicates the heating load. **Right:** A thermal line scan in the  $x$ -direction (thick dashed line) imaging the inner wall surface at position  $z_{S,I}$  reveals the local variations in thermal resistance. (Qualitative sketch showing no calculated or measured temperatures.)

### 3.2.2 Application examples

Several practical examples of applications in the building sector will be discussed where infrared thermography (IRT) is being applied along with other methods for *non-destructive evaluation* (Wu, Busse 1998; Carino 1998). Each example will be discussed under these aspects:

- Problem definition - what is the nature of the problem, possible causes and effects?
- Significance - adverse impacts, why should we care about the problem?
- Thermophysical effects - detectable symptoms, thermal coefficients affected?
- IRT detection - how is IRT applied today, how could it be applied in the future, limitations?
- Other methods of detection - how else can the problem be detected, which other diagnostic sensors or procedures exist?

The examples are listed in table 3-2 together with a thermophysical coefficient explaining the symptoms and the direction of property changes, e.g. rising or falling. If such a coefficient exists, it will likely be found also in a detailed simulation model and its value can be fitted to approximate and thereby explain the actual thermal measurements. Otherwise, an entry '*Meas. error*' indicates that no coefficient can be adjusted to minimize (regress) the measurement error, at least not in an obvious and understandable fashion, although the thermal images deviate from the predictions and thereby show detectable signs of the problem.

NDT problem	Thermophysical coefficients
Insulation defects	Conductivity ↑
Material compliance	Depending on material
Thermal bridges	Conductivity ↑
Delamination	Conductivity ↓, heat capacity ↓
Moisture	
Insulation	Conductivity ↑
Material (high-density)	Heat capacity ↑, conductivity ↗
Surface wetness	<i>Meas. Error</i>
Leakages	<i>Meas. Error</i>
Airtightness	Convective heat transfer coefficient ↑, air exchange rate ↑
Structural damage	Surface emissivity
Coating	Surface emissivity, reflectivity or transmittance
Aging VIP (vacuum-insulated panels)	Conductivity ↑

Table 3-2: Nondestructive testing examples in the building sector

This list is far from complete; other potentially useful applications are, for example, inspections of the mechanical and electrical HVAC installations of a building; detection of loose or corroded electric cable connections; clogged air intake or exhaust filters; overheated motors, bearings, pumps or transformers (Balaras, Argiriou 2002). These examples of *condition-based maintenance* in general are not specific to the building area. A broad and in-depth overview of diagnostic tools used to commission residential houses and to assess component performance is found in the report (Wray et al. 2002).

#### **Insulation defects**

Problem: Parts of the thermal insulation of a roof, attic, curtain wall, window frame, or HVAC pipe duct are missing or were not installed correctly; for example, insulation panels are not well aligned with the frame or are loose. RESNET (RESNET 2010) contains many examples of insulation defects.

**Significance:** This is a *construction* problem which should be dealt with during *commissioning* (initial or retrofit) of a building with consequences of *warranty* or *litigation*. In rare cases, after long use or after intrusion of moisture and subsequent drying, insulation may shrink (sinter); this constitutes a problem of *aging*. In any case, missing or defective insulation loses more heat and causes further problems of reduced *airtightness* and less resistance to *vapor*.

**Thermophysical effects:** Despite the low conductivity of air, an air-filled cavity has a *higher effective thermal conductivity* than the same void filled with insulation material because of the *radiative exchanges* between cavity boundaries. Since all radiation is trapped inside the void, it will eventually be absorbed similar to a blackbody. Radiative exchanges inside small pores of insulation material are negligible<sup>15</sup>, however. In large vertical void spaces, *convective exchanges* cause temperature increases from bottom to top thus increasing heat transfer.

Since a wall with voids has higher effective conductivity, the temperature *difference* between *inside* and *outside* surfaces is smaller than for an insulated wall as explained in figure 3-2. Warmer and cooler spots therefore are detected on the bounding surface under steady-state thermal conditions.

**IRT detection:** In practice, a temperature difference  $\Delta T \geq 10^\circ\text{C}$  should exist between inside and outside (RESNET 2010). The table below summarizes how to distinguish well insulated parts from voids.

Season	During Heating	During Cooling
<b>Side of inspection</b>		
From Inside	Warmer / <u>cooler</u>	Cooler / <u>warmer</u>
From Outside	Cooler / <u>warmer</u>	Warmer / <u>cooler</u>

Inspecting subsurface insulation is a highly developed area of building thermography, e.g. (Grinzato et al. 1998; RESNET 2010; Brooks 2007; Snell 2008). Clear guidelines and standards exist as to how and when to inspect, how to interpret the data, and how to grade defects (ISO 6781). Since the thermal symptoms are not limited to insulation defects, other possible causes must always be considered.

**Other methods of detection:** The cheapest and best method is *visual* inspection *before* the drywall is applied, i.e. performing ‘early’ or *collateral commissioning* during construction. However, this is at odds with business processes in the building trade. When presumed spot locations are more or less known and easily accessible, heat flux meters are used. Still, IRT is the most effective method of *screening* large surfaces from a distance.

### **Material compliance**

**Problem:** By mistake or in order to save money, different kinds of construction material were chosen than had been specified. Various parts of the building envelope could be affected, e.g. an inferior type of insulation, a different make of window fabric, concrete of a porosity or density contrary to specifications. Responsibility is assumed to lie on the *integration* side (procurement, building construction), not on the *component* side (*manufacturer*). The latter’s task would be material testing: checking if the product supplied meets the manufacturer’s own design specification.

**Significance:** Like all *construction* faults, these should be discovered during initial *commissioning*, entailing possibly legal consequences or, if unnoticed, late problems ranging from degraded energy performance or occupant discomfort to reduced durability of the construction.

---

<sup>15</sup> Since the net radiative power exchange grows by  $\Delta T^4$ , larger holes imply higher *temperature differences*!



Thermophysical effects: Many building materials have specific thermal properties, i.e.

- *Conductive* coefficients: thermal resistance, heat capacity or specific density, sometimes derived parameters such as thermal diffusivity and effusivity (Colantonio, Wood 2008; Sargentis et al. 2009);
- *Optical / radiometric* surface properties of glazing: emissivity, reflectance or transmittance.

When a material has distinctive conductive properties and separates two zones of different temperatures, the measured *difference* between surface *temperatures* on both sides deviates according to conductivity and characterizes the material. When radiometric properties are distinctive, the sample material emits thermal radiation at a higher or a lower level and *appears* warmer or cooler than the reference material at the same temperature.

IRT detection: Several conditions must be met before IRT may be used to distinguish the materials:

- a) The components must be made of thermally distinguishable material (as against different kinds of steel, parts differing solely in functional performance ...).
- b) Samples of components must be installed in the building which exhibit observable temperature differences (as against most components in the building core).
- c) For the *target material*, *temperatures* and their *uncertainty* must be measurable or computable under the same *ambient conditions* as for the inspected building material.

These restrictive conditions prevent the use of IRT in detecting discrepancies between materials on the spot. Moreover, this research area is still in its infancy.

Other methods of detection: Again, the most effective test method is on-site observation *during* construction supported by visual or other NDT techniques, such as ultrasonic sensors. For component testing, manufacturers and NDE institutions use specialized laboratory test setups equipped with sensors tailored to the performance criterion tested, such as structural resilience, air tightness or watertightness, sound transmission etc.

### ***Thermal bridges***

Problem: Two layers of building material separated by an insulating barrier are connected by elements of different materials such as metal bars, bolts or concrete slabs, mostly for attachment or structural reasons. In this way, thermally conducting bridges are created which bypass the thermal barrier.

Significance: Unintended thermal bridges are construction faults to be detected in commissioning. Thermal bridges serving structural purposes should be seen instead as design faults or errors in model validation if they were ignored in energy simulation. Ever rising requirements and improvements in the thermal insulation of façades and multi-layer walls imply that the *relative importance* of even minor heat losses due to cold bridges increases (Zalewski et al. 2010).

Thermophysical effects: As thermal resistance is decreased locally, so is the temperature *difference* between the inner and the outer surfaces, i.e. bridges appear as warmer spots on the cool side and as cooler spots on the warm side, similar to insulation voids. The visible effect is similar as with insulation voids; only, it is caused by increased conduction rather than convection and radiation.

IRT detection: Passive IRT is applied widely to detect and visualize thermal bridges, e.g. (Sargentis et al. 2009; Brooks 2007; Snell 2008; Zalewski et al. 2010). The cross section of the bridge head should not be too small compared to the insulated area; thin steel bars may not be detectable due to limited spatial resolution but will contribute to thermal performance only marginally, anyway. The

thermal contrast between insulated and bridged sections is often sharper than in insulation voids. A quantitative method of estimating heat loss from temperature differences ( $|T_{A,I} - T_{S,I}|$  in figure 3-2) has been proposed recently (Asdrubali et al. 2011).

Other methods of detection: As was said under 'Insulation defects', thermal bridges are discovered best visually before the construction is complete. As an alternative, and assuming the location is known, heat flux meters are used.

### **Delamination**

Problem: Several layers of different materials bonded into a composite structure, e.g. a façade, are detached from each other. This can be due to aging processes such as glue resolving or thermal stress acting on layers with different coefficients of thermal expansion.

Significance: Unlike insulating materials, laminates require *good conductive heat transfer* by close contact between layers as in a water pot on a hotplate. For example, solar heat is to be delivered from a curtain wall to the large thermal mass of a concrete wall behind or floor underneath. Delamination impairs thermal heat transfer and causes further damage as moisture infiltrates the air gap.

Thermophysical effects: A detaching layer warms up more and faster than a layer in good contact with a thermal mass in the back (see figure 3-3 below). As the degree of detachment varies over the surface, thermal variations are clearly visible on the detaching side. However, under ambient conditions, these effects are offset partly by convective cooling or other disturbances.

IRT detection: Layered structures have been modeled and measured by IRT, e.g. by Chiang (Chiang et al. 2006) and Grinzato (Grinzato et al. 1998). The latter authors applied lock-in thermography to detect delamination by heating the specimen with a  $1\text{KW/m}^2$  heater for 10 minutes. They reported thermal signals,  $\Delta T > 1^\circ\text{C}$ , where passive IRT under steady-state conditions produced barely detectable signals of  $\Delta T \approx 0.1^\circ\text{C}$ , even for a  $20^\circ\text{C}$  temperature difference between the innermost and the outermost layers. Inspection should be performed from the side closest to the delaminated layer, and detection may fail if the fault is buried too deeply.

Other methods of detection: Delamination can be detected also acoustically, e.g. by manual knocking or ultrasonic echo sounding. These contact methods require accessibility; they are too inefficient for screening.

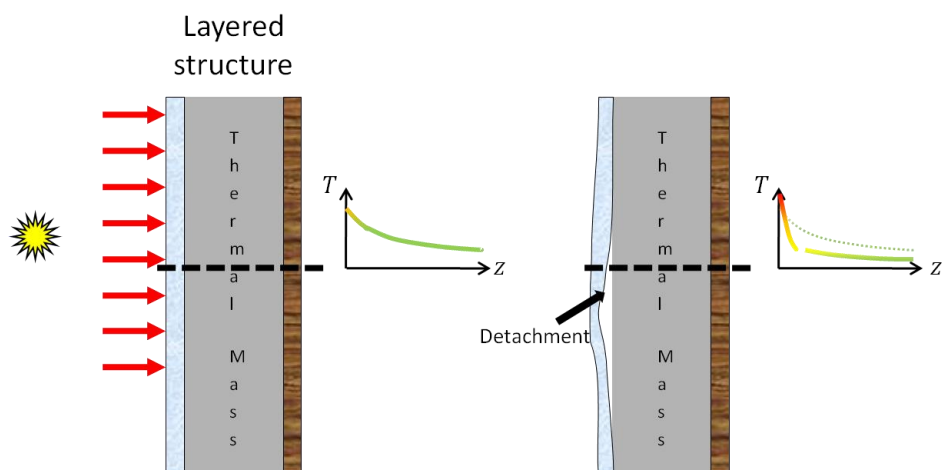


**Figure 3-3:** Thermal response of a layered structure under solar heating (left: normal condition, right: detached layer).

## Moisture

**Problem:** Moisture in buildings exists in many forms, including soaked masonry, wood, or insulation material as well as exposed surface wetness. Moisture may have remained from the very beginning due to imperfect drying of the building structure, or it can penetrate from the ground or through the roof via heavy rainfalls or melting snow, develop as dew on cold surfaces, be advected by humid air, or result from water damage (→Leakage). Therefore, moisture issues come up during the commissioning and the operational phases alike.

**Significance:** Moisture is one of the severest threats to a building life. Patterns of damage range from mould growth jeopardizing occupant comfort and health to long-term structural damage (steel corrosion, freezing-thawing cycles in concrete, swelling). Economic and cultural impacts are felt most severely in the building stock, especially in historical buildings.

**Thermophysical effects:** Intrusion of moisture causes thermal effects which can cancel out in part and are therefore difficult to detect. Water increases the heat capacity of materials but decreases thermal resistance, respectively, increases conductivity. Important cases and possibilities of detection include:

- i. Moisture absorption by low-density insulation material: Thermal *resistance* is *decreased* greatly but the increase in heat capacity is negligible because of the low material density. The net effect of moisture-affected insulation therefore resembles that of a thermal bridge or an insulation void. Hidden pieces of moisture-loaded insulation appear as warmer spots on the cool side and as cooler spots on the warm side of an insulated wall, assuming a *permanent* temperature difference on opposite sides due to heating or cooling load. This can be detected by *passive* IRT.
- ii. Moisture absorption by high-density building materials such as concrete, brick, or wood: Specific heat *capacity* is *increased* greatly while the decrease of thermal resistance as a function of the water content depends on the material and is less pronounced. Because of increased heat capacity, the wet material *lags behind* its dryer surroundings in both heating up and cooling down. Detection therefore requires *transient heating or cooling* of the test object and requires *active* thermography, in general.
- iii. Exposed surface wetness: The measured IRT image deviates from the predicted one but the *measurement error* which is only locally high cannot be eliminated simply by parameter fitting. Humidity condensing on cool surfaces (dew) appears warmer than its surroundings; wet spots on heated surfaces are subject to evaporative cooling. When phase changes are insignificant, or heating or cooling offset endothermic or exothermic phase changes, indeterminate heat patterns can be observed.

**IRT detection:** Numerous examples of humidity detection on building façades, roofs, walls, and floors using IRT in outdoor and more frequently in indoor surveys have been reported<sup>16</sup>. Under heating conditions, as a rule, the suspected humidity appears as warmer patches in outdoor surveys and as cooler ones in indoor surveys, always relative to their surroundings. Passive IRT lends itself well to fast screening and mapping of affected areas, but is not sufficient to confirm or quantify damage. Condensing humidity (dew) can be detected but rarely is in practice because the surfaces affected are not exposed well enough. Active thermography has been used to map moisture damage in historical buildings (Grinzato et al. 1998; Meola, Carlomagno 2004). Sham (Sham 2008) presents an

---

<sup>16</sup> For example, Colantonio, Wood 2008; Grinzato et al. 1998; Langlais, Klarsfeld 1984; ISO 10051; Said 2004; Sham 2008; Brooks 2007; Snell 2008.

application of active flash thermography to masonry and concrete walls, including quantification of the diameter and the depth of a defect.

Other methods of detection: Damage caused by moisture must be confirmed and analyzed further by *moisture sensors* detecting the change in electrical resistance or capacitance (ISO 10051; Said 2004). These meters, most of them hand-held, operate at close distance and are inefficient in screening large surface areas. If a building is vulnerable to *condensation* in certain areas or under specific conditions such as air cavities, window frames, concave creases and corners, laundry and cooking activities or, generally, buildings in humid climates, then it makes more sense to install a 'watchdog' or real-time monitoring function based on *hygrometers* rather than using IRT.

#### **Leakages (liquids)**

Problem: A leak is a loss of fluid in a contained duct system, such as a buried steam or water line, an underground sprinkler system, or a floor heating loop. Leaks can affect vital public infrastructure at district or urban levels (district heating, sewage ducts...).

Significance: Unless a leak can be seen clearly, early detection and quick countermeasures are crucial in preventing further damage, such as environmental *pollution* or persistent *moisture-induced damage*. An independent task sometimes is *mapping* and *locating* pipe ducts or confirming their presumed location, e.g. in planning maintenance work, retrofitting, or upgrading.

Thermophysical effects: Contrary to moisture, where a liquid has assumed approximately ambient temperatures, a leaking liquid often has a *distinctive* temperature level. The fluid acts as a *heat source or sink*, transferring heat to or from the surroundings by convection and conduction. Either the liquid itself or the enclosing duct is thermally visible. The thermal images *locally* deviate from the expectation (predicted images), producing a higher *measurement error* which cannot be explained well by thermal coefficients and should not be minimized by parameter fitting.

IRT detection: The 'leaky' image areas have fuzzy borders where the heat or cold spills beyond the well-defined contours delimiting an intact pipe duct. The ability to detect a leak depends on its depth beneath the surface and on the thermal conductivity of the covering layer. If the insulating material around a pipe fully absorbs the leaking fluid, the leakage is not visible directly but only subsequent humidification of the insulation is detected as described under →Moisture.

Other methods of detection: *Pressure* sensors measuring loss of pressure, and *flow* meters making up the balance of flows entering and leaving the pipe network can detect, but not precisely locate, a leak.

#### **Airtightness**

Problem: *Airtightness* of the entire building envelope acting as a barrier against unwanted cold, heat, or humidity is a primary concern. Equally important is efficient ventilation ensuring a high level of air quality and building comfort while avoiding draught and excessive ventilation losses.

Significance: Increased rates of air change compromise energy performance in the form of unwanted heat losses and gains. The NIST (U.S. National Institute of Standards and Technology) estimates that an increase of up to 43% of heating and 26% of cooling energy are due to (air) infiltration (Emerich S.J. et al. 2005). Ventilation is a long-time and complex issue to measure, control, and optimize.

Thermophysical effects: Unlike liquids, air flows are not visible in the thermal spectrum, but they leave traces on adjacent wall surfaces struck or touched by the air flow. On a larger scale, *convective*

*heat transfer coefficients* or *air exchange rates* due to indoor ventilation can be identified from thermal images if these parameters are represented in the associated building model.

IRT detection: Under ambient pressure conditions IRT already clearly indicates the *presence of air leakages*. Even small spots, like cracks, window seals or gaskets, show noticeable differences in intensity and are spatially resolved at short distances. *Confirming airtightness* of a building, on the other hand, requires pressurization / depressurization (**blower door** testing, an invasive method). Shortly ( $\approx 1-2$ h) afterwards, the paths of increased air filtration into or out of the building envelope leave a thermal signal. IR images are captured both from outside and inside. Airtightness is an established domain in building thermography (Colantonio, Wood 2008; Brooks 2007; Snell 2008).

Other methods of detection: Flow meters and, above all, visible *tracer gases* are used in connection with blower door tests.

### **Structural damage**

Problem: Detecting cracks, micro-cracks, or spalling of a concrete structure or brick masonry is part of *structural damage assessment* in historic buildings.

Significance: Structural damage assessment is important in the preservation of cultural heritage (Meola, Carlomagno 2004). Other potential applications include these:

- Assessment of non-apparent damage after vibration shocks caused by minor earthquakes, geo-thermal concussion, or mining activity.
- Safety inspection of public infrastructure systems, notably bridges.
- Assessment of commercial or residential buildings after persistent water damage.

Thermophysical effects: Surface roughness is often increased near cracks or spalling zones. Radiometric surface properties change locally both in the visual and the thermal IR ranges. As multiple reflections increase, the surface moves closer to a blackbody and its emissivity rises. Thermal emissivity can be measured when the surface temperature is known independently, e.g. (Griffith, Arasteh 1999; Avdelidis, Moropoulou 2003).

IRT detection: Active *flash thermography* using a xenon flash lamp has been applied successfully by Sham (Sham 2008) to detect and, under certain conditions, also quantify damage patterns on brick masonry and concrete walls. The IR images are captured immediately after a strong but very short light pulse (duration  $\approx 3$ ms,  $\lambda \approx 400$  nm) is emitted. Micro-cracks of  $< 0.5$ mm width on marble plates produced a more pronounced contrast in the IR images than in the visible spectrum when a digital color camera was used. To aid IRT detection, the plates were sprayed with water which increased their thermal conductivity locally because water accumulated in the micro-cracks. The images were captured by a high-resolution IR camera from a distance of  $\approx 1$ m. These IRT applications are in a laboratory stage.

Other methods of detection: Many structural damage patterns require different types of sensors, i.e. ultrasonic sensors (Carino 1998), inspection under visible light, or Ground Penetrating Radar.

### **Coating**

Problem: Reflective paintings or rendering coats deteriorate due to soiling, dust, smog, chemical reaction, microbial growth, or UV fading on building envelopes (Platzer 2006). Similar mechanisms affect the protective sealing of translucent surfaces, mainly glass façades and high-performance window glazing.

**Significance:** Preserving the functional and energetic performance of coatings is a requirement in condition-based maintenance. An ever-rising degree of sophistication invested in modern building materials to reap even marginal performance benefits makes components vulnerable to aging and damaging and requires careful monitoring of their performance, often simply to decide when cleaning is needed, or when a self-cleaning coat (Nano-material) starts deteriorating. Reflective paintings on roofs and pavements, in particular, may take part in urban or regional strategies to mitigate the urban heat island effect by counteracting *radiative forcing*.

**Thermophysical effects:** Changes in surface emissivity, reflectance, and transmittance attend and indicate performance degradation. These changes often can be detected in thermal images when the sample temperature is known independently, or when adjacent material of known radiometric properties exists in good thermal contact with the sample (Griffith, Arasteh 1999; Avdelidis, Moropoulou 2003). Subsequently, an impact on performance must be calculated from the changes in coefficients.

**IRT detection:** Cases of practical application of IRT in the building sector are still few and far between. Bison et al. (Bison et al. 2007) monitored thermal barrier coatings by pulsed thermography; however, they estimated a different thermal property of the coatings, i.e. their thermal diffusivity<sup>17</sup>.

**Other methods of detection:** Cameras in the visible or near-infrared spectra; chemical sensors ('electronic noses') are alternatives if volatile chemical compounds are diffused as a result of degradation.

#### **Aging VIP's**

**Problem:** Very high-performance material insulations, especially Vacuum Insulation Panels (VIP), are affected by gradual performance degradation due to rising internal air pressure and, accordingly, absorption of moisture.

**Significance:** As mentioned above, VIP's are sophisticated components which may lose their specific advantages in terms of energy performance unless properly monitored.

**Thermophysical effects:** The degree of deterioration is related to a measurable thermo-physical coefficient, the thermal resistance or, conversely, the conductivity of a panel.

**IRT detection:** Thermal resistance should be measured on the cold side under winter conditions. Rough screening is achieved quickly by scanning an entire façade containing VIP's. After adjusting thermal coefficients in the simulation model, individually or in a lumped fashion, a performance estimate for the *whole building* is derived. If a noticeable loss compared to previous estimates is found, individual panels are inspected more thoroughly. Accurate measurements of their thermal resistance require controlled conditions in a test box; see Nussbaumer (Nussbaumer et al. 2006).

**Other methods of detection:** Heat flux meters can be used to determine the thermal resistance of individual VIP components. Moisture contents can be determined by precision-*weighing* and comparing the result to the panel weight as delivered.

#### **Discussion**

The majority of building thermography today remains *qualitative* in nature, detecting, visualizing and interpreting anomalies in thermal images. Human expertise and prior experience are required at

---

<sup>17</sup> Diffusivity is defined as the quotient,  $\lambda/(\rho c)$ , of conductivity and heat capacity; it indicates how fast a temperature change diffuses through the material.

a high level. Therefore, the costs are considerable and the degree of automation is low. This is why building thermography still is not used routinely or area-wide. On the other hand, *quantitative* techniques estimating temperatures or defect properties mostly rely on active heating; they are applied at the component level in dedicated test chambers, not at the whole-building level and not in occupied buildings at a large scale. In some papers the term *Quantitative Thermography* denotes, in a narrow and precise sense, estimating the *size* or *depth* of a defect such as a crack directly from IRT images with *no thermodynamic model* describing the processes in the test object. In our work, the property of interest is the impact on building energy performance and, perhaps, the probable residual service life of a component. These quantities require that the IR images be coupled to an *existing BIM and a thermodynamic model (BPS/BES)* that is calibrated from the images acquired.

### 3.3 Building Information Modeling (BIM)

Building information models assist in lifelong analysis of buildings and form the core of our SW architecture sketched in chapter 2 (figure 2-1 2). Reviewing the BIM technology, evaluating or comparing the features of specific BIM schemas in detail are beyond the scope of this report. A state-of-the-art introduction into the topic is found in the BIM Handbook (Eastman et al. 2008).

#### 3.3.1 Definition

According to Eastman (Eastman et al. 2008) there is no single, widely accepted definition of building information modeling. The authors define BIM as a digital spatial (3D) representation of a facility achieving *intelligent simulation of architecture*. For our purposes, let the facility be a building or an aggregation of buildings, i.e. a district or city, embedded in the urban topography and infrastructure. The BIM representation must be (Eastman et al. 2008), p. 13:

1. measurable (quantifiable, dimension-able, and query-able),
2. comprehensive (encapsulating and communicating design intent, building performance, constructability, and including sequential and financial aspects of means and methods),
3. accessible to the entire team (owner, architect, engineers, and construction staff) through an interoperable exchange standard, and
4. durable (usable through all phases of a facility's life).

More specific features characterizing a BIM schema can be listed: the representation

5. carries numerous topical data and material properties (**'attributes'**) distinguishing the parts beyond their geometry, in order to carry out diverse analysis applications, such as structural, cost, acoustic, daylight, or thermal analyses,
6. aggregates components hierarchically, i.e. is structured and in all cases accessible as a **part hierarchy**, and can be viewed as a hierarchical **scene graph** known from 3D graphical rendering,
7. supports **parametric modeling**: components are parameterized object classes providing **relations** to other objects such as adjacent or hierarchically nested ones and embodying **rules constraining** the parameter values of several **related** objects.

Properties 5, 6, and 7 make BIM **semantic** (product) data models. The rules in 7 implement predefined or user-defined domain knowledge about how components are constructed and fabricated. When the user enters changes in one object, the rules assure automatic and consistent updating of all **related** objects by propagating the changes to neighboring parts and through the relational

graph. For example, door or window openings that *belong to* one wall object must lie *inside* the wall boundary and be *disjoint* to each other. A wall *abuts* on the *adjacent* floor, ceiling, and wall so as to enclose a watertight space. Therefore, wall heights will automatically adapt to a changing story height. This concept applies not only to geometrical shape, placement or size, but to all properties described by attributes: For example, changing the thickness of a wall affects its *heat transfer coefficient* in the same way as choosing a different wall material does.

An example of parametric modeling of key importance to energy simulation is the *relation of correspondence* between *architectural entities* and *thermal engineering entities*. The former ones refer to structural or decorative building elements and their enclosed spaces or rooms; the latter ones to the thermal zones and to HVAC components such as inlets and outlets, ducts, fans, pumps, heat exchangers, sensors, and control points. To build and run detailed models for thermal analysis, it must be known which sensors and thermostats control which zones, how zones and rooms (spaces) correspond geometrically, and how fluid flows and HVAC components cohere into functional units. BIM exchange schemas like IFC and gbXML are powerful and general enough to express these relations. However, the authors do not know if and to what extent exploiting these features and filling BIM instance documents with precise information on this is common practice.

### 3.3.2 BIM exchange standards

In this research project, only BIM representations offering an open exchange standard have been considered. Proprietary data models implemented by architectural CAD tools such as [ArchiCAD \(Graphisoft\)](#), [Revit \(Autodesk\)](#), or [Bentley Systems](#), which meet all of the above criteria except for 3, have been ignored because they provide no interoperable exchange format. Three well-known candidates have been considered: IFC, CityGML, and gbXML.

#### ***Industry Foundation Classes (IFC)***

IFC (IAI 2006, 2008-2011) constitute the most ambitious and comprehensive product data model available to date supporting the entire building life cycle. IFC is the outcome of standardization efforts undertaken by ISO-STEP (**Standard for the Exchange of Product Model Data**) and is being advanced and certified by the **International Alliance for Interoperability (IAI)**. Its syntax is based on the EXPRESS language. IFC provides broad and general definitions of objects from which more task-specific models are derived, and therefore is referred to as an extensible framework model. The IFC architecture provides three main layers: the **Resource Layer** at the bottom defines re-usable base entities from 26 categories; the **Interoperability Layer** provides elements shared by different applications, whereas the top **Domain Layer** contains specific extensions for nine application domains, including Building Architecture, HVAC, Buildings Controls, and Structural Analysis. The Institute of Applied Informatics at KIT has played a role in IFC standardization and developed several publicly available software tools (in C++) for import and export, visualization (*IfcViewer* Häfele, Isele 2011) and manipulation (*IfcExplorer* Häfele, Isele 2011) of IFC models. Still, the authors find IFC rather mighty and difficult to comprehend and master fully. Even basic entities, such as an *IfcWall*, are nested deeply in the class hierarchy. IFC highlights the business *process view*, modeling all roles, responsibilities and activities during construction and operation of buildings, which are marginal issues in the thermography part of this project.

#### ***CityGML***

CityGML (OGC 08-007r1; OGC 2007; Benner et al. 2011) is an XML-based specification developed by the Open Geospatial Consortium (OGC) to represent urban objects and 3D city models. CityGML



defines the classes and relations modeling the important topographic objects of cities and regional models with respect to their geometrical, topological, semantic, and appearance properties. Included are generalization hierarchies between thematic classes, aggregations, relations between objects, and spatial properties. CityGML's scope being large-scale modeling of urban landscapes (geometry, topology, and visualization), it currently seems to lack the full support required for energy analysis applications (thermophysical and material properties), i.e. it does not yet fully meet BIM criteria 2, 5, and 7 in its present form.

CityGML models are distinguished by their level of detail (LOD), ranging from LOD 1 (representing houses as block models) to LOD 4 (buildings containing interior zoning and HVAC equipment); intermediate levels (LOD 2 and LOD 3) are concerned with progressive refinement of roofs and façades. Energy analysis of individual buildings requires LOD 4, in general, while the bulk of implemented CityGML models focus on the outer structure and appearance of buildings at levels LoD 1 to LoD 3.

### **gbXML**

gbXML ('green building XML' gbXML 2010) is an XML-based schema developed to transfer information needed for preliminary **energy analysis** of buildings, specifying their envelopes, zones, mechanical equipment, and HVAC components. Buildings are spatially embedded in their natural environment including vegetation. The gbXML format supports geometry specifications from major CAD vendors and interfaces to several energy analysis programs, among them DOE, EnergyPlus, IES, and Ecotect. gbXML seems to reconcile (relative) simplicity with completeness regarding our main application, which is energy simulation (Dong et al. 2007); therefore, it is our first choice for pivotal development and proof of concept. However, this choice is preliminary, not backed by experience, and switching to IFC later is envisaged if demands should exceed gbXML capabilities.

## **3.4 Energy Performance Simulation**

Several tools and development platforms for building performance simulation are reviewed briefly in this section, motivated by the need to decide on a *technology platform to implement and test* QGT. After all, the new technique is intended for on-site monitoring and inspection of *occupied* buildings, not for use in dedicated thermal chambers. Simulating real buildings requires knowledge of their geometry, to begin with. In many cases, the geometry data will exist already in CAD or BIM documents which, according to figure 2-12, lie at the heart of the concept. Ideally, the building simulator should draw on information from the BIM as far as possible. Therefore, interoperability between energy simulators and semantic data models is a major issue and selection criterion.

Secondly, only case studies examining a variety of building models showing different patterns of thermal behavior will reveal how reliably and accurately parameter estimation by mobile sensors works. A set of realistic 'pre-cooked' building models serving as a benchmark could be obtained most easily by using a special-purpose *simulation package*. In general-purpose simulation languages or development frameworks much effort would go into developing a base layer of building physics models.

At this point, conflicting demands appear on our list of wishes, such as access to internal software structures (data, code) required to build a mobile observer interface and a parameter calibration interface. Integration of a camera model needs the simulator also as a platform for *software and interface development*. Generality in the modeling of heat, mass, and moisture transfer seems more important than libraries for specific solutions, like advanced HVAC systems or façade elements for

passive houses. The necessary flexibility is expected rather from a component-based simulation environment with powerful application programmer interfaces (API).

For a review of the capabilities of building simulation packages to practitioners' needs reference is made to a Web site maintained by the U.S. Department of Energy and providing a long list of software tools and vendors: [Building Energy Software Tools Directory](#) (DOE 2011). Some information has been derived from that source. A survey by Crawley et al. (Crawley et al. 2005) updated since 2005 as a live document compares the capabilities of twenty major building energy simulation programs. The comparison is based on information provided by the tool developers in 14 categories and includes general modeling features, building envelope and daylight, multi-zone airflow, HVAC systems and components, climate data, as well as user interfaces and data import/export facilities to other programs.

#### 3.4.1 EnergyPlus

The [EnergyPlus](#) simulation program was developed at the Lawrence Berkeley National Laboratory (LBNL) and introduced in 2001. It implements the ASHRAE building energy calculation framework, in particular the transfer function model according to the EnergyPlus calculation reference (DOE 2010). EnergyPlus is the most widely used BES tool in the USA today. Licenses are available free of charge.

Compared to its predecessors, DOE-2 and BLAST, EnergyPlus implements more accurate simulation concepts and is well suited to all lifecycle phases of a building (Maile et al. 2007). New interfaces were provided to the **S**imulation **P**roblem **A**nalysis and **R**esearch **K**ernel (SPARK) and also to a multi-zone air flow model (COMIS), allowing air flow to be simulated as occurring in naturally ventilated buildings, and allowing user-defined HVAC components to be created. Like other BES tools, EnergyPlus simulates ideal HVAC component behavior and not degraded performance.

EnergyPlus supports interoperability: IFC files can be converted into the native IDF (Input Definition Format) by a tool named IDFGenerator developed by LBNL; a similar conversion tool for gbXML files is available from third-party vendors.

EnergyPlus has formed the basis of further developments in the BES research community. For example, the *MIT Design Advisor* (Urban 2007) was designed with a user-friendly graphical interface to quickly assess a limited set of building design options. According to Urban, EnergyPlus is '*intended for highly experienced technical users ... usability is compromised for the ability to model complex building scenarios ... it has many underlying assumptions without being explicitly evident to the casual user*'. The MIT Design Advisor was an independent software development and did not have EnergyPlus as a development platform but rather as a repository for energy calculation formulae (DOE 2010) and as a reference for comparison of results.

#### 3.4.2 ESP-r

[ESP-r](#) (Environmental System Performance – research) (Clarke 2001), developed at the University of Strathclyde, Glasgow, UK, is one of the most complete, best documented and most widely used tools for building performance simulation to date. It is capable of simulating innovative or cutting-edge technologies such as daylight utilization, natural ventilation, and photovoltaic façades. Users are granted an open-source GNU-Linux license.

With regard to building physics, ESP-r covers the transport of air, moisture, and thermal energy between components called *control volumes*, as well as fluid flow within HVAC ducts. Radiative heat

transfer implies short-wave and long-wave radiation and calculation of geometric view factors. Different components can be integrated using independent time steps ranging from seconds to hours.

The ESP-r data model (Hand 1998) consists of a *site* description and a number of *buildings*. A site specifies a *location* embedded in a terrain, and a *context* repository specifying climate, fuel supply and other boundary conditions. Each building includes a geometry description in terms of *thermal zones* linked by explicit *contiguity relations*. A thermal zone denotes an air volume in a polyhedral enclosure at a uniform temperature. HVAC *plant components* refer to the zone containing it, have *control algorithms* attached to them, and are represented by volumes with plant connections. A building model also specifies properties necessary for numerical solution, e.g. gridding schemes of domains of fluid dynamics. *Operation schedules* specify time series of occupancy, heat gain, or shading.

ESP-r imports the AutoCAD DXF format and International Graphics Exchange Standard (IGES). The IFC exchange standard is supported only indirectly via the Ecotect tool.

ESP-r has been used as a research and development platform for major software developments (Citherlet, Hand 2002; Nakhi 1995; Hand 1998). Nakhi (Nakhi 1995) focuses on the relation between geometric model refinement and thermophysical model simulation (meshing, gridding). He distinguishes full 3D-mesh, partly and fully lumped models according to the space dimensions considered in the numerical heat transfer, and he develops an ESP-r extension allowing different levels of detail of heat conduction and variable thermophysical properties, such as thermal conductivity described as a function of the moisture content.

Hand (Hand 1998) extended ESP-r by designing a novel project manager with facilities for model definitions of sites, context, buildings, zones, environmental systems, etc. This application controls all aspects of simulation-based design and supports decision making. Hand's work, a precursor of the DAI initiative, was an attempt to integrate energy simulation into building design.

ESP-r has been implemented in FORTRAN and C. An executable simulator is obtained by generating internally a sparse system (energy) matrix of algebraic equations. To include a new equation, one has to know the system matrix implementation routine and needs to calculate the self and cross coupling coefficients (Mazzarella, Pasini 2009). More recent efforts extending ESP-r capabilities seem to avoid direct work on the code base and explore new avenues, such as the cooperation of independent simulation tools by run time coupling and message passing (Trcka et al. 2006).

### 3.4.3 Ecotect

Autodesk® [Ecotect™](#) is an environmental design and analysis tool coupling an intuitive 3D-modeling interface with extensive functions for solar, thermal, lighting, acoustic, and cost analysis. Ecotect is designed to provide visual and analytical design feedback during (early) conceptual design and accepts even simple sketch models (Attia 2011). Towards the final design, as progressively more detailed information becomes available, a design validation may be desired. Ecotect delegates part of this task, thermal energy analysis, to more focused tools, such as EnergyPlus or ESP-r.

Ecotect boasts of a high level of data interoperability supporting IFC, gbXML, and CityGML input besides native CAD formats (ArchiCAD 10). As mentioned above, data export to BIM alone does not imply fully automatic transformation providing complete and consistent input to the charged analysis tool.

From a developer's point of view, a person planning to extend the functions of Ecotect would deal with the tool delegates, e.g. EnergyPlus or ESP-r, discussed above.

### 3.4.4 TRNSYS

[TRNSYS](#) (Transient System Simulation Program), developed in the 1970's at the Solar Energy Lab of the University of Wisconsin, has been used for manifold analytical problems: HVAC sizing, multizone thermal and airflow, electric power simulation, solar design, analysis of control algorithms etc. TRNSYS is one of the most complete and thoroughly validated energy simulation packages and has a good run time performance. The use of TRNSYS incurs appreciable license fees.

The TRNSYS package includes a graphical interface, a simulation engine, and a library of components. The 3D-geometry (building envelope) can now be created in the TRNSYS 3D plugin for Google SketchUp™ and edited in the TRNBuild interface. Component models are encapsulated in so-called TYPEs, such as the multizone building model, TYPE56, which are FORTRAN subroutines with standard arguments. Many TYPEs implement their own mathematical solvers. To define a system model, the output of one TYPE is declared to be an input to other TYPEs, using an editor such as the TRNSYS Simulation Studio (Wetter, Haugstetter 2006). In this way, new components not existing in the standard package are created.

Correctly solving differential and algebraic equation systems described by coupled components (TRNSYS TYPEs) requires careful consideration of their proper interconnection and calling sequence in the numerical solution. Component parameters adopt fixed roles, being input or output arguments (Sowell, Haves 2001). Put differently, a graphical simulation studio with drag-and-drop functions alone cannot offset fundamental limitations of the programming language and the software architecture, e.g. mixing of modeling issues with equation solving, lack of generic interfaces and object-oriented concepts (inheritance, hierarchical composition) which help build fully re-usable components.

### 3.4.5 Modelica

[Modelica](#) is an object-oriented, declarative language for component-oriented modeling of complex systems in various engineering domains, including building energy simulation (Wetter, Haugstetter 2006; Mazzarella, Pasini 2009; Sodja, Zupančič 2009). To build and run simulations, the user needs

- a simulator kernel with debugging facility and graphical user interface, and
- a development environment for visual editing, model parsing, and code generation.

She or he may either choose an open-source (OpenModelica) or a commercial visual simulation studio, such as Dymola.

Key goals pursued by Modelica are separating modeling from numerical simulation and assuring extensibility and code re-use. In contrast to procedural or *input-output* oriented model specifications, a modeler in Modelica writes *equations* describing *equality* but not predefined *causality*. Equations are used to define module behavior and interconnections. The simulation environment manipulates these equations symbolically to decide at run time whether terms are inputs or outputs, and determines their execution order; then it selects the numerical routine for solving the entire system (Mazzarella, Pasini 2009).

Modelica supports many features known from object-oriented languages such as C++ or C#: class declarations and instance variables, nesting of classes (composition), (multiple) inheritance, generic (parameterized) classes, hierarchical namespaces, packages, and libraries. Besides equations, also traditional algorithms can be programmed by using input-output functions, assignments, iterations, and while-loops. Array (matrix) arithmetic is provided in a MATLAB-like style. For the simulation of mechanical and electrical systems, couplings between classes are provided in the form of *connector*

*classes* implementing energy flows with constraints. Dynamic behavior is specified by discrete events raised upon time elapse (clock events) or when conditions become true.

Wetter and Haugstetter (Wetter, Haugstetter 2006) compared Modelica and TRNSYS as development frameworks for creating multizone BES models, and claimed a five- to tenfold reduction in development time for Modelica compared to the TRNSYS multizone component, TYPE56. Major benefits stemmed from the hierarchical model building which facilitates debugging of large models and re-using sub-models. On the other hand, the authors (Wetter, Haugstetter 2006) found computation times three to four times longer in Modelica than in TRNSYS, but conceded unexplored optimization potential in Modelica<sup>18</sup>.

Symbolic equation manipulation and automatic differentiation, inverse model solving, and sensitivity analysis are further features recommending Modelica for parameter estimation tasks in particular.

On the other hand, the role of geometry and topology appears somewhat underdeveloped in Modelica models. Also, the authors are not aware of any import or export of BIM (IFC or gbXML) or architectural design documents. This weakness owes to Modelica being a general-purpose 'physics simulation' environment not specifically designed for building simulation.

### 3.4.6 Matlab based platforms (HamLab)

[HamLab](#) (Heat, Air and Moisture Simulation Laboratory) is a collection of tools and functions in the Matlab / Simulink / FemLab environment including

- multi-zone building models,
- detailed physics models for heat, airflow, and moisture transport in up to three dimensions (HAMBASE, HAMSYS, HAMDET),
- modules for optimum building operation and control provided by another library, HAMOP.

HAMLab is a research tool derived from van Schijndel's dissertation (van Schijndel 2007). Development in HAMLab requires a license for, and understanding of, Matlab / Simulink / FemLab.

Powerful matrix algebra capabilities and advanced control algorithm development are merits inherited from the Matlab and Simulink base.

The authors do not know of any conversion tools for importing complex building geometry (IFC or gbXML format) into HamLab.

### 3.4.7 IES

The [IES-VE](#) (Integrated Environmental Solutions <Virtual Environment>) building energy analysis tool offers an extensive set of features by incorporating a whole suite of modules for special analyses, e.g. estimates of heating and cooling loads by the ASHRAE Heat Balance Method, modeling transient heat transfer by the ApacheSim simulation tool, daylight and solar analysis based on the Radiance tool, and airflow simulation by a CFD module. The software also highlights very diverse calculable

---

<sup>18</sup> The time to develop TYPE56 in TRNSYS was not measurable directly so a C++ based model of similar complexity was built for comparison. Comparing the run-time performance required imposing *equal accuracy* of both *solutions* because absolute running times, depending on the integration time step and the error tolerance set by the iterative solver, are not comparable directly.

performance measures, e.g. comfort analysis or environmental impact of a building, and can be used to assess early design sketches.

IES-VE has been designed for interoperability with BIM in mind and, among other formats, supports gbXML. However, it is a commercial tool, neither freeware nor open-source. We know nothing about its use for detailed model development or as a research platform for extensions. For example, can it be extended to integrate new observer interfaces? How are internal parameters to be calibrated from sensor measurements?

#### 3.4.8 Discussion and conclusion

A general-purpose, object-oriented open development platform such as Modelica or Hamlab, oriented towards dynamic systems and control system applications, seems more useful than a packaged solution such as EnergyPlus, ESP-r or TRNSYS, because modularity and extensibility are must-requirements for developing the new interfaces for mobile observers. Modelica is preferred because it supports symbolic equation manipulation and automatic differentiation. On the other hand, Modelica currently lacks facilities for the import of complex building geometry as provided by EnergyPlus, for example, which is seen as an obstacle. In the future, geometry import from ifc and gbXML may become possible indirectly, by using a Modelica plug-in developed for EnergyPlus (See et al. 2011).

### 3.5 Validation and Calibration of Building Simulators

Verification, validation, and calibration (or parameter identification) denote different methodical aspects serving one common purpose: ensuring that a simulation model accurately predicts the corresponding behavior of a real system being simulated, and does so under different input conditions. In the simulation domain, verification asks whether an *implemented model* yields correct solutions with respect to an intended *conceptual model* (physical or mathematical) while validation investigates whether the *model* (conceptual or implemented) explains a section of *real behavior* faithfully, assuming that measurements from the real world are available for comparison (Sargent 2009). In building energy simulation, the terms have assumed slightly different meanings (Judkoff et al. 2008). *Verification* compares simulation output to results from a reference model possessing a known, *analytically calculable* solution and serving as ground truth. This is a special case of *validation*, which includes *empirical* output comparisons as well as comparisons of different simulation programs, e.g. code-to-code comparison. In the building simulation domain, validation is thus used as a generic term including verification.

*Calibration* determines *internal* variables of the model called *empirical parameters*, to be distinguished from *input variables*, by means of measurements. Parameter values, reflecting the condition of a building, must be determined such that simulated output *best approximates* measured output under identical *input* conditions. The error function should consider statistical uncertainty of measurements by covariance or by upper and lower bounds, i.e. uncertainty intervals (Del Barrio, Guyon 2003). Further statistical analysis of the error residuals is necessary to detect bias or model mismatch. Finally, model calibration needs a mechanism to decide whether the best agreement is *acceptable* taking into account the measurement uncertainty. Calibration is therefore closely linked with *model validation*.

There is no generally accepted definition of parameters; it depends on the definition of the model interface (system boundary) and the purpose of analysis. Table 3-3 presents a list of parameters in building simulation models which can be targeted and identified by QGT.

*Validated* building models are essential for application to *existing buildings* (Neymark et al. 2002; Torcellini et al. 2006; Judkoff et al. 2008; Bowers et al. 2010). Validation and identification are required especially when the model is used for *optimum control*, e.g. for implementing energy efficient HVAC control algorithms (Sun 2004; Liu, Henze G.P. 2005; Dong 2010).

### 3.5.1 General Methodology

Major validation efforts have gone into building simulation programs in general, not into individual building models. On an international level, the *Energy Conservation in Buildings and Community Systems Programme* (International Energy Agency IEA / ECBCS Beausoleil-Morrison 2007) notably focused on energy supply systems and co-generation schemes. Validation methodologies have led to international and national standards, e.g. IEA BESTEST Task 22 (Neymark et al. 2002) and US ASHRAE Standard 140 (Judkoff et al. 2008). On a European level, the PASSYS validation methodology was established by the Commission of the European Communities in 1986 (Jensen 1995; Del Barrio, Guyon 2003).

In a newly prepared report (Judkoff et al. 2008) results were published from a study performed by the U.S. Solar Energy Research Institute (SERI) in the early 1980's. A validation methodology was developed in that study and, after empirical data had been collected, applied to several BES simulation programs in use at that time (DOE-2.1, BLAST, DEROB, SUNCAT). Key causes of difference between calculated and observed energy results were identified and classified as **external** or **internal causes**. The external causes include

- Differences of the actual weather / microclimatic conditions;
- Differences of the actual occupant behavior;
- Invalid model assumptions or invalid parameters describing the actual building geometry or its material including thermal properties;
- User errors in supplying a correct building input file, often related to the user interface.

Internal causes include modeling errors due to the underlying model assumptions and simplifications (Judkoff et al. 2008, table 3.1 pp.32) or to the numerical solution techniques:

- Incorrect modeling of heat transfer mechanisms within a zone;
- Incorrect modeling of interactions between zones;
- Implementation bugs.

Several validation techniques in use are discussed in the article (Judkoff et al. 2008):

- Comparison between different simulation programs, including code-to-code comparisons.
- Comparison with analytical models of heat transfer which can be solved for simple test cases.
- Empirical verification with data measured at instrumented test sites, both single-zone and multi-zone.

The research topic of this paper focuses on the validity of models representing **particular** buildings throughout their life cycle, i.e. it is concerned with external rather than with internal causes which bear on the correctness and accuracy of solutions implemented in a simulation package.

Type	Example Parameters	Association Building physics	Building Components	Model level of detail	Unit
Heat transfer coefficient	Conductivity	Conduction	Solids (envelope, thermal mass, composite structures); Liquids (HVAC)	all	W/(m K)
	Heat resistance	Conduction	Solids (layered / composite)	medium	Km <sup>2</sup> /W
	Heat capacity	Conduction	Solids (thermal mass)	medium	J/(kg K)
	Diffusivity	Conduction	Solids (layered)	detailed (diagnostic)	m <sup>2</sup> /s
	Effusivity	Thermal adaptivity			-
	Air exchange rate, infiltration	Convection	Air zones	coarse	m <sup>3</sup> /s
	CHTC <ul style="list-style-type: none"> <li>• ventilation-driven</li> <li>• buoyancy-driven</li> <li>• stratified</li> </ul>	Convection	Air zones	medium	W/(m <sup>2</sup> K)
	Roughness index	Convection	Bounding Surfaces (e.g. roof)	detailed	-
	Emissivity, Absorptivity	Radiation thermal/ solar	Bounding Surfaces (envelope thermal mass)	all	-
	Reflectance	Radiation thermal/ solar/ visible	Bounding Surfaces (envelope thermal mass)	all	-
	Transmittance	Radiation thermal/ solar/ visible	Air, Glazing	all	-
Solar heat gain	Radiation thermal/ solar/ visible	Glazing	all	-	
Mass transfer coefficient		Air and moisture transport	Zone, insulation	detailed (CFD)	m/s kg/s
Machine coefficients	Capacity	Thermal heating or cooling power (supply)	HVAC pump / fan	coarse	W
	Flow rate		HVAC pump / fan	medium	m <sup>3</sup> /s
	Supply / Return temperatures	Parameter affecting thermal HVAC efficiency	HVAC boiler / chiller loop (set points)	medium	K
	Coefficient of Performance	Fuel consumption	HVAC	coarse	-
	Fouling factor	Fractional degradation of Convective heat transfer	HVAC heat exchanger	detailed	-
Miscellaneous non-measured input	Ground temperature	Conduction through floor	Building Environment	all	K
	Ground reflectance	Solar radiation	Building Environment	all	-

**Table 3-3:** Candidate parameters for QGT calibration in building performance simulation

A general methodology of calibrating simulation models by means of measured energy data is proposed in a study by Reddy and Maor (Reddy, Maor 2006). The calibrated models serve for quantitative comparison of methods of saving energy, taking uncertainty into account. Utility bills showing energy consumption for a year are the only performance data available for calibration. The specific results apply to models implemented in the DOE-2 simulation program; a case study was performed with two simulated buildings and one real building. The authors concede that model calibration is feasible and cost-effective only for large public buildings, such as hospitals, schools, office buildings or hotels.

As to the types of models calibrated, the study (Reddy, Maor 2006) discusses several methods:



- 'black box' validation using abstract models of input/output behavior, for example, Neural Network (Lundin et al. 2004) or ARMAX models (Jimenez et al. 2008)),
- 'gray box' parameter estimates for models based on thermal physics, and
- simulation programs, i.e. computer implementations of models.

There are six levels of calibration differing in the time needed and the performance data available.

Calibration needs a criterion showing goodness of fit. The authors use an index distinguishing among several energy 'channels' (heat, gas, electricity). They demand that the normalized error be less than 6%. An objective function including 'soft constraints' is proposed which penalizes parameter values outside their bounds but avoids explicitly performing constrained minimization. The errors in measurement prediction are weighted against deviations of the actual parameter values from the 'preferred' ones (Carroll, Hitchcock R.J. 1993). The uncertainty (covariance) in measurement data determines the weights.

The mean squared measurement error is a highly non-linear function of all parameters and has many local minima; the solution often is under-constrained, given the measurement data available. As the authors state, "*A simulation output close to the measured output is no guarantee that all the individual knobs (parameters) are tuned correctly*" (Reddy, Maor 2006). In order to compare certain energy saving measures, the most influential input knobs impacting energy savings should be known and should be tuned most carefully and individually. To solve the multidimensional global minimization problem, the authors propose a hierarchical four-stage approach (Reddy, Maor 2006) roughly summarized as follows:

1. Identify a subset of *influential* input parameters (typically  $\approx 20$  out of  $\approx 300$ ), guided by human expertise. Define best-guess estimates and ranges of variation of their values depending on building type. Typically, a parameter has three characteristic values: *min*, *max*, and *base* values.
2. *Perform a coarse grid search*: Sample the product space of the value ranges of all influential parameters by Latin Hypercube Monte Carlo (LHMC) sampling<sup>19</sup>. Run the simulation for each combination sampled and evaluate the resulting measurement errors in order to find regions containing local minima. Then inspect all parameter vectors lying in local minima regions: find the *strong parameters*<sup>20</sup> taking one dominant value which occurs most often in the solution set. Using a  $\chi^2$  test, distinguish them from *weak parameters* with roughly uniform occurrence of all values.
3. Retain those samples from step 2 in which all *strong* parameters actually take their values in the dominant value interval. If the solution set is still considered too large, re-iterate the filtering process after *freezing* the strong parameters, i.e. excluding them from further sampling. Go back to step 2 and examine the pruned sample set to identify further strong parameters.

<sup>19</sup> LHMC generates samples from a high-dimensional parameter vector space where the range of values of each scalar component is divided into equally likely intervals (classes, e.g. denoted *low*, *medium* and *high*). Interval bounds are chosen according to the values' probability density function (pdf). Samples are generated by *first* drawing the class of each component parameter (using uniform sampling, i.e. all classes get equal likelihood) and *then* picking a random value from the sub-interval associated with that class. The goal is to assure uniform coverage of the value ranges with comparatively fewer samples needed than with direct sampling.

<sup>20</sup> This method selecting the strong parameters is called 'regional sensitivity analysis', but sensitivity is based here on frequency counts and not on the partial derivatives of the error with respect to parameters.

4. Use the final sample set to determine the uncertainty in measurement prediction, and use the samples as *starting values* for a *local* optimization algorithm, e.g. gradient-based search. The authors feel that keeping a small number ( $\approx 10$ ) of top feasible solutions is more robust in predicting the effect of energy saving measures than solely relying on the 'best' solution whose ranking may be due to random noise.

The methodology (Reddy, Maor 2006) was tested in synthetic and real examples where several large office buildings were simulated employing the DOE-2 energy analysis program.

#### 3.5.2 Case studies, sensors, and measurements

In the thesis (Sun 2004), a systematic methodology was developed for calibration and optimum control by BES. The approach focuses on specific aspects of air distribution in HVAC systems and optimum control of heating and cooling systems; to this end, the simulation models must be detailed and calibrated accurately. Only limited measurable performance data are available for calibration, mostly utility bills and electricity used by the cooling system. A systematic approach similar to (Reddy, Maor 2006) called analytic optimization is developed which performs a guided refined search for calibrating BES programs. The approach includes four basic steps:

- Sensitivity analysis - calculating normalized relative sensitivity coefficient vectors.
- Identifiability analysis - selecting the identifiable parameters. Their number is derived as the rank of the Hessian matrix of the measurement error as a function of the parameters (identifiability matrix). The condition number of the identifiability matrix is calculated numerically.
- Numerical parameter optimization.
- Uncertainty analysis - using Latin hypercube Monte Carlo sampling similar to (Reddy, Maor 2006).

Automatic differentiation (AD) techniques were used to obtain the derivatives. In a case study of a simple cooling plant, the calibrated model was shown to be useful for supervisory control (Sun 2004).

In several calibration projects, temperatures are monitored alone or combined with energy metering. Experiments are usually performed in test cells or dedicated test houses (Lundin et al. 2004; Park et al. 2004; Gutschker 2008; Dong 2010) or in buildings selected for demonstration projects (Heidt et al. 2003); in one case, the test building was an industrial manufacturing unit (Bowers et al. 2010).

The parameter identification study (Lundin et al. 2004) was performed in order to assess and analyze energy efficiency measures in buildings during commissioning. Parameters to be identified on a daily or hourly basis include the *factor of heat gain* due to electrical equipment and the unknown building occupancy, the *heat loss* coefficient due to transmission and ventilation, and the total *heat capacity* and the *time constant* of the building, respectively. For experiments, a single test cell was equipped with 15 thermocouples to capture air and surface temperatures; artificial heat sources (0-250W) were installed to simulate the heat gain caused by occupants. Parameter values were learnt by a neural network, which is a black-box model assuming no prior knowledge of the functional dependency of parameters. Neural network training utilizes information of the temperature difference between inside and outside, the heat supplied, and the free heat available. Results reported for the root mean square relative error are between 2.5% and 12% for different parameters, but no accuracy levels are given for the parameters proper or their impact on energy efficiency.

Simulation models of four residential low-energy buildings of different construction types in North-Rhine Westphalia, Germany, are described in the paper (Heidt et al. 2003). TRNSYS simulation predicts energy use and thermal comfort in the occupied demonstration buildings. Validation serves to develop guidelines for the cost efficiency of measures saving energy. Ample measurement data are available every 15 minutes: indoor air temperatures of each room and some wall temperatures, heat energy delivered based on the temperature level and the flow of the heat transport medium, electricity requirement of ventilation and household, domestic hot water consumption, and weather data (solar irradiation, outdoor temperature, wind, and humidity).

Many interior parameters were estimated in the study, e.g. the heat transfer coefficients (U-values) and the solar absorption of floor, roof, wall, and window surfaces [ $\text{W}/\text{m}^2\text{K}$ ], the heat capacitance of zones, infiltration rates, and several HVAC parameters such as efficiency of heat recovery, heat losses in the tank and pipe ducts, maximum heating power per zone and dead band control temperature. Most parameter values are known in principle from the construction plans and subsequent measurements while the parameters of the building as erected deviate within limits (Heidt et al. 2003). Very accurate predictions of the heating energy demand ( $\approx 0.5\%$  relative error in heating periods of one to four months) and also of zone air temperatures ( $\approx 0.1\text{K}$  mean deviation) were obtained by adjusting the parameters within their admissible value bounds. The authors discuss ways to determine load schedules: e.g. changes in heating and ventilation controls are detected by examining the electricity demand of pumps, and user events like operating shading devices or opening windows and doors are detected by the rate of temperature decrease in the heating period.

An evolutionary algorithm is used in (Bowers et al. 2010) to determine optimum parameter values for a steady-state model (840 parameters) in comparison with a dynamic thermal model (514). A time-dependent mutation operator controls the temporal rate of parameter changes. The method was tested on benchmark simulation models in Energy Plus and also in a real industrial building. The steady-state model ignores the dynamic effects due to thermal masses. It contains five parameters of which hourly values had to be estimated independently during a whole week: heating energy load [kWh], target temperature and heat transfer coefficient for heating and cooling, respectively. Energy consumption, external temperatures, and solar radiation data were available from measurements. The second model assumes a single thermal mass at uniform temperature and, therefore, needs only three hourly parameters: heating load and target temperatures for heating and cooling. Heat transfer through the thermal mass is described by ten constant parameters.

Several studies apply calibrated building models for optimum HVAC controls, e.g. (Park et al. 2004; Yoon et al. 2011; Dong 2010).

A double-skin façade system providing different air flow regimes is analyzed in the study (Park et al. 2004). Six convective heat transfer coefficients characterizing the bounding surfaces of the glazing and the louver slats were estimated. The heat transfer model is used for performance assessment of energy, comfort, and daylight, and for optimum control of louver slat angle and air inlet / outlet dampers. A demonstration unit equipped with a weather station (thermocouples, pyranometer, and anemometer) provides very detailed measurements of local solar radiation, wind speed, and temperatures.

The authors conclude that their model accurately predicts temperatures and air cavity velocities, is reliable for performance studies and efficient enough for model based control. However, the calibration effort has to be repeated for every size, type, position and orientation of a façade system, even inside the same building. An on-line self-calibrating procedure is developed in a follow-up study (Yoon et al. 2011) to avoid laborious off-line calibration. Pre-wired, plug-and-play façade units are proposed which would come to the construction site equipped for internet connection and with sensors and after assembly they would start communicating with a central server. We presume that

a mobile, portable weather station with internet access would be advantageous in measuring weather conditions.

Real time optimum control strategy is proposed for HVAC in the Ph.D. thesis (Dong 2010), suggesting a smart-home scenario of ubiquitous surveillance. One key focus is accurate capture of the building load, i.e. local weather forecasting, predicting the number of occupants and their occupancy by means of Hidden Markov models and by observing indoor relative humidity. CO<sub>2</sub> content, lighting, motion and acoustics, power consumption of electrical appliances are measured at over 100 sensor points.

A heat transfer model was developed for a dedicated test building, the Decathlon solar house at Carnegie Mellon University. Still, its construction materials and associated properties of heat capacitance, thermal resistance, convective and radiative heat transfer coefficients were *unknown* and had to be estimated (Dong 2010). Wall and roof, indoor and outdoor temperatures, and solar irradiation were recorded every minute for a whole month. The estimation, progressing from the envelope parameters towards the interior zones and constrained by lower and upper value bounds, was implemented as an Artificial Neural Network in MATLAB.

### 3.5.3 Discussion and conclusion

The remarks below apply to validation and calibration methods in general.

- In most studies, measurement data are collected from *test cells* or selected *demonstration houses*; (re-)calibration is not performed routinely as part of an ongoing commissioning process or on a large scale. Preparing a house for data capture is time consuming and intrusive. Often, data are insufficiently diverse and dense to disaggregate all parameters to be estimated.
- A whole-building simulation model contains very many, typically hundreds of parameters to be estimated simultaneously. Grid search, evolutionary algorithms, and neural networks have been used for non-linear minimization of the error function. However, there are still the risks of error compensation (Reddy, Maor 2006; Maile et al. 2010a) and of being stuck in local minima. An incremental, *spatially focused* calibration strategy seems to be missing; a new method will be introduced in section 4.3. Recently, a similar calibration methodology has been proposed which is guided by a hierarchy of the sources of evidence and works with version histories (Rafferty et al. 2011). A detailed methodology is proposed how to define the thermal zones in a BPS/BES model.
- The authors know of relatively few publications in which infrared images were heavily used for parameter identification of thermal building models, e.g. (Griffith, Arasteh 1999; Cehlin et al. 2002; Chiang et al. 2006), see section 3.6. In most projects contact temperature measurements were applied. IR cameras are deployed mostly in thermal chambers with fixed measurement geometry and are not truly employed as autonomous mobile observers.

## 3.6 Thermographic Analysis

This section reviews some *relevant* work on thermal image analysis covering at least one of the following aspects beyond image processing in the thermal range:

1. Infrared camera models; prediction or simulation of thermal images.

2. Model calibration using IR images for measurement.
3. IR image analysis and scene interpretation based on thermal models.

As to relevance criteria, our primary focus is on *building applications* and performance assessment, while suitability of the *methods* applied ranks second.

Domains 1 and 2 overlap significantly in the estimates of emissivity and reflectivity properties of surfaces: these are important parameters of every infrared camera model which need to be determined accurately and, sometimes, compensated for.

### 3.6.1 Radiometric camera models

All bodies above 0°K (absolute zero) emit electromagnetic radiation which can be detected by infrared cameras mostly in spectral ranges where atmospheric transmittance reaches its maximum, i.e. in mid-range (2-5.6  $\mu\text{m}$  wavelength) and especially in thermal infrared range (8-14 $\mu\text{m}$ ). Objects emit most of their radiant power in the thermal range at the low temperatures found in buildings. IR cameras sense radiosity, not temperatures. Radiosity depends on the emissivity of a material, on radiation reflected by the background, in particular sun and sky, and on the geometric view factors specifying the shares of radiation due to each object. Thus, important features of radiometric camera models are the following ones:

- Estimating emissivity and reflectivity values or, more generally, the bidirectional reflectance distribution function (BRDF) of a surface, and correcting for the reflection.
- Modeling solar and atmospheric radiation as well as atmospheric transmittance in the case that the camera is far away from the objects.
- Calculating the geometric view factors.

An introduction to radiometric sensors and measurement procedures is given in the report (SMSSG 2010).

Why is it important to model the thermographic measurement process and its disturbances in detail? The primary objective of thermographic imaging often is simply accurate **temperature measurement**, i.e. direct conversion of a radiance image into a thermal image. Other purposes are obtaining estimates of the states or parameters of the thermal process behind the surface, detecting or classifying objects from their thermal signatures, and assessing their condition or state of degradation. Models of the genesis of radiance images also allow their synthesis (thermal image simulation) to be performed.

Thermal image simulators were first developed for target recognition in military applications, as described in an early U.S. army report (Weiss et al. 1992) and later by the Swedish Defense Research Agency (Nelsson et al. 2005). These reports refer to commercial programs for thermal signature prediction, such as

- **CAMEO-SIM** (Camouflage Electro-Optic Simulation by Insys Ltd., U.K.), an IR scene simulation program producing high fidelity physics based images, and
- **RadThermIR** (by ThermoAnalytics Inc., USA), a 3D heat transfer program originally developed for thermal and IR signature prediction of targets such as vehicles. This software considers BRDFs after the Sanford-Robinson model and models sensor dynamics and camera optics. Different sources of noise (diffraction, lens imperfection, and motion blur) are taken into account.

WinTherm (Johnson et al. 1995) is a thermal analysis package including a thermal network solver for buildings and urban areas, an image viewer for thermal display, and a pre-processor for model edit-

ing. The program supports radiative heat transfer and view factor calculation and displays thermal images of the scene from any view point, but does not strictly implement a radiometric camera model accounting for disturbances or modeling solar and atmospheric radiance. Emissivity values must be known; no identification based on image data is described.

A tool named OSIRIS, simulating images of 3D landscapes and urban areas in the thermal infrared range (3-14 $\mu$ m) and in high spatial resolution, is proposed in (Poglio et al. 2001, 2003; Poglio et al. 2006). Its main applications lie in remote sensing. Radiative object interactions including solar and atmospheric radiation are covered, and so is BRDF, but no methods were reported how to estimate the BRDF shape or parameters. Landscapes are represented in terms of 3D elements which are extruded from a flat oriented surface with polygon enclosure. 3D elements possess a homogeneous flux normal to the surface and a layered depth structure for modeling heat conduction. Facets are dynamically divided into elements according to the degree of partial shadowing.

### 3.6.2 Estimates of emissivity and reflectivity

As mentioned above, modeling and determining emissivity and reflectivity is crucial for infrared image simulation and image interpretation alike. Notably, the U.S. Lawrence Berkeley National Laboratory (LBNL) conducted detailed experimental investigations in thermal chambers, e.g. (Türler et al. 1997; Griffith, Arasteh 1999; Griffith et al. 2001). In the report (Griffith, Arasteh 1999), the steady-state heat flow through building envelopes was studied by means infrared cameras under heating conditions in winter. Measurements were made on the warm side of a wall specimen dividing the test cell into a warm and a cool (refrigerated) compartment. The purpose of this setup was to produce spatial 3D-distributions of the wall temperature acting as boundary values for heat flow simulation (finite-element / CFD programs). The thermal fields on the test site were obtained basically by *inverting* radiosity images, using spatial markers for spot localization. A complicated background correction accounting for self-viewing surfaces was applied<sup>21</sup>.

The *reference emitter* method to determine the emissivity of an unknown surface is described in detail. A test surface and an abutted surface of *known emissivity* are both kept at the same arbitrary temperature, and the *apparent temperatures* as-imaged are recorded for both materials. The latter ones are obtained by turning off emissivity correction in the IR camera, i.e. setting  $\epsilon=1$ . The true background temperature must also be known; it is obtained by viewing a background mirror with the camera. In fact, this needs to be done for each camera position. A formula is also presented to quantify the uncertainties of emissivity-corrected temperatures when values of apparent temperature, emissivity, and background temperature are given and their respective uncertainties are also known. Arrays containing many different background temperatures produce more accurate measurements than a single background temperature for the entire image, which is what most IR cameras today provide (Griffith, Arasteh 1999). Of course, permanently adapting corrective values for the background radiation to the changing view point by hand would be impractical.

The materials research study by Avdelidis and Moropoulou (Avdelidis, Moropoulou 2003) reviews emissivity measurement techniques and highlights the importance of emissivity values for health diagnostics of historical buildings containing very diverse building materials. One focus is on emissivity as a function of wavelength and temperature. Emissivity values of selected building materials, e.g. types of plaster, marble, limestone, and porous stone, were determined at various tempera-

---

<sup>21</sup> Modeling the radiative exchange between arbitrary surfaces - self-viewing or not - may be delegated to a thermal simulation model of the environment. However, this was not available.

tures (0°C, 48.8°C, 100°C), in the mid-wave (3-5.4  $\mu\text{m}$ ) and long-wave (8-12  $\mu\text{m}$ ) spectra. Two different techniques were applied: the ASTM standard E1933-97 (ASTM E1933 - 97) and an empirical method in which a reference emitter made of electrical tape with known emissivity was attached to the test specimen. One research question asked was if higher-than-ambient temperatures (100°C) could produce higher emissivity values and, being less prone to disturbing background reflection, yield more accurate temperature measurements in building diagnostics.

Part of the ambient radiation received by the infrared camera detector is radiation reflected at the surface viewed, diffuse or specular. Several papers address ways of how to handle reflections in IR thermography.

(Datcu et al. 2005) lists several existing methods of reflectivity correction:

1. Modulated photothermal effect: The test object is warmed up locally. This affects the emitted part of radiation whereas the reflected portion remains constant and can be eliminated.
2. Two-color technique: The test object is viewed at two different wavelengths, but at the same temperature, assuming wavelength-independent emissivity and known background radiation.
3. Explicit determination of the reflected heat, for example by means of a hemispherical mirror collecting the background radiation.

The method (Datcu et al. 2005) quantifies the reflected heat flux and operates in a controlled test chamber. The background objects are assumed to be far away and randomly distributed, emitting uniform and isotropic infrared radiation, which leads to the assumption of a uniform *equivalent background temperature*. It can be determined by viewing a hemispherical mirror made of highly reflective and diffusive aluminum. In fact, the mirror itself had non-negligible and angle-dependent emissivity; therefore, its value and the mirror temperature had to be determined. The mean surrounding temperature obtained on the mirror surface turned out to be close to the blackbody temperatures of the walls. Validation studies were carried out on a multi-layer wall with an insulation fault placed inside, and on a real building wall with a window viewed from inside during winter time. Although the methodology and the experiments are described in detail and in depth, it remains unclear when and why the high effort of reflectivity determination is justified and whether there are any alternatives.

Accurate temperature measurement of the glass cover of solar collectors and photovoltaic modules is important for their performance assessment (Krenzinger, de Andrade 2007). Outdoor thermography can produce *specular reflection* errors. A method of correcting these errors is proposed and validated experimentally. Reflectance values of glass in the thermal infrared spectrum are calculated by the Fresnell equation, with the incident and refracted angles and the refractive indices for air and glass being known. (Krenzinger, de Andrade 2007) presents also a method for estimating a thermographic equivalent sky temperature.

An experimental study (Cehlin et al. 2002) in Sweden focused on thermal comfort analysis of low-velocity diffusers (fans) in displacement ventilation. Thermography as a thermal field measuring technique was applied in a test chamber to visualize the thermal patterns of the air flow. Imaging the cool air flow as an occupant in the room would feel it rather than viewing its trace left on an outer wall, yet avoid disturbing the air flow by the experiment was a major objective. Therefore, a paper screen of high emissivity was placed *parallel* to the air stream and imaged. Because of the low air speed, convective heat transfer to the paper screen is low, but so is the thermal mass of the paper. The screen also receives disturbing background radiation from the warmer surrounding walls. The convective heat transfer coefficient was estimated without the explicit use of parameter identification methods. Error analysis expressed the difference between the true air temperature and the screen temperature measured as a function of three uncertain variables, mean wall temperature,

convective heat coefficient, and screen emissivity. The uncertainty of the predicted air temperature was found to vary between 0.62°C and 0.98°C (Cehlin et al. 2002).

#### 3.6.3 Model validation and calibration

Parameter estimation and calibration of thermo-spatial models by IR thermography are found in several disciplines, such as microelectronics (Zawada 2005) and medical diagnostics (Jiang et al. 2010) but apparently are not yet common in whole-building simulation models. Several researchers studied inverse heat transfer problems at the component level, e.g. (Nair et al. 2004; Wawrzynek, Bartoszek 2002). Nair et al. dealt with thermal nondestructive evaluation by thermosonics or vibrothermography. They suggested a novel input parameterization scheme and developed a regularization term based on the maximum entropy method, to cope with parameter identification being ill-posed. Wawrzynek and Bartoszek estimated thermal conductivity and specific heat coefficient of concrete or, specifically, cementitious cylindrical specimens (Wawrzynek, Bartoszek 2002). The building parts showed non-homogeneous heat loss patterns with location and temperature dependent heat coefficients. The 2D heat conduction equation (Fourier law) yields the forward model; the inverse model for parameter estimation, driven by the squared differences of temperatures as the objective function, is solved by means of sensitivity coefficients. Temperatures were assumed to be simply measurable by thermography and to not require an explicit IR camera model.

Zawada (Zawada 2005) describes a distributed parameter system, modeling in two space dimensions the waste heat dissipation of thick-film modules made on alumina and ceramic substrates. Several important model parameters were estimated simultaneously: convective and radiative heat transfer coefficients, and thermal conductivity. Heat generation is assumed to be either spatially uniform or concentrated in one point. In the steady state, constant temperatures were assumed in the normal direction (thin-layer assumption). Parameter estimation works with a repeated non-iterative least squares algorithm (RLSQA). A sensitivity analysis to the measurement and the heater positions was performed. The test samples were coated with black paint; thermography measurements therefore yielded an array of temperatures directly without any correction of emissivity.

Jiang et al. (Jiang et al. 2010) develop a thermography-based method for screening breast cancer focusing on deeper and smaller tumors. The breast tissue model consists of tetrahedral finite elements with spatial constraints. Both forward and inverse models serve to estimate each patient's individual *thermal tissue properties*, i.e. conductivity, blood perfusion, and metabolic heat generation. Available distributions of thermal properties of the population average are employed as regularization constraints since parameter identification is underdetermined. It is not tissue property data as such, but the *thermal contrast* in an image which makes the tumor indicator (*tumor-induced thermal contrast* Jiang et al. 2010). But thermal contrast becomes *predictable* only if tissue properties were estimated accurately. There is a methodological analogy to QGT: the *energy impact* predicted by a whole-building simulation makes the diagnostic signal in QGT, not parameter values as such or thermal images. However, prediction of the impact requires that heat coefficients be estimated accurately which, in turn, relies on up-to-date thermal images of critical areas.

#### 3.6.4 Quantitative thermal image analysis

An early example of model-based thermal image analysis and scene interpretation is found in (Nandhakumar, Aggarwal 1988). Its main purpose was land cover classification in outdoor scenes illuminated by bright sunlight and viewed by an IR camera in the 8-12 $\mu$ m range. Surface temperatures were estimated by a simple radiometric model ignoring the spectral response of the detector



and atmospheric attenuation. A key idea underlying the approach is the *fusion* of registered infrared and visual images. Surface orientation and absorptance were estimated from the visual image, heat flux and temperatures from the IR image. To distinguish different types of land cover such as vegetation, pavement, vehicles, and buildings, the authors employed the relation between two heat fluxes: external solar irradiation and heat conduction into the ground. Although the absolute values of both quantities varied with the ambient conditions, their ratio persisted; the lowest values were found for cars, the highest ones for vegetation.

Garbe et al. (Garbe et al. 2003) analyze infrared image sequences to identify transport models at the surface of an ocean turned up by wind and waves. At the topmost boundary layer of water, heat is exchanged with the environment by diffusion (conduction to air, radiation to sky) whereas heat and mass transfer with the bulk of water underneath are driven by turbulent transport. Elements of water from deeper layers are injected into the boundary layer while particles from the boundary layer disappear following a statistical process of surface renewal. The probability density function (pdf) of surface renewal events is modeled after a logarithmic normal distribution. Estimated parameters were the temperature difference across the thermal boundary layer, the parameters of the surface renewal pdf, and the heat flux at the surface.

The ocean surface is a highly dynamical process observed in a thermal image sequence. From the temperature changes measured at *fixed* image points, the thermal dynamics of *moving* water particles are estimated by optical flow analysis, allowing for constant brightness changes where brightness is assumed proportional to temperature. A motion transformation of locally constant unknown velocities on the surface is assumed. These assumptions lead to an extended brightness change constraint equation from which the motion parameters can be estimated by total least squares. Furthermore, the total derivative of sea surface temperature is estimated with respect to time.

(Garbe et al. 2003) is an excellent example of model identification using thermographic measurements. The mathematical complexity resides here in the *transport model* proper and in optical flow analysis; these requirements are unique and greatly differ from building models. On the other hand, no *measurement model* was required and developed. Thermography (done at night-time) is treated like ordinary surface temperature measurement enjoying a high resolution in space and time. Measurement geometry does not matter because emissivity, reflectivity, and radiation between objects are ignored; actually, the camera position is fixed.

Several recently published papers report on IR thermography used in *quantitative assessment* of heat losses in *buildings*, thus advancing the state of the art beyond temperature measurement and qualitative diagnosis.

One paper (Chiang et al. 2006) discusses IR thermography applied to the inspection and defect characterization of layered concrete building walls (internal voids, → section 3.2). A finite element analysis of heat transfer in the multi-layered system was carried out, based on the conductive heat equation in two dimensions (Fourier diffusion equation). The authors found that the time to the maximum thermal contrast observable increases with the depth of internal voids. Several restrictions are mentioned: Convective heat transfer is ignored, the initial boundary conditions of the solution to the heat equation are unknown, and heat flux is assumed to be uniform.

Zalewski (Zalewski et al. 2010) characterizes the impact of thermal bridges on the performance of complex buildings walls. Objects under study were light construction walls with a steel frame and insulating material packed between the metal trusses. The walls came equipped with rain water and vapor barriers and with naturally ventilated air layers on the outside. Several existing methods for *thermal bridge* assessment are reviewed in the article, such as linear thermal transmittance according to the ASHRAE handbook (2005 ASHRAE handbook 2005; ISO 9164; EN ISO 13790) and 2D / 3D numerical simulations. The authors applied thermography to *visualize* the thermal bridges that are

visible on the vertical frame and on the horizontal spacers separating layers of air. Predictions of heat loss were obtained differently, using a numerical 3D heat transfer model of the wall in steady-state which was calibrated from readings of three heat flux meters installed in the frame. The thermography temperatures were found to be too inaccurate for calibration. The predicted heat loss due to the thermal bridges amounted to  $\approx 26\%$  in total. Replacing the inside layer of air by insulation material reduced this figure to  $\approx 13.5\%$ .

In a recent paper (Asdrubali et al. 2011, 16-18 May), a *quantitative thermographic* method is proposed for evaluating thermal bridges in buildings, especially in multi-layered walls and windows. Heat loss through thermal bridges is related to the overall heat flux in a homogeneous wall. This so-called *incidence factor* is obtained from the spatial temperature field alone, without performing heat transfer simulation of the laminar wall for known material properties (U-values). *Temperature differences* between the *inside air* and the *inner wall* surface as measured in the disturbed zones and weighted by their respective areas are related to the respective temperature differences for a homogeneous wall weighted by its total area. IR images corrected for emissivity and background radiation furnish the wall temperatures. Experiments were conducted in an environmental chamber containing a window with an artificial bridge installed between the frame and the glazing and in situ with a bridge installed between a real building floor and an adjacent wall. For validation, an empirical heat flow analysis was carried out with thermometers and heat flux meters installed, and also an independent numerical analysis. Good agreement was found between the incidence factor method proposed by the authors, the measured and the numerically determined values of heat loss, all being in the 10-20% range.

The method requires steady-state conditions. How to ascertain when they hold in practice constitutes a problem. Also, from building physics principles one would expect the observable differences of surface temperature to depend strongly on the depth of a thermal bridge. The difference should be negligible for a thermal bridge deeply buried in a layered construction, even if the true impact on the energy flux were the same. Also, the existence of a single and constant 'laminar coefficient' resembling a heat transfer coefficient is assumed, in the disturbed zones or elsewhere. Still, the method seems to be promising in order to obtain quick comparative assessments.

### 3.7 Allinson's Aerial Thermography

The study (Allinson 2007) addresses the following research question: is it possible to distinguish loft insulation (its existence and thickness) in residential housing by measuring *roof surface temperatures* in large-scale aerial thermographic surveys? The work relates to earlier studies with similar objectives performed by the ASHRAE and the CIBSE as early as in the 1980's and scrutinizes popular yet delusive theses:

1. Poorly insulated buildings have warmer roofs, in winter.
2. Aerial thermography efficiently captures large urban areas.
3. Therefore, aerial thermography can quickly assess the retrofitting demand.

This work is closely related to QGT in several respects:

- Geo-referenced thermography: Aerial images are registered with a 3D terrain map by using GPS in an airplane and assuming known fixed measurement geometry.
- A camera model exists to predict the IR measurements when roof temperatures are known;
- A building zone model exists to predict roof temperatures for known thickness of insulation.

To determine the insulation as the *goal variable* from measurements, the models would have to be inverted, run backwards. One key contribution of Allinson's work is quantifying the *sensitivity* of both models with respect to the goal variable and with respect to ambient conditions. These imprecisely known disturbances affect the main system components as shown in figure 3-4. As a result, variations of the actual or aerially measured roof temperatures due to disturbances *outweigh* the influence of the insulation. This **disproves** conclusion 3 above. As a matter of fact, *better* insulated roofs may *appear warmer* than poorly insulated ones.

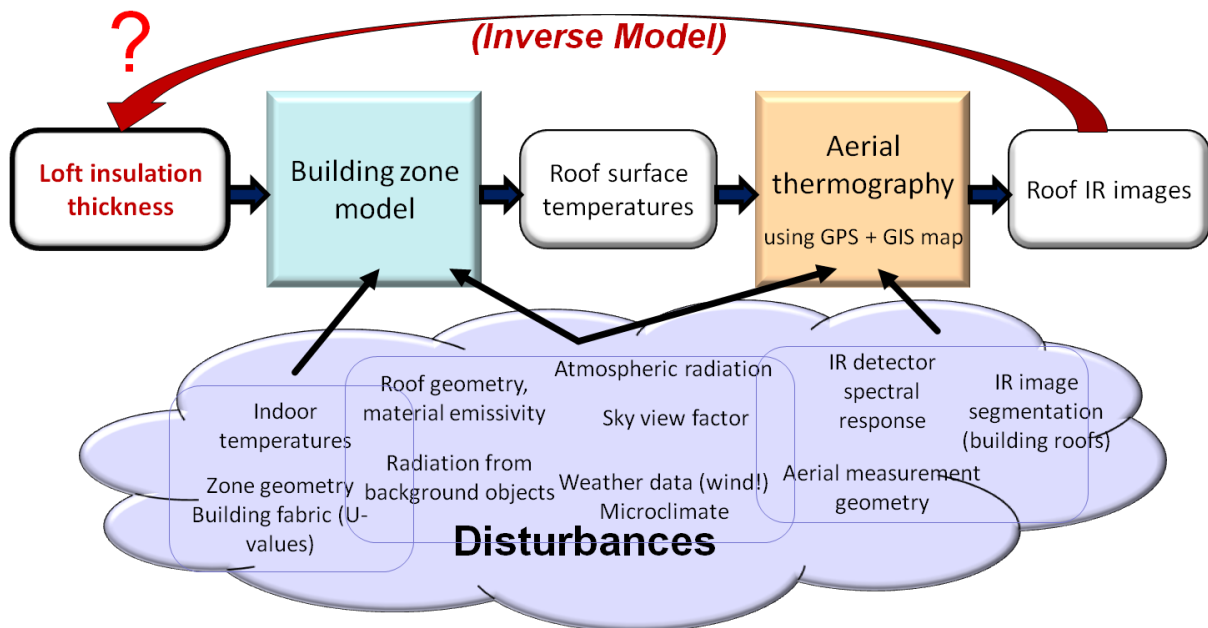


Figure 3-4: Analysis of loft insulation by aerial thermography after fig. 3-7 in (Allinson 2007)

### 3.7.1 Scope of survey

A number (96) of fairly aged terraced apartment houses built in the 1930's were selected for the study from four different urban districts in the city of Nottingham, U.K. The houses had different roof shapes such as gable roofs for the mid-terrace houses and half-hipped or hipped roofs for the end-terrace houses. Roofs were further distinguished by their sloping angles (1:3 or 1:1 pitch) and by the material of roof tiles (clay or slate shingles). These construction details were surveyed on site; a few photos from (Allinson 2007) are shown in figure 3-5.

One important assumption is made on all houses surveyed: Heat insulation, varying between 0mm and 250mm in thickness, is attached to the *ceiling* of the *uppermost story* and *not* to the outer roof fabric. In other words, houses have 'cold', unshielded and undeveloped loft air spaces. This property is responsible for poor aerial observability. As the houses were owned by the city council, ground truth information about the real condition of heat insulation could be obtained from an owners' database.

Surveys were undertaken during clear and relatively cold ( $\approx 2^{\circ}\text{C}$ ) winter nights and at low wind speeds on the ground ( $< 2.4$  m/s). Meteorological and atmospheric conditions (air pressure, temperature, relative humidity, dew point, wind direction, wind speed, and others) were captured in great detail and to the highest possible accuracy by collecting 'radio soundings' from the closest weather

station  $\approx 10$  km away. The MODTRAN 4 software (Berk et al. 1999) was applied to the weather data to estimate transmittance of the atmosphere as well as radiance up-welled and down-welled from the atmosphere.

The airplane flew at an altitude of about 760 m and was equipped with a thermal line scanner operating in the spectral band [8, 14  $\mu\text{m}$ ], scanning downwards in the nadir direction with the scanning plane perpendicular to the flight path. A spatial resolution of roughly one pixel per square meter [ $\text{m}^2$ ] was thereby achieved. The scan lines or strips were registered to a digital terrain map using GPS for airplane localization. After correction of geometric distortions and 2D projection, individual houses were cut out of the thermal image by using boundary polygons from a floor map (Ordnance Survey Landline in GIS) with a buffer one pixel wide drawn around them. Each house contributed one thermal radiosity value, the average over all pixel values inside the boundary.



Figure 3-5: Photographs of houses surveyed (Allinson 2007), figure 10-2 (image courtesy D. Allinson)

### 3.7.2 Sensitivity analysis

Measuring roof surface temperatures by installing thermocouples on a number of roofs was found neither practicable nor helpful, as it had produced only one *value* for each house. A correlation expressing the roof temperature  $T$  as a *function* of the insulation thickness  $D$  and all disturbance parameters (vector  $\mathbf{p}$ ) was sought instead. To this end, a simplified building model was developed describing the loft air space of each house by a single zone. The zone model  $Z$  calculates the roof temperature  $T$  in steady state as  $T_z = Z(D, \mathbf{p})$ . The roof temperature is derived independently as  $T_c = C^{-1}(I, \mathbf{p})$ , where  $I$  denotes an infrared image containing the particular roof and the letter  $C$  refers to the *camera model*, which is inverted in this case (figure 3-6). Figure 3-7 illustrates the building zone model and the assumptions made about the construction and the heat transfer mechanisms.

All parameter values and their uncertainties had to be determined as accurately as possible. Each parameter component  $p$  was modeled individually by a normal distribution  $(\mu_p, \sigma_p)$  with mean  $\mu_p$  and standard deviation  $\sigma_p$  producing a standard uncertainty interval  $[\mu_p + \sigma_p, \mu_p - \sigma_p]$ . For example, the inside air temperature  $T_{inside}$  was determined to be  $18 \pm 1^\circ\text{C}$ . The crucial emissivity values of roof tiles were calibrated in a thermal test chamber to a high accuracy obtaining  $\varepsilon = 0.881 \pm 0.003$ . The parameters are listed in table 3-4 for the thermography model and in table 3-5 for the zone model, respectively. The mean values are referred to as ‘reference’ values in fig. 3-6 and in the tables.

Name	Unit	Meaning	Reference value(s)	Uncertainty ( $1\sigma$ )
$\tau$	-	Transmittance of atmospheric layer below the airplane	0.83	0.016
$\varepsilon$	-	Emissivity of roof tiles	0.881 clay, 0.925 slate	0.003
$L_u$	W/m <sup>2</sup>	Up-welled radiation intensity of the atmosphere below the airplane (in the spectral band of the IR detector)	3.51	0.07
$L_d$	W/m <sup>2</sup>	Down-welled radiation intensity of the hemisphere reflected from the roof towards the camera (in the spectral band of the IR detector)	7.41	0.14
$L_{bg}$	W/m <sup>2</sup>	Background radiation intensity reflected from the roof towards the camera (in the spectral band of the IR detector)	derived/equated	?
$F$	-	Sky view factor	0.734, 0.832	0.02
$\theta$	°	Roof sloping angle	45, 18.43	0.4
$DN$	-	Detector output for each roof surface, averaging the associated roof pixels and all 12 house types	104.9	1.3

**Table 3-4:** Input parameters of the radiometric camera model (Allinson 2007)

Name	Unit	Meaning	Reference value(s)	Uncertainty ( $1\sigma$ )
$T_{air}$	°C	External air temperature	4.5	0.4
$T_{inside}$	°C	Inside air temperature	18	0.8
$T_{sky}$	K	Clear sky temperature (broad band)	261.0	1.2
$T_{bg}$	°C	Background temperature from other buildings/objects	derived/equated	?
$\varepsilon$	-	Emissivity of roof tiles	0.881, 0.925	0.003
$F$	-	Sky view factor	0.734, 0.832	0.02
$v$	m/s	Wind speed	2.4	0.5
$l_{bg}$	m	Building length	5.9	0.04
$w_{bg}$	m	Building width	6.4	0.04
$\theta$	°	Roof sloping angle	45, 18.43	0.4
$D$	mm	Loft Insulation thickness (uppermost ceiling)	50, 150, 250	6
$n$	h <sup>-1</sup>	Air exchange rate of roof air space	2	0.8

**Table 3-5:** Input parameters of the building zone model (Allinson 2007)

The impact of input uncertainty on the calculated temperatures was analyzed, next. In a first step, the sensitivity of roof temperatures to single-parameter variations ( $\pm 10\%$  around their reference values in steps of 2%) was estimated, while all other parameters were fixed at their reference values. The roof temperatures estimated from the infrared camera model turned out to be most sensitive to atmospheric transmittance  $\tau$ , followed by roof emissivity  $\varepsilon$ , up-welled radiation  $L_u$ , and the averaged sensor output ( $DN$ ), shown in table 3-4. Roof temperatures estimated in accordance with the zone model were most sensitive to these six parameters, in order: external air temperature  $T_{air}$ , sky view factor  $F$ , sky temperature  $T_{sky}$ , emissivity  $\varepsilon$ , wind speed  $v$ , and air exchange rate in the loft space. The background temperature  $T_{bg}$  was equated with the roof temperature for the sake of simplicity (Allinson 2007). It is rated a sensitive parameter as well if specified in °C instead of Kelvin because a moderate mere 1°C difference causes a large relative error.

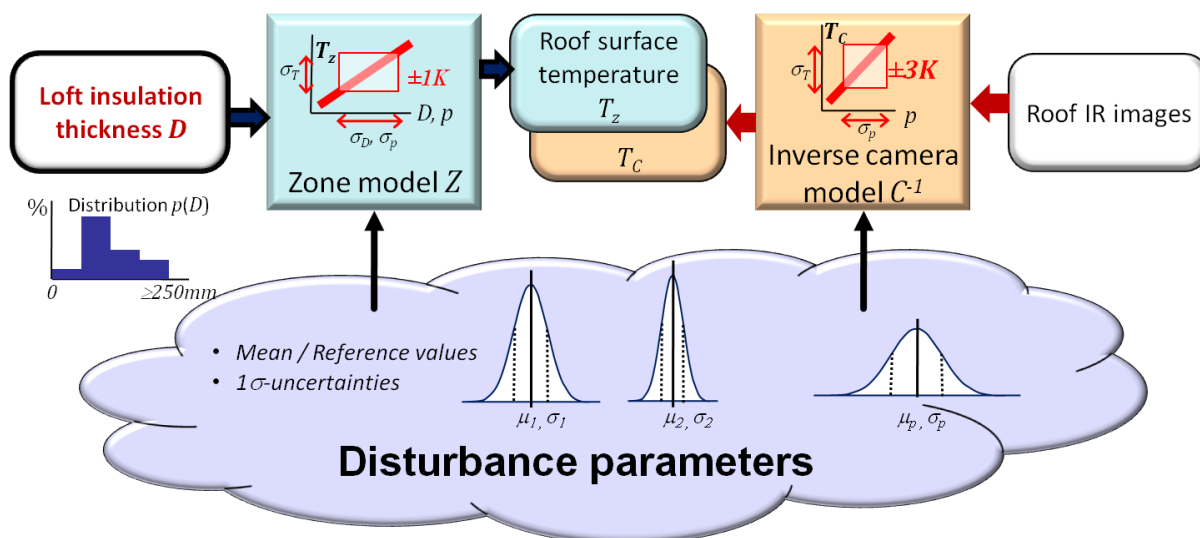


Figure 3-6: Overview of Allison's sensitivity analysis (author's illustration after Allison 2007).

An expected difference of  $\approx 0.5^\circ\text{C}$  in the roof temperature, only, distinguishes a well-insulated house from a poorly-insulated one but it could also result from a mere 1% error in transmittance or 2% error in emissivity estimates.

In the second step, all input parameters were varied jointly in 1000 Monte-Carlo simulation runs, and roof temperatures were calculated for 12 types of houses in both models: two roof types (clay roof with 1:1 sloping or shingle roof with 1:3 sloping) combined with two postures (mid or end terrace) and three insulation thicknesses (50/150/250 mm). Empirical normal distributions of the resultant roof temperatures were then construed for each case.

Varying the thickness of insulation between 0 mm and 250 mm and also the disturbance parameters in the zone model within  $1\sigma$  intervals caused roof temperature variations of only  $\approx \pm 1^\circ\text{C}$  for  $T_z$  whereas  $1\sigma$  parameter perturbations of the camera model caused roof temperature variations as large as  $\approx \pm 3^\circ\text{C}$  for  $T_c$  (figure 3-6). In other words, the impact of the goal variable of insulation thickness on roof temperature is dominated by, or lost in, the uncertainties of aerial infrared measurements.

In order to derive a binary decision criterion "*Needs retrofitting*", an insulation thickness of 175 mm was set as a threshold and converted to a corresponding threshold of the roof temperature predicted by the zone model. The latter threshold was then used in thermography evaluation to classify the roofs, and the results were compared to the known values of insulation thickness. In the resultant confusion matrix, the ratio of correct classifications reached only 54% on the average, though varying with the types and locations of houses. This finding implies a random classification result.

The negative outcome is partly due to the top-down sensor geometry and to roof designs allowing insulation to be observed only indirectly through the loft air space with an extremely high thermal resistance. The sky radiation reflected from the roof and the (partly compensating) convective heat gains by wind in clear and cold winter nights, as well as atmospheric transmittance, have a huge impact on calculated temperatures, but are hard to determine accurately. This result should be suggestive to anybody planning large-scale outdoor surveys and attempting naïve interpretation of imagery, i.e. not backed by accurate thermodynamic modeling of the urban environment.

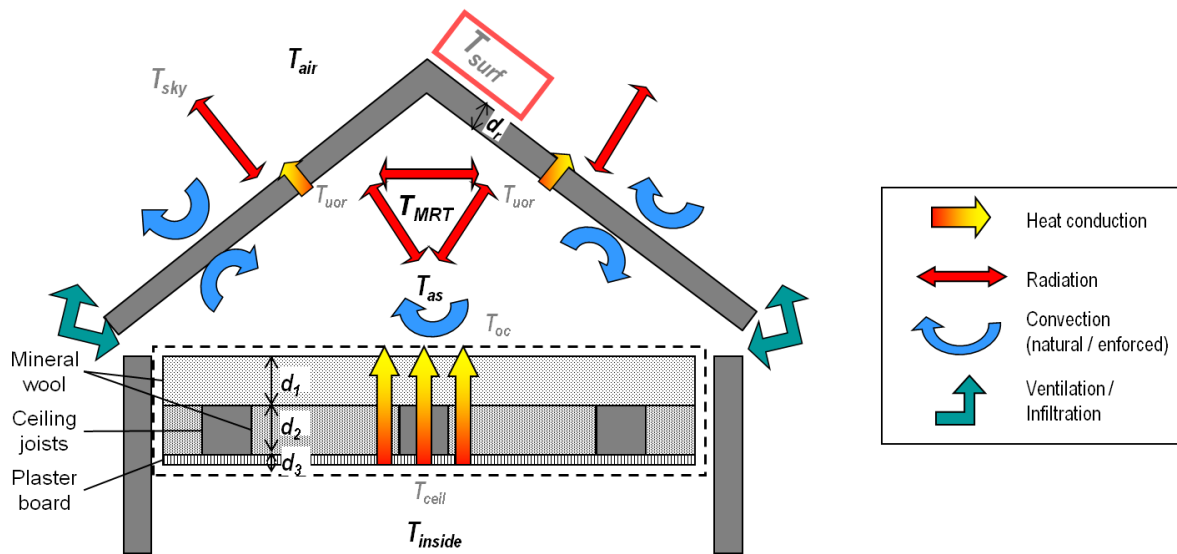


**Figure 3-7:** Building zone model, constructional assumptions, and heat transfer mechanisms considered; adapted from figures 5-3, 5-4, 5-5, and 6-1 in (Allinson 2007). Black letters symbolize air temperatures, gray letters object or surface temperatures. Radiative exchange in the closed loft air space is modeled by the **mean radiant temperature network** ( $T_{MRT}$ ).

### 3.7.3 Problems and limitations

Several sources of inaccuracy remaining in aerial thermography were identified and are summarized below. The five listed first may be eliminated gradually by improved software support, in particular by relying on accurate semantic building or city information models. Three remaining problems seem to be intrinsically tough owing to large-scale aerial surveying carried out from a long distance.

- ✓ Precise **emissivity** estimates of many different **roof tile materials** are difficult and cumbersome to make, but they are crucial to accurate temperature measurement, constituting an obstacle to large-scale thermography application. Ideally, one would expect building information models to hold material coefficients individually, including emissivity values, and keep them up to date for repeated surveys.
- ✓ Calculating the **effective emissivity** of an **entire roof surface** is inaccurate because it is not known which pixel belongs to which roof surface patch. This is a minor restriction due to the lack of image *segmentation* and outside the scope and purpose of Allinson's work.
- ✓ Calculating more accurate individual **sky view factors** is important and can be performed very efficiently assisted by GPU rendering of 3D city models.
- ✓ Equating **background temperature** with roof surface temperatures appears to be the single most problematic assumption or simplification in the camera model. It could be avoided by coupling thermography with a 3D city model to predict radiation from background objects individually. If this is considered too costly, the class of background surfaces viewing the sky could still be distinguished from those that don't.
- ✓ Similarly, real building **occupancy**, **inside temperature**, and **air change rates** could be captured more accurately but also more costly, by running calibrated BPS models with accurately determined load conditions.

- Local **wind direction** and **wind speed** near houses are sensitive parameters changing quickly. Accurate real-time measurement is essential for correct IR image interpretation and parameter identification, possibly by using mobile local weather stations at selected sites.
- **Urban topography** and **microclimate** (small valleys or hollows, hillsides, street canyons, urban heat island, smog,...) greatly influence parameters of the transient thermal load, such as air and ground temperatures, local wind, atmospheric transmittance, up-welled radiation etc., and thus affect thermographic results. However, in no case would the computational expense be justified employing a detailed *urban climate model* to predict these effects.
- Condensation of **moisture** (dew), **rain** or **snow** on roof surfaces greatly complicate thermographic analysis or even make it impossible.

The objectives of quantitative geo-reference thermography (QGT) and the type of surveys planned here differ from Allinson's study in several aspects; the main differences are summarized in table 3-6. However, the comparison should not falsely represent that error sources analyzed by Allinson will be simply avoided and therefore not be an issue in our project. In a sense, our promises and claims are broader and more general; therefore one might argue QGT being even more prone to errors. Performing quantitative sensitivity analyses of various disturbances along Allinson's line of work will be a key research question which will become evident in the following chapter.

	<b>Aerial thermography</b> (Allinson 2007)	<b>QGT</b> [HGF/TIG Sub-Topic 2.5.5]
<b>Objective</b>	"One-off" scenario: Estimating <b>absolute</b> parameter values and properties from a <b>single survey</b> .	Estimating parameter <b>changes</b> due to aging or discrepancies design ↔ as-built, comparing <b>different</b> surveys and simulations.
<b>Methodology</b>	<b>House 'templates'</b> ; anonymous / partially known houses. No 3D city model used. Goal variables estimated via roof temperatures, separating BES from IR camera model. <b>Fixed</b> measurement geometry.	Houses <b>modeled individually</b> (3D BIM / BES). IR camera model integrated into building simulation as a mobile observer; <i>goal parameters</i> estimated directly from radiance images, not temperatures (inverse model). <b>Variable</b> measurement geometry.
<b>Surveying conditions</b>	Nocturnal <b>aerial</b> (top-down) survey. Long distance (e.g. 760 m), low spatial resolution. Disturbances by up-welled and down-welled radiation and atmospheric transmittance. Targets (insulation) thermally shielded from the IR camera by the loft air space beneath the roof.	Day or night surveys mostly at <b>ground</b> level Outdoor, similar to (Stilla, Hoegner 2008), and indoor ⇒ Shorter distances (1-50m), higher spatial resolution, less atmospheric disturbance, but <b>solar radiation</b> . Targets (windows, walls / façades, insulations) may be more exposed.
<b>Speed, cost</b>	Very fast, completely non-invasive.	Slower, slightly more invasive Much higher surveying cost.

**Table 3-6:** Main differences between the conditions of aerial thermography after (Allinson 2007) and QGT.



## 4 Quantitative Geo-referenced Thermography

In this chapter, the systems-theoretic concept underlying quantitative geo-referenced thermography (QGT) is defined and key research ideas and problems are outlined. The concept is closely linked to building energy simulation (BES) models as dynamic systems represented in state space (section 4.1). Simulation model extensions for mobile measurement and parameter identification are proposed in section 4.2 and the errors introduced thereby are analyzed. In section 4.3, innovative applications to the building lifecycle are proposed and the potential benefits are discussed. Two technical details, the mobile observer interface and the localization of the infrared camera, are covered in section 4.4. Building simulators offering new interfaces for remote identification (QGT) and lifelong monitoring of buildings require support from the semantic data model (BIM) lying at the root; preliminary specifications to meet these requirements are proposed in section 4.5. Finally, the research questions and agenda to be addressed in the remaining project phase are summarized in section 4.6.

### 4.1 Thermodynamic building model

Modeling the heat flux between thermal nodes in a network forms the core of (transient) building energy simulation. The *thermal nodes* carry temperature attributes and represent either *volumes*, or *bounding surfaces* of volumes, such as reflective window glazing. Volumes are divided into *building elements* made of solid material (e.g. concrete slabs, steel or wooden frames, glass façades, multi-layered insulation) and in *air zones*. Heating and cooling energy demand and primary energy input are the simulation goal variables and are calculated from the heat flux by means of efficiency or utilization factors (Hirschberg 2008; DIN V 18599).

Heat transfer inside an element is modeled by subdividing the volume into (infinitesimal) small elements  $\Delta V$ . The temperature  $T(\mathbf{x}, t)$  of an element  $\Delta V$  at position  $\mathbf{x} = (x, y, z) \in \mathbb{R}^3$  in Cartesian coordinates and at time  $t$  changes at a rate proportional to the sum of all gains and losses in terms of heating power [W], or power per unit volume [W/m<sup>3</sup>] (see figure 4-1 for illustration):

- the heat flux  $Q_{dif}$  conducted to or from *neighbor* elements  $\Delta V'$  (*diffusion* in  $x$ ,  $y$  or  $z$  direction),
- the remaining heat flux  $Q_S$  (*sources/sinks*) not captured by  $Q_{dif}$ , due to one of the following:
  - S1 Different modes of heat transfer, i.e. *convection* or *radiation* with other thermal nodes in the network;
  - S2 Heat sources or sinks of arbitrary type *inside*  $\Delta V$ <sup>22</sup>;
  - S3 Heat sources or sinks *external* to the network and acting as model input, e.g. gains and losses due to weather influences and to heating or cooling units.

By the law of energy conservation, the total rate of heat gain or loss at  $\Delta V$  equals

$$\rho c \frac{\partial T}{\partial t} = \underbrace{Q_{dif}}_{diffusion} + \underbrace{Q_S}_{source} = \kappa \underbrace{\left( \frac{\partial^2 T}{\partial x^2} + \frac{\partial^2 T}{\partial y^2} + \frac{\partial^2 T}{\partial z^2} \right)}_{divergence \nabla^2 T := \nabla \cdot (\nabla T)} + Q_S \quad eq. (4-1a)$$

<sup>22</sup> Chemical (exothermic or endothermic) reactions or phase changes inside the material act as heat sources or sinks which, for instance, is exploited in innovative thermal storage systems. In building simulations today they still play a minor role and are therefore ignored in the theoretical exposition.

Where  $\rho$  [ $kg/m^3$ ] and  $c$  [ $Ws/(kg\cdot K)$ ] denote the specific weight and the heat capacity, respectively. The partial differential equation (4.1a) known as Fourier's law (Çengel 2003) holds for *constant heat conductivity*,  $\kappa$  [ $Wm^{-1}K^{-1}$ ]. Conductivity is assumed independent of the direction of heat diffusion, the temperature  $T$  and the material properties. The diffusion term  $\nabla^2 T$  in eq. (4.1a) expresses the divergence of *spatial heat flux*  $\nabla T$  inside the volume, heat flowing in the direction of steepest temperature change which is the gradient direction  $\nabla T = (\partial T/\partial x, \partial T/\partial y, \partial T/\partial z)^T$ .  $\nabla T$  vanishes if the element adopts uniform temperature or has zero extent in the gradient direction. With a constant temperature gradient, temperature changes linearly in space and  $\nabla^2 T$  vanishes; therefore, the partial differential equation in (4.1a) reduces to an ordinary one:  $\rho c \partial T/\partial t = Q_S$ . The heat equation is actually specified in (4.1a) as heating power *per unit volume* [ $W/m^3$ ], or *power density*; multiplying with the volume  $V$  of the element  $\Delta V$  gives the more familiar form

$$V\rho c \frac{\partial T}{\partial t} = mc \dot{T} = VQ_S [W]. \quad eq. (4-1b)$$

Conduction is completely characterized by heat capacity and conductivity in eq. (4-1a). When a volume element contains neither internal heat sources or sinks (S2) nor control inputs (S3), the remaining source term  $VQ_S$  is a summation of all convective and radiative heat fluxes due to external objects (S1) and interacting via  $\Delta V$ 's *bounding surface* (areas  $A_i$ ). This may be written as<sup>23</sup>:

$$mc \dot{T} = VQ_S = \sum_i A_i H_i (T_i(t) - T(t)). \quad eq. (4-1c)$$

Each term in (4.1c) is proportional to the driving temperature difference with a *heat transfer coefficient*  $H_i$  [ $W/(m^2K)$ ] explained below.  $Q_S$  may be nonzero for arbitrary fluid elements or transparent solids, but in the most common case of opaque building materials, it is nonzero only for elements  $\Delta V$  located at the volume boundary.

Under steady-state conditions defining a 'thermal equilibrium' ( $\dot{T} = 0$ ):

$$\sum_i A_i H_i (T_i - T) = 0. \quad eq. (4-1d)$$

#### 4.1.1 Thermal coefficients

Riveting next on radiation and convection, the heat transfer between elements  $i, j$  assuming temperatures  $T_i, T_j$  is specified by coefficients  $H_{i,j}^{rad}, H_{i,j}^{conv}$ , respectively.

As to radiation, the total power emitted by a black body equals  $Q^{rad} = \sigma \cdot T^4$  [ $W/m^2$ ] (Stefan-Boltzmann constant,  $\sigma$ ). The *net radiation* exchanged among  $n$  gray bodies depends on their emissivity values  $\varepsilon_i, 0 \leq \varepsilon_i \leq 1$  and the *geometric views factor*  $0 \leq F_{ij} \leq 1$  describing mutual visual relationship. The net radiative heat flux (gain or loss)  $Q_i$  experienced by the  $i$ -th body is approximately linear in temperatures, i.e. may be written as a linear combination of temperature differences:

$$Q_i \approx \sum_{k,l} A_k H_{k,l}^{rad} (T_k - T_l) \quad (1 \leq k, l \leq n) \quad [W/m^2K]. \quad eq. (4-2a)$$

---

<sup>23</sup> Since the heat energy flows from the warmer to the cooler body, the flux  $Q_{Si}$  is positive (indicating heat gain) for  $T_i > T$  and negative (heat loss) for  $T_i < T$ .

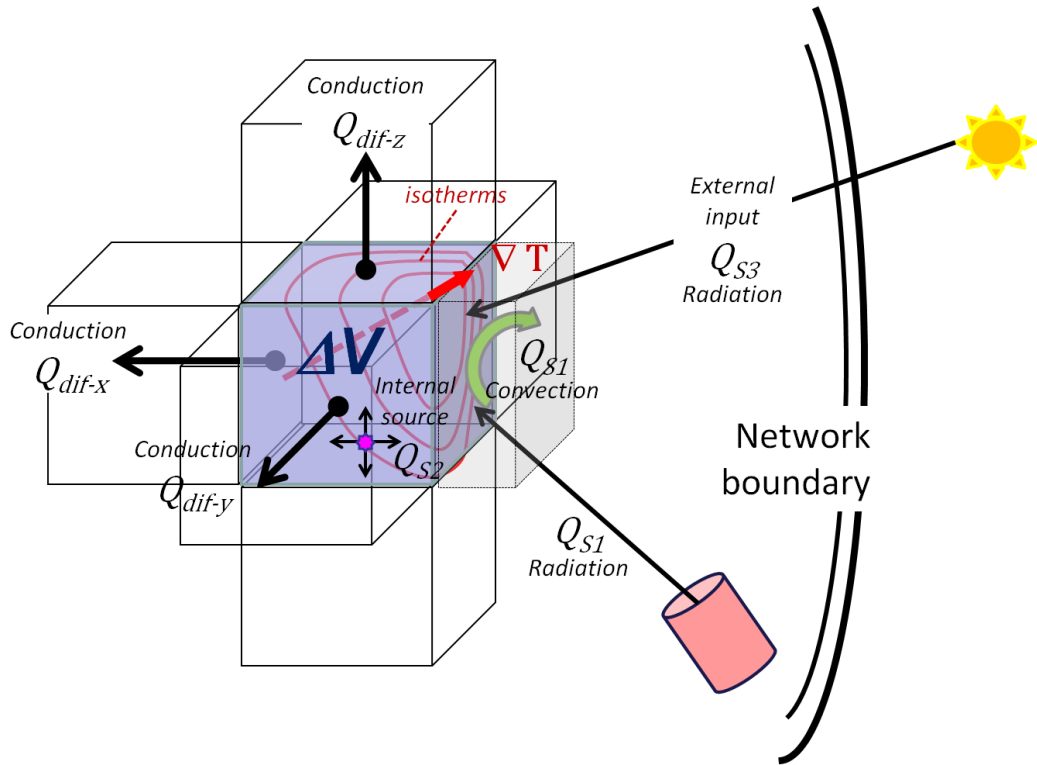


Figure 4-1: Heat balance of a volume element  $\Delta V$  in a thermal network (see text).

The radiative heat transfer coefficients (RHTC)  $H^{rad}$  are temperature dependent on their part, growing with the third power of some mean temperature, see Appendix A.4 for details.

A *view factor*  $F_{ij}$  indicates the fraction of total radiant power emitted by an object  $i$  impinging on object  $j$ . The *sky view factor* of a flat (roof or window) surface captures the fraction of hemispherical area viewing the sky; it is a special case. View factors are important in this work, for instance, to explain the radiosity received by a *detector surface* element of an infrared camera, see appendix A.2 for details. We keep in mind that view factors are purely geometric properties calculable from distances, sizes, and relative orientations of object surfaces. Therefore, emissivity values are the only unknown quantities to calculate the RHTC in eq. (4.2a).

As for convective heat transfer coefficients (CHTC)  $H^{conv}$ , a plethora of correlations have been derived for different cases occurring in practice, such as natural convection, indoor ventilation distinguishing stably-stratified and buoyancy-driven conditions in buildings, and forced convection onto the envelope under wind pressure (DOE 2010)). Some formulae have been found empirically, others were derived by analytical models reducing convection to heat conduction occurring at boundary layers. CHTC may be temperature dependent on their part, modeled by some slowly-growing rational function of temperature difference. For natural convection, Allinson uses the formula (Allinson 2007 eq. 6-4)

$$H_{air,surf}^{conv,n} \propto (T_{air} - T_{surf})^{1/3} \quad [W/m^2K] \quad eq. (4-2b)$$

and for forced convection, a correlation depending on the local wind speed  $v$  [m/s] but not on the temperatures is quoted (Allinson 2007 eq. 6-12):

$$H_{air,surf}^{conv,f} \propto v^{1/2} \quad [W/m^2K]. \quad eq. (4-2c)$$

The proportionality indicated in both formulae depends on terms calculable from the geometry, such as roof surface orientation, perimeter, and area, while other terms may be unknown, such as the surface roughness index.

### 4.1.2 Numerical solution

The heat equations (4.1a, b, or c) are numerically solved using finite difference approximations of the derivatives and assuming known initial states (for  $t = 0$ ) and known boundary temperatures, for arbitrary  $t$ . Often, a uniform quantization of space  $\Delta x$ ,  $\Delta y$ ,  $\Delta z$  and time  $\Delta t$  is performed, obtaining the simplest possible discrete approximation as follows:

$$\begin{aligned} \frac{\partial T(\cdot, t)}{\partial t} &\approx \frac{T(\cdot, t+\Delta t) - T(\cdot, t)}{\Delta t} \\ \frac{\partial^2 T(x, \cdot)}{\partial x^2} &\approx \frac{T(x+\Delta x, \cdot) + T(x-\Delta x, \cdot) - 2T(x, \cdot)}{(\Delta x)^2} \end{aligned} \quad \text{eq. (4-3a)}$$

Employing a *location-based* geometry representation such as a uniform grid for heat transfer is not essential, however. *Feature-based* geometries mixing finite elements of arbitrary shape and choosing individual dimensions of heat transfer (1D-, 2D- or 3D) lead to state vector representations as well (Nakhi 1995). Collecting all node temperatures in an  $N$ -dimensional state vector  $\mathbf{T}$  and evaluating the equations (4-1a, b) with the approximation (4-3a) at discrete time steps yields the following discrete-time matrix system ( $\mathbf{T}[k] := \mathbf{T}(k \cdot \Delta t)$ ):

$$\mathbf{T}[k + 1] = \mathbf{A} \cdot \mathbf{T}[k] + \mathbf{B} \cdot \mathbf{u}[k] \quad (\mathbf{A} \in \mathbb{R}^{N,N}, \mathbf{B} \in \mathbb{R}^{N,M}). \quad \text{eq. (4-3b)}$$

The *system matrix*  $\mathbf{A}$  contains all interactions between thermal nodes of type (S1) mentioned above and is often rather sparse. All source terms due to weather influences and HVAC input (S3) are pooled in the control vector  $\mathbf{u}$ . Though the system equation (4-3b) is linear in the state  $\mathbf{T}$  because of the form of equations (4-1a,b,c) and (4-3a), it is neither strictly linear nor time-invariant because the matrices  $\mathbf{A}$  and  $\mathbf{B}$  contain nonlinear, time dependent, and occasionally even state dependent *coefficient functions*, as seen in eq. (4-2a, b), for example, and explicated further below.

Equation (4-3b) is quoted being in *explicit form* (Nakhi 1995) because the new state  $\mathbf{T}[k+1]$  directly results from previous state values. In *implicit form*, the new state appears as an unknown quantity in an algebraic equation that needs to be solved for. The implicit form enjoys better *numerical stability*. When the explicit solution is calculated with time steps  $\Delta t$  too large in relation to the spatial resolution  $\Delta \mathbf{x}$ , numerical oscillations and even instability may occur. As long as a unique solution for  $\mathbf{T}[k+1]$  exists, implicit and explicit forms are functionally equivalent, i.e. we may assume the explicit form (4-3b) without loss of generality.

Time steps in building simulations often follow the hourly available weather data ( $\Delta t = 1h$ ). Accurate simulation of large thermal masses like floor slabs, however, requires much finer time resolution of  $\Delta t \approx 1min$  to ensure numerical stability (Urban 2007).

### 4.1.3 Simulation model

Next, the system equation (4-3b) is written more verbose to make the information structure explicit and group the influence factors according to their meaning in the building domain:

$$\mathbf{T}[k + 1] = \mathbf{A}(\mathbf{T}, \mathbf{g}, \mathbf{p}) \cdot \mathbf{T}[k] + \mathbf{B}(\mathbf{T}, \mathbf{g}, \mathbf{p}) \cdot \mathbf{u}[k] \quad \text{eq. (4-3c)}$$

Where

- **g** embodies all **geometric** and **topological** properties. The interconnection structure encoded in matrix **A** reflects the adjacency of components, spatially or in terms of heat flow, and thus forms the backbone of the heat transfer model. Dimensions (component sizes) and view factors influencing the HTC come under the geometry properties and therefore appear in matrix coefficients. Strictly speaking, the *choice* of state vector reflects a geometric decision of its own. To make **T** independent and concentrate all geometry information in **A**, the state vector **T** could be defined on an 'ultra-fine' base grid to which any finite-element geometry could be mapped via a binary interconnection matrix.
- **p** denotes the vector of **parameters** characterizing the **condition** of building components or materials numerically, *at the respective level of detail* represented by the model. The reader is referred to table 3-3 listing the candidate parameters to be identified. Parameters should be irreducible computationally and *independent of time, state, and geometry*. In other words, parameters are *atomic* quantities neither computable from other quantities nor queryable from a database, catalogue or BIM document, nor known constants of building physics or directly measurable quantities. Too many parameters will remain, anyhow, rendering identification and condition estimation under-determined. Therefore, we avoid diluting the estimation accuracy further by including variables that could be determined by other means. A few examples will help to clarify this important point.
  - The *conductive HTC* through a one-dimensional layer is described by the formula  $H^{cond} = \kappa/D$  with thermal conductivity  $\kappa$  of material and layer thickness  $D$  [m]. When conductivity on its part is not constant but temperature dependent,  $\kappa$  may be modeled as a polynomial function of object temperature  $T$ :  $\kappa(T) = a_0 + a_1T + a_2T^2 + \dots$ . At this particular level of model detail, the coefficients  $a_0, a_1, a_2, \dots$ , are the **only** parameters to be estimated and found in the vector **p**.  $T$  is a computable state variable,  $D$  a geometric property 'looked up in the BIM file', the resulting coefficient  $H^{cond}$  is a compound expression, but none of these is considered a 'parameter'.
  - A *window shading coefficient* indicates the time-integrated fraction of window area which is not exposed to sunlight; it can and should be *calculated* from the building and environment geometry, the solar equation at the geographical site, and possibly a weather profile indicating cloud cover. Hence it is *known* in principle and should not be considered a free variable to be calibrated.
  - On the other hand, a *window U-value* for a *specific window* (unlike the U-value for new windows of this type obtained from a catalogue of building components) may be a calibration parameter.
- **B·u[k]** captures the **load** acting upon the building. The vector **u** comprises **weather data** (outdoor air and soil temperature, humidity, wind speed, cloud cover, and solar irradiation) and **occupancy schedules** as far as the thermal building load is affected. Occupants change HVAC setpoints, they open windows or operate shading devices<sup>24</sup>, act as heat gains by their sheer presence, and operate electrical devices acting as heat sources or sinks of their own. The index  $[k]$  indicates time dependence, i.e. the load is specified as a time function or time series.

Our sharp distinction between 'load' variables and 'parameters' is not grounded in building *physics* but in the logic of dynamic systems identification: building load is a free (independent) *input* variable awaiting to be set (predefined) while calibration parameters are *output (dependent)* variables. We

---

<sup>24</sup>From the perspective of the *building* model taken here, occupants' actions are *inputs* whereas thermal comfort is an *output* (goal) variable. From the opposite perspective, thermal comfort (or the lack thereof) is input to the *user* and his/her *reaction*, i.e. changes in HVAC settings, operating windows or blinds, is the output!

seek parameter values that minimize the measurement error *under all* possible inputs, in a weighted mean sense; and thereby reflect the *building condition*. Initial states and load for measurement prediction are *forced* to match the conditions of each corresponding measurement campaign. Our task is *not* to *determine some* load schedule under which the model best fits the measurement data.

Determining accurately the load schedules of an occupied building is laborious and difficult and, in several studies, poses a major goal of its own (Heidt et al. 2003; Sun 2004; Torcellini et al. 2006) and is referred to as calibration or model identification, as well. But this task never comes under the term of parameter identification in our work.

At this point, we introduce some extra notation which is due to the overloaded use of *parameter collections*, or *parameter vectors* in this report. For the purpose of system identification, a *vector*

$$\mathbf{p} = (p_1, \dots, p_m)$$

has the standard mathematical meaning of an ordered set of scalar components (values!)  $p_i$  being a member of a normed *vector space*, the Cartesian product of component spaces (fields) endowed with a vector norm  $\|\cdot\|$ . On the other hand, a parameter vector also denotes a collection of variables possessing names, values, and types. In the representation

$$\mathbf{p} := (\mathbf{p}_1, \dots, \mathbf{p}_m)$$

each  $\mathbf{p}_i$  is a *triple*  $(id_i, p_i, \mathbf{P}_i)$ ,  $id_i$  denoting the *name* or unique *identifier* of the  $i$ -th parameter,  $p_i$  its current *value*, and  $\mathbf{P}_i$  the set (or *type*) of possible values it may take. In this notation, the parameter vector resembles a STRUCT in a programming language like C++ or C# allowing heterogeneous components. In particular, parameter vectors may be distinguished or compared as *unordered sets of identifiers* where two members appearing in different models are considered equal if they denote the *same physical quantity* in a building.

Let  $\mathcal{P} = \{id_i\}_{1 \leq i \leq m}$  denote the set of identifiers of a parameter vector  $\mathbf{p}$  with  $m$  components.

To avoid unnecessary subscript/superscripts, this shorthand notation is applied to arbitrary symbols; for instance,  $\mathbf{P}$ ,  $\mathbf{P}'$ ,  $\mathbf{Q}$ , respectively, denote the value sets and  $\mathcal{P}$ ,  $\mathcal{P}'$ ,  $\mathcal{Q}$  the identifier sets of some parameter vectors  $\mathbf{p}$ ,  $\mathbf{p}'$ , and  $\mathbf{q}$ .

Before proceeding with the identification methodology, one more aspect of the modeling architecture is discussed. Henceforth, building models will be drawn by simplified diagrams with one input, the load, and two outputs denoted measurement and goal variables, respectively (fig. 4-2, all input and output signals are understood as being time functions). The distinction between the two output variables simply is as follows:

- *Goal variables* comprise whatever items the *simulation user* (architect or engineer) is interested in, including consumption of energy of different carriers [ $kWh$ ], functional building performance, and derived efficiency figures such as the functional building performance delivered per unit of input energy, which was mentioned in chapter 2.
- *Measurement* output, e.g. temperature fields, is designated for *identification*. Some output quantities may be measurable and goal variables at the same time, for instance, energy consumption.

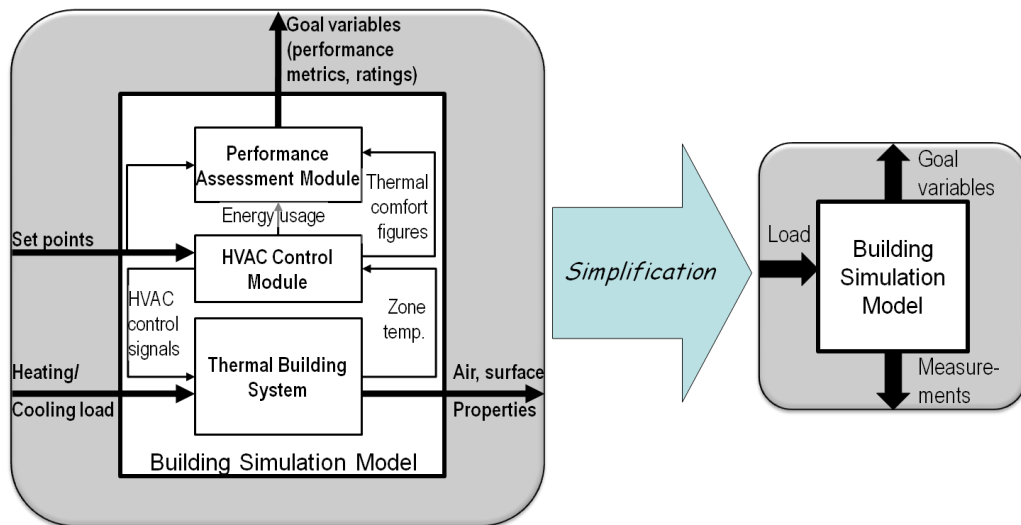


**Figure 4-2:** Simplified building model (right) and the explicit control architecture imagined and actually implemented in a simulation (left).

The internal model structure realizing the behavior could be complex, providing separate, *hierarchically coupled* subsystems of measurement and control (fig. 4-2 left). The *control output* at one layer specifies *set points* for the next-lower layer while the *goal output* provides *measurement* input to the next-higher layer. Heat and mass flow between air zones, building envelope, and thermal masses are simulated on the bottom layer, their input being the weather load and the HVAC control signals commanding heating and cooling power, i.e. binary values (ON|OFF) or real-valued thermostat set points. Temperature and humidity measurements are sent to the HVAC *control algorithm module* on the middle layer. Information relevant to assess thermal comfort is forwarded to the *performance assessment* layer on top. Lower layers often contribute details in the form of diagnostic goal variables explaining where and why building performance leaves to be desired, such as periods of simultaneous heating and cooling observed, part load operation, or coefficients of performance of a ventilation unit (Hitchcock R.J. 2002).

#### 4.1.4 Heat, air, and moisture transfer

A range of tasks require models of **heat, air, and moisture** transfer (HAM) combined. This applies to performance assessment of ventilation, thermal comfort and air quality, natural ventilation in multi-layer façades, or estimation of the condensation risk. HAM models are frequently being implemented by modern BES such as HAMLAB (van Schijndel 2007; Li et al. 2009). Similar to the case of pure heat transfer, a zone-based geometry is taken as a basis, assuming well-mixed air zones. The state variables then consist of temperatures and moisture content or mass per zone (Nakhi 1995). The temporal process of moisture diffusion and advection is driven by the spatial gradient of vapor pressure acting as the potential, similar to the heat diffusion equation. Only laminar air flow can be modeled under these assumptions and by means of zonal HAM models.

Analyzing also turbulent air flow or irregular distributions of moisture requires advanced hygrothermal models from **computational fluid dynamics** (CFD). The space is divided into *control volumes*, forming a grid much finer in resolution than thermal zones. The state variables per control volume encompass temperature, pressure of air and water vapor, and air velocity. Solutions are based on the ideal gas equation and the conservation laws of energy, mass, and momentum applied to each

control volume. The state values initially ( $t=0$ ) and at the boundary layer of the grid must be known; at the building walls, zero air speed is assumed. In several simulations, fine-grained CFD models near critical points, such as the inlet or outlet points of a ventilation duct or major openings in the envelope, are coupled with zonal HAM models of the interior building zones (Zhong, Braun 2008; Mirsadeghi et al. 2009; Steeman et al. 2009; Steskens P. 2009). The CFD submodel receives initial and boundary values at the wall surface from the enclosing HAM zone and sends back the calculated grid values to the HAM model which forms an averaged zone value again.

In this report, we deal with pure heat diffusion and do not quote or analyze the hygrothermal extensions and their governing equations, i.e. Fick's law, Darcy's law or Luikov's equation for HAM, and the Navier-Stokes equations for CFD models, see (Heiselberg et al. 1998). However, marking out the class of transport models identifiable by means of QGT or similar mobile cameras remains a relevant research question (section 4.6.1) and will require looking closer at HAM or CFD models.

Needless to say, hygrothermal building models need their own empirical parameters to be estimated, for example, convective *mass transfer coefficients* analogous to HTC, vapor permeability, and moisture diffusivity (Plagge et al. 2005; Zhong, Braun 2008; Desta et al. 2011). Their identification demands sensors targeted to the measurement of humidity, pressure, and air flow (Desta et al. 2011; van Belleghem et al. 2011). Hygric properties of materials influence the thermal submodel via the system couplings and, therefore, may be observable *indirectly* from thermal images. However, reliable and stable estimates seem unlikely to be obtained from thermal images alone. Anyway, air flow and vapor included in the thermal model do have a major impact on temperature predictions. Narrowing down to heat coefficients and their identifiability, how does a model representing the state of moisture explicitly differ in this respect from a lumped model using a convective coefficient? This is one of the research questions posed in section 4.6.1.

## 4.2 Measurement and identification framework

Many types of processes and discrete events running at different time scales act upon building systems and influence energy consumption, as illustrated in figure 4-3. Most of the 'fast' events are weather- or occupancy-related, while processes evolving inside the building system tend to be slower. The slowest dynamics is found in degradation processes and in infrequent events such as HVAC operating strategy changes, component failure and replacement, energetic retrofitting, or changes of the building construction. Some events occur only once in the building life, for instance, initial commissioning or retro-commissioning.

The main purpose of thermographic surveys is to quantify parameter changes associated with slow processes or rare events. Slow parameters are assumed not to change significantly and are treated as being constant during the rather short duration of a survey (in the order of minutes, as shown in fig. 4-3). On the other hand, the monitoring interval, i.e. the time between consecutive surveys, is chosen long enough to detect significant changes of the variables such as component aging. In most cases, surveys are scheduled deliberately to assess specific transitions, e.g. design conditions compared to as-built ones, or performance before and after retrofitting.

Events occurring at a time scale comparable to or shorter than surveying, i.e. changes of weather or occupancy (the building load) must be captured *during* the survey, and their time functions must be imposed on the simulation model for accurate prediction. Only when the initial model state and the load trajectory accurately match the actual surveying conditions, can deviations between predicted thermal images and the actually captured ones be explained by as yet undetected parameter changes.



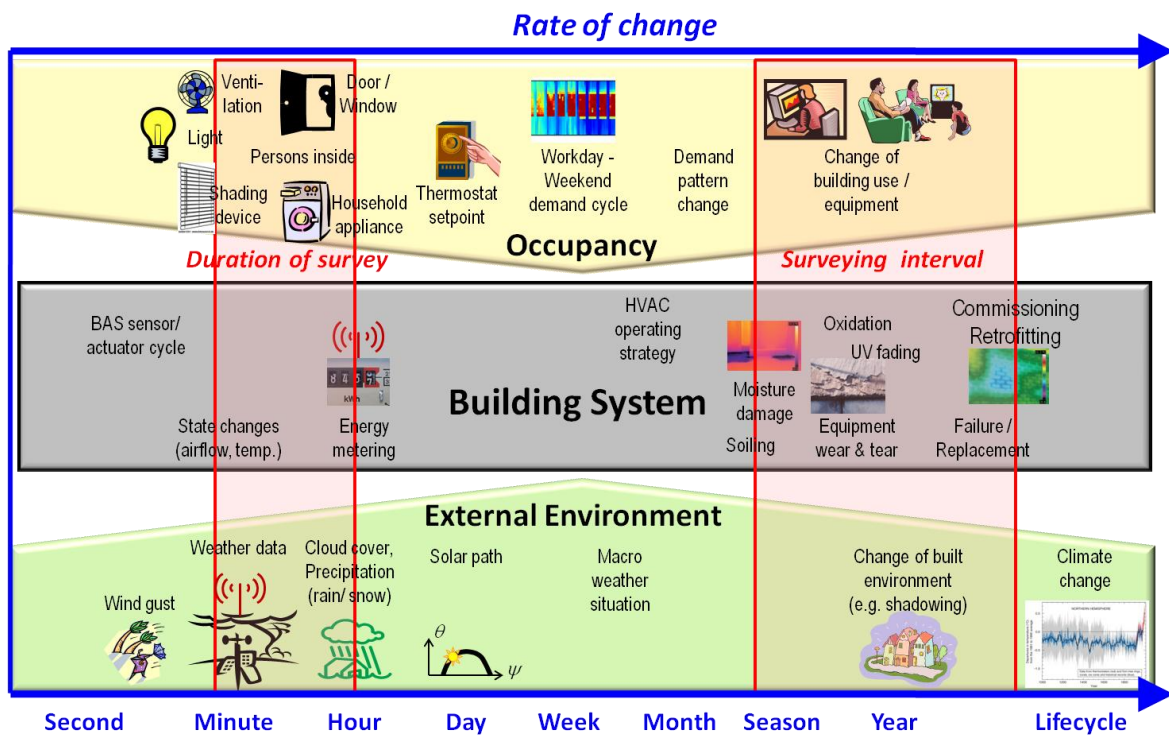


**Figure 4-3:** Time scales of building dynamics, ordered by duration, mean arrival time or rate of change. The duration of QGT surveys and the interval between surveys are indicated by red bars.

### 4.2.1 Mobile camera model

Infrared (IR) cameras sense in a specific spectral band the *radiant* heat emitted by surfaces at temperatures above 0 K; cameras for building thermography mostly operate in the *long wave* band (8-14 $\mu$ m). An IR image captures the radiation falling within a *view cone* with opening angle given by the ratio of detector array size and camera focal length; the apex is located in the optical center. The detector array dimensions determine the spatial resolution (a typical value: 320x240 pixels). Each pixel measures radiant power per unit of *solid angle* ('steradian' *sr*, [W/sr]) which is converted to unit area [ $W/m^2$ ] when the surface distances from the camera are known.

Unlike contact temperature measurements, radiant power is a complex function of the surface temperatures, their interactions including the external environment, and the detector properties, as illustrated in figure 4-4 and detailed in the appendices A.1-A.3.

1. First, the camera optics and geometry including image resolution have to be modeled. The foot print of a pixel may hit portions of several objects contributing by partial view factors. As is the case for visual cameras, geometric distortion due to lens diffraction, motion blur and, in case of a vehicle-mounted or hand-held camera, shaking must be considered.
2. For each object adopting a known temperature, the pixel value is proportional to *integral spectral power* according to the Planck equation. Spectral contribution at each wavelength depends on the spectral sensitivity as specified by the detector's *spectral response function*.
3. For each pixel, the background radiation *reflected* at the surface viewed must be determined accurately. In *outdoor* applications, sky emissivity, *up-welled* and *down-welled sky irradiance*, and apparent sky temperature are important parameters to capture, which are not

found in the building model. Packages for computing atmospheric radiation such as MOD-TRAN are widely used for that purpose (Poglio et al. 2003; Allinson 2007).

4. At longer distances, for example in airborne surveys undertaken at high altitude (Allinson 2007), the IR attenuation by the atmosphere becomes non-negligible (*transmissivity*  $\tau < 1$ ).
5. Emissivity, reflectance, and transmittance depend on the angle of incidence and/or the wavelength, though constant values are often used across wide angular or spectral ranges. In any case, *specular reflections* at windows or glass façades require special consideration and are often modeled as mixture distributions (BRDF) comprising diffuse (Lambertian) and specular terms of reflection (Krenzinger, de Andrade 2007).

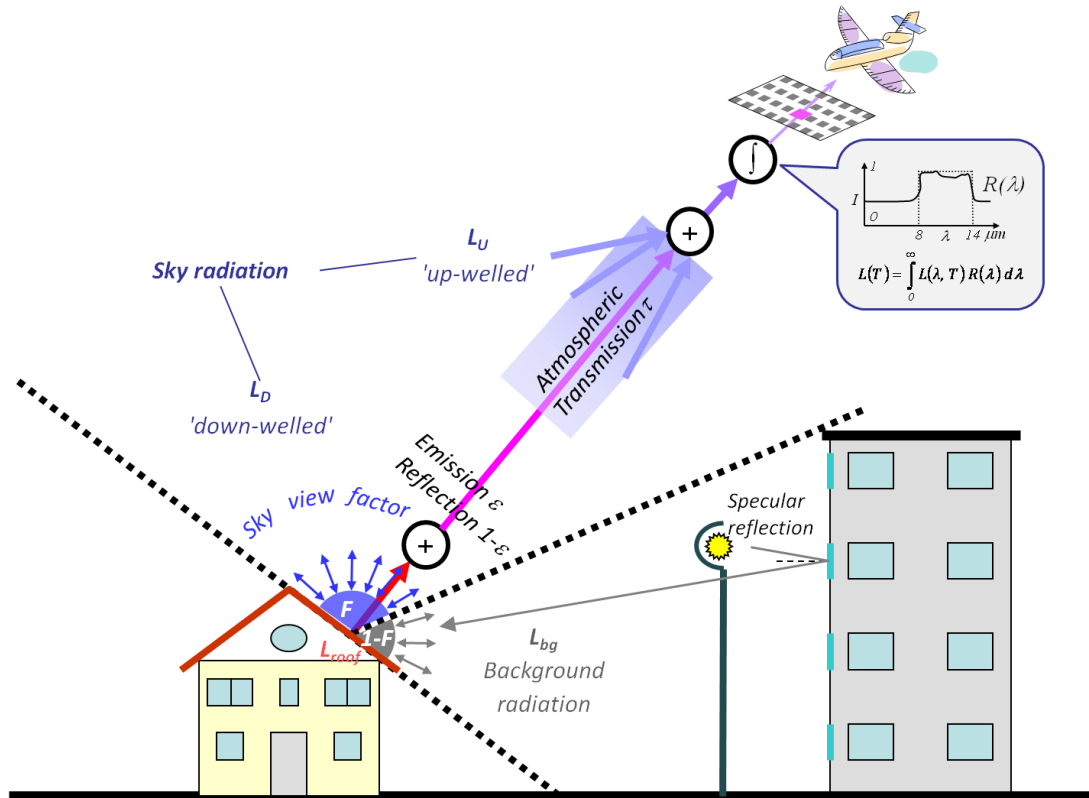


**Figure 4-4:** Illustration of a camera model for aerial thermography after (Allinson 2007). The detector mounted on an airplane (on top) receives a portion  $\varepsilon$  of thermal radiation emitted from the roof surface (bottom left) and a portion  $(1-\varepsilon)$  of radiation diffusely reflected at the roof. A rate  $F$  (sky view factor) of the latter is down-welled sky radiation and the rest  $(1-F)$  comes from the background, possibly including specular reflection at third-party surfaces. A fraction  $\tau < 1$  of radiant energy, only, is transmitted through the atmosphere which emits up-welled sky radiation on its part. The radiation arriving at the detector is spectrally weighted by its sensitivity  $R(\lambda)$  and integrated to yield the final detector value.

These influences are combined in the radiometric **IR camera model** or **measurement equation** which is added to the state equation (4-3b, c). Camera models have been developed before (Johnson et al. 1995; Poglio et al. 2003; Allinson 2007). Notably the latter study reveals that accurate calibration of the parameter values is difficult. Most camera models assume a fixed measurement geometry, for example an IR scanner looking down from an airplane in Nadir direction.

In general terms, the measurement equation reads

$$\hat{\mathbf{y}}^{IR}[k] = C(\mathbf{T}[k], \mathbf{g}^{mob}, \mathbf{u}^{IR}[k], \mathbf{p}^{IR}) + \xi[k] \tag{eq. (4-4)}$$

Where

- $\hat{\mathbf{y}}^{IR}[k]$  denotes an IR camera image *predicted* at instant  $k$  by executing the measurement equation  $C$ . The image proper is an array of pixel values. Prediction requires the state  $\mathbf{T}[k]$  depending on the initial value  $\mathbf{T}[0]$  of the survey, the load schedule  $\mathbf{U}_{[k]}$  up to time  $k^{25}$  and the unknown parameters  $\mathbf{p}$ .
- $\mathbf{g}^{mob}$  encodes the *measurement geometry*, i.e. the *mobile* camera pose. From  $\mathbf{g}^{mob}$  the components that would be seen by the camera in each pixel are known and their optical and thermal properties can be queried. The pose  $\mathbf{g}^{mob}$  has six free parameters, three for translation and three for orientation of the camera with respect to the building coordinate system.
- $\mathbf{p}^{IR}$ ,  $\mathbf{u}^{IR}$  denote vectors of empirical parameters and load, respectively, required to interpret the measurement correctly.  $\mathbf{p}^{IR}$  comprises radiometric properties, e.g. the emissivity of roof tiles or the transmittance of atmosphere, which may but need not belong to the system parameters  $\mathbf{p}$ . Therefore, in general, neither  $\mathcal{P}^{IR} \subset \mathcal{P}$  nor  $\mathcal{P} \subset \mathcal{P}^{IR}$  holds. The input  $\mathbf{u}^{IR}$  comprises down-welled atmospheric radiation which affects the thermal measurement directly.
- While function  $C$  explains the deterministic part of the measurement function, the term  $\xi$  models random noise. Unless its statistical properties are precisely known, white Gaussian noise is assumed, identically distributed and independent for all pixels of the image.

There are several *assumptions* implicit in the form of the camera model or measurement equation. First, the IR camera senses only heat radiated from the visible surfaces; conductive or convective heat transfer from ambient air to the detector via camera casing is neglected. Second, eq. (4-4) is an instantaneous measurement equation, i.e. the camera has negligible thermal inertia. Third, observations do not interfere with the building system: heat emitted back into the scene from the camera or computer is neglected, and so is disturbance of convective airflow by the equipment. In other words, the model treats the detector as an ideal heat sink with of zero heat capacity.

The camera model mimics the function *actually implemented* by the camera which should therefore be chosen as simple as possible because imprecisely known functional details will cause inaccuracy. Therefore, *raw values* of radiance are preferable to emissivity-corrected temperatures calculated by most IR cameras. If the device does not support this, the simplest possible temperature conversion should be chosen (set  $\varepsilon=1$  and deactivate background correction), and the conversion used by the camera must be included also in the measurement function  $C$  as its outermost function.

## 4.2.2 Parameter identification

Forward evaluation of the heat equations with known parameter values and known initial values yields the network temperatures, and executing the measurement equation (4-4) predicts the radiosity measured from view pose  $\mathbf{g}^{mob}$ . Thus, the camera model becomes a thermal image simulator (see dataflow diagram 4-5) predicting the spatial distribution of *radiant power* emitted from the system and received at the view pose. We need to solve the *inverse heat transfer* problem as well (Wawrzynek, Bartoszek 2002): having real IR images  $\mathbf{y}^{IR}$  and corresponding predictions  $\hat{\mathbf{y}}^{IR}(\dots, \mathbf{p}, \dots)$  from eq. (4-4) written as a function of the unknown coefficient vector  $\mathbf{p}$ , determine the values so as to minimize the **measurement error (residual)**  $E(\mathbf{p})$ , see figure 4-5:

---

<sup>25</sup> We use the shorthand notation  $\mathbf{U}_{[k]}$  to denote a *time series* of load  $(\mathbf{u}[j])_{j \leq k}$  up to time instant  $k$  and the notation  $\mathbf{U}_{[t_0, t_1]}$  for a continuous-time function of an interval  $\mathbf{U}: [t_0, t_1] \rightarrow \mathbb{R}^m$ .

$$\hat{\mathbf{p}} = \arg \min_{\mathbf{p} \in \mathbf{P}^{mob}} \left( \sum_i \sum_k \frac{\|\mathbf{y}_i^{IR}[k] - \hat{\mathbf{y}}_i^{IR}(\mathbf{p})[k]\|^2}{E_i(\mathbf{p})[k]} + w \|\mathbf{p} - \mathbf{p}_{ref}\|^2 \right) \quad eq. (4 - 5a)$$

$$\text{where } \hat{\mathbf{y}}_i^{IR}(\mathbf{p})[k] = C(\mathbf{T}_i[k], \mathbf{g}_i^{mob}[k], \mathbf{u}_i^{IR}[k], \mathbf{p})$$

$$\mathbf{T}_i[k] := \mathbf{T}(\mathbf{T}_i[0], \mathbf{U}_{i,[k]}, \mathbf{p})$$

The outer summation in the measurement error minimized in eq. (4-5) runs over different thermographic surveys or experiments (index  $i$ ), the inner one over discrete time (index  $k$ ). For each experiment, the initial and boundary values  $\mathbf{T}_i[0]$  and the load schedule  $\mathbf{U}_{i,[k]}$  describing the prevailing conditions during the  $i$ -th survey must be determined to predict the measurements, and so must be the mobile camera poses  $\mathbf{g}_i^{mob}[k]$  from where IR images are captured. Estimating the camera pose is 3D localization using images and a 3D building map and is discussed in section 4.4.2.

A regularization term  $w \|\mathbf{p} - \mathbf{p}_{ref}\|^2$  has been included in the objective function (4 - 5a) to prevent unstable or oscillating numerical solutions (Beck et al. 1996), e.g. by penalizing large deviations from some reference value  $\mathbf{p}_{ref}$  which might be obtained simply as the previous parameter value  $\hat{\mathbf{p}}_{i-1}$ . It is not clear whether such term will be necessary, which form it should take, which prior knowledge about ranges of values is usable, and how large the relative weight  $w$  should be chosen, see subsection 4.6.1.2.

The parameter components of  $\mathbf{p}$  to be minimized have their range of values confined to the set  $\mathbf{P}^{mob}$  which is defined as follows. Only a subset  $\mathcal{P}^{mob}$  of coefficients in the *visual scope* of the camera are free variables and may be assigned values; the remaining ones keep their previous values  $p_j$  frozen:

$$\mathbf{P}^{mob} := \prod_{j=1}^m \mathbf{P}_j^{mob} \quad \text{where } \mathbf{P}_j^{mob} := \begin{cases} \mathbf{P}_j & \text{if } id_j \in \mathcal{P}^{mob} \\ \{p_j\} & \text{else} \end{cases}.$$

The set of free variables depends on some set of measurement poses taken during the current survey  $i$  or possibly some prior surveys, where the functional dependence  $f$  is as yet undefined:

$$\mathcal{P}^{mob} = f(\{\mathbf{g}_i^{mob}[k]\}) \subset \mathcal{P} \cup \mathcal{P}^{IR}.$$

The idea of visual scope will be discussed in subsection 4.3.1; it leads to simpler, localized optimization problems, more likely to adopt a unique minimum and, therefore, amenable to gradient search. Solving the inverse heat transfer problem eq. (4-5) for the coefficient set  $\mathcal{P}^{mob}$  is called *spatially focused calibration* of a simulation model.

As to the choice of the error function, additional measurements not shown in eq. (4-5) such as energy consumption or zone air temperatures may be included. The error function becomes a linear combination of different error terms. As a general rule, the terms should be attuned to and be most *sensitive* to the particular parameters estimated in each case, expressed by the Fisher information criterion (section 4.3.3). Specifically, the error function should be kept simple and avoid combining terms some of which depend on the parameters while others do not. *Measured electricity consumption* depending on the operation schedules of all electrical devices, and *thermal images* of the building envelope put together in a single error function would be pointless, violating the sensitivity and orthogonality principles. However, combining *delivered heat energy* (HVAC) with *measured thermal images* may be a reasonable choice to calibrate parameters that affect *both* measurements. In another experiment, electricity consumption alone would be measured to estimate parameters specifically characterizing the electrical equipment.

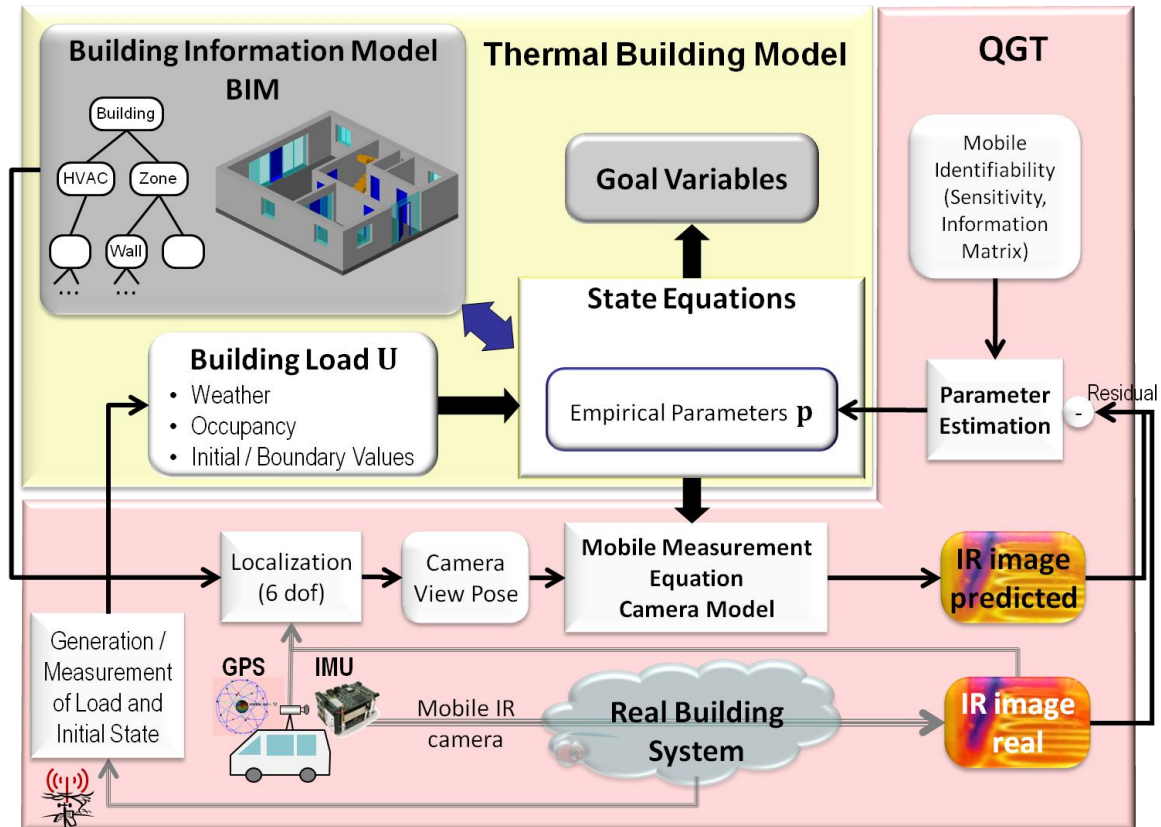


**Figure 4-5:** Functional block diagram of Quantitative Geo-referenced Thermography (QGT) observing a building. Arrows symbolize the directed flow of information between ‘passive’ data repositories and ‘active’ processing instances. Sensor measurements providing data from the real world are shown by gray arrows. GPS and IMU (inertial measurement unit, section 4.4.2) serve to localize the camera platform (vehicle); a weather station with Internet access suggested on the bottom left provides load measurements for the simulation.

### 4.2.3 Residual Analysis

The residual (eq. 4-5) integrates deviations between predicted and measured radiance images to which several different errors actually contribute (figure 4-6). In the remainder of section 4.2, these error sources will be discussed in detail.

#### a) Model mismatch / Model simplification

Model mismatch explains the discrepancy between the simulated discrete state and the actually evolving immeasurable physical process under identical boundary conditions. Discrepancy is caused by the assumptions and simplifications of reality by the model, as well as quantization errors present in the numerical solution. As an example of the former, a single thermal zone with one temperature set point may be assumed for an office building where actually several zones exist, equipped with individual radiators and thermostats. Or, the efficiency of a boiler is calculated for known supply and return temperatures but the actual return temperature differs. The mismatch here lies in the assumption that return temperature behaves ‘as commanded’, i.e. as an *independent design* variable, where in fact it *depends* on the performance of heat distribution into the zone.

### b) Measurement prediction errors

Real infrared images captured in a building deviate from simulated ones even if they were predicted from a perfect building model, because 3D camera localization is inaccurate ( $\Delta g$ ) and, at times, unreliable and because the camera model is imperfect ( $\Delta y$ ). E.g. too simplistic models have been adopted for surface reflectance or spectral IR detector sensitivity (see Appendix A.1-A.3 for details of the camera model). As a matter of fact, these are instances of model mismatch as discussed under a) but distinguished here because the measurement model is not part of the building model proper but an artifact created by our identification method.

### c) Input (load) uncertainty

The initial model state value must be set according to the actual building conditions resulting in a discrepancy  $\Delta T_0$  of initial zone temperatures, for instance. Load discrepancies ( $\Delta U$ ) have an immediate impact on the calculated solar gains and ventilation gains or losses (CHTC). On the part of the building model, certain internal gains may have been covered inadequately or simply been 'forgotten' to model as control input, and occupants' actions on HVAC set points, on windows and shading devices are hard to capture. Measuring accurately the entire building load is difficult and costly. Many building experts would agree that input uncertainty is the severest among the error sources discussed here. Still, it is not clear how big the *impact* of inaccuracies, especially high-frequency signals, on thermal measurements and simulation goal variables actually is, and how far errors may be statistically aggregated.

### d) Parameter mismatch

Some empirical parameters or coefficients are not adjusted to their 'proper' values. This situation tacitly assumes the *absence* of model mismatch a), i.e. model and reality agree at least in *having* the same parameter. Strictly speaking, this is impossible: empirical parameters are modeling artifacts with no counterpart in 'reality'; they always serve to represent (hide) *un-modeled detail* of a physical process that could be modeled theoretically, e.g. at a molecular scale.

In any practical situation, *all* types of error interfere with each other and contribute to the residual while *only* parameter tuning d) is available to minimize it. Minimization of squared errors is statistically valid under the assumption of a correct model and white (zero mean, stationary) measurement noise. Errors in the model and its input bias the residual, however (Borguet et al. 2008). Parameter fitting under these circumstances abuses the parameters as mere 'tuners' or 'tweaks' of a faulty model (Volponi 2008), defeating the goal to characterize the equipment condition proper. The bias problem could invalidate the QGT approach if left unresolved.

Borguet (Borguet et al. 2008) and Volponi (Volponi 2008) proposed empirical ('black-box') models to essentially predict and compensate the residual bias in engine models (aircraft propulsion gas turbines). After compensation, residuals become unbiased (white noise) for the optimal parameter values. Empirical parameters are now put back in place as indicators of the true plant condition. The bias model runs aside a physics-based engine model for performance monitoring. In fact, different bias models were devised to cover different operating regions, and all were trained off-line as multi-layer perceptron neural networks taking measurement residuals from a *particular* engine and engine model as training data. Health monitoring of aircraft engines is of critical importance and justifies the training effort in each special case. Investing a similar effort repeatedly on buildings, having often more parameters than engine models, could not be justified. In order to mitigate the problem of model mismatch, we should first isolate the errors of each kind and model their effects separately, developing independent bias models:

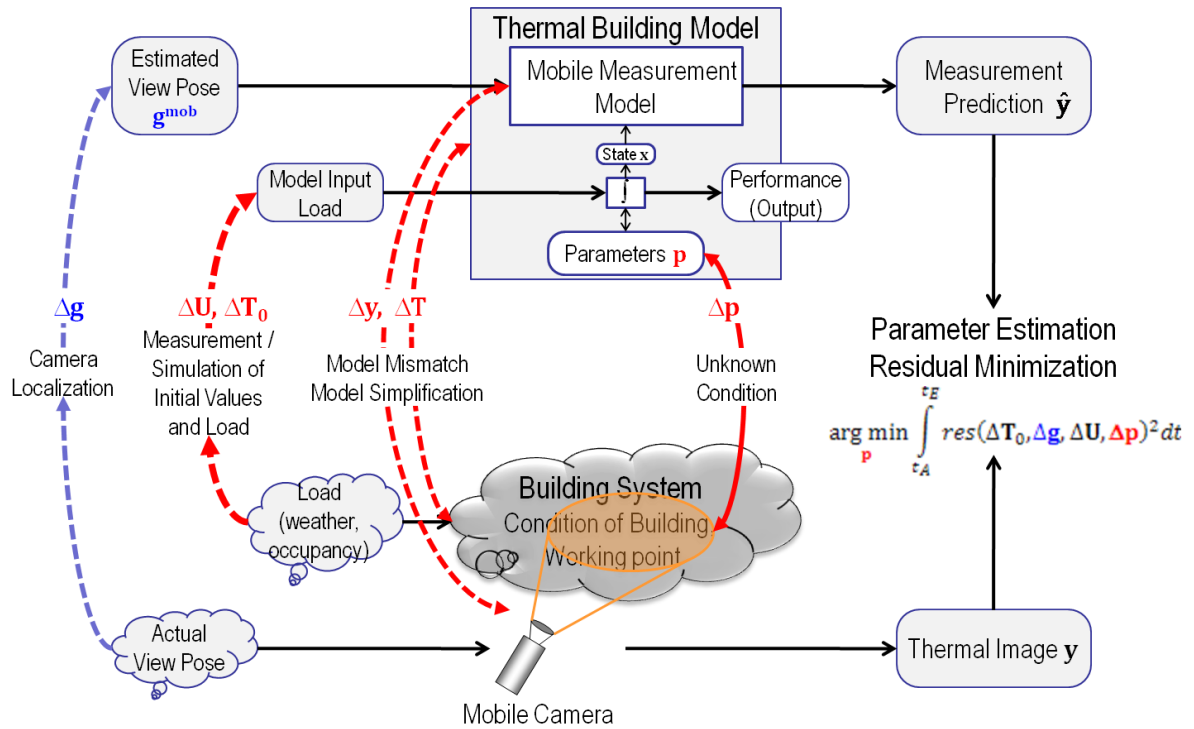


Figure 4-6: Errors contributing to the measurement residual in QGT.

- Before launching a new IR camera and its camera model, measurement prediction and camera localization errors b) should be analyzed and compensated separately, excluding other sources of error. To this end, it is suggested to test both items jointly in a *thermal chamber* providing independently calibrated and densely recorded *temperature measurements* of object surfaces. In this way, the camera model does not need access to any simulated temperatures from the building model. Thereby, model mismatch a), parameter tuning errors d) and erroneous model input c) are excluded. An empirical model compensating the bias due to the particular camera and camera model could be trained in a similar fashion as in (Borguet et al. 2008).
- To tackle the bias due to uncertain building load c), all variables of weather (temperature, radiation, relative humidity, wind direction and wind speed) and occupancy (presence, activity level, door and window opening, operating shading devices, electric light and other appliances, thermostats and set points of HVAC units etc.) should be listed completely. Sensitivity analysis is then performed to select the few ( $\leq 5$ ) most influential load variables, i.e. the ones producing the highest output uncertainty, by proceeding along the lines of Reddy (Reddy, Maor 2006) as discussed in section 3.5.1 or similar to (Allinson 2007). Next, an empirical model of bias may be trained by applying Borguet's method where in our case the term 'biased' refers to a model at least one influential input of which differs from the 'unbiased' model input. Multiple input errors and different error levels play the role of the different operating regions in (Borguet et al. 2008). Training will rely on one generic building model with few parameters characterizing envelopes (glazing) and thermal masses; the validity of such a simplistic approach remains to be tested. In any case, bias models are trained in the simulation domain and not affected by interfering mismatch of type a), b), or d) where real measurements are performed in a real building.

- Model mismatch a) will be addressed, next. A generic approach is needed that learns to *recognize* (classify) different types of mismatch in building models from residual shapes, rather than training for a specific, well known building object each time. Mismatch due to model implementation bugs or to numerical solution problems will be excluded, i.e. a *verified* simulator is assumed. As in the previous item, we suggest to *simulate* mismatch by comparing models of different *level of detail* (either more specific or more general ones), instead of measuring in *real buildings*. A structured approach studying typical *cases of model refinement* lends itself to learn about the residual bias when comparing the measurements. Important cases include:
  - Subdivision of a thermal zone into several sub-zones;
  - Structural decomposition (horizontally / vertically) of compound façades, window systems, and thermal masses;
  - HVAC (heat exchanger) systems represented in different functional detail.
- An extendable library of model transformations similar to *case-based reasoning* systems could be developed, and two main tasks need to be solved:
  - Training: Apply the known model transformations to different building models (contexts) and study, i.e. statistically analyze the time series of residual resulting from each type of transformation. Is it possible to characterize and distinguish them by statistical features describing the temporal and spatial patterns of the measurement residual?
  - Application: Apply the statistical features to residuals from real buildings corresponding to models containing unknown mixture of mismatch. Is it still possible to recognize the *dominant* type of model simplification present, and thereby (partially) compensate it?

### 4.2.4 Simulating non-measured load

Condition estimation and diagnostics benefit from fast changes of load, and sometimes demand situations where those occur. For accurate model prediction, time series of weather data capturing solar irradiance, degree of clearness or cloudiness, wind pressure or rainfall should be recorded at high frequency during a survey, i.e. every minute. A mobile weather station serving that purpose may not be available on site. What is probably available are weather data at a *lower frequency* from a meteorological station *nearby*, providing daily mean, minima and maxima of temperature, average wind speed, and total precipitation. Often, some minimal weather data are recorded *on-site* and *once* during a survey, such as temperature, wind force, cloudiness, or general type of weather. Finally, *statistical parameters* may be known capturing the *short-term dynamics* of typical weather phenomena for the climate zone of the building site.

The problem then is to *simulate* unavailable high-frequency weather data which

- a) are realistic, i.e. contain stochastic variations and comply with basic laws of physics and meteorology,
- b) show plausible patterns of behavior taking into account empirical knowledge of the climate at the building site,
- c) preserve the 'gross energy impact' of actual values measured on site or nearby during the survey, e.g. by assuming conformant mean values.

Specifically, the (expected) average temperature or wind speed of the time series should agree with the value measured once during the survey or, if no measurement exists, with the value of a sinusoidal function adjusted to the surveying date and interpolated at the hour of surveying. Solutions for



this **temporal disaggregation** problem of weather time series have been proposed and reviewed, for instance by (Srikanthan, McMahan 2001), and consist of three main steps (figure 4-7):

1. Determine the probability distribution  $f_{dts,\omega}$  characterizing time series of weather for the date, time, and site of survey ( $dts$ ) and at the time scale (or frequency  $\omega$ ) desired. Methods depend on the available training data<sup>26</sup>; for example, the mean and variance of the density function  $f_{dts,\omega}$  may be regression-fitted to high-frequency data captured at nearby locations.
2. Generate new time series  $\mathbf{U} = (\mathbf{U}[k])_{k=0,1,\dots} \sim f_{dts,s}$  (Monte Carlo sampling).
3. Normalize (scale)  $\mathbf{U}$  to obtain  $\bar{\mathbf{U}}, \bar{\mathbf{U}}[k] := \mathbf{U}[k] \cdot \mu_{dts,\omega} / \mu_{\mathbf{U}}$  where  $\mu_{dts,\omega}$  denotes the mean (average) value known from the survey and  $\mu_{\mathbf{U}}$  the mean (average) value of  $\mathbf{U}$ .

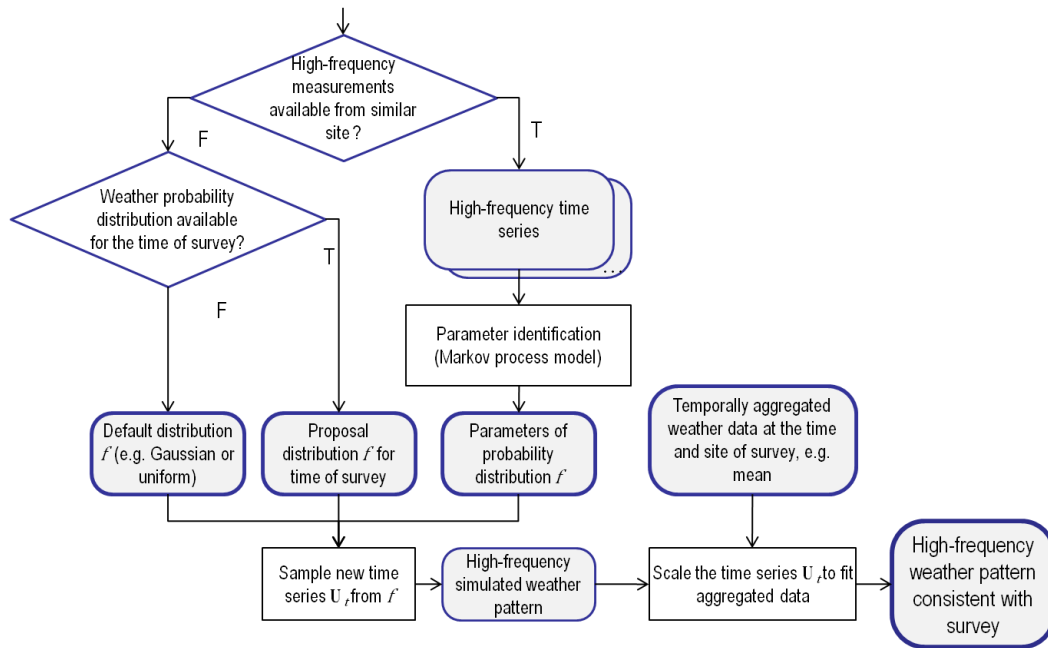


Figure 4-7: Data flow diagram for temporal disaggregation of weather schedules.

Coming back to the identification task, images obtained from a survey under *real* but unmeasured weather  $\mathbf{U}$  will now be compared to images predicted from *simulated* trajectories  $\hat{\mathbf{U}}_j$ . The correlation between real and simulated weather is a rather indirect one:  $\hat{\mathbf{U}}$  should preserve  $\mathbf{U}$ 's gross impact on heating or cooling load, e.g. by preserving the mean value  $\mu_{\mathbf{U}}$  of temperature or wind speed, and it should be sampled from a probability distribution  $f_{dts(\mathbf{U}),\omega}$  chosen to match with the available on-site information, such as date, time, geographic location and general type of weather during the survey. The weather data will be provided in the desired sampling rate  $\omega$ . An open question remains as to which statistical parameters besides the mean (higher moments of the PDF of  $\mathbf{U}$ ?) best preserve the *gross impact of weather*, minimizing the impact of deviations on the building behavior. A modified measurement residual will then be put in place taking the form

<sup>26</sup> Stochastic models used to explain or simulate weather patterns  $\mathbf{U}$  include auto-regressive processes of type AR(1) and first-order Markov models (Srikanthan, McMahan 2001) for which two probability distributions are to be specified, one specifying the probability of the initial state  $P(\mathbf{U}_0)$  and one the transition probability  $P_t(\mathbf{U}_k | \mathbf{U}_{k-1})$  ( $k > 0$ ). The statistical parameters depend on the date, time, and geographic location of the survey as well as on the sampling frequency, and must be determined.

$$E(\mathbf{p}) := \sum_{\substack{\hat{\mathbf{U}}_j \sim f_{dts(\mathbf{U}),\omega} \\ \mu_{\hat{\mathbf{U}}_j} = \mu_{\mathbf{U}}}} w_j \int_{t_A}^{t_E} \left\| \mathbf{y}(\mathbf{U}_{[t_A, t_E]}(\tau)) - \hat{\mathbf{y}}(\hat{\mathbf{U}}_j, [t_A, t_E](\tau), \mathbf{p}) \right\|^2 d\tau. \quad eq.(4.5b)$$

The same real measurement  $\mathbf{y}(t)$  is now compared to several predictions  $\hat{\mathbf{y}}(t)$  obtained by sampling different time functions  $\hat{\mathbf{U}}_j$  from the distribution  $f_{dts(\mathbf{U}),\omega}$ , and a weighted mean squared error is formed (the remaining arguments which are identical in the measurement and the prediction, such as initial state and geometry in eq. 4 - 5a, have been omitted).

A similar procedure as for the weather should deal with occupancy schedules.

### 4.2.5 Input design problem

It goes without saying that the ability and performance to estimate parameters depends on the *input* (building load) *as such*, not only on the accuracy in determining it. This is true already in simple special cases, such as linear time invariant (LTI) systems. Thermal building models after spatial discretization are approximately LTI systems, according to the equations (4-1) to (4-3):

$$\dot{\mathbf{T}}(t) = \mathbf{A}(\mathbf{p}) \mathbf{T}(t) + \mathbf{B}(\mathbf{p}) \mathbf{u}(t).$$

Their parameter dependent response  $\mathbf{T}(t, \mathbf{p})$  at time  $t$  to a trajectory  $\mathbf{U}$  starting from the initial value  $\mathbf{T}_0 = \mathbf{T}(t_A) := \mathbf{0}$  is therefore given by the *transition function*<sup>27</sup> of the thermal state:

$$\mathbf{T}(t, \mathbf{p}) = \int_{t_A}^t e^{\mathbf{A}(\mathbf{p})(t-\tau)} \cdot \mathbf{B}(\mathbf{p}) \cdot \mathbf{u}(\tau) d\tau. \quad eq.(4-6)$$

The *prediction error*  $E(t) = \|\mathbf{y}(t) - \hat{\mathbf{y}}(t)\|$  where both  $\mathbf{y}(t) := \mathbf{T}(t, \mathbf{p})$  and  $\hat{\mathbf{y}}(t) := \mathbf{T}(t, \mathbf{p}_0)$  are derived by the same model for different parameter values only, the current value  $\mathbf{p}$  being estimated and the reference value  $\mathbf{p}_0$ , clearly depends on the input trajectory  $\mathbf{U}$ . So does the error minimizing parameter value<sup>28</sup>. The sensitivity matrix  $\mathbf{S}(t) := \partial \hat{\mathbf{y}}(t) / \partial \mathbf{p}$ , a key indicator of estimation uncertainty (see section 4.3.3), depends on  $\mathbf{U}$  as well.

Therefore, QGT seems to be a case for *optimal input design* for system identification (SI) which attempts to maximize the information content about model parameters to be identified, by choosing the input data within the limits imposed by some constraints. This topic in experiment design has been studied thoroughly and for several decades, e.g. (Mehra 1974; Isermann, Münchhof 2010). Application to thermal building models, though possible, raises questions to be investigated before:

- Building environments impose known constraints on *amplitudes* and on *sampling rates* of weather and occupancy, which should be utilized in input design. Also, as parameters

<sup>27</sup> The system is nonlinear in parameters  $\mathbf{p}$  and weakly nonlinear in the state  $\mathbf{T}$  because parameters appearing in coefficients of the system matrix themselves depend on the thermal state. The system can be linearized about the starting value  $\mathbf{T}(t_A)$  used as operating point:  $\Delta \dot{\mathbf{T}}(t) \cong \mathbf{A}(\mathbf{p})|_{\mathbf{T}_0} \Delta \mathbf{T}(t) + \mathbf{B}(\mathbf{p}) \mathbf{u}(t) + const$  where  $\Delta \mathbf{T}(t) := \mathbf{T}(t) - \mathbf{T}(t_A)$ ,  $\Delta \mathbf{T}_0 := \Delta \mathbf{T}(t_A) = \mathbf{0}$ . For simplification assume that the state is directly measurable,  $\mathbf{y} := \Delta \mathbf{T}$ ; in fact, the measurement  $\mathbf{y}$  is a nonlinear function of state according to eq. 4-4.

<sup>28</sup> Ignoring all other sources of prediction error discussed in section 4.2.3 and substituting, for small parameter changes  $\Delta \mathbf{p} := \mathbf{p} - \mathbf{p}_0$ , a first-order Taylor approximation of matrices  $\mathbf{A}$  and  $\mathbf{B}$  around  $\mathbf{p}_0$  into the transition function eq. (4-6), the dependency of the  $\mathbf{E}$  and  $\mathbf{S}$  trajectories on the load schedule  $\mathbf{U}$  becomes apparent:

$$\mathbf{A}(\mathbf{p}) \approx \mathbf{A}(\mathbf{p}_0) + \Delta \mathbf{A}(\Delta \mathbf{p}) \text{ where matrix } \Delta \mathbf{A}(\Delta \mathbf{p}) := [(\partial \mathbf{A}_{ij} / \partial \mathbf{p})^T \Delta \mathbf{p}]_{ij}, \text{ similarly } \mathbf{B}(\mathbf{p}) \approx \mathbf{B}(\mathbf{p}_0) + \Delta \mathbf{B}(\Delta \mathbf{p}).$$

change slowly, they can be estimated as bounded changes of known previous values. First estimates are obtained from the design values of the building components.

- Unlike machines with defined electrical input signals, the input of a building in *natural environment* cannot be imposed or *commanded* to produce the desired response; only general types or spells of weather might be chosen deliberately. How *expressive* are the input conditions encountered during surveys with respect to the probability distribution of conditions expected in practice? This important question will be further discussed in section 4.2.6.
- SI focuses mostly on *frequency domain* tools employing the spectral decomposition of input functions for optimization. The spectral idea is also exploited in *active thermography* where artificial sinusoidal heating patterns are imposed on the specimens under study. Building load signals admit periodic behavior at the time scales of daily or seasonal weather patterns and weekly operation schedules. For the short time dynamics, such as minute-by-minute changes in wind speed or solar radiation, the benefit gained by spectral analysis remains obscure. Valuable information is expected mainly in the *spatial distribution* (location) of parameters: specific parameters require targeted camera positions and suitable weather for their identification.

#### 4.2.6 Representative load schedules

Sensitivity of parameter estimation to weather is discussed here at an example in building diagnostics. A window consisting of double glazing with highly *reflective* ('low-e') *coating* and an *evacuated gap* is considered. Heat transfer occurs through the glass and through the frame, the latter one mostly by infiltration through the opening mechanism and the seals. Assuming that the three major window functions should be tested independently<sup>29</sup> (figure 4-8 on the right) the following can be stated:

- i. Glazing and coating properties are expressed by the *radiative* resistance  $R_r$  (alternatively, the solar heat gain coefficient) which, on its part, depends on the absorptance, reflectance, and transmittance in the solar spectrum for both panes. To estimate these parameters from temperature fields measured outside and inside, the window should be exposed to bright sunshine, or to strong variations of *solar radiation*. Other factors such as outdoor temperature have no influence.
- ii. Quality of vacuum insulation is shown in the *conductive* resistance  $R_c$  of the gap. The parameter is estimated best from a large temperature difference between outer and inner panes, i.e. under *cold outdoor temperatures*.
- iii. Infiltration losses through the frame and sealing are captured by the *convective* heat transfer  $h_{cv}$  or, inversely, the resistance  $R_{cv}$ . It is estimated best under significant pressure difference, e.g. by blower door testing or, when dispensing with ambient conditions, by picking a spell of *stormy weather* with the window oriented windward. Specific problems, such as condensation on window edges of air-conditioned buildings in warm, humid climates, show up under even more specific conditions (windy, high relative humidity, and large temperature difference).

---

<sup>29</sup> By 'testing' we always determine the *system* contribution of components in situ, e.g. the condition of a window and its impact on a specific building. We do not try to assess the quality of windows as work pieces at a manufacturer's location!

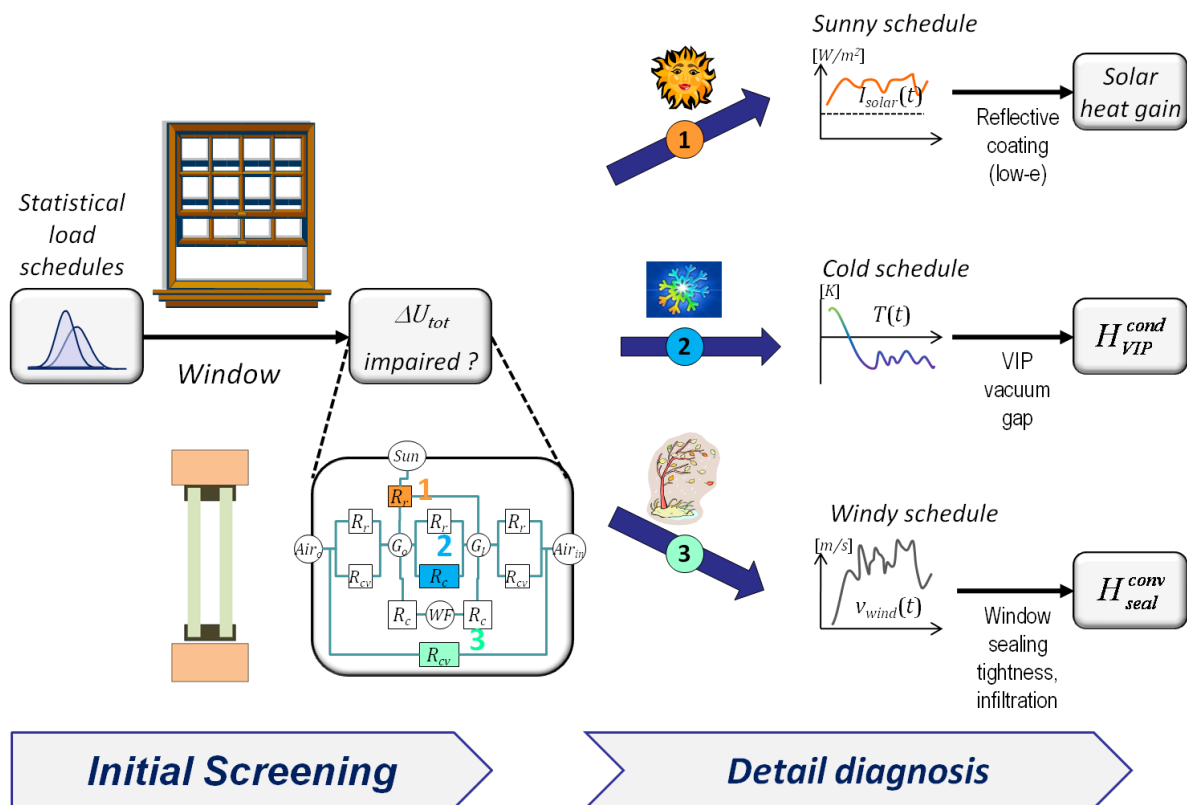


**Figure 4-8:** The influence of load (weather) schedules on the performance of window diagnostics. Which conditions are optimal to detect *any* system change  $\Delta U_{tot}$  regardless of the component causing it? If the cause of the problem were known, the conditions indicated on the right would be optimal. Circles in the RC network on the bottom denote component states ( $Air_{o/i}$ ,  $G_{o/i}$ : outside and inside air zone and glazing, respectively,  $WF$ : Window frame); rectangles symbolize thermal resistances ( $R_c$ : conductive,  $R_{cv}$ : convective,  $R_r$ : radiative) and lines serial or parallel heat flows. Total heat transfer  $U_{tot}$  or resistance  $R_{tot}$  are determined from the respective component quantities according to the Kirchhoff laws. The surrounding wall connected to the frame  $WF$  and the heat capacities of the glass panes have been omitted for simplicity.

Each weather schedule is suited (targeted) to detect a narrow set of problems. Building diagnostics, performed routinely or upon occupants' complaints but lacking a clear suspicion about the cause, must work in *reverse order, top-down* (figure 4-8 on the left). At first, the entire window or its surrounding façade are screened and the *system* thermal resistance or *U-value* denoted  $U_{tot}$  is estimated. Next, more detailed diagnostic steps will be taken, but only if some deterioration is manifest. If the particular weather during initial screening is insensitive to the defect actually causing the problem, no significant change in  $U_{tot}$  will probably be detected. What will be best conditions or strategy for this initial screening step?

It is conjectured that a building operator stands the best chance to detect *any possible* defect by surveying *several* times exploring *extremes*, i.e. sunny, windy and cold weather, which is better than picking at random or selecting 'a-bit-of-everything' weather. Surveys may be viewed as random sampling from a probability distribution of weather time series. How *representative* are the weather samples in the sense that the building responds to many different (unknown) problems, allowing in all cases to detect parameter changes and reveal the true condition? This is a relevant and nontrivial question because it is *external* stimuli of weather and occupancy that have the most impact on building dynamics, and their statistical characterization is difficult.

## 4.3 New application scenarios

However coarse and schematic our discussion has been so far, several novel and promising application scenarios can be identified immediately.

### 4.3.1 Spatially focused calibration

Calibrating a building simulation model involves many, typically hundreds, of parameters. Estimating them simultaneously from sparse measurements is under-determined. Different parameters may have offsetting effects on measurements, e.g. due to the zone interactions, and changing them may give a small error in eq. (4-5) despite a faulty model (Reddy, Maor 2006; Maile et al. 2010a).

QGT enables *incremental*, one-at-a-time calibration focusing on the parameters associated with the building zone or component in the visual focus of the IR camera. Parameters 'out of focus' or parameters barely observable from the measurements should be left untouched, *frozen* to their prior values: fewer degrees of freedom reduce the risk of inadvertently tuning 'unrelated' parameters.

However, to avoid chicken-and-egg problems picking the parameters in the right order, an initial and already roughly calibrated simulation model should exist *before* tuning any parameters from IR camera images. This primary model should predict reasonable *energy consumption* values under a *variety of load schedules*. We suggest that *energy consumption measurements*<sup>30</sup> be used to calibrate those HVAC parameters having the greatest impact on *simulated energy consumption*, such as coefficients of performance, rates of ventilated air change, maximum heating power, or dead band temperature used by HVAC control systems (Heidt et al. 2003; Reddy, Maor 2006). As to parameters describing the building envelope and the thermal zones, reasonable initial values can be obtained from the final design specification or from a database of building materials. This adjustment of the model called *initial global calibration* (see figure 4-9) is required to reduce the model mismatch (section 4.2.3).

By requiring the initial calibration we do not imply that HVAC parameters can *only* be tuned from energy consumption. During building operation, QGT may serve as a diagnostic tool for HVAC units, e.g. inspect air and water ducts, determine temperature levels, detect losses in the heating system, or re-estimate parameters of functional performance of HVAC units.

Figure 4-9 illustrates calibration steps reflecting changes in the behavior of a particular building component. It is shown how to assess its *impact* on the energy performance of the whole building. The data in the simulation model flow *vertically*, showing from bottom to top:

- Input (load) schedules  $\mathbf{U}$ ;
- Internal model parameters  $\mathbf{p}$  before and after calibration;
- Measurement signals  $\mathbf{y}$  and predictions  $\hat{\mathbf{y}}$ , respectively, as well as performance variables  $\mathbf{z}$ .

Time flows *horizontally* from left to right. At first, an *initial global calibration* estimates a version  $\mathbf{p}_G^{(0)}$  of the *entire* parameter vector obtaining satisfactory energy predictions under a *broad range* of input conditions, including different weather types and operation schedules specified by a probability density function (pdf). The energy consumption figures going into initial calibration may have taken several months to measure.

---

<sup>30</sup> From an operational rating, if available, otherwise using estimates from similar building projects.

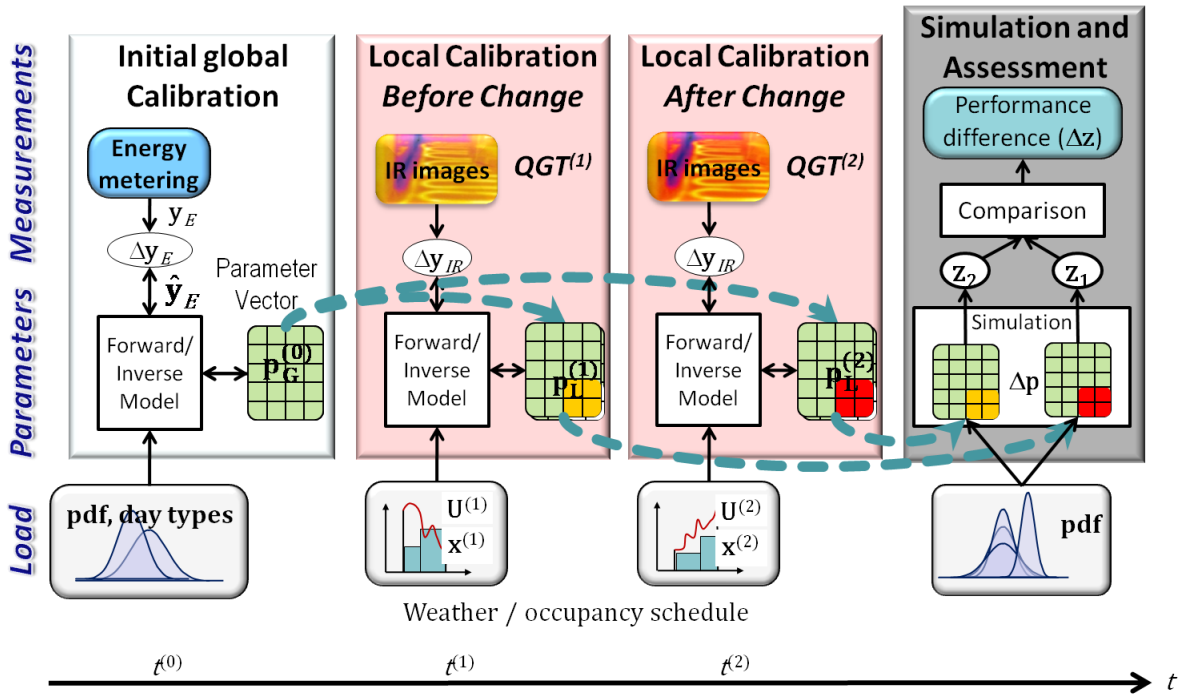


Figure 4-9: Sequence of Incremental calibration steps and quantitative assessment of the estimated changes.

In the future, local parameter sub-vectors  $\mathbf{p}_L$  attributable to the location of survey are estimated by means of QGT while the remaining parameters  $\mathbf{p}_G$  are frozen. The parameter values estimated,  $\mathbf{p}_L^{(1)}$ ,  $\mathbf{p}_L^{(2)}$ , capture the component state at times  $t^{(1)}$ ,  $t^{(2)}$  'before' and 'after' some change, respectively. In between, the component ages or is being repaired or replaced. The contribution to the system energy performance made by these changes is finally assessed.

The load conditions of the two QGT inspections denoted  $\mathbf{U}^{(1)}$ ,  $\mathbf{U}^{(2)}$ , respectively, may be different. Still, the calibration results  $\mathbf{p}_L^{(1)}$  and  $\mathbf{p}_L^{(2)}$  should reflect true conditions of the component and not just be a random outcome of weather conditions. As was discussed before (section 4.2.6), the stability of parameter estimation under different load puts a *requirement* on experiment design, and cannot be taken for granted. It should be noted also that QGT calibration may *increase* the error in predicting *energy consumption* compared to initial calibration because energy consumption is not part of the error function in eq. 4-5a for QGT, i.e. deviations of energy consumption are not minimized.

For performance assessment, the calibration results are plugged back into the parameter vectors,  $(\mathbf{p}_G^{(0)}, \mathbf{p}_L^{(1)})$ ,  $(\mathbf{p}_G^{(0)}, \mathbf{p}_L^{(2)})$ , and their effect on the goal variables is compared by *simulations* run under *identical load*. Load cases representing a *broad range of operating conditions* drawn from a pdf should be statistically averaged to measure the impact under different conditions. Statistical load for assessment purposes is independent of the actual load encountered during calibration.

### 4.3.2 Learning individual aging functions

Walls, façades, insulations, windows, coatings, HVAC equipment and many other building components gradually deteriorate during their lifetime. Mechanical and thermal stress, UV sunlight, soiling, moisture, chemical pollution or biological agents (plant or mould growth) are the key drivers in this

process. The effect greatly depends on the conditions of exposure, the quality of materials, their installation and maintenance. Often, the decay is attended by a loss of (energy) efficiency which can be read from the changing thermo-physical parameters. Systematically logging long-term histories of individual building components *under use* could offer several advantages. But the costs of surveying, calibration, and simulation are substantial, and a 'short-cut' is desirable exploiting the experience gathered for a specific building. Inspections may be summarized as correlations

$$\underbrace{\{\mathbf{y}_i[k]\}}_{\text{IR image set}} \xrightarrow{\text{Calibration}} \underbrace{\mathbf{p}_i}_{\substack{\text{parameter, e.g.} \\ U\text{-value}}} \xrightarrow{\text{Simulation}} \underbrace{z_i}_{\substack{\text{System Energy} \\ \text{Performance}}}$$

resulting in a temporal sequence  $(t_i, z_i)$  of energy performance values between 0 and 1 (equivalently, 0% and 100%). To predict the future service life of a component or to plan its replacement, a parameterized aging function  $af(a_1, \dots, a_n)(t)$  with free coefficients  $a_j$  may be fitted to the empirically derived temporal sequence<sup>31</sup>. Such an aging function is individual, representing a component and its contribution to the *system* performance under specific conditions of exposure.

Learning detailed guidelines for diagnostic purposes is also possible, e.g. to predict the amount of infiltration (air leakage) through a window frame *directly* from IR images without re-calibrating the entire simulation model each time. A thermal image gallery of the window could be generated from calibrated simulations under different weather conditions (outdoor temperatures) and for different values of CHTC. When a new image is presented, the situation matching it most closely would be identified.

### 4.3.3 Mobile measurement design

Buildings often operate at near ambient temperatures making the estimation of HTC difficult. On the other hand, weather exposure and occupants reacting to the load are important factors to observe. Most building components are exposed and accessible to thermal inspection<sup>32</sup>. IR cameras - hand-held or vehicle-mounted - are *mobile observers* that can be placed in time and space so as to observe and exploit the 'natural' transient behavior that would be artificially imposed by active thermography methods. Figure 4-10 illustrates the point.

Specifically, the observer structure in eq. (4-5) can be *designed* to observe or identify properties of building components *in the best way*. This problem of *optimally placing mobile* sensors in distributed parameter systems and sensor networks received considerable scientific attention in recent years (Uciński 2005).

One quantitative criterion to assess the degree of observability for different sensor geometries is provided by the *Fisher information matrix* (FIM) (Uciński 2005; Uciński, Patan 2007). The FIM is based on the *sensitivity* of each observation to all coefficients  $p_i$  ( $i=1 \dots m$ ) of the parameter vector  $\mathbf{p}$  being estimated. Although the camera image is an array of values, let us assume that the measurement  $\mathbf{y}$  yields a suitable *scalar* criterion  $y$ , such as the mean value or variance in a specific region, being a differentiable function of all parameters. The *sensitivity vector*  $\mathbf{s}$  comprising partial derivatives with respect to all parameter coefficients and evaluated at the current values  $\mathbf{p}^0$  reads

<sup>31</sup> For instance, a polynomial  $af(t) = a_0 + a_1t + a_2t^2 + a_3t^3$ , or a function of exponential decay  $af(t) = a_0e^{-a_1t}$ .

<sup>32</sup> This contrasts the situation in *chemical plants* which are usually shielded from their external environment and measured with stationary (built-in) sensors.

$$\mathbf{s}(\mathbf{T}, \mathbf{g}^{mob}, \mathbf{u}) = \left[ \frac{\partial y(\mathbf{T}, \mathbf{g}^{mob}, \mathbf{u}, \mathbf{p})}{\partial p_1} \Big|_{\mathbf{p}^0} \dots \frac{\partial y(\mathbf{T}, \mathbf{g}^{mob}, \mathbf{u}, \mathbf{p})}{\partial p_m} \Big|_{\mathbf{p}^0} \right]^T \quad eq. (4 - 7a)$$

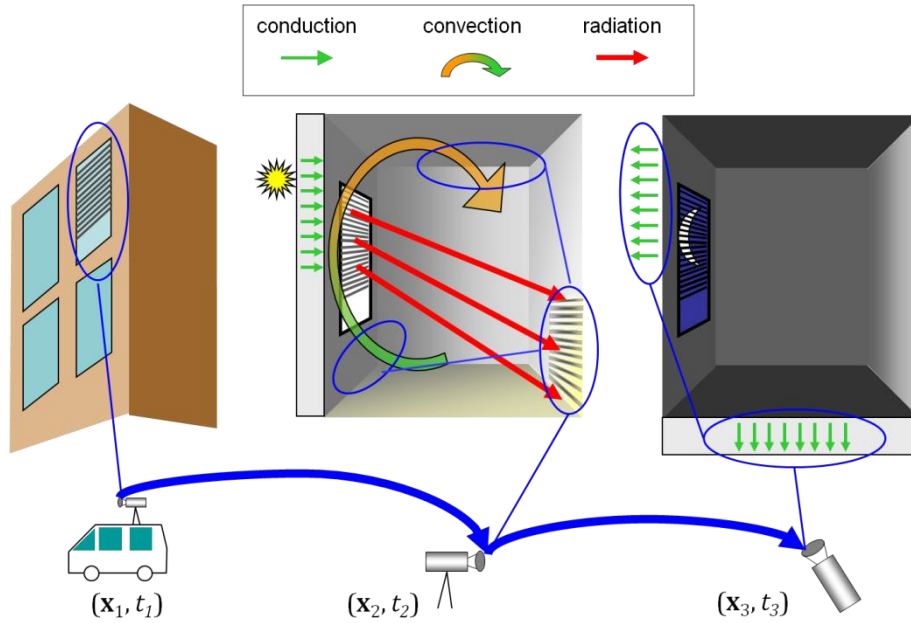


Figure 4-10: Mobile observation of heat transfer coefficients, blue arrows symbolizing the measurement path.

The sensitivity vector depends

- on the system state  $\mathbf{T}$  as well as on the control input (load)  $\mathbf{u}$ , and
- on the *mobile measurement geometry*  $\mathbf{g}^{mob}$ , i.e. distances and orientation angles of the camera with respect to building surfaces imaged.

When the magnitude of derivative is large, the measurement strongly depends on the estimated parameter which means good estimating conditions obtaining low variance estimates. Several maximization criteria have been employed in experiment design; the one suggested by (Uciński, Patan 2007) is the logarithm of the determinant of the  $m \times m$  FIM constructed from the outer product of sensitivity vectors  $\mathbf{s}$  and integrated over an appropriate domain  $\Omega$  of state values  $\mathbf{T}$ :

$$\mathbf{g}^*(\mathbf{u}) = \arg \max_{\mathbf{g}^{mob}} \log \det \left( FIM(\mathbf{g}^{mob}, \mathbf{u}) \right) \quad eq. (4 - 7b)$$

$$where \quad FIM(\mathbf{g}^{mob}, \mathbf{u}) = \int_{\mathbf{T} \in \Omega} \mathbf{s}(\mathbf{T}, \mathbf{g}^{mob}, \mathbf{u}) \mathbf{s}(\mathbf{T}, \mathbf{g}^{mob}, \mathbf{u})^T dT_1 \dots dT_N$$

In practice, the costs to realize the measurement geometry in terms of accessibility or other constraints must also be considered. The computational cost of *optimization* in the style of eq. (4-7b) may be prohibitive and must be justified by the expected benefit. In any case, the FIM framework provides a good starting point to systematically *assess* and *improve* observability as a function of measurement geometry.



### 4.3.4 Thermography-guided geometry refinement

How to partition a building model into zones, surfaces, and surface elements is an important design decision with great impact on accuracy, computation and memory demands of the simulation. *Homogeneity* of thermal properties of surfaces and of air zones being well-mixed is a common assumption. Initial model versions start with a coarse division into few large zones which is refined as necessary. At the other end, a detailed investigation of the thermal comfort in a public building may require a full-fledged CFD program simulating a mesh of thousands of surface or volume elements to accurately model the transport of heat, air, and moisture, which is resource-intensive. Clear guidelines are missing as to precisely where and how to refine.

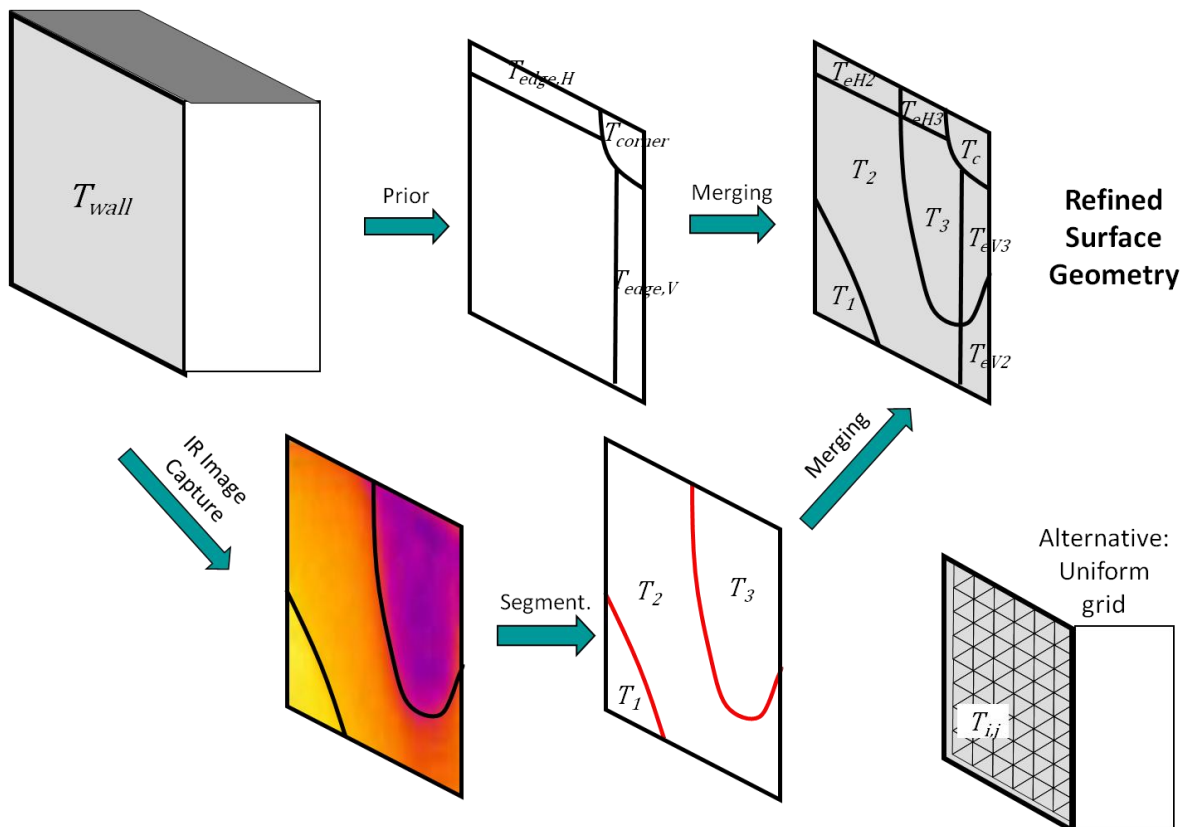


**Figure 4-11:** Thermography-guided refinement of wall geometry. The uniform wall model is decomposed into edge and corner regions based on prior knowledge or experience (top). A different segmentation is derived from the measured thermal distribution (bottom). Both segmentations are merged into a single decomposition (upper right) which is more efficient for heat calculations than the uniform grid (bottom right) and more faithful and accurate than uniform wall geometry.

Geo-referenced thermography captures *spatially dense* thermal fields providing useful feedback to *refine* the geometry (semi-)automatically. When comparing simulated to measured thermal distribution, not primarily the mean or integral *magnitude* of error but the *spatial distribution* of prominent deviations of temperatures provides a guideline for possible refinement. As IR images are captured from a wall modeled initially as a thermally uniform slab, the heat texture is automatically mapped onto spatial coordinates in the frame of the wall surface; two spatial coordinates  $x, y$  will suffice. Building walls adjacent to the envelope often exhibit spatially non-uniform heat distribution, espe-

cially near the *edges* to adjacent walls and near the *corners*. Because of nonzero wall thickness, the ratio between surface areas internally and externally changes there (Nakhi 1995).

Further spots due to moisture or airflow skimming along the wall may be discovered as regions where measurement errors, i.e. differences between measured and predicted heat flux, are *locally* big. Notwithstanding the diagnostic approach taken, accurate simulation of the heat transfer as such suggests that the surface be split into several thermally distinct regions of edges, corners, and other areas, see figure 4-11. Large and uniform regions remain in the wall center. There is no need for *gridding* the entire wall surface as done in a CFD simulation. By combining thermal and geometric criteria of homogeneity, a partition of the image (*segmentation*) can be obtained returning regions with area, connectivity, and bounding contour lengths, from which the refined heat diffusion equations are calculated via geometric transformations reflecting the region decomposition into cells.

### 4.3.5 QGT applications in the life cycle

A long-term benefit to the life cycle of buildings is expected from improved modeling and monitoring of energy consumption. Our overarching motivation is closer ***change control***. Viewing the life cycle as a chain of *versions* of the building model and its real counterpart, the intention is to fully understand the transitions and their impact on energy performance prior to optimization. In the long run, a contribution to the *persistence* of measures improving the energy efficiency is expected as well.

Several brief scenarios explain the mission of QGT applied to different phases in the life cycle.

#### ***Verification of BES***

Verification is an atypical example as it focuses on the simulator software, on correct modeling and correct model implementation, rather than on particular building models. Debugging a simulator may be difficult when only goal variables such as predicted *energy demand or consumption* can be displayed graphically but internal diagnostic variables are lacking. The program output may deviate from analytical calculation results (available for very simple models) or from simulation results of the same or a similar building obtained with a different simulator. Or it may not significantly, or under specific and rarely tested operating conditions, deviate, and still have offsetting internal errors (Judkoff et al. 2008). In any case, the goal values neither reveal possible causes in case of deviation, nor can tallying values substantiate our trust in model correctness.

QGT offers improved *diagnostic support* by *visualizing* and comparing *internal* surface temperature distributions (*simulated* thermography, in high spatial resolution) to prior expectations obtained from measurements or calculations.

#### ***Validation of building models***

The validity question asks: does a particular simulation model reflect the building *design intentions* and *expectations* and conform to the *design data* underpinning the certification? Measurement data from the actual building do not yet exist for comparison. Ideally, the final design details (geometry, material, equipment and parameters) are documented completely in the building model which is *simulated* by running a *verified* BES. Baselines of energy performance such as required by an asset rating (section 3.1) should now be reproducible in the simulation. Simulated thermal distributions are helpful for testing and diagnosis, having checked that crucial parameters of thermography simulation, such as surface emissivity values, contain no gross errors and produce reasonable thermal images.

The primary importance of the validation phase lies in the definition of *test cases* for future actual QGT surveys. Simulated thermal distributions will be produced for different load conditions and documented together with model details (parameter values) as a reference or baseline to which future measurements are compared.

### ***Initial commissioning***

Commissioning deals with the *actual construction*, i.e. the components and materials built into a new, usually certified building and the execution of construction work. The *implemented building* and its energy performance is for the first time compared to the final design specification (Fischer et al. 2006). Examples of constructional misfits include differing layer thickness, missing pieces of insulation or unintended thermal bridges. Also, manufacturer data of actually built-in HVAC equipment are checked against design specifications.

To assist in commissioning, QGT measurements are made in the building and compared with *corresponding* simulation images from the validation phase. However, preparatory work needs to be carried out on the simulation model before meaningful comparative results may be expected:

1. Confirm that the *geometry* actually built reflects the validated design model (BIM, BES).
2. Determine the BES *load schedules* using time series of weather data (meteorological station), statistical occupancy data, and recordings of occupants' control actions on the HVAC control system.
3. Perform initial global calibration runs (4.3.1) with measured energy consumption data.

The last task, in particular, takes much more time than the commissioning procedure proper, i.e. uses several months of energy consumption. The three steps will explain major differences between simulated and captured thermal images and cause the already validated BES model to be updated and modified. For example, important energy consumers may have been neglected or simply been forgotten in the model. Not until then may discrepancies between the adjusted model and the surveyed building be attributed to possible deficiencies of construction or building materials used.

### ***Characterizing the building stock***

Unlike new buildings, existing ones need neither have a valid building model nor be certified, at least not according to a contemporary rating standard. To meet overall energy performance goals in the building sector, upgrading the building stock is vital because of the long lifespan of buildings. A new BPS model of the geometry as-built must be developed, HVAC equipment and material properties must be investigated before drawing any benefit from QGT. Under favorable conditions, an up-to-date *urban information model* exists to extract the floor plan and properties of the *building environment* from, as to supply of daylight, shading, sky view, and solar gains. Methods of reverse engineering for automatic map building from 3D point clouds may be helpful to determine outer and inner geometry and wall thicknesses. However, obtaining an accurate performance model of the HVAC equipment may be cumbersome, to say the least. With incomplete documentation, determining the composition of building materials consumed in a multi-layer wall or façade will rely on knowledge of the state-of-the-art at the time of construction, or draw on analogy to similar buildings by age.

Initial global calibration (4.3.1) is performed first, comparing measured energy consumption and air zone temperatures to predictions. When the BPS model has stabilized, focused parameter identification by thermography is performed zone by zone, proceeding from the envelope inward towards the building core. QGT may be used in transient heating or cooling processes to infer material parame-

ters like thermal conductivity or capacitance, assuming initial values not too far off reality are known, even if the building materials themselves remain unknown.

From then on, the calibrated simulation model serves as a *design substitute* and provides a performance baseline based on which alternative scenarios of upgrading and retrofitting can be played through, balancing energy performance gains with costs of retrofitting.

### **Degradation monitoring**

Critical components to be inspected regularly and patterns of typical damage are in the focus. Several examples have been discussed in section 3.2 and are not repeated here. This is the realm of building thermography and building diagnostics with the added benefit of whole-building simulation providing quantitative impact analysis. Technically, spatially focused calibration (4.3.1) explains aging processes by changes in thermal coefficients. Selecting viewpoints with good or even optimal observability (4.3.3) is important for accurate recalibration of these coefficients from thermal images. As soon as a history of QGT survey data of a specific part has been collected, a lumped aging function of the component may be estimated as described in section 4.3.2.

### **Ongoing commissioning**

Unlike initial commissioning, OC focuses on the *building operation*, specifically on how and why HVAC performance deviates from expectations. The building operator attempts to *adjust* the HVAC control to the *actual* load in contrast to a *statistical* load which it was designed and optimized for, and tries to reconcile the occupant's specific desires or habits with energy performance goals.

In order to reproduce peculiar operational patterns, the settings of the load in the BES must be carefully determined and some HVAC coefficients may need re-calibration because operating points of HVAC equipment have changed from the situation during initial commissioning. I.e. some work carried out during initial global calibration may need to be redone. In order to explain in detail properties related to air comfort or daylight supply, the modeled building geometry may also need local refinement (4.3.4). QGT imaging thermal distributions in high resolution, e.g. displaying traces of air draught on a wall, may help to assess if the overall control strategy meets the needs of individual users in specific rooms.

## **4.4 BIM-integrated thermography**

Predicting IR camera images accurately requires that the corresponding view pose  $\mathbf{g}^{mob}$  of the IR camera in the building coordinate system be *known* during the survey. A link from the 2D image domain into the 3D model is thereby provided. Before discussing how to solve this localization task, the benefits may be appreciated by briefly looking at the situation in building thermography today.

Most infrared camera manufacturers offer their users administrative software, easing the tasks of organizing infrared images, documenting environmental conditions during image capture, and generating inspection reports. There are also efforts ongoing to integrate thermographic inspection into *facility maintenance* systems. Still, large image collections are being organized, accessed, and searched mostly in *directory-like structures*. The primary ordering criteria are by time, project (name), or type of problem. This organization of measurement data has several drawbacks:

- a) Images and features are not associated uniquely with *building components*; even obtaining efficiently a history of *all* IR images showing a specific part ('anamnesis') is not trivial.

- b) Images viewing the same part at different times cannot be directly compared since the precise 3D view pose to rectify or align images and create an 'overlay' structure is missing.
- c) Comprehensive and accurate documentation of *all relevant* external conditions to correctly interpret or compare images and to reproduce measurements is unavailable. Inspections comprise annotated image files and textual reports.

The concept of **geo-referenced thermography** was developed by Stilla and Hoegner and tested on a street vehicle with two IR cameras (covering different spectral bands) mounted on a pan and tilt unit to capture the building façades (Stilla, Hoegner 2008). The authors proposed and implemented a method to estimate the vehicle pose with respect to a building/district model represented in CityGML. *Object-centered monitoring* with spatially and temporally ordered inspections, and *automatic mapping* of heat textures onto the 3D geometry (BIM) are key advantages of this method. The paper (Stilla, Hoegner 2008) mentions the possibility to extract details from the IR image like heating pipes, line or surface features, and states current limitations of CityGML to properly represent these features.

#### 4.4.1 Mobile observer in detail

The new concept of **BIM-integrated thermography** provides in addition camera-based calibration of thermal models and, equivalently, model-guided quantitative evaluation of IR images. Figure 4-12 refines the data flow shown in figure 4-5, illustrating how to provide access to the building parameters and measurement equations, i.e. how to link the IR image domain with the 3D BIM.

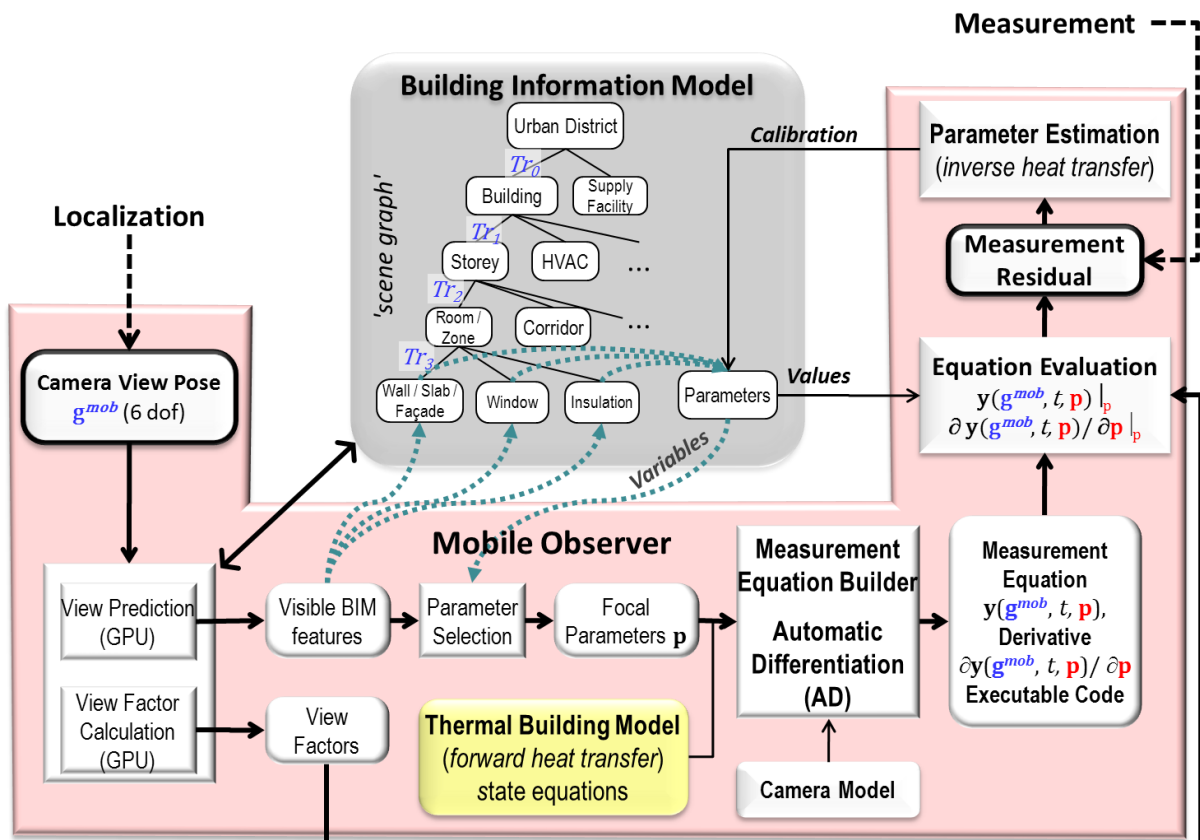


Figure 4-12: Data flow diagram of the mobile observer cooperating with the BIM.

In the image center the BIM part hierarchy is shown as a 'scene graph' linking each element to its parent by a coordinate transformation denoted  $Tr_i$ . Elements are located in the BIM coordinate system by applying the composition  $Tr_0 \circ \dots \circ Tr_n$ . 'IR localization' on the left-hand side estimates the transformation  $\mathbf{g}^{mob}$  that maps coordinates in the IR camera frame onto the BIM 'world' frame.

When the intrinsic camera parameters (opening angle or focus distance and image resolution) are also known, the entire 3D $\leftrightarrow$ 2D camera transformation is available. For each image pixel capturing part of an object surface, the associated building component is known. These *visible features* refer to BIM components shown as dotted arrows in fig. 4-12, with the following exceptions:

- No object may be returned and regions of the sky or building environment such as streets or vegetation are seen instead; this may frequently happen in outdoor surveys.
- A barely visible object is seen the surface of which lies almost parallel to the viewing direction.
- An object is partly occluded by foreground objects, such as people, furniture or mobile equipment which may alter the thermal behavior of the inspection targets. Foreground objects become distinguishable from targets under two assumptions. Firstly, the localization should tolerate partial occlusion and register *persistent* building features but not *mobile equipment* with corresponding elements in the BIM. Secondly, 3D vision via stereo camera or range sensor is available along with the IR camera to distinguish and excise foreground objects, based on distance comparisons to BIM components.

The view factors (on the bottom of fig. 4-12) for a given pixel return the share of radiosity emitted or reflected from other objects; they are essential for predicting the detector output. Visible features and view factors are efficiently computable by GPU (graphical processing unit) assisted scene rendering operations (Robinson, Stone 2005).

*Thermo-physical parameters* associated with the *imaged* (solid) *building component*  $i$  are primary candidates for parameter calibration. Further parameters associated with *adjacent* components may be added, by defining an *area of influence* of components around the  $i$ -th component. The following selection criteria may be used in combination:

- **Connectivity:** components  $k$  directly influenced from the  $i$ -th component via the system matrix  $\mathbf{A}$  in eq. (4-3b), i.e. entries  $\mathbf{A}_{k,i} \neq 0$ . In fluid flows described by a process flow graph, these are typically immediate neighbors downstream of component  $i$ .
- **Proximity:** components  $k$  *spatially closest* to  $i$ .
- **Sensitivity:** components  $k$  parameters of which have largest sensitivity values (eq. 4-7) with respect to the measurement, evaluated for the current state values and the captured image. Only components represented in the state vector or algebraically coupled with state variables can have nonzero sensitivity because the measurement equation is directly linked to the state equation.

All parameters directly visible or in the area of influence of visible parameters except the ones designated as frozen (section 4.3.1) form the set  $\mathcal{P}^{mob}$  of free variables and are called **focal parameters**.

For each pixel  $(u, v)$  there exists a **measurement equation** predicting the radiance  $\hat{y}_{uv}^{IR}$  as a function of the variable focal parameters and the fixed remaining ones. With actual radiance measurements  $y_{uv}^{IR}$  available, the inverse heat problem in eq. (4-5) can be solved with nonlinear minimization algorithms such as conjugate gradients, Levenberg-Marquardt, or simpler Newton-like algorithms. Whatever algorithm will be used, the measurement equation and its derivatives  $\partial y / \partial \mathbf{p}$  must be evaluated for many different parameter values. Furthermore, derivatives are essential to analyze the

sensitivity of measurements to parameters, to calculate the Fisher information matrix or to find optimum view poses (4.3.3).

Contrary to fixed measurement geometry (inline gauges), the measurement equation cannot be written down off-hand in closed form because the building model (BIM) has irregular finite-element geometry, and there are infinitely many measurement poses. Pre-calculating a representation of the workspace by finite aspects, though possible, would entail quantization errors. Therefore, the precise measurement equation will be extracted at run time when the measurement pose is known. The *measurement equation builder* in fig. 4-12 provides this equation and its derivative as executable code, invoking an automatic differentiation tool (AD) (Bischof et al. 2003). To keep the computational overhead manageable, it is divided into terms executed at run time (view dependent terms) and view-independent terms calculated offline (figure 4-13). First, the measurement function is written as two concatenated mappings  $\mathbf{T}$  and  $\mathbf{L}$  (function arguments of initial values, boundary values, and load have been dropped from the notation since known values independent of  $\mathbf{p}$  can be substituted for them):

$$\mathbf{p} \xrightarrow{\mathbf{T}} \{T^{view}(\mathbf{x}, t, \mathbf{p}), T_1^{refl}(t, \mathbf{p}), \dots, T_r^{refl}(t, \mathbf{p})\} \xrightarrow{\mathbf{L}} \hat{\mathbf{y}}_{u,v}^{IR}.$$

Where  $T^{view}(\mathbf{x}, t, \mathbf{p})$  denotes the temperature of the imaged component at the location  $\mathbf{x}$  of the pixel foot print, assuming for simplicity that at most one component is hit;  $T^{refl}(t, \mathbf{p})$  denote temperature(s) of components from where the imaged component receives and reflects thermal radiation. All temperatures are members of the state vector  $\mathbf{T}$  which is calculated by integrating the heat transfer equation from simulation time  $t_0$  to  $t$  corresponding to the real time span  $t-t_0$  elapsed since the most recent state initialization when the current image is captured. The view pose  $\mathbf{g}^{mob}$  determines the 3D location of the pixel footprint and *selects* the relevant object temperatures in the mapping  $\mathbf{T}$ .

The second mapping  $\mathbf{L}$  embodies the *camera model* proper, expressing the radiosity  $\hat{\mathbf{y}}_{u,v}^{IR}$  at pixel  $(u, v)$  as a function of all temperatures contributing. At each wavelength, the spectral radiosity is a *linear combination* of  $N$  blackbody radiosity values  $E_b$ , and is weighted by the detector sensitivity and integrated over the spectral band, obtaining the following form:

$$\hat{y}(\mathbf{g}^{mob}, t, \mathbf{p}) = \sum_{i=1}^N \int_{\lambda_0}^{\lambda_1} \alpha_i(\mathbf{g}^{mob}, \lambda, \mathbf{p}) \cdot E_B(\lambda, \mathbf{T}_i(t, \mathbf{p})) d\lambda \quad eq. (4-8)$$

The factors  $\alpha_i$  reflect the sparse interconnection structure between state variables and measurements:  $\alpha_i = 0$  if the  $i$ -th object has no effect on what is seen from the current view pose  $\mathbf{g}^{mob}$ , neither directly nor indirectly via reflection. A factor  $\alpha_i \neq 0$  functionally includes some coefficient  $\varepsilon_i(\lambda)$  of emissivity or reflectance which may or may not belong to the focal parameter set  $\mathcal{P}^{mob}$ , and  $\alpha_i$  depends on the geometric view factor  $F_i$  of the object surface. Pulling the detector sensitivity  $R(\lambda)$  inside the factor  $\alpha_i$  obtains a function  $\alpha_i(\mathbf{g}^{mob}, \lambda, \mathbf{p})$ . Differentiating the measurement equation (4-8) with respect to the parameters  $\mathbf{p}$  obtains the following expression:

$$\begin{aligned} \frac{\partial y(\mathbf{g}^{mob}, t, \mathbf{p})}{\partial \mathbf{p}} &= \sum_{i=1}^N \int_{\lambda_0}^{\lambda_1} \underbrace{\frac{\partial \alpha_i(\mathbf{g}^{mob}, \lambda, \mathbf{p})}{\partial \mathbf{p}}}_{\text{pose dependent}} \cdot E_B(\lambda, \mathbf{T}_i(t, \mathbf{p})) d\lambda + \\ &\quad \sum_{i=1}^N \int_{\lambda_0}^{\lambda_1} \alpha_i(\mathbf{g}^{mob}, \lambda, \mathbf{p}) \cdot \underbrace{\frac{\partial E_B(\lambda, \mathbf{T}_i(t, \mathbf{p}))}{\partial \mathbf{T}_i}}_{\text{pose independent}} \cdot \underbrace{\frac{\partial \mathbf{T}_i(t, \mathbf{p})}{\partial \mathbf{p}}}_{\substack{\text{pose independent} \\ \text{(state equ.)}}} d\lambda \end{aligned} \quad eq. (4-9)$$

Only the pose dependent functions  $\alpha_i$  and their derivatives  $\partial \alpha_i / \partial \mathbf{p}$  must be calculated at run time, whenever the camera is moved about. In many cases, derivatives take a simple form, being either zero (if  $\alpha_i = 0$  or  $\alpha_i$  does not depend on  $\mathbf{p}$ ) or constant, independent of  $\mathbf{p}$ .

For example, let  $\alpha_i = (1 - \varepsilon_i) \cdot F_i \cdot R(\lambda)$  with the view factor  $F_i$  of the  $i$ -th object, and let emissivity  $\varepsilon_i$  be an inaccurately known calibration parameter appearing as the  $j$ -th component in vector  $\mathbf{p}$ . Then

$$\frac{\partial \alpha_i}{\partial \mathbf{p}} = \left( 0, \dots, 0, \underbrace{-F_i \cdot R(\lambda)}_{j\text{-th}}, 0, \dots, 0 \right)^T.$$

All derivatives in the second summation of eq. (4-9) are pose-invariant and can be *provided* as executable functions at design time. Still, they must be *evaluated* at run time for different parameter values. The derivatives of blackbody radiation function  $E_b(\cdot)$  are evaluated only for the current temperature (state), not for different values of  $\mathbf{p}$ . Derivatives of the state vector are obtained from the state equation (4-3b) as a (discrete-time) recurrence formula:

$$\begin{aligned} \frac{\partial \mathbf{T}[k+1]}{\partial \mathbf{p}} &= \mathbf{A} \frac{\partial \mathbf{T}[k]}{\partial \mathbf{p}} + \left[ \frac{\partial \mathbf{A}}{\partial p_1} \mathbf{T}[k], \dots, \frac{\partial \mathbf{A}}{\partial p_m} \mathbf{T}[k] \right] + \left[ \frac{\partial \mathbf{B}}{\partial p_1} \mathbf{u}[k], \dots, \frac{\partial \mathbf{B}}{\partial p_m} \mathbf{u}[k] \right] \quad (\text{for } k > 0); \\ \frac{\partial \mathbf{T}[1]}{\partial \mathbf{p}} &= \left[ \frac{\partial \mathbf{A}}{\partial p_1} \mathbf{T}[0], \dots, \frac{\partial \mathbf{A}}{\partial p_m} \mathbf{T}[0] \right] + \left[ \frac{\partial \mathbf{B}}{\partial p_1} \mathbf{u}[0], \dots, \frac{\partial \mathbf{B}}{\partial p_m} \mathbf{u}[0] \right]. \end{aligned} \quad \text{eq. (4-10)}$$

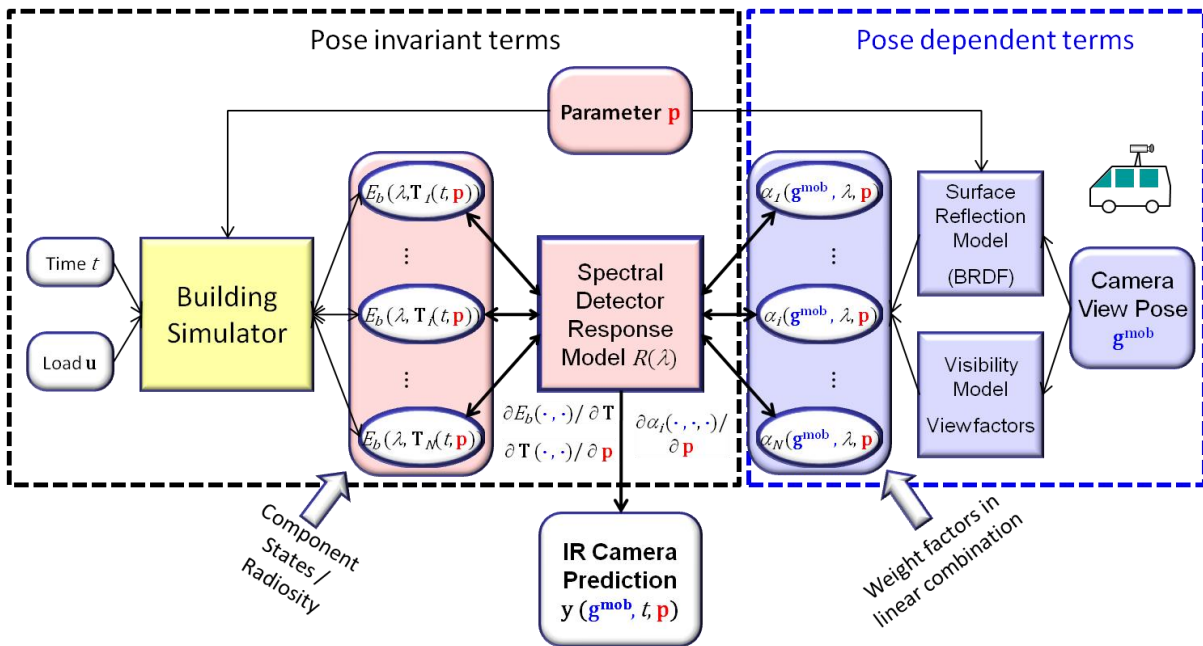


Figure 4-13: Calculation scheme for mobile measurement equation containing pose-dependent and invariant terms.

### 4.4.2 Localizing the infrared camera

When a visual sensor or camera takes *measurements* in a known way described by a sensor model and in an environment described by a *map*, the likelihood or probability density function of measurements can be predicted for any given *view pose*. *Localization* (Borenstein et al. 1996) is the in-



verse problem "Where am I?": finding the *unknown view pose* from which a *given measurement* becomes most likely. In this report, a building information model (BIM) forms the known 3D map. *Expanding* a map from measurements while exploring an *unknown* environment, known as *simultaneous localization and mapping* (SLAM), is a broader and deeper problem (Thrun et al. 2005) which is not considered in our context.

Camera localization in fact comprises two parts: determining the position and orientation (six degrees of freedom) of the infrared camera frame with respect to the Cartesian BIM frame, and finding the transformation between camera frame and 2D image coordinates. The second part, taking care of projection and possibly lens distortion, is solved by *camera calibration* and not discussed here.

Localization works in principle similarly for an IR camera as for a digital color camera, except that thermal features are dealt with. A vast amount of mathematical methods, algorithms and prototype systems for camera-based localization and navigation have been published by the robotics and the photogrammetric communities in several decades, though comparatively few of them working in the infrared domain. Methods depend on the environment, the type of survey (indoor or outdoor survey, airborne or terrestrial) and on the available sensors. To date, no general, fool-proof method working reliably and accurately in any situation exists. Yet, localization technology has crossed the edge from basic research to real applications, such as mobile city guides, and seems mature enough to venture building new applications on-top if one is aware of the assumptions and limitations of each method.

From a practical point of view, we distinguish between *coarse* absolute and *fine* relative localization. The former estimates an initial pose ("Which building do I see, which façade, from where do I enter? In which room am I?"), the latter refines an *existing* pose estimate, usually by minimizing a distance function of predicted and measured visual features. Identical or very similar features may be seen from totally different view poses. Therefore, coarse localization is required for pose disambiguation, not only for initialization. Coarse localization identifies a global maximum of probability in the pose space, whereas fine localization converges to the closest local maximum. Successful localization algorithms were proposed by (Früh, Zakhor 2003; Boström et al. 2004; Mayer 2007; Stilla, Hoegner 2008) and many others under the topic headline of '3D modeling and texturing urban environments'. Typically, combined range, video, and infrared image sequences are captured for localization and / or texturing. Figure 4-14 shows two examples of thermal textures mapped onto a 3D geometry model.

Important assessment criteria for the localization sensors and methods include the following:

- Accuracy: as a rule of thumb for indoor surveys, we quote 1‰ of relative positional error (e.g. 10mm deviation per 10m of range), and 2° of angular orientation error. These figures indicate standard deviations, assuming unbiased estimates.
- Reliability and robustness with respect to measurement outliers and partial occlusion of BIM features, e.g. by furniture or mobile equipment inside or vegetation outside;
- Generality, i.e. broad applicability to indoor and outdoor surveys, imposing few restrictions and assumptions such as requiring special localization infrastructure inside a building.
- Engineering criteria (equipment costs, sensor size and weight, handling, usability, and comfort experienced by the operator; effort to install and calibrate the sensors, operator skills required to conduct surveys);
- Algorithm complexity with regard to development effort and running time.

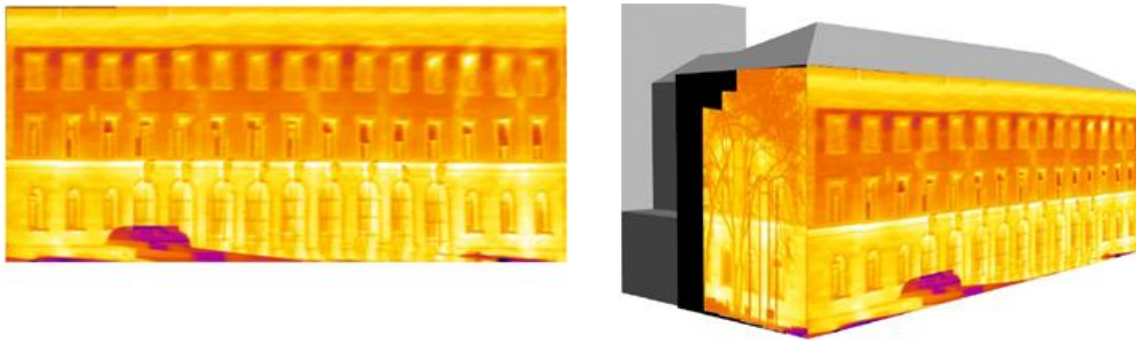


**Figure 4-14a:** Infrared texture generated from 20 partial textures, registered and mapped onto a 3D building model (Hoegner, Stilla 2007, figures 8 and 11, without permission).

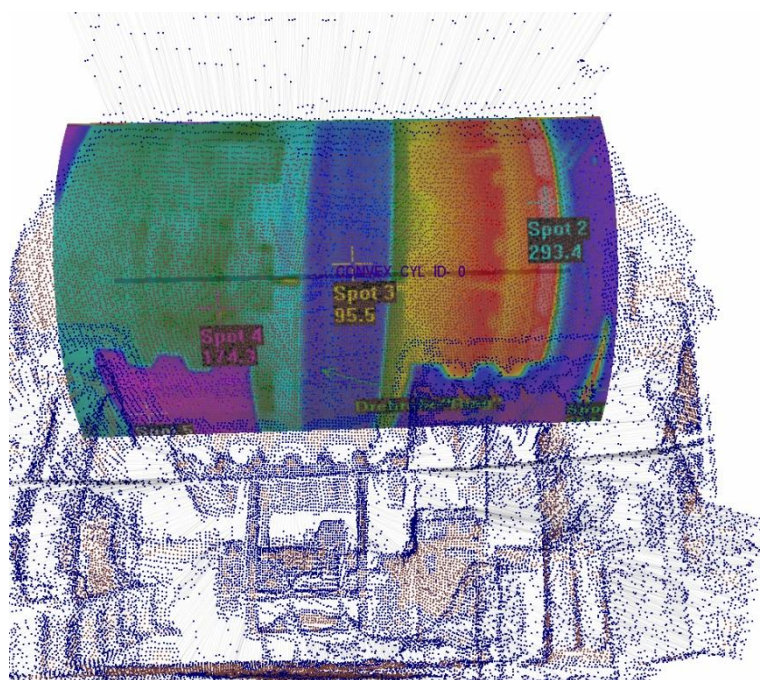


**Figure 4.14 b:** IR image registered and mapped to a cylindrical kiln model of the THERESA plant reconstructed from laser scan data (Kohlhepp 2009, figure 1-1).

### **Coarse localization**

In *outdoor surveys*, the camera is mounted on a carrier platform (vehicle, airplane) which may have a GPS receiver to obtain global position estimates. Higher accuracy is obtained with techniques known as 'differential GPS', GPS-RTK (real-time kinematic), or CP-GPS (carrier phase) (Schall et al. 2009). GPS delivers *position* and not orientation directly. When surveying continuously, a recorded path of GPS view poses may be interpolated by a smooth curve, such as a spline function, and coarse *orientation* estimates can be obtained from its tangent assuming that an initial orientation is known, using a compass or magnetometer.

Inertial sensors like wheel encoder, inclination sensor, gyroscope, accelerometer, magnetometer, 6D mouse, or head-mounted display provide alternatives to GPS. Methods based on inertial measure-

ment units (IMU) *maintain* a coarse global view pose and are applicable in outdoor and in indoor surveys, but they provide *no starting pose*. Contrary to independent GPS readings, these methods are plagued by *accumulating* uncertainty, because they integrate differential changes (in velocity or pose). This is why pose uncertainty must be estimated and updated regularly (by propagating covariance), and combined with results of fine localization to reduce the uncertainty by covariance intersection (Uhlmann, Csorba 1997). Therefore, inertial methods are not self-sufficient for localization.

Occasional loss of GPS signals may occur in densely built-up areas, narrow street canyons or heavily occluded spaces. Resorting to old signals instead increases the uncertainty as well. For indoor inspections, GPS usually is not a viable option. Large public or commercial buildings possibly dispose of in-house localization equipment. An inexpensive and more flexible alternative may be RFID (radio-frequency identification) tags dispersed for localization (Miller 2006). However, applicability is restricted because the RFID reader must stay within short range (<1m) of a locatable RFID tag.

3D laser scanners capturing point clouds together with algorithms to extract surface features are frequently used for absolute (global) positioning in a 3D geometry model. For instance, the 'Orthogonal Surface Assignment' algorithm (OSA) (Kohlhepp et al. 2006) developed as part of a SLAM framework building new surface maps from range views is applicable to existing maps as well to localize the sensor pose. Its basic assumption that every range view contains *some orthogonal* surface features will fail in many *outdoor* environments. Methods for solving the 'kidnapped robot problem' (See et al. 2011) also localize a robot (mostly in 2D) with no valid prior sensor information.

### ***Fine localization***

Fine localization methods use prior pose estimates together with a region of uncertainty as the starting point, respectively, the search region to find the transformation aligning features in the model with corresponding image features with a minimum error. A feature correspondence or *association* (best match) must be found in a robust way so as to preserve geometric relations and account for spurious or missing features.

This task becomes easiest if model and image features agree in dimension (3D) and type. Therefore, laser scanners preserving metric distances are very popular for data capture. Variants of the ICP algorithm (Iterative closest point Rusinkiewicz, Levoy 2001) are frequently employed for the tasks of feature matching and registration. For each image point (3D) the model feature with shortest (orthogonal) distance is selected as correspondent. Next, a rotation and translation is calculated moving all model features closest to their image correspondents. Correspondence and transformation steps iterate until the error converges.

For intensity images captured by a moving camera or binocular stereo camera, 3D image features must be recovered first by stereo matching (Burschka 2008). Lowe's scale invariant feature transformation (SIFT Lowe 2004) has become a 'gold standard' to find corresponding features in different images. The SIFT algorithm extracts key points (descriptors) as features that are invariant to image translation, rotation, and scaling. It provides efficient key point matching and also estimates the motion transformation between key points. Recently, efficient simplifications of this algorithm have been proposed, such as the SURF algorithm (Bay et al. 2008).

Comparatively little experience is available with thermal infrared features as key points. Key points extracted in the thermal band may be much sparser than those in the visual range, and may require adapting the key point description and matching methods. Matching thermal image (2D) features to 3D geometry features is difficult mainly because thermal edges do not correspond to geometric edges in the BIM, as reported in (Stilla, Hoegner 2008, 2007).

## 4.5 BIM for design, analysis, and monitoring

Thermographic surveying proposed for performance monitoring and model identification should be embedded in an environment for building design and analysis and be rooted in a building information model (BIM). In this section we discuss possible implications on the advancement / evolution of future BIM technology, picking two examples. Subsection 4.5.1 highlights the key role of geometry which CAD design tasks and thermal analysis put very different demands on, the new mobile observer standing in between (4.5.1). In subsection 4.5.2 future BIM development specializing in the support of lifelong performance monitoring of buildings is sketched.

### 4.5.1 Linking design and thermal analysis

As the focus in a building design process changes, so too does the role of the 'parameters' (figure 4-15). An architect or engineer thinks of *design parameters* chosen from a discrete option space, such as picking different types of façade or makes of space heating, window fabric, or insulating material. Working with a suitable design frontend system, her or his decisions eventually enter the semantic building model (BIM) where corresponding *property values* reflect the design choices. For energy analysis, this BIM is transformed into an executable simulation model automatically (more on this further down in this section), in a way hidden from the user and driven by needs of numerical accuracy and efficiency. Calibration adjusts the internal parameters of this final simulation model.

Although design options are related to simulation parameters, for instance, different types of fabric differ in heat coefficients, there is no one-to-one correspondence. A single design choice may affect many parameters and, conversely, several design decisions contribute to one simulation parameter. In order to translate the calibration results back into user language, all rules governing model transformations must be accessible explicitly and be applicable in forward and in reverse order.

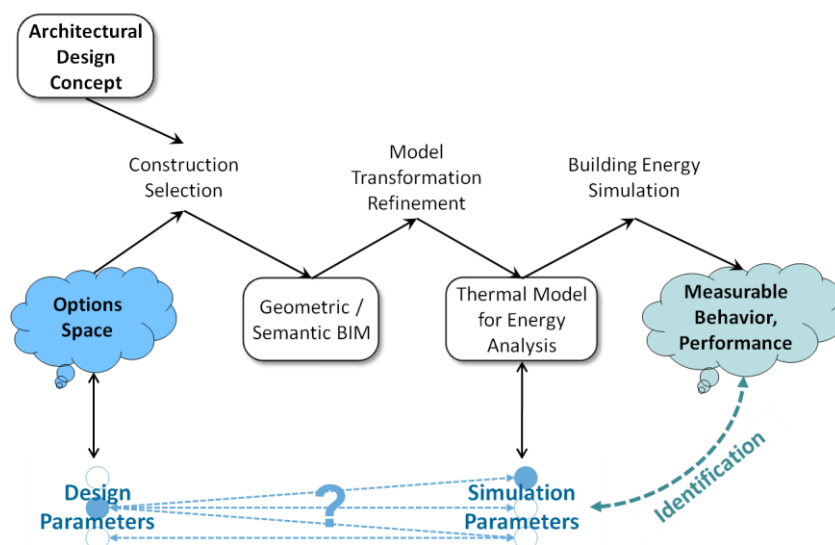


Figure 4-15: Design and simulation parameters

The link found in BIM between the aspects of (architectural, CAD) design and thermal analysis / simulation have been investigated thoroughly by Maile and others (Maile et al. 2007; Maile 2010) and, recently, in Schlüter's PhD dissertation (Schlüter 2010). Figure 4-16 highlights a core subset of BIM

classes forming the link between these two views. We discuss the relation between semantic building model and thermal simulation at some length because of its implications on the new interface to be designed for the IR camera.

Creating a thermal simulation model from a BIM requires, in all but the simplest cases, far more than exporting a few U-values, envelope surface areas and zone volumes that are readily calculated from the BIM geometry. There is a correspondence or duality, but not an identity, between design and analysis concepts:

- *Spatial aggregations* serving a building purpose from the architect's or owner's view, and *functional aggregations* from a process engineering viewpoint, such as a complete HVAC system;
- *Geometric enclosures* (spaces, rooms) defined by the enclosing solid components, and *thermal zones* as the units of heat and air transfer, including sensor and control points;
- *Geometry* representation according to CAD needs (construction, 3D rendering, Boolean operations, ...) and geometry as a domain for solving HAM transport problems (*Transport Geometry*), balancing computational efficiency with physical accuracy;
- *Topological relations* between *geometric entities* (e.g. *adjacent* walls enclosing a space or spaces sharing a bounding wall, parametric relations expressing constructional constraints), and adjacency of *functional units* forming a coherent fluid flow in a HVAC system.

A process flow graph describing a HVAC system consists of nodes (class *Flow\_Comp*) and edges (class *Flow\_Interface*) shown in figure 4-16. Concrete types of HVAC units such as ducts, pumps, heat exchangers, inlets and outlets are derived from the abstract node class.

Functional units as parts of building service systems are assigned to solid objects such as façade elements, walls, and floors defining the building structure by means of *Placements*, analogous to the inhabitation and hosting concepts in (Schlüter 2010). In this way, HVAC components are placed within the building structure. E.g. air inlet and outlet nodes of an AHU are fixed to a wall or a slab, a radiator is attached to a wall, a duct runs inside a wall or slab, and the layout of a cooling coil may be defined with respect to a thermally activated slab. Thus, service components obtain their preferred position, orientation, and space demand, specified by an oriented bounding box (OBB). By placing also the sensors and actuators in each control loop, the space (*ThermalZone*) controlled by one HVAC system becomes completely defined and linked with the CAD geometry. Geometric dimensions needed for heat calculations such as the surface area of a heat exchanger become available.

From a thermal zone, the domain for the numerical solution of heat and mass transfer called *TransportGeometry* is generated. Its level of detail, i.e. number of dimensions (1D, 2D, 3D) and principal directions considered in heat conduction and convection, grid sizes etc., should allow to be chosen individually for different parts (Nakhi 1995) and independently of CAD geometry representation. For instance, airflow around the inlet placement of an AHU is resolved into a fine 3D grid while treating the surrounding space as one 'well-mixed' air zone. Heat conduction through a wall in normal direction may be 1-D by default but two- or three-dimensional near corners or edges where several walls join. The shape of a thermal zone and the transport geometry generated are not determined fully automatically but influenced by deliberate engineering decisions (zone merging or splitting) and by requirements of simulation accuracy. The necessary interfaces to the design engineer are not shown in figure 4-16.

A second link from architectural CAD to building physics is defined by the class *Material*, which embodies material properties of all solids including their bounding surfaces that are relevant to the simulation of heat conduction, convection, and radiation. A direct association arrow from *Solid* to *Materials* has been drawn in figure 4-16; in practice, there exist intermediate classes describing

composite structures in detail, such as several *layers* of materials or complex *frame walls* (*SolidComposite*).

Two main implementation strategies exist for developing a thermal simulation model from a BIM: the transformation solution and the integrated solution.

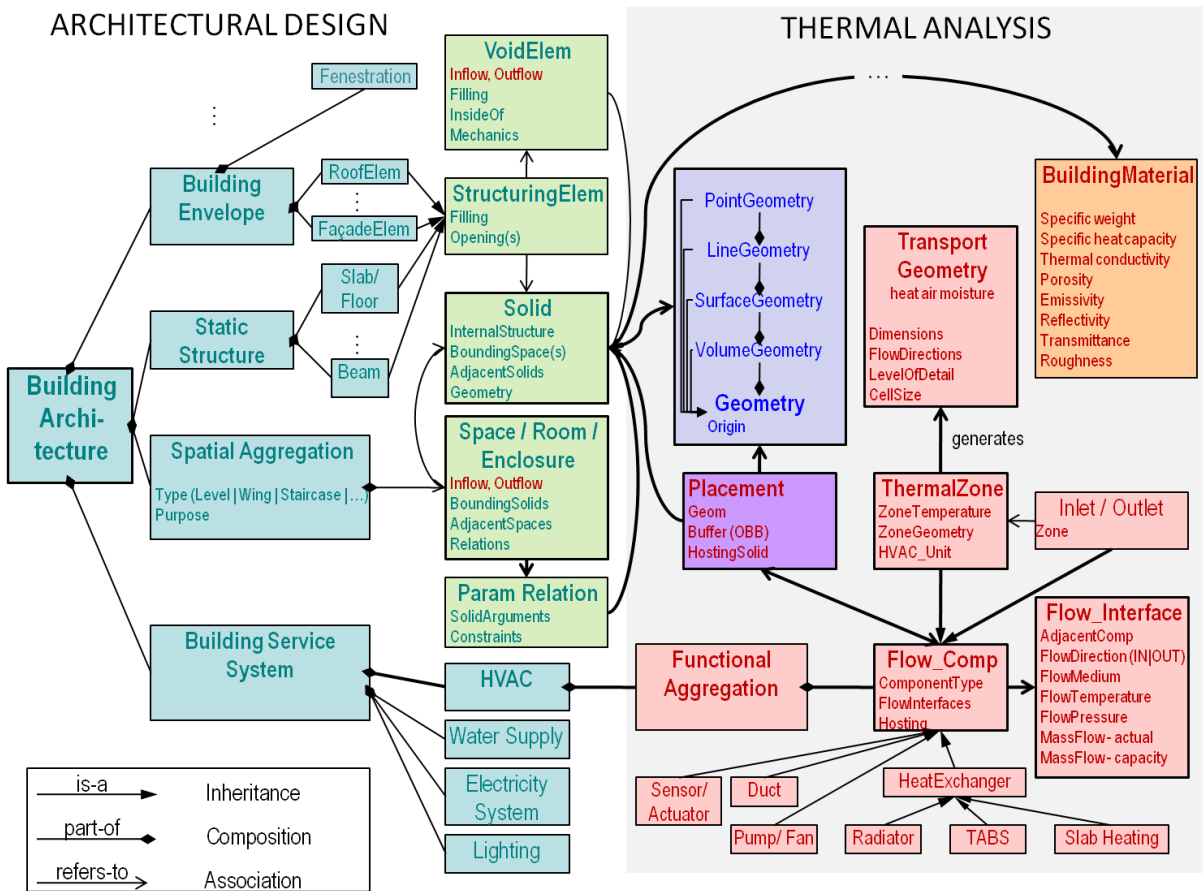


**Figure 4-16:** BIM classes at the interface between architectural design and thermal simulation. Important links are drawn in bold; key properties are shown textually as class attributes. Not shown on the thermal analysis side (right) are all classes modeling input schedules (climate, weather, and occupancy), requirements (demands), simulation output (performance), internal numerical solutions or calculation results, and GUI classes. Adaptation from UML diagrams by (Schlüter 2010).

**Transformation solution** (figure 4-17)

A new interface to an existing building simulator is provided by converting the BIM into, and by exporting the simulator’s native input description. Conversion requires explicit semantic knowledge about the dependencies, rules, and relational constraints existing between the CAD designer’s viewpoint and the functional viewpoints of process engineering. The correspondence between BIM attributes and simulation model parameters has been explained above as one aspect of different semantic domains. The transformation solution requires checking whether the BIM presents complete and consistent (plausible) information to the simulation, and is not a one-to-one translation of BIM elements. The transformation approach is best practice today when bringing BIM and BES expertise together (e.g. ifc to EnergyPlus Maile et al. 2010b). The two main advantages are:



1. CAD design requirements are clearly separated from simulation requirements, and
2. Building simulators existing on the market can be interfaced.

On the backside, developing big applications will entail more communication overhead. Imagine the simulation side suggesting structural changes to make the building more energy-efficient: these changes must be transferred back to the original BIM design document (*bidirectional* transformation, which is not shown in figure 4-17 but would be needed). Changes could also affect *coherent* architectural details essential to architectural design but missing (being omitted) in the simulation model. These details must be adapted consistently by the rules of parametric modeling (Maile et al. 2007; Eastman et al. 2008, page 176ff in section 3.3.1). Before accepting the architectural updates, we need to check that no design intent or constraint has been violated.

Another point is extendibility to add novel features to the simulation such as a mobile camera interface. Placing the camera (virtually) within the building model to pick the objects seen pleads for a 3D scene graph organized as a part-of hierarchy (figure 4-17 on the upper-left) which is common in rendering applications including CAD systems. Camera placement, however, is a novel feature required by the mobile observer interface *dynamically* (at simulation run-time) and, therefore, *must* be provided by the *thermal simulator*. One has to live with whatever geometry representation the simulation framework provides, which may be rudimentary.

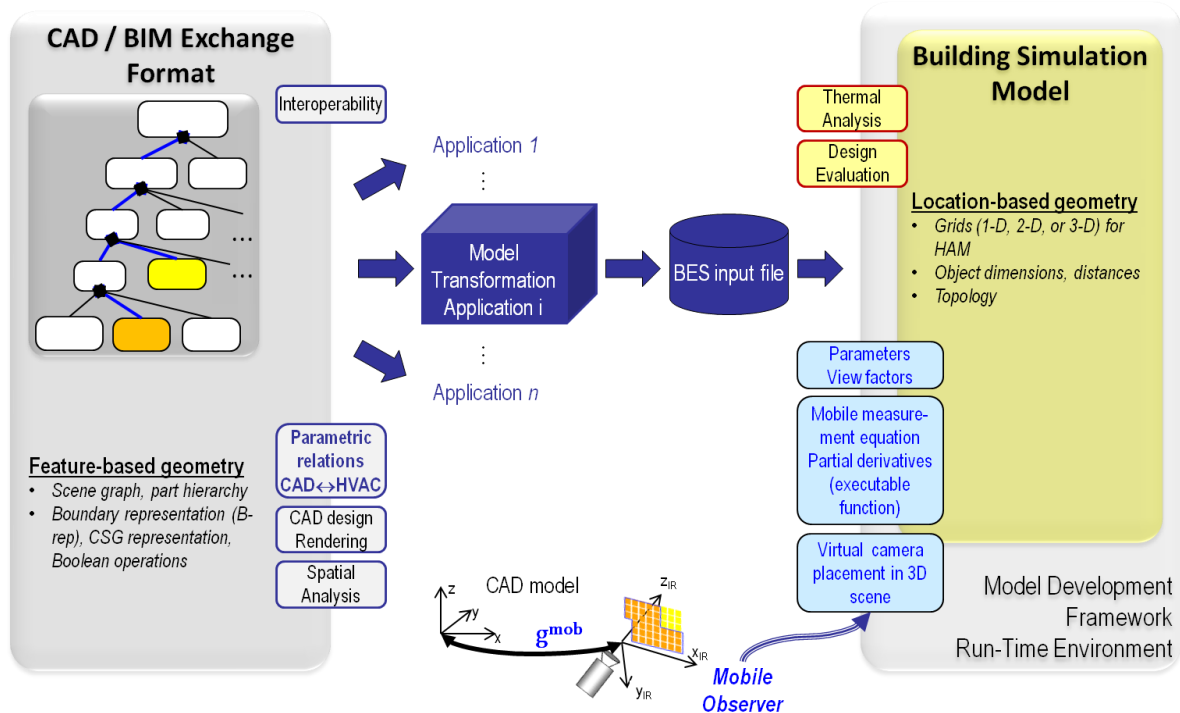


**Figure 4-17:** Transformation of the BIM into an input file for a simulation environment. Rounded small rectangles show various capabilities offered and required for different purposes. For mobile observers, in particular, access to model parameters and view factors, access to measurement equations and derivatives, and virtual camera placement are essential (bottom right, in light blue). Feature geometry (left) is optimal for CAD design tasks including 3D rendering, spatial analysis, room layout, visibility assessment, navigability, maneuverability, clash detection, and allocation. Location (grid or cell) based geometry is tailored to accurate and efficient numerical heat transfer solution. Camera placement would opt for the CAD geometry but has to cope with the thermal simulator geometry.

### Integrated solution

An integrated approach does not need native input file representations like a building simulator. Thermal analysis as one application runs directly on the BIM data structure; climate files and occupancy schedules, only, must be provided via external interfaces. Re-using parts of existing simulator kernels to develop an integrated solution faster may not be easy. The software architecture drawn in figure 2-12 in fact depicts a prototype of integrated software architecture.

Most interface classes for thermal analysis shown in figure 4-16 (on the right) will be implemented by the simulation tool, in one or the other way. It is suggested to store (serialize) the calculated intermediate information about thermal zones, HVAC component placements, topological relations and constraints in the BIM document. In this way, the transport geometry can be reconstructed or regenerated efficiently. The first BIM-integrated tool implementation, to our knowledge, is the Design Performance Viewer proposed by (Schlüter 2010), which is intended for energy performance evaluation in early building design phases. Integrated solutions are not yet available widely. Their key advantage will be tighter interaction between design and simulation in the future, shortening the cycles of performance assessment and subsequent modification. We believe that integrated solutions built 'around' the BIM will facilitate making extensions like mobile camera interfaces for several reasons: because of the unified and powerful geometry representation inherited from CAD systems, because of advanced features for spatial and semantic analysis and, in general, a more advanced programming environment compared to what is available most building simulators.

### 4.5.2 Lifelong performance monitoring

Monitoring a building and collecting performance data throughout the life cycle is part of an *ongoing commissioning* process (section 3.1). The task can be greatly assisted with a suitable building information model (BIM) the requirements of which are briefly outlined in this section. Figure 4-18 highlights the situation of energy modeling and monitoring but applies to condition-based maintenance tasks in general. The presentation is independent of a particular BIM representation schema.

To motivate and justify the development of an exchange format for lifecycle monitoring, it should be noted that monitoring is part of Computer-Aided Facility Management systems (CAFM) or Computerized Maintenance Management Systems (CMMS) (Neelamkavil 2009). Therefore, the distinction between semantic data models for monitoring and maintenance systems remains fuzzy and somewhat arbitrary.

CAFM systems organize and supervise the maintenance work in terms of time schedules, cost, and resources required. Primarily, they schedule and control *work orders* including inspection and monitoring events; i.e. their main focus is on future and present events and not the past. CMMS also perform inventory control of spare parts and tools. Moreover, they keep track of issues defined in maintenance contracts such as warranty. CAFM/CMMS provide packaged software solutions around their internal data structures. Interoperability and the exchange of *maintenance data* among different tools via an open standard are no major issues.

Examples of commercial systems from the building sector include [Morada](#), [Speedikon](#), and [PRO-TEUS](#). The latter, specifically, links continuous commissioning to the LEED process and interfaces with intelligent Building Automation System (BAS), by generating work orders out of alarms issued by the BAS. A web site of CAFM/CMMS on the market is maintained by [Jens Nävy](#).

Our focus rather is on the data (schema) specification than on features supporting specific maintenance tasks. Our BIM extensions will focus on the monitoring history, i.e. the past, aiming at performance tracking, analysis (measurement and simulation), diagnosis, and documentation, at the com-



ponent and the whole-building levels. Using geo-referenced imagery for comparison requires performance analysis to be strongly linked with building geometry, part hierarchy, and functional part association. On the other hand, scheduling work orders is disregarded, and the future is only considered by trend analysis or in estimating remaining service life of a component<sup>33</sup>. Business processes and workflow of maintenance are already represented in existing BIM standards (ifc).

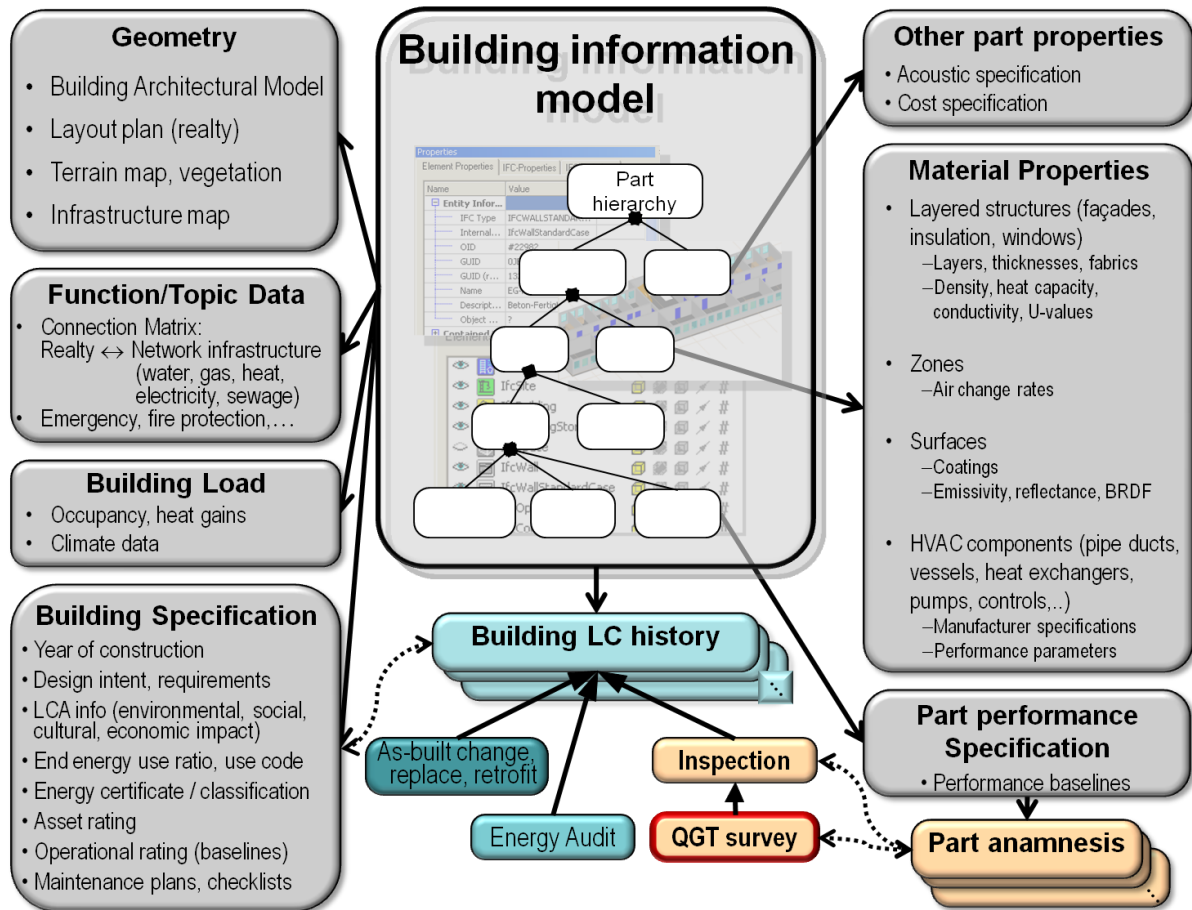


**Figure 4-18:** Semantic model of a building in an urban context, focusing on lifelong performance monitoring.

Properties describing the building *as a whole* are shown on the left in fig. 4-18, i.e. geometry, functions and topic data, load, and specification documents. Two aspects are emphasized: the embedding in the urban context (district level) with interfaces and connections to the networks of infrastructure, and the building specification and documentation. The latter scope includes

- Building design contracts,
- Estimated life cycle impacts and costs (environmentally, economically, socially, and culturally),
- Specification of energy performance (asset rating, operational rating, energy efficiency class),
- Manuals of building operation and maintenance.

<sup>33</sup> Of course, the distinction between 'future', 'present' and 'past' is indiscriminate as today's future becomes the past on the day after tomorrow and, conversely, today's history may be essential for planning future maintenance tasks. The same kind of IT support, e.g. historical databases, will be essential for both tasks.

Properties on the right of fig. 4-18 belong to individual *components* in the part hierarchy shown in the image center, including the parameters needed in the simulation and subject to calibration.

**Maintenance inspections** along with **actions** and **modifications** carried out will be documented in the **Building LC history** (BLCH) shown on the bottom of fig. 4-18. Such measures are taken either to resolve manifest performance problems, or to improve energy performance in general. Replacement of HVAC parts, changes in HVAC control settings, retrofitting of windows, roofs, façades, insulation material, and structural modifications fall into this category. Monitoring events documented in the BLCH usually follow a general maintenance plan. The underlying rules and strategies, inspection targets, time schedules, and responsibilities may be specified in a separate document residing in an external facility management system and referred to from the BIM (bottom left).

Inspections performed and results obtained are documented accurately and comprehensively in the monitoring, or inspection, events. The following information is considered most essential.

### ***Inspections in general (base class):***

- I-1 Time of survey (primary ordering criterion) and duration of survey.
- I-2 Person / institution in charge.
- I-3 Reason causing the inspection (scheduled event, alarm signal, occupant's complaint, ...).
- I-4 Phase in the life cycle (building design, construction, post-construction,...).
- I-5 Building components affected / inspected – a link to the part hierarchy and part performance specification.
- I-6 *Type of data surveyed (measured or simulated);*
- I-7 *Description of data (sensors / data points / variables, assumptions and limitations of data capturing);*
- I-8 Readings or trend logs of values<sup>34</sup>.
- I-9 Association with other inspection data, such as a link from measurements to simulated values.
- I-10 Diagnostic result of inspection, e.g.: no fault, degradation, malfunction, component failure, ...
- I-11 Facility condition index - a value between 0 and 100% indicating the component's condition.
- I-12 Consequences drawn and decisions made, e.g.: no action, deeper diagnostic effort prospected, replacement scheduled, retrofitting planned,...

### ***QGT survey (derived class, new attributes)***

Thermographic surveys by QGT involve partial *calibration* of the BPS *model* and require documenting the necessary information to reproduce the simulation and calibration results. A validated simulation model reflecting the current state of building or building design will be re-calibrated when building conditions have changed, but under *different ambient conditions* which deeply affect the measurement data. Normalization and comparison of results becomes possible as described in section 4.3.1. The required information includes:

- T-1 Details of the IR camera equipment and BES model used (link to camera specification, software version number referring to a revision history to deduce specific features of the simulation program and the implemented building model from).
- T-2 Measurement geometry (view pose  $\mathbf{g}^{mob}$  of the IR camera, intrinsic camera parameters).
- T-3 Link to the set of time-stamped **thermal images** (pairs of measured and simulated images) captured during survey.
- T-4 Building component(s) in the visual focus (section 4.4.1);

---

<sup>34</sup> For examples of measurements, see table 3.1 in section 3.1 showing minimal data for ongoing commissioning.

- Focal parameters (section 4.4.1), i.e. names of the 'free variables' estimated.
- T-5 Specification of error function for inverse model: error terms, regularization term; Results of parameter estimation: initial and final parameter values; residual measurement error.
  - T-6 Initial and boundary values for simulation (for instance, a state vector of air / fluid temperatures, one for each thermal zone). Initial values are needed only for *transient* energy simulation.
  - T-7 Schedule of building occupancy and ancillary weather conditions during survey (section 4.1.3).
  - T-8 Diagnostic results for component or entire building (see examples in section 3.2 on degradation).
  - T-9 Energy impact estimated with respect to previous QGT survey or previous simulation (section 4.3.1).

The version history of QGT surveys bears similarities to the IT support proposed for the evidence-based calibration strategy by Raftery et al. (Raftery et al. 2011).

Inspections serving ongoing monitoring and QGT surveys in particular cover specific building components, units or assemblies, and therefore link to their part descriptions (QGT.4). As an inverse reference, a **part anamnesis** is proposed associating each part with a linked list of all monitoring events concerning it (a sub-list of the BLCH). A specification document of component performance provides a reference or *performance baseline*, specifying acceptable ranges of parameter values.

In a series of QGT inspections, the same part may have been captured from many different viewpoints, producing variations in spatial resolution and affine image distortion. For overlaying and comparing images, we propose transforming (interpolating) all images of the part anamnesis into a uniform, *component-centered* grid in planar or, depending on the object surface, cylindrical coordinates. The transformation is determined by the view pose  $\mathbf{g}^{mob}$  and the component geometry.

One positive side effect of the part anamnesis should be mentioned. The link from the part geometry in the BIM to the thermal images provides *visual features* how the part appears in the thermal spectrum, such as *thermal edges*, and these features have 3D coordinates. This is an advantage for the localization of the IR camera.

A semantic building model mainly serves the operation and maintenance of a particular *building*. At a higher level, it may convey valuable information about actual energy performance and building conditions of an ensemble of buildings, i.e. a *district*. Future patterns of building activity and their likely impact on the consumption of energy fuels may be predicted more accurately by exploiting the BIM as a data repository. For instance, this is essential to the planning of *district heating networks* operating with biomass or waste heat supply because their profitability is sensitive to changing patterns of heating demand.

## 4.6 Research questions and agenda

Remote identification of building models by IR cameras as mobile geo-referenced observers is a *new* concept. Therefore, top priority is given to develop a *functional prototype* demonstrating capability to estimate the condition of a spatially distributed thermodynamic system through remote parameter identification. At a coarse level, the research questions are structured as follows:

### 1. Proof of concept

By applying results from dynamic systems identification to the class of models relevant for heat, mass, and moisture transfer in buildings, characterize the degree of observability of parameters and the information gained from thermal images.

Develop solutions to three key engineering problems: reliable IR camera localization using the BIM as map, accurate IR camera model for thermography prediction / simulation, and in-

terfaces to the BPS (simulation model) to predict the mobile measurement equation and set up the inverse model.

**2. Error Analysis**

Analyze quantitatively the errors and their effects on parameter estimation due to the 'casual' QGT type of surveying occupied buildings, which greatly differ from active thermography using a controlled experiment setup such as a thermal chamber. Is QGT able to estimate the building condition, i.e. the effect of aging or the discrepancy between design and 'as-is', by means of parameter estimation? Does QGT cope with transient load conditions that are encountered during a short period of time and barely controllable?

Are state-of-the-art BPS systems able to assess the energy impact of small and uncertain parameter changes estimated, by running building loads sampled from a suitable probability distribution? I.e. can the user be provided with a significant estimate of the difference in energy efficiency or cost that would result from an estimated difference of building parameters in the long term?

**3. Evaluation**

Perform field testing for thorough technical assessment, accompanied by economic and social assessment.

Define the preconditions that the IR cameras, localization sensors, building maps (BIM), building simulation software, and experimental design must fulfill for QGT to become feasible both technically and economically. Can the energy efficiency gains expected by applying this method at a broad scale be estimated quantitatively?

Estimate the costs of equipment, surveying, and evaluation, as well as economic benefits, e.g. new business models in maintenance. Analyze social impacts on building stakeholders, regarding privacy and data protection.

In the remainder of this section, our detailing of these research questions is explained in work items.

The research questions are grouped into four problem areas: energy systems modeling (4.6.1), BIM integration (4.6.2), experimental evaluation of technical issues (4.6.3), and socio-economic impact analysis (4.6.4). As to the first two areas answers to the detailed research questions posed will lead to achieve our milestones as stated in the proposal for the Helmholtz Research Programme 'Technology, Innovation and Society', section 2.5.5.3.

Milestone	Year
Part-based, semantically attributed geometry and thermodynamic models for buildings	2012
Integrated approach for assessment and monitoring of energy efficiency of buildings	2014

Field testing (4.6.3) and impact analysis (4.6.4) are also essential to establish QGT but can be tackled only in collaborative projects with additional funding, and will greatly exceed the current time frame (POF-II, end of 2014).

## 4.6.1 Energy system model

### 4.6.1.1 Model definition and development

The main research goal is to develop and test a generic extension of BES/BPS aiming at easy and lifelong identification of model parameters from mobile camera measurements. Since this activity cross-cuts existing simulator technology and is not bound to a particular simulation language, platform, or library of building components, the scope of models considered for pivotal development must be defined mathematically or in terms of dynamic systems in general.

- **State equations**

Delimit the class of building models, considering taxonomy of increasing generality of heat transfer:

*Steady-state heat balance* → *Transient spatial (1D→2D→3D) heat transfer* → *Heat, air, and moisture transport (HAM)* → *Computational fluid dynamic model (CFD)*.

How do the calibration parameters and their roles change with increasing model complexity? How much model realism is lost in progressively simplified models, and what may be gained on the other hand from simpler observer interfaces and (possibly) improved observability? Answers to the general question depend on the observability analysis (subsection 4.6.1.2) and will develop with the case studies performed under 4.6.2.

Define the geometry representation: a *feature* representation by polyhedral volumes with individually detailed heat transfer (1D, 2D or 3D) allows more efficient and accurate simulation than a uniform *mesh* or *grid*, but technically complicates the state and measurement equations and thereby the identification task, by needing additional geometric transformations.

- **Parameter selection for building diagnostics**

Make a table of the building *performance degradation* problems discussed in section 3.2. Many types of problems find expression in thermal model parameters that can be identified (a subset of the parameters listed in table 3-3). For each parameter, specify type, value range, and representation, such as primitive value or function with unknown coefficients. The table depends on the level of detail in the model; for example, convective heat transfer may be a *parameter* in a lumped model but a *state variable* in a more detailed model.

- **Mobile observer interface development**

Develop the radiometric camera model predicting the radiosity sensed  $\mathbf{y}(\mathbf{g}^{mob}, t, \mathbf{p})$  as a function of camera view pose  $\mathbf{g}^{mob}$ , simulation time  $t$ , and focal parameter vector  $\mathbf{p}$ , for all image pixels  $(u, v)$ .

$\mathbf{p}$  and time  $t$  are *internal* parameters of the building energy simulator, whereas  $\mathbf{g}^{mob}$  and mobile observer output  $\mathbf{y}$  are *external*, not supported by existing building simulators. Therefore, a new *interface* linking the mobile observer to the simulator must be defined. The work is divided into several subtasks.

- Getting the *visible model components* under  $\mathbf{g}^{mob}$  depending on how the simulator represents and organizes building geometry. Ideally, the model geometry is accessible as a (hierarchical) 3D scene graph: when the camera is placed in the scene using the transformation  $\mathbf{g}^{mob}$ , the scene graph is rendered graphically and the foreground objects are extracted.

- Selecting and accessing the focal parameters  $\mathbf{p}$  to be estimated. These parameters are attached to *components* that are directly *visible* or are immediate *neighbors* (upstream) in the heat and mass flow, and must *not* have their current values *frozen* (section 4.3.1). Each model parameter must provide access to its current *value* and its (variable or function) *name*.
- Forming the measurement function  $y_{u,v}(\mathbf{g}^{mob}, t, \mathbf{p})$  and the derivatives  $\partial y_{u,v}(\mathbf{g}^{mob}, t, \mathbf{p})/\partial \mathbf{p}$  with respect to the focal parameters  $\mathbf{p}$ , as executable code, using a tool for symbolic processing and automatic differentiation (AD) as described in section 4.4.1. Available AD tools will be investigated, and a suitable one for the building simulation platform (4.6.2) be selected and installed. An open question remains as to where precisely 'place' the AD tool between building simulator and observer, and when and how to invoke it.
- **Radiometric camera model** (observer equation and details of thermography simulator)

Allinson's model developed for *aerial* thermographic surveys (Allinson 2007) (see appendix A.1) provides a good starting point for aerial and ground surveys alike. However, several details must be examined.

  - Delimitation: To what extent will air transmittance<sup>35</sup> be considered and represented?
  - Delimitation: which types of BRDF (bidirectional reflectance density functions, appendix A.3) are relevant for building materials?
  - Geometric view factors: Select an accurate and fast GPU assisted approximation algorithm calculating view factors for arbitrary system geometry and measurement poses<sup>36</sup>.
  - Modeling the imaging errors (camera lens distortion, thermal blurring<sup>37</sup>, ...?).
  - Determine the spectral response function of the infrared detector for the camera at hand<sup>38</sup>.

### 4.6.1.2 Parameter estimation (inverse heat transfer)

- Determine the **observability** of parameters numerically from thermal images (condition number, quantitative degree), calculating the Fisher information matrix (FIM) and the sensitivity vectors for the measurement equations.

Which thermal parameters from the building diagnostic set in 4.6.1.1 are unobservable or barely observable from thermal images, and which ones are best observable?
- **Experimental design**: which factors affect identifiability most when using an infrared camera?

---

<sup>35</sup> Atmospheric transmittance ( $0 < \tau_{air} < 1$ ) must be modeled accurately at long viewing distances (Allinson 2007, see section 4.2.1 and appendix A.1); at short distances (<100 m?) one may set  $\tau_{air}=1$ . Window glass and transparent façades are usually assumed opaque with respect to *thermal* radiation ( $\tau_{glass}=0$ ). However, the bulk of solar radiant energy is transmitted in the *visible* and NIR ranges. Advanced glazing materials merit special consideration even in the thermal range ( $\tau > 0$ ?).

<sup>36</sup> View factors between building objects and the camera detector field must be calculated in real time.

<sup>37</sup> A single pixel footprint may hit *several* objects or surfaces, averaging their radiosity values.

<sup>38</sup> An inquiry from the manufacturer (NEC) of the *Thermo Tracer TH7800* available in this project obtained no useful answer. In Appendix A.1 an alternative procedure to estimate the spectral response function is outlined.

- i. Space: viewing from different points, changing object distances and orientations?
- ii. Time: viewing transient behavior in a particular period of time?
- iii. Load: selecting particular weather or occupancy input for parameter estimation?

Under which circumstances do observation equations become singular (rank-deficient)? Simple criteria are sought to recognize camera view poses as redundant, yielding no additional information. Does observability depend on the view pose at all in case of diffuse reflection (Lambertian surfaces), or do viewing distance and angle matter only if surfaces exhibit complicated, anisotropic BRDF's?

To characterize the parameter sensitivity with respect to load (iii), an analytical assessment will be attempted under strong simplifications. A single-zone linear time invariant (LTI) building model will be developed as a reference, preferably one for an available demonstration building. The goal is to derive bounds of the load impact on parameter estimation analytically; the transition function approach sketched in section 4.2.5 will be tried as the first (most obvious) analysis method. Outreach research activities as to the statistical representativeness of load for identification purposes (section 4.2.6) cannot be tackled within the current HGF funding.

- How much is observability affected by the **low temperature differences** found in building environments?
- Choice and analysis of computational procedures:

Select and test **nonlinear regression** methods to estimate parameter values, such as Newton-like schemes (e.g. sensitivity coefficients Wawrzynek, Bartoszek 2002), conjugate gradients, or Levenberg-Marquardt.

Specify and test suitable regularization terms in the residual to make the estimation problem less ill-posed.

Determine the range of validity of the (first-order) approximation of the measurement equation around reference values of parameters, by numerical simulations. How sensitive are parameter optima with respect to the current and fixed values of other parameters? How sensitive are parameter optima with respect to different control input (load schedules)?

## 4.6.2 BIM integration

This work package covers the interfacing of QGT with a building model (BIM) and an energy simulation platform.

- **IR camera localization method**

The IR camera is to be localized, i.e.  $g^{mob}$  to be determined, in the Cartesian building coordinate system of the BIM, reliably and accurately in 6 degrees of freedom. A cost-effective and user-friendly solution is sought for indoor and outdoor surveys *from the ground*.

Referring to section 4.4.2, several important engineering decisions must be made:

- How to divide the work among coarse/absolute and fine/relative localization?
- Which features are used (thermal and visual cues, depth, 3D features such as surfaces, edges, and corners, ...)?
- Auxiliary sensors for reliable localization (GPS, inertial sensors, inclinometer, stereo head, range sensor)?
- Cost, weight, and performance of the entire construction should be taken into account.

The localization accuracy will be quantified statistically, by numerical error analysis; reliability of localization should be evaluated empirically with a focus on object clutter not represented in the building model.

The BIM serves as a 3D map providing the necessary topological and geometric features for localization. It is suggested to design a generic interface for accessing the map information independently of the particular BIM schema used ('feature-extracting filter for localization').

- **Simulation Platform**

The building information model (BIM) schema chosen must adhere to an open standard for information exchange, preferably gbXML (section 3.3).

Modelica is the preferred candidate platform for simulation development and testing, because of its support of symbolic processing, automatic differentiation, and object-oriented modeling (sections 3.4 and 4.4.1).

Building model export from gbXML to Modelica is an open problem. Also, the suitability of gbXML and Modelica remains to be tested for the extensions planned. One possible alternative to gbXML is IFC; HAMlab and ESP-r are the alternatives to Modelica considered.

Two main test cases shall be developed.

- Virtual buildings: A complex *multi-zone model* of a *virtual* building will be implemented for thorough testing of the mobile camera model.
- Real building: Testing the IR camera in an existing building requires a simplified (single-zone) building model to simulate whatever work space the IR camera will actually be operating in. Preference will be given to a demonstration building available on KIT South Campus.

- **BIM extension for monitoring**

The goal is to specify a building information model supporting ongoing monitoring in general and capturing *histories* of *QGT inspections* in particular, grounding on the requirements outlined in section 4.5.2. The specification could extend an existing BIM schema, similar to the concept of application domain extension (ADE) known from CityGML, or, if need be, could lead to a new schema.

- **BIM ↔ BES interoperability**

A key cross-cutting problem discussed in section 4.5.1 is how to transform the information from a BIM into an executable energy simulation model, correctly and efficiently. Issues touched range from the import of BIM geometry (e.g. gbXML→ Modelica) via automatic or semi-automatic tools to convert or transform geometry and material properties, to future energy simulators operating BIMs *directly* and as their *sole* data repository, except for the load schedules which must be supplied by separate sources.

This project has no work capacity left for interoperability issues. However, the progress on this topic shall be monitored by literature reviews and by personal contacts to research institutions (e.g. Tobias Maile, CIFE, Stanford University, or Arno Schlüter, ETH Zürich).



### 4.6.3 Experimental investigation and field testing

- **Residual analysis**

In section 4.2.3, the contamination of measurement residuals by model mismatch and inaccurately known load has been discussed, raising two immediate research questions:

- Which statistical criteria are suitable to decide whether the measurement residual is affected by errors of types a), b), or c) (section 4.2.3)? Can we find quantitative error criteria (e.g. thresholds) when the degree of contamination *invalidates* parameter estimation results?
- Is it possible to *discriminate* the dominant source of error from the residuals?

- **Comparison to traditional building thermography**

How does QGT compare to best-practice methods used in building thermography, performing manual surveys and following standardized procedures of evaluation and diagnostics, such as detecting heat loss caused by insulation defects or thermal bridges (ISO 10051; ISO 6781; ISO 9164; EN ISO 13790) ?

- **Comparison to other calibration methods for BPS/BES**

How do thermal images for parameter estimation compare to measured energy consumption or conventionally measured air and surface temperatures (advantages and drawbacks)? Can QGT supplement or improve conventional calibration methods, and does the *spatially focused* approach (one-parameter-at-a-time) keep the promises made in section 4.3.1?

- **Focal parameter determination**

QGT identifies thermal parameters of those parts *directly viewed* by the camera. Beyond that, the focal parameters may be extended to cover a *neighborhood*, as proposed in section 4.4.1. Is it possible and advantageous to estimate several parameters at a time, and how many? Can we specify criteria how to choose the neighborhood or 'catchment area' of a building part?

- **Emissivity calibration**

Can QGT estimate *emissivity* and *reflectivity* of building surfaces accurately enough while surveying a building in use, i.e. outside thermal chambers or dedicated test sites? A comparative experiment should be performed using a reference emitter or reflective mirror for calibration.

- **Comparison with active thermography**

QGT has been proposed to observe the transient behavior of occupied buildings under heating or cooling operation. Can the types of degradations in buildings discussed in section 3.2 be discovered in this way? For which problems does *active thermography*, imposing *artificial* heating patterns or *artificial* pressure variations, remain indispensable?

- **Design of QGT surveys**

Different types of surveys can be distinguished as to measurement geometry, carrier platforms and auxiliary sensors needed, data capturing strategies etc. Their advantages and drawbacks in general terms are characterized in table 4-1. Can these expectations be substantiated? Which 'critical' building components should QGT inspections concentrate on? Can we find efficient (coarse-to-fine) screening strategies?

#### 4.6.4 Impact analysis

Assuming that the technical soundness and feasibility of QGT could be demonstrated in the previous work packages, its economic and societal impacts remain to be analyzed, preferably by field testing in a substantial municipal test area.

- If QGT inspection were routinely performed at a large scale, and the evaluation be largely automated, could we expect a significant impact on primary energy use / energy efficiency in the building sector, more so than with conventional building thermography? Does improved monitoring during the building lifecycle pay off from the owner's or occupant's perspective, and can their awareness be increased in this way?
- What are the economic costs of performing QGT routinely, at a large scale, in a largely automated fashion? What are main economic and societal obstacles to make it happen?
- How can QGT be performed least invasively and intrusively to building occupants and owners, respecting their privacy and their data? Can it be used in a way avoiding feelings of being under surveillance?

Survey Type	Advantages	Drawbacks / Problems
Airborne remote sensing	<ul style="list-style-type: none"> <li>+ Very fast and efficient (large areas)</li> <li>+ Least invasive</li> <li>+ 3D localization (GPS, air plane) is reliable, simple, and efficient</li> </ul>	<ul style="list-style-type: none"> <li>- Limited view (only roofs), very poor spatial resolution</li> <li>- Inspection targets are often thermally insulated (e.g. loft air spaces)</li> <li>- Severe disturbances (atmosphere transmissivity, sky temperature)</li> <li>- Expensive</li> <li>- Demanding as to weather conditions (clear, cold winter days!)</li> </ul>
Terrestrial scanning (outdoor)	<ul style="list-style-type: none"> <li>+ Many sensible inspection targets are exposed directly (curtain walls, windows)</li> <li>+ Moderate cost (mounted on public vehicle or cable car)</li> <li>+ Reasonably efficient</li> <li>+ Fairly large temperature differences</li> </ul>	<ul style="list-style-type: none"> <li>- Partial occlusion (accessibility)</li> <li>- Limited field of view or poor resolution of high vertical façades</li> <li>- Performing reliable, accurate 3D localization is rather difficult</li> <li>- Survey not related to building use, not targeted to occupants' needs</li> <li>- Disturbances (e.g. wind gusts)</li> </ul>
Built-in inspection devices (indoor)	<ul style="list-style-type: none"> <li>+ Can be targeted to problem spots</li> <li>+ No localization problem</li> <li>+ High spatial resolution</li> </ul>	<ul style="list-style-type: none"> <li>- Not useful for the building stock</li> <li>- Static views yield limited information</li> <li>- More invasive, may violate need of privacy</li> </ul>
Mobile indoor inspection (hand-held or vehicle-mounted camera)	<ul style="list-style-type: none"> <li>+ Good visibility, high spatial resolution</li> <li>+ Can be targeted to occupant needs (thermal comfort)</li> <li>+ Less affected by disturbances than inspection from outside (wind, convection)</li> </ul>	<ul style="list-style-type: none"> <li>- Reliable, accurate 3D localization is difficult</li> <li>- Relatively slow and costly</li> <li>- Low temperature differences <math>\Rightarrow</math> limited observability?</li> <li>- More invasive, may violate privacy</li> </ul>

**Table 4-1:** Ways of performing thermographic surveys

## 5 Conclusion and Outlook

Exergy+ and Thermography+ have been proposed in this report for energy efficient design and life-long performance monitoring of buildings. The promises held by the new concept elaborated in this report are summarized as follows:

- Exergy-based building design and assessment, unlike conventional energy flow analysis based on the first thermodynamic law, makes the thermodynamic efficiency of the energy conversion processes explicit that occur in and around buildings. Exergo-economic-environmental analysis allocates thermodynamic inefficiency to particular HVAC components and permits trading operational efficiency against overall life cycle costs and environmental impacts, at the level of building components and materials and in the same way for the entire building system.
- Performance simulation models linked tightly to the semantic building model (BIM) enables shorter cycles of design, feedback, and improvement. Repeated model identification by means of mobile geo-referenced IR camera surveys allows carrying over simulation-based assessment to the operational phase under uniform performance criteria. Major events and processes in the lifecycle, especially initial and ongoing commissioning, retrofitting, and condition monitoring are thereby monitored. Assessing the contribution of components to specific buildings in situ provides a novel way to learn the true impact of energy-related decisions in practice.
- Quantitative geo-referenced thermography lifts well-known merits of building thermography to the level of quantitative impact analysis through a co-running simulation model. It helps answering essential questions: Does a suspected thermal image reveal truly a degradation shown by changed heat transfer coefficients or related building parameters? Is it relevant to the building user, and what might be the expected long-term cost of a defect? QGT is model-based IR image analysis and camera-based condition estimation via model calibration. The following features add to its flexibility: the ability to simulate thermal images of building parts at design time, serving as a baseline; the transformation and normalization of real images to different viewpoints or different ambient conditions; the spatially focused (one-at-a-time) parameter calibration.

QGT combines the *geo-referenced thermography* by Stilla (Stilla, Hoegner 2008) with elements of *active thermography* as a nondestructive testing method. This innovation will come at a price, requiring many synchronized technical solutions and thorough field testing accompanied by social research. In this report the major research questions and problems were analyzed.

- Firstly, the IR camera must be located and oriented in six degrees of freedom, inside buildings and outside from street level alike. Localization should expect no dedicated infrastructure, e.g. camera network or RFID radio network, except for the BIM serving as a 3D map. For reliability and accuracy, information from several sensors such as IMU, compass, GPS, and visual image features must be fused and matched with 3-D BIM features. Dissimilarity between thermal features in IR images and geometric BIM features leads to added localization overhead. Despite that, an affordable solution is desired, giving handy and manageable equipment to the operator. Autonomous localization and navigation are becoming ubiqui-

tous services in transportation and communication; still no solutions exist that are universal and light-weight, accurate and robust at the same time.

- Predicting the outcome of mobile measurement as a function of the parameters to be estimated is the key feature for identification. Actually, the numerical solution computed by the simulator is sought, not the analytical solution of the heat transfer equation which is not available in most cases. First, the section in the building map corresponding to the camera pose is located (virtual camera placement), then the simulation components in the visual focus and the empirical parameters characterizing their condition are accessed. Finally, the measurement equation must be formed at run time, executed, and differentiated. Therefore, new interfaces to building simulators are required in order to exploit mobile sensors, and the simulators must offer strong geometry support. These arguments favor the development of new building simulators rooted in, i.e. *running directly on* the building model, rather than extending proven simulators like EnergyPlus with their native input and geometry files.
- Most demanding from the viewpoint of dynamic systems theory is analyzing all the *errors* contributing to the measurement residual *besides* the parameters reflecting the building condition: errors in camera localization, mismatch of the numerical model with respect to real building response, errors in capturing weather trajectories, building occupancy, and initial states. It is these error sources that discriminate QGT against *active thermography* bearing on a controlled scenario like 'work piece in a mock-up under sinusoidal heating'. Empirical bias models proposed for aircraft engine monitoring might help compensating the residual bias, but a 'generic' model and a faster and inexpensive method of training should be found for the application in buildings.

Which class of heat, air and moisture models in buildings admits identification by mobile sensors at all? How big is the influence of the load uncertainty on the identification results, specifically weather? Do we have statistical criteria whether transient load during a survey is representative of the conditions in practice? How can the mobility of the IR camera in space and time be exploited in the best way?

- Another challenge is the attending support by *facility management* software. Long-term histories of surveying campaigns including ancillary conditions and results will be stored and retrieved to ensure reproducibility and comparability of measurements and to document the maintenance process. Since buildings are being operated for decades, software support for monitoring should outlast many versions of simulation software and camera hardware. In this report, the idea of a domain extension in the BIM *exchange standard* proper was advocated for performance monitoring, as an alternative to specialized CAFM data structures.
- QGT should pass through extended field tests in thermal chambers, in demonstration buildings and in occupied ones considering different platforms (hand-held cameras, street or airborne vehicles) and different procedures for surveying. Following that, the concept needs economic and social assessment. Can the claimed advantages of improved building monitoring be substantiated? Does testing in-situ provide new insights into aging of building materials, improve owner awareness of efficient building operation, or architect awareness of design decisions? And do these advantages eventually pay off in buildings becoming quantifiably more energy-efficient? How much do regular surveys and evaluation cost; will added value be created in the maintenance branches? Can the monitoring technology be implemented in a way to be accepted by owners and tenants, or does it raise adverse feelings of supervision and intrusion; i.e. what will be the social impact? Could it be a wasteful 'technology-driven' effort in the end?

The detailed concept and work program with work packages to solve the technical problems and answer the aforementioned questions have been developed in this report. Time need goes beyond the end of current POF 2 program period (2014); quicker progress, deeper and/or broader methodological analyses will require third-party funding.

QGT for buildings should be seen in a wider application context, the simulation of urban environment and transformation of the energy system towards integrated networks of electricity, heat, and transportation. For instance:

- District heating networks based on biomass or waste heat require quite accurate forecasts of demand, both short-term demand and long-term prediction of subscriber rates, taking into account the actual building condition and utilization and the demographic change expected. Remote thermographic surveying is already considered and being asked for as one tool.
- Climate models at the urban scale, e.g. to assess efforts such as reflecting roofs planned to mitigate the heat island, will gain increasing importance. They are instances of spatially wide-spread transport models calling for remote identification by means of aerial thermography. At this scale, the individual building energy models will be simplified greatly but may still be present.

Further QGT applications include condition estimation and health monitoring of thermal plants, e.g. in petrochemistry, and networks of infrastructure such as district heating pipelines. We conjecture QGT to be useful for remote state estimation of damaged or partially destroyed plants.

---

## A Radiometric camera models

In this appendix, formulae and techniques needed for the development of infrared camera models are reviewed. Appendix A.1 begins with Allinson's model for aerial thermographic surveys. Appendix A.2 contains the definition and formulae for calculating geometric view factors of polyhedral object surfaces where detector pixels take the role of receiving surfaces. Appendix A.3 deals with cases where surface emissivity and reflectivity are not isotropic and described by one parameter each, but are directionally dependent and represented as bi-directional reflectance distribution functions (BRDF). The implications of dealing with BRDF on the parameter estimation task are discussed. In Appendix A.4, the basics of radiation networks (enclosures) are reviewed and radiative heat transfer coefficients derived.

### A.1 Summary of aerial thermography model after Allinson

The following formulae from Allinson's work (Allinson 2007) are summarized to underpin sections 3.7, 4.2.1, and 4.4.1. First, the correlations between object temperature and radiant power (Planck's law and Boltzmann's law) for blackbodies and gray bodies are quoted; they may be found in any textbook on radiation heat transfer, e.g. (Çengel 2003).

$E_b(\lambda, T) = \frac{2\pi hc^2 \lambda^{-5}}{e^{hc/\lambda KT} - 1} \cdot 10^{-6}$	<b>Spectral emissive power density</b> [W/m <sup>2</sup> μm] of a blackbody at temperature T [K] and wavelength λ [μm]
where	<b>(Planck's law)</b> eq. (A-1)
$h = 6.62606896 \cdot 10^{-34}$ [Js]	Planck's constant
$K = 1,3806504 \cdot 10^{-23}$ [J/K]	Boltzmann constant
$c = 2.99792458 \cdot 10^8$ [m/s]	Speed of light
$E_b(T) = \int_0^\infty E_b(\lambda, T) d\lambda = \sigma \cdot T^4$	<b>Total emissive power density</b> [W/m <sup>2</sup> ] ( <b>radiosity</b> ) of a <b>blackbody</b> at temperature T [K] per unit surface area ( <b>Stefan-Boltzmann's law</b> )
where	eq. (A-2)
$\sigma = 5.6704 \cdot 10^{-8}$ [W/m <sup>2</sup> K <sup>4</sup> ]	Stefan-Boltzmann constant
$\varepsilon(\lambda, T) = E(\lambda, T)/E_b(\lambda, T) \leq 1$	<b>Emissivity</b> of a gray body emitting <b>spectral radiosity</b> E(λ, T) [W/(m <sup>2</sup> μm)] at temperature T and wavelength λ [μm]
$\varepsilon(T) = E(T)/E_b(T) \leq 1$	<b>Emissivity</b> (spectrally averaged) of a gray body emitting <b>total radiosity</b> E(T) [W/m <sup>2</sup> ] at temperature T
$L_b(\{\lambda, \} T) = E_b(\{\lambda, \} T)/\pi$ $L(\{\lambda, \} T) = E(\{\lambda, \} T)/\pi$	<b>Radiance</b> , i.e. radiosity per <b>solid angle</b> (steradian) [W/m <sup>2</sup> sr] of a blackbody (L <sub>b</sub> ) or gray body (L); λ wavelength in case of spectral radiance; Assuming a perfectly diffuse emitter (Lambertian surface).

An *ideal* detector would integrate spectral radiosity values according to the Boltzmann law eq. (A-2), attaching *equal* weight 1 to all wavelengths and ending up with the radiosity  $E_B(T)$ . *Real* infrared detectors produce a slightly distorted analogue output signal  $L_R(T)$  where wavelengths are weighted

according to the *spectral detector sensitivity*, specified by the **spectral response function**  $R(\lambda)$ ,  $R: [0, \infty] \rightarrow [0, 1]$ . Sensitivity values may be assumed to be normalized by their maximum value, i.e.  $0 \leq R(\lambda) \leq 1$ . Digital output  $DN(T)$ , after A/D conversion, is proportional to  $L_R(T)$  with **slope** (gain)  $m$  and **intercept (offset)**  $c$  coefficients mapping the range of temperatures of interest.

<b>IR detector output</b>		
$L_R(T) = \int_0^\infty L(\lambda, T) \cdot R(\lambda) d\lambda$	Analog detector output	eq. (A-3)
$DN(T) = m \cdot L_R(T) + c$	Digital detector output	

### **IR detector calibration (known SRF)**

To determine the coefficients  $m$  and  $c$  in eq. A-3, object(s) at known temperatures  $T_i$  (measured by contact thermometer) and with known emissivity values  $\varepsilon_i$  should be imaged, obtaining actual detector output values  $DN_i$ . The corresponding radiance values  $L_i := L_R(T_i)$  are *calculated*, by integrating products of spectral radiance, emissivity  $\varepsilon_i$ , and detector sensitivity  $R(\lambda)$ . The spectral response function should be known from the camera manufacturer in the form of a table.

A regression line  $y = m \cdot x + c$  is finally fitted through the pairs  $(L_i, DN_i)$ .

### **IR detector calibration (unknown SRF)**

In our case (infrared camera *Thermo Tracer TH 7800*) the SRF is unknown. For estimating an unknown SRF, we outline a simplistic regression method treating the camera as a black box. A more accurate but, in our case, too costly alternative would be *measuring* spectral radiosity directly with a spectrometer. The unknown spectral sensitivity is estimated by a known temperature distribution (spread) imposed on a test object, exploiting the nonlinear correlation between temperature and radiances. For simplicity, the following assumptions are made (see figure A-1 for illustration):

- A **blackbody** as test specimen should be available for which  $\varepsilon(\lambda) \approx 1$  holds with good accuracy in the spectral band of interest  $[\lambda_{min}, \lambda_{max}] = [8\mu\text{m}, 14\mu\text{m}]$  and in the thermal range  $[T_{min}, T_{max}]$  relevant to buildings, e.g.  $[-20^\circ\text{C}, 60^\circ\text{C}]$ . The ranges are attuned in a way that the overwhelming fraction of radiance, and also detector sensitivity, are concentrated in the band  $[\lambda_{min}, \lambda_{max}]$ .
- The blackbody will be heated or cooled to  $M > N + 1$  distinct temperature levels  $T_j$  within  $[T_{min}, T_{max}]$ , which will be determined independently by the IR camera as  $\tilde{T}_j$  ( $1 \leq j \leq M$ ).
- SRF values are negligible outside the band  $[\lambda_{min}, \lambda_{max}]$ , in any case constant (specified by two constants  $R_{min} \neq 0$  and  $R_{max} \approx 0$ ). Inside the band, SRF is approximated as a *piecewise linear* function with coefficient values  $R_i$  ( $0 \leq i \leq N$ ) at equidistant points:  

$$\lambda_i := \lambda_{min} + i \Delta\lambda \quad (0 \leq i \leq N), \quad \lambda_N := \lambda_{max}.$$
- SRF coefficients only depend on wavelength, not on temperature.
- Let the spectral blackbody radiance  $L_b(\lambda, T)$  also be piecewise linearized in each interval  $[\lambda_i, \lambda_{i+1}]$  about the center point value  $L_{b,i}(T) := L_b(\lambda_i + \Delta\lambda/2, T)$ .

The setup yields  $M$  equations for blackbody radiances  $L_j$  corresponding to the IR temperatures measured ( $L_j := L_b(\tilde{T}_j) = \sigma/\pi \cdot \tilde{T}_j^4$  by Stefan-Boltzmann eq. (A-2). Each equation is linear in the  $N+1$  unknown camera parameters  $R_i$ :



$$\begin{aligned}
L_j &= \int_0^\infty L_b(\lambda, T_j) \cdot R(\lambda) d\lambda \underset{\substack{\approx \\ \lambda_0 = \lambda_{min} \\ \lambda_N = \lambda_{max}}}{\approx} \sum_{i=0}^{N-1} \int_{\lambda_i}^{\lambda_{i+1}} L_b(\lambda, T_j) \cdot R(\lambda) d\lambda \approx \\
&\sum_{i=0}^{N-1} L_{b,i}(T_j) \underbrace{\int_{\lambda_i}^{\lambda_{i+1}} \left( R_i + \frac{\lambda - \lambda_i}{\Delta \lambda} (R_{i+1} - R_i) \right) d\lambda}_{(R_i + R_{i+1}) \cdot \Delta \lambda / 2} = \sum_{i=0}^N l_{ij} \cdot R_i \quad \text{where} \\
l_{ij} &:= \left( L_{b,i}(T_j) + L_{b,i-1}(T_j) \right) \cdot \frac{\Delta \lambda}{2} \quad (0 \leq i \leq N, 1 \leq j \leq M), \\
L_{b,-1}(T_j) &:= L_b \left( \lambda_0 - \frac{\Delta \lambda}{2}, T_j \right).
\end{aligned}$$

In vector and matrix notation the coefficient vector is found by linear regression:

$$\mathbf{r} := [R_0, \dots, R_N]^T, \quad \mathbf{l} := [L_1, \dots, L_M]^T, \quad \mathbf{L} := \begin{bmatrix} l_{01} & \dots & l_{N1} \\ \vdots & \ddots & \vdots \\ l_{0M} & \dots & l_{NM} \end{bmatrix}$$

$$\mathbf{r}^* = \arg \min_{\mathbf{r}} \|\mathbf{l} - \mathbf{L} \cdot \mathbf{r}\|^2 \Rightarrow \mathbf{r}^* = \mathbf{L}^\dagger \cdot \mathbf{l}$$

(superscript ‘†’ denoting the pseudo-inverse).

For enhanced numerical stability, constraints on the derivatives imposing smoothness of the SRF may be introduced as regularization terms. A low third derivative ( $\ddot{R}(\lambda)$ ) constraint included in the minimization with a weighting factor  $w$  would favor quadratic SRF shapes:

$$\mathbf{r}^* = \arg \min_{\mathbf{r}} \left( \|\mathbf{l} - \mathbf{A} \cdot \mathbf{r}\|^2 + w \int \|\ddot{R}(\lambda)\|^2 d\lambda \right).$$

Finite-difference approximations linear in the coefficients  $R_i$  are obtained for the third derivatives as

$$\ddot{r}_i \approx \frac{R_{i+3} - 3R_{i+1} + 3R_{i-1} - R_{i-3}}{8\Delta\lambda^3} \Rightarrow \ddot{\mathbf{r}} = \mathbf{D} \mathbf{r}.$$

The regularization becomes a quadratic form with symmetric positive definite banded matrix  $\mathbf{D}^T \mathbf{D}$ :

$$\sum_i \|\ddot{r}_i\|^2 = \mathbf{r}^T \mathbf{D}^T \mathbf{D} \mathbf{r}.$$

For an actual experimental setup including numerical evaluation, a few technical details must be resolved:

- The condition number of the matrix  $\mathbf{A}$ , coefficients of which depend on the distribution (spread) of temperatures in relation to wavelengths, governs the estimation uncertainty. How should temperatures be chosen to maximize the condition number?
- How to select the weight factor  $w$ ?
- Instead of a piecewise linear function, we could have chosen a 4<sup>th</sup> degree polynomial or a spline function from the first to reduce the number of coefficients. Several publications claim that even a Gaussian distribution function (bell curve) approximate the SRF well, which we cannot confirm from plots of calibrated SRF's reported in the literature. Our choice is owing to the fact that we simply do not know the type of function shaping SRF's of typical thermal infrared imagers.

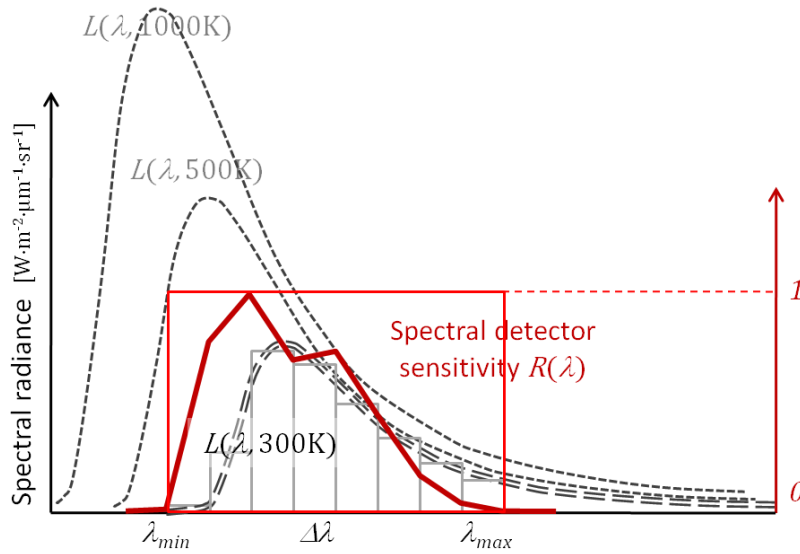


Figure A-1: Approximations of the spectral radiance and the spectral response function.

### Surface Temperatures

Total radiosity per solid angle  $L(T)$  can be inverted to estimate the temperature  $T$  directly, using an approximation formula by Singh (1988) cited in (Allinson 2007):

$$\underbrace{\ln(L(T))}_{=:y} \cong a + b \cdot \underbrace{\frac{1}{T}}_{=:x}$$

Where the as yet unknown coefficients  $a$ ,  $b$  depend on the particular SRF and are determined as regression coefficients of a line fitted to data pairs  $(1/T_i, \ln DN(T_i))$ .  $T_i$  denote temperatures in a narrow interval  $[T_{min}, T_{max}]$  measured together with the raw detector output  $DN(T_i)$ . Temperatures are not estimated explicitly by our camera model but empirical parameters of the thermal process behind are estimated from radiance or, if appropriate, from camera-converted temperature values.

In general, several objects such as inspection targets, background, and sky jointly contribute to the (spectral or total) radiance received by the detector. We cite Allinson's formula of the at-sensor radiance but will take a different approach, relying on the *thermal building simulator* to handle all radiant heat exchange between *arbitrary objects* while using the view factor method in eq. (A-2) to calculate the radiance at the *detector* due to the directly visible *object* surfaces.

**At-sensor radiance** The radiance  $L_{Sens}$  received at a detector pixel is assumed to come from a single target object  $L_b^{obj}$  and a uniform background  $L_{bg}$ . It further depends on the atmosphere between target and camera (transmittance  $\tau$ , up-welled radiance  $L_u$ ) and on the down-welled atmospheric radiation  $L_d$  reflected at the target and redirected toward the camera.

The following formula (Allinson 2007, 4-5) applies to each temperature  $T$  and wavelength  $\lambda$ ; for simplicity, these arguments have been omitted.

$$L_{Sens} = \underbrace{\tau}_{\substack{\text{Atmosph.} \\ \text{transmiss.}}} \cdot \left( \underbrace{\varepsilon \cdot L_b^{obj}}_{\substack{\text{Emitted,} \\ \text{target obj.}}} + \underbrace{(1 - \varepsilon)}_{\text{Reflected}} \cdot \left( \underbrace{F}_{\text{Sky}} \cdot L_d + \underbrace{(1 - F)}_{\text{Background}} \cdot L_{bg} \right) \right) + \underbrace{L_u}_{\substack{\text{Atmosphere} \\ \text{between object and sensor}}} \quad \text{eq. (A-4)}$$

where

$\tau$	Transmittance of the air layer between camera and object
$L_u$	Up-welled radiance of the air layer between camera and object
$\varepsilon$	Emissivity of the target object surface
$L_b^{obj}$	Radiance of the target <i>object</i> if it were a <i>blackbody</i>
$F$	Sky view factor, $0 \leq F \leq 1$ , the portion of the surface hemisphere covered by the sky.
$L_d$	Down-welled radiance from the entire sky (atmosphere), reflected at the target surface
$L_{bg}$	Radiance from background objects reflected at the target surface

The following parameters in eq. (A-4) must be known, i.e. must be determined:

- **Atmospheric** parameters  $\tau$ ,  $L_d$ ,  $L_u$ : methods are found in (Allinson 2007), chap. 7.
- **Target object** (building) parameters  $\varepsilon$ ,  $F$ : methods are given in (Allinson 2007), chap. 8.
- **Background** radiance  $L_{bg}$  is equated with the target radiance in (Allinson 2007).

Knowing the at-sensor radiance  $L_{sens}$ , the atmospheric parameters  $\tau$ ,  $L_d$ ,  $L_u$ , and the target object parameters  $\varepsilon$ ,  $F$ , and **assuming** that the background radiance  $L_{bg}$  **equals** the target blackbody radiance  $L_b^{obj}$  sought, the latter may be solved for (Allinson 2007, formula 4-7):

$$L_b^{obj} = \frac{(L_{sens} - L_u)/\tau + (1 - \varepsilon) \cdot F \cdot L_d}{\varepsilon + (1 - \varepsilon)(1 - F)}.$$

Next, atmospheric sky radiation is considered. These formulae, usually, are not required for indoor building thermography with windows closed (the entire envelope including glazing is opaque with respect to thermal radiation), but for outdoor surveys from street level because of reflections at window glazing.

#### **Determining atmospheric parameters $\tau$ , $L_u$**

Both parameters depend on

- angle of deviation  $\theta$  of the viewing ray from the nadir direction and sensor altitude  $h$ ,
- wavelength  $\lambda$  and air temperature  $T$ ,
- atmospheric properties, i.e. air pressure, humidity, and gas composition in different layers.

Allinson calculates **transmittance**  $\tau(\theta, h, \lambda, T)$  and upwelled **atmospheric radiance**  $L_u(\theta, h, \lambda, T)$  for discrete arguments, employing the [MODTRAN 4 software](#) from remote sensing. The atmospheric properties needed in c) were received from a nearby weather station at the day of surveying (*radio soundings*).

**Approximations** independent of wavelength and temperature,  $\tau(\theta, h)$  and  $L_u(\theta, h)$ , are derived as the slope and the offset, respectively, of a regression line that correlates raw detector output without atmospheric transmission with the respective output accounting for it, for any target object radiance. To obtain the data pairs for line fitting, *artificial blackbody* radiances  $L(\lambda, T) = E_b(\lambda, T)/\pi$  are generated for *different values* of *temperature* and *wavelength* in their respective bands and integrated by eq. (A-3), obtaining detector output  $L_R(T)$  with transmittance ignored. Corresponding values with atmospheric transmission ( $L_u > 0$ ,  $\tau < 1$ ) are obtained by substituting at-sensor radiance  $L_{sens}$  after equation (A-4) where, for simplicity,  $\varepsilon$  is set to 1, i.e. reflected background radiance is ignored. Calculations are performed independently for different angles  $\theta$  but at constant height  $h$ :

$$\begin{aligned}
L(\theta, h, T) &= \int_0^\infty \left( \underbrace{\overbrace{\tau(\theta, h, \lambda, T)}^{\substack{\text{Transmittance} \\ \text{MODTRAN}}} \cdot \overbrace{L(\lambda, T)}^{\substack{\text{Blackbody radiance} \\ \text{after Planck}}} + \overbrace{L_u(\theta, h, \lambda, T)}^{\substack{\text{Upwelled} \\ \text{MODTRAN}}}}_{L_{Sens} \text{ after eq. (A-4) for } \varepsilon=1} \right) \cdot \underbrace{R(\lambda)}_{\text{known}} d\lambda \equiv \\
&\quad \underbrace{\tau(\theta, h)}_{\substack{\text{Desired factor} \\ \text{independent of } \lambda}} \cdot \underbrace{\int_0^\infty L(\lambda, T) \cdot R(\lambda) d\lambda}_{\substack{L_R(T) \text{ calculated for} \\ \text{different values of } T}} + \underbrace{L_u(\theta, h)}_{\substack{\text{Desired coefficient} \\ \text{independent of } \lambda}} \cdot \underbrace{\int_0^\infty R(\lambda) d\lambda}_{\text{constant } R_0} = \\
&\quad \underbrace{\tau(\theta, h)}_{\text{Slope}} \cdot \underbrace{L_R(T)}_{\substack{\text{independent} \\ \text{variable}}} + \underbrace{L_u(\theta, h)}_{\text{Offset}} \cdot R_0 \qquad \qquad \qquad \text{eq. (A-5)}
\end{aligned}$$

For each angle value  $\theta$ , a regression line with slope  $\tau(\theta, h)$  and offset  $L_u(\theta, h)$  is fitted through the set of pairs  $(L_R(T_i), L(\theta, h, T_i))$  where equidistant temperatures  $T_i$  in the interesting range of outdoor temperatures  $[-5^\circ\text{C}, 5^\circ\text{C}]$  are chosen. The results (fig. 7-2 in Allinson 2007) show a very close-to-linear correlation between radiances with and without atmospheric transmittance. Within the narrow temperature range, the radiances  $L_R(T_i)$  are spaced out evenly, i.e. give an almost linear function of temperature.

In a further step, the transmittance  $\tau(\theta, h)$  and the up-welled radiation  $L_u(\theta, h)$  are approximated by 4<sup>th</sup> order polynomials of the angle  $\theta$ :

$$\tau(\theta) = \sum_{0 \leq k \leq 4} a_k \theta^k, \quad L_u(\theta) = \sum_{0 \leq k \leq 4} b_k \theta^k$$

Results (diagrams 7-3, 7-4 in Allinson 2007) show that the transmittance  $\tau$  decreases with the declination angle  $\theta$  whereas the up-welled radiance  $L_u$  increases.

### **Determining atmospheric parameters $L_d, T_{sky}$**

Directional down-welled sky radiation represented as a function  $L_d(\theta, \phi)$  [ $\text{W}/\text{m}^2$ ] of declination angle  $\theta$  and azimuth angle  $\phi$  was calculated with the MODTRAN software. Atmospheric properties required for calculation at the day of surveying were captured from the weather station. The entire hemispherical radiance incident on a horizontal ground surface follows from double integration over  $\theta$  and  $\phi$  where independence of azimuth angle was assumed (formula 7-7 in (Allinson 2007)).

$$L_d = 2 \int_0^{\pi/2} L_d(\theta, \varphi) \cdot \cos \theta \cdot \sin \theta d\theta \qquad \qquad \qquad \text{eq. (A - 6)}$$

The apparent sky temperature  $T_{sky}$  was estimated from the downwelled radiation using the Stefan-Boltzmann law, eq. (A-2):

$$T_{sky} = (L_d / \sigma)^{1/4}.$$

Under clear sky conditions and measured air temperature of  $+4^\circ\text{C}$  (277K) the sky temperature was calculated as  $T_{sky} = 261 \pm 3\text{K}$ .

## A.2 A note on view factor calculation

The *view factor*<sup>39</sup>  $F_{ij}$  of (from) a surface  $F_i$  to a surface  $F_j$  denotes the fraction of diffuse *radiant energy* leaving  $F_i$  that strikes  $F_j$  directly. For a small flat differential surface element  $dF_j$  of area  $dA_j$ , located at a distance  $r_{ij}$  from a differential element  $dF_i$ , the view factor  $F_{ij}$ , i.e. the fraction of  $dF_i$ 's radiation reaching  $dF_j$ , is calculated by the formula (Çengel 2003)

$$dF_{ij} = v_{ij} \frac{\cos \theta_{ij} \cdot \cos \theta_{ji} \cdot dA_j}{\pi r_{ij}^2}, \quad v_{ij} = \begin{cases} 1, & \text{if } dF_j \text{ is visible from } dF_i \\ 0, & \text{otherwise} \end{cases} \quad \text{eq. (A-7)}$$

Where  $\theta_{ij}$  denotes the angle that the normal vector of surface  $i$  (*first* index) includes with the line of sight connecting both surfaces; the angle cosine product models two attenuations in series caused by diffuse reflection, one occurring at the 'sender' side and one at the 'receiver'. The view factor of a large surface  $F_i$  with respect to another surface  $F_j$  is obtained by doubly integrating over differential patches, normalizing by the area of the sending surface  $A_i$  so as to obtain a value  $\leq 1$ :

$$F_{ij} = \frac{1}{A_i} \int_{A_i} \int_{A_j} v_{ij} \frac{\cos \theta_{ij} \cdot \cos \theta_{ji}}{\pi r_{ij}^2} dA_j dA_i \leq 1 \quad \text{eq. (A-8a)}$$

At this point, some well-known and useful rules for calculating view factors of discrete surface patches are summarized.

Reciprocity rule:

$$A_i F_{ij} = A_j F_{ji} \quad \forall i, j.$$

The reciprocity rule follows from eq. (A-8) by exchanging the indices  $i, j$ , because the integrations over the finite areas  $A_i, A_j$  can be performed in any order.

Summation rule:

For a surface set  $\{S_j\}_{j=1, \dots, n}$  forming an *enclosure* with no external sources or sinks of radiation:

$$\sum_{j=1}^n F_{ij} = 1 \quad \forall i.$$

$F_{ii} = 0$  for convex or flat surfaces but  $F_{ii} > 0$  for concave ones.

Superposition rule:

If the 'receiving' surface  $S_j$  in  $F_{ij}$  is split into disjoint patches  $S_j = \dot{\cup}_k S_k$ , then

$$F_{ij} = \sum_k F_{ik}$$

but, conversely,  $F_{ji}$  with the 'sending' surface  $S_j$  being subdivided is a weighted mean of the constituent view factors  $F_{ki}$ :

$$A_j F_{ji} = A_i \underbrace{F_{ij}}_{=\sum_k F_{ik}} = \sum_k A_k F_{ki} \Rightarrow F_{ji} = \sum_k \frac{A_k}{A_j} F_{ki}.$$

<sup>39</sup> Common alternative terms: form factor, shape factor, or configuration factor

**Planar and spherical view factors**

The *planar* view factor eq. (A-8) describing the interaction between planar surfaces depends on the relative orientations of *both* surfaces with respect to their common line of sight. It differs from the *spherical view factor*  $F_{ij}^{sph}$ , denoting the fraction of *hemisphere area occupied* by  $S_j$  when projecting the surface onto the unit hemisphere centered in  $S_i$ . An example is the *sky view factor*  $F_{i,sky}^{sph}$  of  $S_i$  where the sky surface plays the role of  $S_j$ . The relationship between flat and spherical view factor is

$$F_{ij} = F_{ij}^{sph} \cdot \cos \theta_{ij}. \tag{eq. A-8b}$$

This is illustrated by the ‘Nusselt analogy’ in figure A-2 below: the spherical view factor indicates the fraction of occupied *hemisphere area*; the planar view factor gives the respective fraction of occupied *circle area* when the hemisphere patches are projected onto the *base circle*. The relationship is essential for implementing IR camera models:

- When the *detector* array of an *IR camera* is the receiving surface, the share of radiosity falling on each pixel is given by the *spherical view factor*  $F^{sph}$ , *not* the planar view factor  $F$  because the camera lens collects radiosity from a *view pyramid* of constant solid angle per pixel, independently of the orientation of the line of sight with respect to the detector surface. In other words, a *detector surface should be regarded as spherical, always normal to the line of sight* ( $\cos \theta_{ij} = 1$ ), and not as flat.
- Projecting facets onto a hemisphere and calculating their *spherical view factors* is equivalent to *graphical scene rendering* placing a virtual camera with opening angle  $\pi$  in the center. Hidden surfaces have visibility  $v_{ij}=0$ . Graphical rendering in the visible spectrum is efficiently and routinely performed by modern GPU. A discrete approximation of spherical view factors is obtained by assigning each facet a unique color value and counting the screen pixels with that color. To approximate the planar view factor, in addition, pixel counts are weighted by  $\cos \theta$  according to eq. A-8b. The methods described in the literature (Robinson, Stone 2005; Takizawa et al. 2006; Borsdorf et al. 2005) apply to the case of diffuse (Lambertian) reflection. *Specular* reflections, handled by Wallner (Wallner 2009), require more general approaches (bi-directional reflectance distribution function, BRDF).

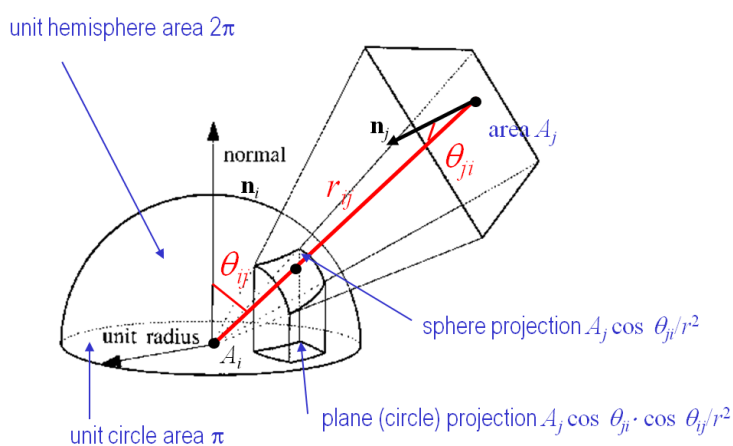


**Figure A-2:** Planar and spherical view factors illustrated by the Nusselt analogy (from <http://www.cis.udel.edu/~chandra/640/Spring05/radiosity.ppt>).

### A.3 Bi-directional reflectance distribution function (BRDF)

From (Poglio et al. 2006), the radiance  $L(\mathbf{x}, \omega_v)$  leaving a surface at a point  $\mathbf{x}$  in the viewing direction  $\omega_v$  comprises the radiance  $L_e(\mathbf{x}, \omega_v)$  emitted by  $\mathbf{x}$  in that direction and the reflected radiances  $L_R(\mathbf{x}, \omega)$  impinging on  $\mathbf{x}$  from all directions  $\omega$ , integrated according to the bi-directional reflectance distribution (BRDF) of the surface at  $\mathbf{x}$ :

$$L(\mathbf{x}, \omega_v) = L_e(\mathbf{x}, \omega_v) + \int_{\Omega} f_R(\mathbf{x}, \omega, \omega_v) \cdot L_R(\mathbf{x}, \omega) \cdot \cos \theta \, d\omega. \quad \text{eq. (A-9)}$$

$\Omega = [0, \pi/2] \times [0, \pi]$  covers all angular directions  $\omega := (\text{elevation } \theta, \text{azimuth } \varphi)$  of the hemisphere attached 'normally' to the surface, centered in point  $\mathbf{x}$ . For all ingoing and outgoing directions  $\omega, \omega_v$ , respectively, the BRDF values  $f_R(\mathbf{x}, \omega, \omega_v)$  indicate the fraction of radiance entering via  $\omega$  at  $\mathbf{x}$  that is reflected via  $\omega_v$ . These values are positive, symmetric with respect to ingoing and outgoing directions, and integrate to at most one (conservation of energy) (Nicodemus 1965):

$$f_R(\mathbf{x}, \omega_v, \omega) = f_R(\mathbf{x}, \omega, \omega_v) \geq 0 \quad \forall \omega, \omega_v, \quad \int_{\Omega} f_R(\mathbf{x}, \omega, \omega_v) \cdot \cos \theta \, d\omega \leq 1 \quad \forall \omega_v.$$

In many cases, the reflective properties encoded in the BRDF neither depend on the azimuth angle  $\varphi$  (they are isotropic) nor on the point  $\mathbf{x}$ .

In a radiometric camera model, equation (A-9) would be applied to each pixel of the IR detector. Let the viewing ray passing through the camera origin and through pixel  $p = (u, v)$  have 3D representation  $l_p^{cam}$  in camera coordinates and  $l_p^{world} = \mathbf{g}^{mob}(l_p^{cam})$  in the building frame where the camera view pose  $\mathbf{g}^{mob}$  was defined in section 4.2.1. Let  $S_p$  be the surface closest to the camera and intersecting the ray  $l_p^{world}$  at point  $\mathbf{x}$ . All quantities are determined by GPU assisted rendering and specifically by placing the rendering camera according to the IR camera pose  $\mathbf{g}^{mob}$ .

The negative direction  $-\mathbf{l}_p$  of this ray and the surface normal  $\mathbf{n}_p$  include an angle  $\theta_v = \cos^{-1}(-\mathbf{l}_p^T \mathbf{n}_p)$  which characterizes the viewing direction  $\omega_v$ . When surface  $S_p$  has directional emissivity  $\varepsilon_v$  and temperature  $T_p$  according to the thermal model,  $L_e$  in eq. (A-9) is determined by the blackbody radiance

$$L_e(\mathbf{x}, \omega_v) = \varepsilon_v \cdot L_b(T_p).$$

$L_b$  is known (computable) whereas the emissivity  $\varepsilon_v$  may be unknown and to be estimated.

In a discrete model world, the contributions reflected at  $\mathbf{x}$  in eq. (A-9) come from a *finite* set of model elements  $S_n$  ( $n=1 \dots N$ ) characterized by viewing directions  $\omega_n$ , or, rather, by finite intervals of directional angles occupied,  $\Omega_n := [\omega_n^{min}, \omega_n^{max}]$ . The directionally integrated radiosity from each  $S_n$  to facet  $S_p$  is approximated by *constant* radiance multiplied by the *view factor*  $F_{np}$  from  $S_n$  to  $S_p$ :

$$\int_{\Omega_n} L_R(\mathbf{x}, \omega) \cdot \cos \theta \, d\omega \approx F_{np} \cdot L_b(T_n) \quad \text{eq. (A-10)}$$

We will also attempt to approximate the continuous functional terms  $f_R$  in the BRDF by piecewise constant values, i.e. a mean value for each interval  $\Omega_n$ :

$$\bar{f}_{R,n} = \frac{1}{|\Omega_n|} \int_{\Omega_n} f_R(\mathbf{x}, \omega, \omega_v) \, d\omega. \quad \text{eq. (A-11)}$$

In practical cases, a 2D vector  $f_{k,m}$  of unknown coefficients is able to represent the directional reflectivity in the BRDF where index  $m$  selects the region of viewing angle  $\theta_v$  and index  $k$  represents the

magnitude of angle between ingoing and outgoing direction,  $|\theta - \theta_v|$ . Then,  $\bar{f}_{R,n}$  is written as a linear combination of coefficients  $f_{k,m}$  determined by  $S_n$ 's view geometry with respect to  $S_p$ . With eq. (A-10, A-11), equation (A-9) simplifies to

$$L(\mathbf{x}, \omega_v) \approx \underbrace{\varepsilon_v}_{\text{unknown parameter}} \cdot \underbrace{L_b(T_p)}_{\text{Emitted by visible model component}} + \sum_{n=1}^N \underbrace{\bar{f}_{R,n}}_{\substack{\text{Known linear} \\ \text{combination of} \\ \text{unknown parameters}}} \cdot \underbrace{F_{np} \cdot L_b(T_n)}_{\text{Reflected from model components}} \quad (\text{eq. A-12})$$

Measurement equation (A-12) belongs to the observer (camera model) while its constituent terms, the radiance terms  $L_b()$  and the view factors  $F_{np}$  characterizing radiant exchange of objects, are computed by the building energy model and need to be accessed via the mobile observer interface. The parameters  $\varepsilon_v$  and coefficient vectors  $\bar{f}_{R,n}$  are specific for each view pose. In general, emitted blackbody radiance is a function  $L_b(\mathbf{p})$  of component parameters to be estimated, as has been discussed in sections 4.2.1 and 4.4.1 (eq. 4-8).

The vector representation  $f_{k,m}$  raises the question of suitable BRDF models. Parameterized BRDF models have been developed with compactness of representation in mind, and may be classified as physical, empirical, or semi-empirical (Shell 2004). Semi-empirical models incorporate some measured data but are also based on the physics of electromagnetic energy and material interactions. They require further parameters such as surface roughness and the complex index of refraction. Often, the BRDF is composed of a summation of specular and diffuse components. Popular semi-empirical BRDF models include the Phong and the Cook-Torrance models (used in computer graphics), and the Sandford-Robertson model in the infrared spectrum used for military target recognition of aircraft from infrared signature (Nelsson et al. 2005; SMSG 2010). Selecting suitable BRDF models for reflective building materials such as glazing and coating is one research question mentioned in section 4.6.1.

## A.4 Radiation networks

In this section, radiative heat transfer in gray-body enclosures is summarized to derive the heat transfer coefficients in the dynamic system model (section 4.1.1) (Mehra 1974; Çengel 2003) (Chap. 13). A blackbody at temperature  $T$  and in thermal equilibrium with its environment emits and absorbs radiation at power density  $E_b = \sigma T^4$  [ $W/m^2$ ]. For gray bodies with emissivity coefficients  $\varepsilon_i < 1$ , the difference between emitted and received radiation must be derived to set up their energy balance correctly. Self-emitted radiation is decreased by factor  $\varepsilon_i < 1$  with respect to a black body while the complementary fraction  $1 - \varepsilon_i$  of radiation received from the environment is reflected. Therefore, the effective radiosity of a gray body becomes:

$$J_i = \underbrace{\varepsilon_i E_{b,i}}_{\text{absorbed / emitted}} + \underbrace{(1 - \varepsilon_i) G_i}_{\text{reflected}} \quad \Rightarrow \quad G_i = \frac{J_i - \varepsilon_i E_{b,i}}{1 - \varepsilon_i}$$

Where

- $J_i$ : Radiosity (power density per unit area, [ $W/m^2$ ]) of gray body, **outgoing**
- $G_i$ : Radiosity [ $W/m^2$ ] of the environment, **incoming**.

The difference between outgoing and incoming radiosity weighted by the actual surface area  $A_i$  indicates the effective gain (<0) or loss (>0) as to radiative power:



$$Q_i = A_i \left( \underbrace{J_i}_{\text{outgoing}} - \underbrace{G_i}_{\text{incoming}} \right) \stackrel{\text{substituting } G_i}{=} A_i \frac{\varepsilon_i}{1-\varepsilon_i} (E_{b,i} - J_i) = \frac{1}{\underbrace{R_i}_{R_i := \frac{1-\varepsilon_i}{A_i \varepsilon_i}}} (E_{b,i} - J_i) \quad \text{eq. (A-13)}$$

Where  $Q_i$ : radiative power [W] entering or leaving the  $i$ -th body,  $A_i$  surface area [ $m^2$ ].

In the theory of *radiation networks* (Mehra 1974) the factor of proportionality in eq. (A-13) is interpreted as the inverse  $1/R_i$  of some *radiative resistance*  $R_i$  causing heat flow  $Q_i$  under the *potential difference*  $E_{b,i} - J_i$ . Surprisingly perhaps, not the difference between the radiosity  $E_{b,i}$  of the blackbody and its environment  $G_i$  is defined as the potential difference, which would lead to the simpler (but pointless) equation  $Q_i = A_i \varepsilon_i (E_{b,i} - G_i)$ , rather the difference between blackbody and effective radiosity  $E_{b,i} - J_i$  makes the relevant potential difference.

### Exact Solution

The radiative interaction between  $n$  bodies is determined by a linear system of equations as follows. The body surfaces need not form a strict enclosure, i.e. the system might have external sources or sinks. The total balance of radiative power  $Q_i$  for the  $i$ -th surface in eq. (A-13), by conservation of energy, can also be expressed as the sum of all pairwise balance terms  $Q_{ij}$ , between surface pairs  $(i, j)$ . Each of these pairwise balances is defined as the fractional radiance from the  $i$ -th surface striking the  $j$ -th one minus the fractional radiance going in the reverse direction:

$$Q_{ij} = A_i F_{ij} J_i - A_j F_{ji} J_j \stackrel{\text{reciprocity of view factors}}{=} A_i F_{ij} (J_i - J_j) = \frac{1}{\underbrace{R_{ij}}_{R_{ij} := 1/A_i F_{ij}}} (J_i - J_j) \quad \text{eq. (A-14)}$$

Where:  $Q_{ij}$  radiative power exchange [W] between a surface pair,  $F_{ij}$  view factor (fraction of radiosity of the  $i$ -th surface striking the  $j$ -th one).  $R_{ij}$  analogous to the inner resistance  $R_i$  in eq. (A-13) is the radiative resistance between a surface pair  $(i, j)$ .

Solving eq. (A-13) for the radiosity and substituting  $J_i$  into eq. (A-14) obtains the following linear system in  $n$  unknown radiation balances  $Q_i$ :

$$Q_i = \sum_{j=1}^n Q_{ij} \stackrel{\text{eq. (A-14)}}{=} \sum_{j=1}^n \frac{J_i - J_j}{R_{ij}} \stackrel{\text{eq. (A-13)} \Rightarrow J_i = E_{b,i} - Q_i R_i}{=} \quad \text{eq. (A-15)}$$

$$\sum_{j=1}^n \frac{E_{b,i} - E_{b,j}}{R_{ij}} - Q_i \frac{1-\varepsilon_i}{\varepsilon_i} \underbrace{\sum_{j=1}^n F_{ij}}_{=1} + \sum_{j=1}^n Q_j \frac{(1-\varepsilon_j) F_{ji}}{\varepsilon_j}$$

Assuming for simplicity a closed space (enclosure) having neither external sources nor sinks of radiation, i.e.  $\sum_j F_{ij} = 1 \forall i$ :

$$\underbrace{\begin{bmatrix} \frac{1}{\varepsilon_1} & \dots & -\frac{(1-\varepsilon_n)F_{n1}}{\varepsilon_n} \\ \vdots & \ddots & \vdots \\ -\frac{(1-\varepsilon_1)F_{1n}}{\varepsilon_1} & \dots & \frac{1}{\varepsilon_n} \end{bmatrix}}_{\mathbf{RQ}} \begin{bmatrix} Q_1 \\ \vdots \\ Q_n \end{bmatrix} = \underbrace{\begin{bmatrix} \sum_{j=1}^n \frac{E_{b,1} - E_{b,j}}{R_{1j}} \\ \vdots \\ \sum_{j=1}^n \frac{E_{b,n} - E_{b,j}}{R_{nj}} \end{bmatrix}}_{\mathbf{E_{bb}}}. \quad \text{eq. (A-16)}$$

By virtue of eq. (A-16) the radiative balance  $Q_i$  of each surface is written as a **linear combination** of *radiosity differences*  $E_{b,k} - E_{b,l}$ , terms admitting a linear (first-order) approximation of *temperature differences*, i.e. state variables, around the mean temperature  $\bar{T} = (T_k + T_l)/2$ :

$$E_{b,k} - E_{b,l} = \sigma T_k^4 - \sigma T_l^4 \approx 4\sigma \bar{T}^3 (T_k - T_l) \Rightarrow$$

$$\frac{E_{b,k} - E_{b,l}}{R_{kl}} \approx 4A_k F_{kl} \sigma \bar{T}^3 (T_k - T_l).$$

$$\mathbf{Q} = \mathbf{R}^{-1} \mathbf{E}_{bb} \Rightarrow$$

$$Q_i \approx \sum_{k,l} A_k H_{k,l}^{rad} (T_k - T_l).$$

eq. (A-17)

Where each radiative heat transfer coefficient  $H_{k,l}^{rad}$ , on its part, is some linear combination of *constant* matrix coefficients  $r_{ij}$  of  $\mathbf{R}$  reading

$$r_{ij} = \begin{cases} \frac{1}{\varepsilon_i} & \text{if } i = j \text{ (for enclosures, } 1 + \frac{1-\varepsilon_i}{\varepsilon_i} \sum_{j=1}^n F_{ij} \text{ for non-enclosures)} \\ -\frac{(1-\varepsilon_j)}{\varepsilon_j} F_{ji} & \text{if } i \neq j \end{cases}.$$

According to eq. (A-17), the essentially linear system dynamics is **preserved** despite radiation heat transfer growing with the 4<sup>th</sup> power of temperature; i.e. heat gains or losses are still roughly proportional to temperature differences as claimed in eq. 4-2a (section 4.1.1).

In the limiting case of blackbodies ( $\varepsilon_i \rightarrow 1$ ,  $1 \leq i \leq n$ ) we obtain

$\mathbf{R}(\varepsilon_1, \dots, \varepsilon_n) \rightarrow \mathbf{I}_n$  (identity matrix) and therefore, as expected:

$$Q_i = \sum_{j=1}^n \frac{E_{b,i} - E_{b,j}}{R_{ij}} = A_i (E_{b,i} - \sum_{j=1}^n E_{b,j} F_{ij}) \quad (1 \leq i \leq n).$$

For perfectly reflecting surfaces (case  $\varepsilon_i = 0$ ) some matrix coefficients are undefined but, since the  $i$ -th surface experiences no net heat exchange,  $Q_i = 0$ . Therefore, the  $i$ -th matrix row and column can be eliminated. There remain a few minor technical questions to be resolved:

- Why, or under what assumption, is the matrix  $\mathbf{R}$  describing the ensemble of radiative resistances nonsingular?
- How to adjust for so-called *reradiating* (thermally isolated, adiabatic) *surfaces*?
- How, and how often to determine the mean temperature(s)  $\bar{T}$ ? The mean could be calculated for each pair  $(k, l)$  as assumed in eq. (A-17), or as the mean of all surfaces forming an enclosure. It could be updated at each time step or kept constant (e.g.  $\bar{T} = 20^\circ\text{C}$ ).

### Mean Radiant Temperature Network

Quite often in practice, radiation balances in enclosures are not solved for exactly, but approximated by means of the Mean Radiant Temperature Network (Çengel 2003; Allinson 2007) which uses the following simplifying assumptions:

- The enclosure consists of  $n$  planar facets  $S_i$ , each one adopting uniform temperature and emissivity, no two of which are co-planar;
- The enclosed space boundary is approximated by a *sphere*.
- By projecting all facets  $S_i$  onto the sphere, spherical patches  $s_i$  with area  $a_i$  covering the entire sphere area  $a_s$  are obtained:  $\sum_i a_i = a_s$ .

In this way, the  $n(n-1)/2$  pairwise view factors  $F_{ij}$  are effectively replaced by  $n$  surface view factors  $F_i$  each of which depends only on the patch area  $a_i$ .<sup>40</sup> Consequently,  $F_i = a_i/\sum_j a_j = a_i/a_S$ . Furthermore, the radiant contribution of the environment to each surface is captured by a single (area-weighted) mean temperature of all surfaces, the mean radiant temperature  $T_{mrt}$ :

$$T_{mrt} := \frac{\sum_j a_j T_j}{\sum_j a_j} = \sum_j F_j T_j \quad \text{eq. (A-18)}$$

In order to apply the mean radiant temperature approximation, the unknown spherical areas  $a_i$  must be determined first, assuming known areas  $A_i$  of their planar counterparts. As a further simplification, spherical facets  $s_i$  are approximated by spherical caps and their planar counterparts  $S_i$  by their base circles. The following geometric correlation holds between the respective planar and spherical patch areas  $A_i$  and  $a_i$ :

$$\frac{A_i}{a_i} = 1 - \frac{a_i}{a_S} \quad (1 \leq i \leq n).$$

The total spherical area  $a_S$  (respectively, the sphere radius  $r$ ) is determined by the additional equation  $\sum_j a_j = a_S (= 4\pi r^2)$ . Assuming black facets for simplicity, the radiation balance  $Q_i$  of the  $i$ -th facet can be written as follows:

$$\begin{aligned} Q_i &= a_i \left( \underbrace{E_{b,i}}_{\text{Emitted}} - \underbrace{\sum_j E_{b,j} F_{ij}}_{\text{Received}} \right) = a_i \sigma T_i^4 - a_i \sigma \sum_j F_{ij} T_j^4 \stackrel{\substack{\equiv \\ \sum_j F_{ij}=1}}{=} \\ & a_i \sigma \sum_j F_{ij} (T_i^4 - T_j^4) \stackrel{\substack{\approx \\ \text{1st order}}}{=} a_i 4 \bar{T}^3 \sigma \sum_j F_{ij} (T_i - T_j) \stackrel{\substack{\equiv \\ F_{ij}=a_j/a_S}}{=} \\ & a_i 4 \bar{T}^3 \sigma \left( T_i - \frac{\sum_j a_j T_j}{a_S} \right) = a_i \underbrace{4 \bar{T}^3 \sigma}_{=: H_i^{rad}} (T_i - T_{mrt}). \end{aligned} \quad \text{eq. (A-19)}$$

For networks of gray facets, an analogy of radiant networks to electricity networks is quoted. According to the *Ohm law*, at any point on a serial path (without branches) the same ‘current’ (heat flow) is observed while the radiosity differences (potential differences  $\triangleq$  ‘voltage drops’) add up between the points, and so do the resistances. According to eq. (A-13) above, each gray facet possesses an ‘inner’ radiative resistance  $R_i := (1 - \varepsilon_i)/(a_i \varepsilon_i)$ , which is *connected in series* with the ‘outer’ resistance that is offered to radiative exchange with the environment. The outer resistance equals the inverse of the heat transfer coefficient in eq. (A-19). Consequently, these two resistances must be added, leading to the following heat transfer equation:

$$Q_i \approx \frac{1}{\frac{1}{a_i 4 \sigma \bar{T}^3} + \frac{1 - \varepsilon_i}{a_i \varepsilon_i}} \cdot (T_i - T_{mrt}) \quad \text{where } T_{mrt} = \frac{\sum_j a_j T_j}{\sum_j a_j} \quad \text{eq. (A-20)}$$

This corresponds to equation (A-17) above for the general case of individual temperatures.

<sup>40</sup> The reason being that view factors in *spherical* enclosures are in fact proportional to *viewing angles* (opening angles) of spherical facets seen from an arbitrary point or an infinitesimally small patch which is located on the same sphere. The viewing angles depend *only* on the *facet area* and not on the location of either facet or point. This follows from a generalization of the circumference rule for circles and chords in 2D, or, as a special case, the Thales rule stating that the periphery angle over a half *circle* is always 90°.

## B List of Figures

<b>Figure 1-1:</b>	Building design process and stakeholders. Source: (Klinge 1994) .....	5
<b>Figure 1-2:</b>	Matrix over life cycle stages of a building and the life cycle supply chain of each building material and component for each stage of a building (Buchgeister et al. 27/08/2007) .....	7
<b>Figure 1-3:</b>	Simple integrated energy model of a building within German EnEV (Schlüter, Thesseling 2009) .....	9
<b>Figure 1-4:</b>	Simplified system architecture (block diagram) of the exergy and the thermography (QGT) tool.....	10
<b>Figure 2-1:</b>	General structure, steps and analogy of the exergoeconomic and exergoenvironmental analysis.....	12
<b>Figure 2-2:</b>	Basic exergy balance of component $k$ . .....	13
<b>Figure 2-3:</b>	General structure and model of the life cycle impact assessment method – Eco-Indicator 99 .....	14
<b>Figure 2-4:</b>	Summary of environmental impact rate of Eco-Indicator 99, CML 2001 and IMPACT 2002 LCIA methods.....	15
<b>Figure 2-5:</b>	Environmental impact balance of component $k$ .....	17
<b>Figure 2-6:</b>	Schematic structure of a heat exchanger HX.....	17
<b>Figure 2-7:</b>	Revenue cost categories for the total revenue requirement (TRR) method (Bejan et al. 1996). .....	21
<b>Figure 2-8:</b>	Expected relationship between investment costs and environmental impact of construction as a function of exergy destruction for the $k$ -th component of an energy conversion system (Meyer et al. 2009).....	23
<b>Figure 2-9:</b>	Example of a building performance measure .....	35
<b>Figure 2-10:</b>	Towards lifelong performance simulation of buildings .....	39
<b>Figure 2-11:</b>	Sensors and measurements applicable for the identification of building simulation models .....	43
<b>Figure 2-12:</b>	Proposed systems architecture (block diagram) of the Exergy+ and the Thermography+ (QGT) tools.....	45
<b>Figure 3-1:</b>	Principle of IRT detecting material properties by observing <i>transient</i> heat transfer. ....	53
<b>Figure 3-2:</b>	Principle of <i>passive</i> IRT observing an insulated wall under <i>stationary</i> conditions. ....	54
<b>Figure 3-3:</b>	Thermal response of a layered structure under solar heating (left: normal condition, right: detached layer). ....	58
<b>Figure 3-4:</b>	Analysis of loft insulation by aerial thermography after fig. 3-7 in (Allinson 2007) .....	83
<b>Figure 3-5:</b>	Photographs of houses surveyed (Allinson 2007), figure 10-2 (image courtesy D. Allinson) .....	84
<b>Figure 3-6:</b>	Overview of Allinson's sensitivity analysis (author's illustration after Allinson 2007). ....	86
<b>Figure 3-7:</b>	Building zone model, constructional assumptions, and heat transfer mechanisms considered; adapted from figures 5-3, 5-4, 5-5, and 6-1 in (Allinson 2007).....	87
<b>Figure 4-1:</b>	Heat balance of a volume element $\Delta V$ in a thermal network (see text). ....	91
<b>Figure 4-2:</b>	Simplified building model (right) and the explicit control architecture imagined and actually implemented in a simulation (left).....	95

---

<b>Figure 4-3:</b>	Time scales of building dynamics, ordered by duration, mean arrival time or rate of change.....	97
<b>Figure 4-4:</b>	Illustration of a camera model for aerial thermography after (Allinson 2007).....	98
<b>Figure 4-5:</b>	Functional block diagram of Quantitative Geo-referenced Thermography (QGT) observing a building.....	101
<b>Figure 4-6:</b>	Errors contributing to the measurement residual in QGT. ....	103
<b>Figure 4-7:</b>	Data flow diagram for temporal disaggregation of weather schedules. ....	105
<b>Figure 4-8:</b>	The influence of load (weather) schedules on the performance of window diagnostics. ....	108
<b>Figure 4-9:</b>	Sequence of Incremental calibration steps and quantitative assessment of the estimated changes. ....	110
<b>Figure 4-10:</b>	Mobile observation of heat transfer coefficients, blue arrows symbolizing the measurement path.....	112
<b>Figure 4-11:</b>	Thermography-guided refinement of wall geometry. ....	113
<b>Figure 4-12:</b>	Data flow diagram of the mobile observer cooperating with the BIM.....	117
<b>Figure 4-13:</b>	Calculation scheme for mobile measurement equation containing pose-dependent and invariant terms.....	120
<b>Figure 4-14a:</b>	Infrared texture generated from 20 partial textures, registered and mapped onto a 3D building model (Hoegner, Stilla 2007, figures 8 and 11, without permission).....	122
<b>Figure 4.14b:</b>	IR image registered and mapped to a cylindrical kiln model of the THERESA plant reconstructed from laser scan data (Kohlhepp 2009, figure 1-1). ....	122
<b>Figure 4-15:</b>	Design and simulation parameters .....	124
<b>Figure 4-16:</b>	BIM classes at the interface between architectural design and thermal simulation.....	126
<b>Figure 4-17:</b>	Transformation of the BIM into an input file for a simulation environment.....	127
<b>Figure 4-18:</b>	Semantic model of a building in an urban context, focusing on lifelong performance monitoring.....	129
<b>Figure A-1:</b>	Approximations of the spectral radiance and the spectral response function.....	146
<b>Figure A-2:</b>	Planar and spherical view factors illustrated by the Nusselt analogy (from <a href="http://www.cis.udel.edu/~chandra/640/Spring05/radiosity.ppt">http://www.cis.udel.edu/~chandra/640/Spring05/radiosity.ppt</a> ). ....	150



---

## C List of Tables

<b>Table 2-1:</b>	Variables used by exergoeconomic and exergoenvironmental analyses .....	22
<b>Table 3-1:</b>	Minimum dataset for continuous commissioning from (Neumann, Jacob 2010) .....	51
<b>Table 3-2:</b>	Nondestructive testing examples in the building sector.....	55
<b>Table 3-3:</b>	Candidate parameters for QGT calibration in building performance simulation .....	72
<b>Table 3-4:</b>	Input parameters of the radiometric camera model (Allinson 2007).....	85
<b>Table 3-5:</b>	Input parameters of the building zone model (Allinson 2007) .....	85
<b>Table 3-6:</b>	Main differences between the conditions of aerial thermography after (Allinson 2007) and QGT. ....	88
<b>Table 4-1:</b>	Ways of performing thermographic surveys.....	138

## D References

1. 2005 ASHRAE handbook. Fundamentals (2005). Atlanta, Georgia, USA.
2. Abeysondra, U. G. Y.; Babel, S.; Gheewala, S. H. (2007): A decision making matrix with life cycle perspective of materials for roofs in Sri Lanka. In *Journal of Materials and Design* 28 (9), pp. 2478–2487.
3. Ahrendts, J. (1974): Die Exergie chemisch reaktionsfähiger Systeme. Erklärung und Bestimmung. Dissertation. Ruhr-Universität Bochum, Bochum.
4. Ahrendts, J. (1980): Reference states. In *Energy* (5), pp. 667–677.
5. Allinson, D. (2007): Evaluation of aerial thermography to discriminate loft insulation in residential housing. Dissertation. University of Nottingham, Nottingham. Available online at <http://etheses.nottingham.ac.uk/284/>.
6. Almond, D.; Patel, P. (1996): Photothermal science and techniques. 1<sup>st</sup> ed. London, New York: Chapman & Hall.
7. Alpuche, M. G.; Heard, Ch.; Best, R.; Rojas, J. (2005): Exergy analysis of air cooling systems in buildings in hot humid climates. In *Applied Thermal Engineering* 25 (4), pp. 507–517.
8. Angelotti, A.; Caputo, P.: The exergy approach for the evaluation of heating and cooling technologies; first results comparing steady-state and dynamic simulations. In : Proceedings of AIVC 28th Conference and Palenc 2nd Conference: Building Low Energy Cooling and Ventilation Technologies in the 21st Century, 27-29 September 2007, Crete island, Greece, Vol. I, pp. 59–64.
9. Asdrubali, F.; Baldinelli, G.; Bianchi, F. (2011, 16-18 May): A quantitative methodology to evaluate thermal bridges in buildings. 3rd Internat. Conf. on Applied Energy (2011, ). Perugia, Italy, 2011, 16-18 May. Available online at [www.crbnet.it/File/Pubblicazioni/pdf/1568.pdf](http://www.crbnet.it/File/Pubblicazioni/pdf/1568.pdf).
10. ASHRAE (2009): American Society of Heating, Refrigerating and Air-Conditioning Engineers Building Energy Quotient. ASHRAE Building Energy Labeling Program: Promoting the Value of Energy Efficiency in the Real Estate Market. Implementation Report. USA. Available online at [http://www.google.de/url?sa=t&rct=j&q=&esrc=s&source=web&cd=2&cad=rja&ved=0CC0QFjAB&url=http%3A%2F%2Fwww.unep.org%2Fsbci%2Fpdfs%2FParis-ASHRAE\\_briefing.pdf&ei=2NBxUOy\\_GM3MsvgamYH4BA&usg=AFQjCNFqY05NdA1zYukFVEJ9YBY7k5UixA](http://www.google.de/url?sa=t&rct=j&q=&esrc=s&source=web&cd=2&cad=rja&ved=0CC0QFjAB&url=http%3A%2F%2Fwww.unep.org%2Fsbci%2Fpdfs%2FParis-ASHRAE_briefing.pdf&ei=2NBxUOy_GM3MsvgamYH4BA&usg=AFQjCNFqY05NdA1zYukFVEJ9YBY7k5UixA).
11. ASTM E1933 - 97, 2010: Standard Test Methods for Measuring and Compensating for Emissivity Using Infrared Imaging Radiometers. Available online at <http://torrentz.eu/z/download/ASTM+Standard+E1933-97/>.
12. Attia, S. (2011): State of the Art of Existing Early Design Simulation Tools for Net Zero Energy Buildings: A Comparison of Ten Tools. Technical Report. Université catholique de Louvain, Belgium. Available online at [www.climat.arch.ucl.ac.be/s\\_attia/attia\\_nzeb\\_tools\\_report.pdf](http://www.climat.arch.ucl.ac.be/s_attia/attia_nzeb_tools_report.pdf).
13. Augenbroe, G. (2002): Trends in building simulation. In *Building and Environment* 37 (8-9), pp. 891–902.
14. Augenbroe, G.; Wilde, P.J. de; Moon, H.J.; Malkawi, A.; Brahme, R.; Choudhary, R. (2003): The Design Analysis Integration (DAI) Initiative. Building Simulation '03, 8th International IBPSA Conference, 2003.
15. Avdelidis, N.P.; Moropoulou, A. (2003): Emissivity considerations in building thermography. In *Energy and Buildings* (35), pp. 663–667.
16. Ayres, R.; Ayres, L.; Martinas, K. (1998): Exergy, waste accounting, and life-cycle analysis. In *Energy* 23 (5), pp. 355–363.
17. Baehr, H. D.; Schmidt, E.F (1963): Definition und Berechnung von Brennstoffexergien. In *BWK* 15, pp. 375–381.
18. Balaras, C.A; Argiriou, A.A. (2002): Infrared thermography for building diagnostics. In *Energy and Buildings* 34 (2), pp. 171–183.
19. Baldo, G. L.; Rollino, S.; Stimmeder, G.; Fieschi, M. (2002): The use of LCA to develop eco-label criteria for hard floor coverings on behalf of the European flower. In *International Journal of LCA* 7 (5), pp. 269–275.
20. Bay, H.; Tuytelaars, T.; van Gool, L. (2008): SURF: Speeded Up Robust Features. In *Computer Vision and Image Understanding (CVIU)* 110 (3).
21. Beausoleil-Morrison, I. (2007): Experimental Investigation of Residential Cogeneration Devices and Calibration of Annex 42 Models. Annex 42 of the Energy Conservation in Buildings and Community Systems Programme. A Report of Subtask B of FC+COGEN-SIM (Simulation of Building-Integrated Fuel Cell and Other Co-generation Systems). International Energy Agency. Available online at [http://www.ecbcs.org/docs/Annex\\_42\\_Experiments\\_&\\_Model\\_Calibration.pdf](http://www.ecbcs.org/docs/Annex_42_Experiments_&_Model_Calibration.pdf).



22. Beck, J. V.; Blackwell, B.; Haji-Sheikh, A. (1996): Comparison of some inverse heat conduction methods using experimental data. In *International Journal of Heat and Mass Transfer* 39 (17), pp. 3649–3657. Available online at <http://www.sciencedirect.com/science/article/pii/S0017931096000348>.
23. Bejan, A.; Tsatsaronis, G.; Moran, M. (1996): *Thermal Design and Optimization*. New York: Wiley.
24. Benner, J.; Häfele, K.-H.; Isele, J. (2011): Semantische Datenmodelle. CityGML Entwicklungen. Karlsruher Institut für Technologie (KIT), Institut für Angewandte Informatik (IAI). Available online at <http://www.iai.fzk.de/www-extern/index.php?id=1126>.
25. Berk, A.; Anderson, G.P.; Acharya, P.K.; Chetwynd, J.H.; Bernstein, L.S.; Shettle, E.P. et al. (1999): *Modtran 4 user's manual*. Edited by Air Force Research Laboratory. Hascom AFB, USA.
26. Bischof, C.; Bücker, H. M.; Lang, B.; Rasch, A. (2003): Solving large-scale optimization problems with EFCOSS. In *Advances in Engineering Software* 34 (10), pp. 633–639.
27. Bisio, G.; Rubatto, G.: Thermodynamic analysis of chemically reacting systems; choice of a reference state for exergy. 35th Intersociety Energy Conversion Engineering Conference and Exhibit, 2000. Available online at [http://ieeexplore.ieee.org/xpls/abs\\_all.jsp?arnumber=870888&tag=1](http://ieeexplore.ieee.org/xpls/abs_all.jsp?arnumber=870888&tag=1).
28. Bison, P.G.; Cernuschi, F.; Grinzato, E.; Marinetti, S.; Robba, D. (2007): Ageing evaluation of thermal barrier coatings by thermal diffusivity. In *Infrared Physics & Technology* 49 (3), pp. 286–291.
29. BMVBS (2007): Bundesministerium für Verkehr, Bau und Stadtentwicklung, Gebäudereport 2007. Berlin. Available online at [www.baufachinformation.de/literatur.jsp?bu=2008069019514](http://www.baufachinformation.de/literatur.jsp?bu=2008069019514).
30. BMWi (2011): Bundesministerium für Wirtschaft und Technologie, Gesamtausgabe der Energiedaten. Nationale und Internationale Entwicklung. Available online at <http://www.bmwi.de/BMWi/Navigation/Energie/Statistik-und-Prognosen/energiedaten.html>.
31. BMWi; BMU (28.09.10): Bundesministerium für Wirtschaft und Technologie (BMWi); Bundesministerium für Umwelt, Naturschutz und Reaktorsicherheit (BMU)Energiekonzept für eine umweltschonende, zuverlässige und bezahlbare Energieversorgung. BMWi (Öffentlichkeitsarbeit); BMU (Abteilung K I). Niestetal. Available online at <http://www.bmu.de/energiekonzept/doc/46394.php>.
32. Borenstein, J.; Everett, H.; Feng, L. (1996): Where am I? Systems and methods for mobile robot positioning. Ann Arbor, MI, USA.
33. Borguet, S.; Dewallef, P.; Léonard, O. (2008): A Way to Deal With Model-Plant Mismatch for a Reliable Diagnosis in Transient Operation. In *J. Eng. Gas Turbines Power* 130 (3), pp. 031601(1-8).
34. Borsdorf, A.; Dachsbacher, C.; Stamminger, M. (2005): Progressive Radiosity auf programmierbarer Grafikkhardware. In : Workshop Hardware for Visual Computing 2005.
35. Boström, G.; Fiocco, M.; Puig, D.; Rossini, A.; Gonçalves, J.; Sequeira, V. (2004): Acquisition, Modelling and Rendering of Very Large Urban Environments. In *3D Data Processing Visualization and Transmission, International Symposium on 0*, pp. 191–198.
36. Bowers, C.P.; Schnier, T.; Wright, J.; Felice, M. de (2010): Evolutionary Parameter Identification of a Building Thermal Model using Energy Consumption Data. Submitted to 'Building and Environment'. Available online at [http://www.cs.bham.ac.uk/~cpb/publications/in-review/thermal\\_model\\_submitted.pdf](http://www.cs.bham.ac.uk/~cpb/publications/in-review/thermal_model_submitted.pdf).
37. Brooks, P. (2007): Testing Building Envelopes with Infrared Thermography; Delivering the “Big Picture”. In *Interface* July 2007, pp. 12–16.
38. Buchgeister, J. (2009): Comparative investigation of exergoenvironmental analysis using two different environmental impact assessment methods on a case study of electricity production. In G. Tsatsaronis, A. Boyano (Eds.): *Proceedings of the International Conference on Optimization Using Exergy-based Methods and Computational Fluid Dynamics*. Berlin, Germany, pp. 55–62.
39. Buchgeister, J. (2010a): Exergoenvironmental analysis - A new approach to support design for environment of chemical processes? In *Chemical Engineering & Technology* 33 (4), pp. 593–602.
40. Buchgeister, J. (2010b): Comparison of exergoenvironmental analysis using three different environmental impact assessment methods in a case of electricity production. In D. Favrat, F. Marechal (Eds.): *Proceedings International Conference on Efficiency, Costs, Optimization and Simulation of Energy Systems (ECOS 2010)*. EPFL Lausanne. Lausanne, Switzerland, pp. 1–8.
41. Buchgeister, J.; Jeske, U.; Klingele, M. (2007): Task sharing on environmental product declaration setup in business to business relations. Life Cycle Management Conference 2007. Zürich, Switzerland, 27/08/2007.

42. Burhenne, S.; Elci, M.; Jacob, D.; Neumann, Ch.; Herkel, S. (2010): Sensitivity Analysis with Building Simulations to support the Commissioning Process. Tenth International Conference for Enhanced Building Operations. Kuwait, 26/10/2010. Available online at <http://repository.tamu.edu/handle/1969.1/94080?show=full>.
43. Burschka, D. (2008): Vision-Based Navigation Strategies. In D. Kragic, V. Kyrki (Eds.): Lecture Notes in Electrical Engineering. Boston, MA: Springer US, pp. 163–185.
44. Carino, N. J. (1998): Nondestructive Test Methods for Evaluation of Concrete in Structures. ACI Committee Report.
45. Carling, P.; Isakson, P. (2004): Model-based functional performance testing of AHU in Kista Entre. In : Proc. 4th Int'l Conf for Enhanced Building Operations. Available online at <http://repository.tamu.edu/handle/1969.1/5036>.
46. Carroll, W.L.; Hitchcock R.J. (1993): Tuning simulated building description to match actual utility data: methods and implementation. In *ASHRAE Transactions* 99 (2), pp. 928–934.
47. Cehlin, M.; Moshfegh, B.; Sandberg, M. (2002): Measurements of air temperatures close to a low-velocity diffuser in displacement ventilation using an infrared camera. In *Energy and Buildings* 34, pp. 687–698.
48. Çengel, Y. A. (2003): Heat transfer. A practical approach. 2nd Edition. Boston: McGraw-Hill.
49. Chantrasrisalai, C.; Ghatti, V.; Fisher, D.E.; Scheatzle, D.G. (2003): Experimental Validation of the EnergyPlus Low-Temperature Radiant Simulation. In *ASHRAE Transactions* 1109 (2), pp. 614–623.
50. Chiang, C.-H.; Pan, C.-L.; Liaw, Y.; Chi, Y.F.; Chu, S.L. (2006): Modeling of Heat Transfer in a Multi-Layered System for Infrared Inspection of a Building Wall. 12th Asia-Pacific Conference on NDT. Auckland, New Zealand, 2006. Available online at <http://130.203.133.150/viewdoc/summary?doi=10.1.1.216.3409>.
51. Cho, S.Y. (2002): The Persistence of Savings Obtained from Commissioning of Existing Buildings. Master thesis. Texas A&M University, USA. Available online at <http://repository.tamu.edu/handle/1969.1/55022?show=full>.
52. Chow, T.T.; Pei, G.; Fong, K.F.; Lin, Z.; Chan, A.L.S.; Ji, J. (2009): Energy and exergy analysis of photovoltaic-thermal collector with and without glass cover. In *Applied Energy* 86, pp. 310–316.
53. Citherlet, S.; Defaux, T. (2007): Energy and environmental comparison of three variants of a family house during its whole life span. In *Building and Environment* 42, pp. 276–284.
54. Citherlet, S.; Hand, J.W. (2002): Assessing energy, lighting, room acoustics, occupant comfort and environmental impacts performance of building with a single simulation program. In *Building and Environment* 37 (8-9), pp. 845–856.
55. Claridge D.E.: Continuous Commissioning Guidebook. Federal Energy Management Program. Energy Systems Laboratory, Texas A&M University. College Station, Texas, USA. Available online at [http://www1.eere.energy.gov/femp/program/om\\_guidebook.html](http://www1.eere.energy.gov/femp/program/om_guidebook.html).
56. Claridge D.E. (2004): Using simulation models for building commissioning. 4th International Conference for enhanced building operation. Paris, 2004.
57. Clarke, J.A. (2001): Energy simulation in building design. 2nd Edition. Oxford: Butterworth-Heinemann.
58. Colantonio, A.; Wood, S. (2008): Detection of Moisture within Building Enclosures by Interior and Exterior Thermographic Inspections. InfraMation, 2008. Available online at [http://www.buildingsciencethermography.com/uploads/InfraMation\\_2008-019\\_Colantonio-Wood.pdf](http://www.buildingsciencethermography.com/uploads/InfraMation_2008-019_Colantonio-Wood.pdf).
59. Cornelissen, R. L. (1997): Thermodynamics and sustainable development - the use of exergy analysis and the reduction of irreversibility. Dissertation. Technical University Twente, Enschede, The Netherlands.
60. Crawley, D.; Hand, J.W.; Kummert, M.; Griffith, B.T. (2005): Contrasting the Capabilities of Building Energy Performance Simulation Programs. Building Simulation '05, 9th Internat. IBPSA Conference. Department of Energy. Washington, DC, USA, 2005. Available online at <http://logiciels.i3er.org/images/logiciels/comparatif.pdf>.
61. Datcu, S.; Ibos, L.; Candau, Y.; Mattei, S. (2005): Improvement of building wall surface temperature measurements by infrared thermography. In *Infrared Physics & Technology* 46, pp. 451–467.
62. Del Barrio, E.P.; Guyon, G. (2003): Theoretical basis for empirical model validation using parameters space analysis tools. In *Energy and Buildings* 35 (10), pp. 985–996.
63. Desta, T. Z.; Langmans, J.; Roels, S. (2011): Experimental data set for validation of heat, air and moisture transport models of building envelopes. In *Building and Environment* 46 (5), pp. 1038–1046.
64. Dewulf, J.; van Langenhove, H. (2002): Assessment of the sustainability of technology by means of a thermodynamically based life cycle analysis. In *Environmental Science and Pollution Research* 9 (4), pp. 267–273.

65. Dewulf, J.; van Langenhove, H.; Mulder, J.; et al (2000): Illustrations towards quantifying the sustainability of technology. In *Green Chemistry* 2 (3), pp. 108–114.
66. EN ISO 13790, 2008: Energy performance of buildings—calculation of energy use for space heating and cooling.
67. DIN V 18599 (2007): Energetische Bilanzierung von Wohngebäuden - Berechnung des Nutz-, End- und Primärenergiebedarfs für Heizung, Kühlung, Lüftung, Trinkwarmwasser und Beleuchtung. Available online at [http://de.wikipedia.org/wiki/DIN\\_V\\_18599](http://de.wikipedia.org/wiki/DIN_V_18599).
68. DOE: EnergyPlus engineering reference. Department of Energy. Washington, DC, USA. Available online at <http://apps1.eere.energy.gov/buildings/energyplus/>.
69. DOE (2011): Building Energy Software Tools Directory. Department of Energy, USA. Washington, DC, USA. Available online at [http://apps1.eere.energy.gov/buildings/tools\\_directory/](http://apps1.eere.energy.gov/buildings/tools_directory/).
70. Dong, B. (2010): Integrated Building Heating, Cooling and Ventilation Control. Dissertation. Carnegie Mellon University, Pittsburgh, USA. Available online at <http://repository.cmu.edu/dissertations/4>.
71. Dong, B.; Lam, K. P.; Huang, Y.C.; Dobbs, G.M. (2007): A comparative study of the IFC and gbXML informational infrastructures for data exchange in computational design support environments. Building Simulation '07, 10th International IBPSA Conference, 2007. Available online at [http://www.ibpsa.org/proceedings/BS2007/p363\\_final.pdf](http://www.ibpsa.org/proceedings/BS2007/p363_final.pdf).
72. Eastman, C.; Teicholz P.; Sacks, R.; Liston K. (2008): BIM handbook. A guide to building information modeling for owners, managers, designers, engineers, and contractors. Hoboken, N.J: Wiley.
73. Emmerich S.J.; Persily A.K.; McDowell T.P. (2005): Impact of infiltration on heating and cooling loads in U.S. office buildings. Building and Fire Research Laboratory. National Institute of Standards and Technology (NIST). Gaithersburg, MD, USA.
74. EnEV 2009: BMVBS (Bundesministerium für Verkehr, Bau und Stadtentwicklung), Verordnung über energiesparenden Wärmeschutz und energiesparende Anlagentechnik bei Gebäuden (Energieeinsparverordnung), 29.04.2009, revised Bundesgesetzblatt Teil I Nr. 23. Available online at <http://www.energieausweis-in.de/enev2009.php>.
75. EU Parliament and EU Council (2002): European Directive on the energy performance of buildings. 2002/91/EC. Source: Brussels. Available online at <http://eur-lex.europa.eu/LexUriServ/LexUriServ.do?uri=OJ:L:2003:001:0065:0071:EN:PDF>.
76. Fanger, P. O. (1982, c1970): Thermal comfort. Analysis and applications in environmental engineering. Malabar, Fla: R.E. Krieger Pub. Co.
77. Fischer, M.; Bazjanac, V.; Maile, T. (2006): Improving and Verifying Building Performance. CIFE Seed Proposal Summary Page. Stanford University. Stanford, CA, USA. Available online at <http://www.stanford.edu/~tmaile/SP>.
78. Frangopoulos, C. (1992): An introduction to environomic analysis and optimization of energy-intensive systems. In A. Valero, G. Tsatsaronis (Eds.): International Conference on Efficiency, Costs, Optimization and Simulation of Energy Systems (ECOS 92). Zaragoza, Spain, pp. 231–239.
79. Frangopoulos, C.; Caralis, Y. (1997): A method for taking into account environmental impacts in the economic evaluation of energy systems. In *Energy Conversion and Management* 38 (15-17), pp. 1751–1763.
80. Frank, M.; Friedman, H.; Heinemeier, K.; Toole, C.; Claridge D.E.; Castro, N.; Haves, P. (2007): State-of-the-art review for commissioning low energy buildings: Existing cost/benefit and persistence methodologies and data, state of development of automated tools and assessment of needs for commissioning. NISTIR Report #7356. National Institute of Standards and Technology (NIST). Gaithersburg, MD, USA. Available online at <http://fire.nist.gov/bfrlpubs/build07/art036.html>.
81. Fratzscher, W.; Brodjanskij, V. M.; Michalek, K. (1986): Exergie: Theorie und Anwendung. Leipzig: Deutscher Verlag für Grundstoffindustrie.
82. Früh, C.; Zakhor, A. (2003): Constructing 3D City Models by Merging Ground-Based and Airborne Views. IEEE Conference on Computer Vision and Pattern Recognition 2003. Madison, WI, USA, 2003.
83. Gane, V.; Haymaker, J. (2008): Benchmarking Conceptual High-rise Design Processes. CIFE Technical Report TR174. Stanford University. Available online at <http://www.stanford.edu/group/CIFE/online.publications/TR174.pdf>.

84. Garbe, C.S; Spies, H.; Jähne, B. (2003): Estimation of Surface Flow and Net Heat Flux from Infrared Image Sequences. In *Journal of Mathematical Imaging and Vision* 19, pp. 159–174.
85. Garcia-Casals, X. (2006): Analysis of building energy regulation and certification in Europe: their role, limitations and differences. In *Energy and Buildings* 38 (5), pp. 381–392.
86. gbXML (2010). <http://www.gbxml.org/index.php>. Edited by The Open Green Building XML Schema Inc.
87. Geiger, A.; Häfele, K.-H.; Bremer, N. M. (2008): Energetische Berechnung und Nachweisführung auf Basis des IFC Datenmodells (in German). Consense Internationaler Kongress und Fachausstellung für nachhaltiges Bauen (June 17-18, 2008). Stuttgart, 2008.
88. Goedkoop, M.; Spiensma, R. (2000): The Eco-indicator 99: A damage oriented method for life cycle impact assessment. Methodology report. Amersfoort, Netherlands. Available online at [www.pre.nl](http://www.pre.nl).
89. Gong, M.; Wall, G. (1997): On exergetics, economics and optimization of technical processes to meet environmental conditions. In C. Ruixan, et al (Eds.): International Conference Thermodynamics Analysis and Improvement of Energy Systems (TAIES 97). Beijing, China, pp. 453–460.
90. Grassmann, P. (1950): Zur allgemeinen Definition des Wirkungsgrads. In *Chemie-Ingenieur-Technik* 22 (4), pp. 77–80.
91. Gratia, E.; Herde, A. de (2003): Design of low energy office buildings. In *Energy and Buildings* 35 (5), pp. 473-491.
92. Griffith, B.T.; Arasteh, D. (1999): Buildings Research Using Infrared Imaging Radiometers with Laboratory Thermal Chambers. LBNL Report 42682. In Proceedings of the SPIE, Vol. 3700. Available online at [http://www.osti.gov/bridge/product.biblio.jsp?osti\\_id=7365](http://www.osti.gov/bridge/product.biblio.jsp?osti_id=7365).
93. Griffith, B.T.; Türler, D.; Goudey, H. (2001): Infrared Thermographic Systems. A Review of IR Imagers and Their Use. LBNL Report Nr. 46590. Lawrence Berkeley National Laboratory (LBNL). Berkeley, USA. Available online at [http://www.google.de/url?sa=t&rct=j&q=&esrc=s&source=web&cd=1&ved=0CCIQFjAA&url=http%3A%2F%2Fgaj.a.lbl.gov%2Fbtech%2Fpapers%2F46590.pdf&ei=duBxUlypH4rGtAavzYHIAg&usg=AFQjCNFEZ4OYV\\_nAsZcYePjURI\\_qJtiInUA&cad=rja](http://www.google.de/url?sa=t&rct=j&q=&esrc=s&source=web&cd=1&ved=0CCIQFjAA&url=http%3A%2F%2Fgaj.a.lbl.gov%2Fbtech%2Fpapers%2F46590.pdf&ei=duBxUlypH4rGtAavzYHIAg&usg=AFQjCNFEZ4OYV_nAsZcYePjURI_qJtiInUA&cad=rja).
94. Grinzato, E.; Vavilov, V.; Kauppinen, T. (1998): Quantitative infrared thermography in buildings. In *Energy and Buildings* 29 (1), pp. 1-9.
95. GSA (2008): BIM Guide Series 05 - Energy Performance and Operations. Version 0.80. Edited by United States General Services Administration (GSA). Available online at [http://www.gsa.gov/graphics/pbs/GSA\\_BIM\\_Guide\\_Series.pdf](http://www.gsa.gov/graphics/pbs/GSA_BIM_Guide_Series.pdf).
96. Günther, A.; Langowski, H.-Ch. (1997): Life Cycle Assessment Study on Resilient Floor Coverings. In *International Journal of LCA* 2 (2), pp. 73–80.
97. Gutschker, O. (2008): Parameter identification with the software package LORD. In *Building and Environment* 43 (2), pp. 163–169.
98. Häfele, K.-H.; Isele, J. (2011): Semantische Datenmodelle. IFC Entwicklungen. Karlsruher Institut für Technologie (KIT), Institut für Angewandte Informatik (IAI). Available online at <http://www.iai.fzk.de/www-extern/index.php?id=1123>.
99. Hand, J.W. (1998): Removing barriers to the use of simulation in the building design professions. Dissertation. University of Strathclyde, Glasgow. Available online at [www.esru.strath.ac.uk/Documents/PhD/hand\\_thesis.pdf](http://www.esru.strath.ac.uk/Documents/PhD/hand_thesis.pdf).
100. Heidt, F.D; Gieseler, U.D; Bier, W. (2003): Combined thermal measurement and simulation for the detailed analysis of four occupied low-energy buildings. In : 8th International IBPSA Conference. Eindhoven, Netherlands. Available online at <http://nesa1.uni-siegen.de/mitarb/ehemalige/PubGieseler/publications.html>.
101. Heiselberg, P.; Murakami, S.; Roulet, C.-A. (Eds.) (1998): Ventilation of Large Spaces in Buildings - Analysis and Prediction Techniques. IEA Energy Conservation in Buildings and Community Systems, Annex 26: Energy Efficient Ventilation of Large Enclosures. Aalborg, DK. Available online at <http://www.ecbcs.org/annexes/annex26.htm>.
102. Hensen, J.L.M. (2004): Towards more effective use of building performance simulation in design. 7th International Conference on Design and Decision Support Systems in Architecture and Urban Planning. TU Eindhoven. Eindhoven, Netherlands, 2004. Available online at [http://www.bwk.tue.nl/bps/hensen/publications/04\\_ddss\\_effictive\\_use.pdf](http://www.bwk.tue.nl/bps/hensen/publications/04_ddss_effictive_use.pdf).

103. Hensen, J.L.M.; Djunaedy, E.; Radošević, M.; Yahiaoui, A. (2004): Building Performance Simulation for better Design: Some Issues and Solutions. In : 21th Conference on Passive and Low Energy Architecture 19.-21. Sep. 2004 (PLEA 2004), pp. 1185–1190. Available online at [http://www.bwk.tue.nl/bps/hensen/publications/04\\_plea\\_bps-issues.pdf](http://www.bwk.tue.nl/bps/hensen/publications/04_plea_bps-issues.pdf).
104. Hirschberg, R. (2008): Energieeffiziente Gebäude. Bau- und anlagentechnische Lösungen; Vereinfachte Verfahren zur energetischen Bewertung. Köln: R. Müller.
105. Hirsig, A. (2010): Finding synergy in simulation modeling by architects and engineers in conceptual design. In : Spring Simulation Multiconference (SpringSim '10). Available online at <http://doi.acm.org/10.1145/1878537.1878732>.
106. Hitchcock R.J. (2002): Standardized Building Performance Metrics. Final Report - Task 2.1.2. Lawrence Berkeley National Laboratory (LBNL). USA (High-Performance Commercial Building Systems Program). Available online at <http://btus.lbl.gov/HPCBS/pubs/E2P21T2d-final.pdf>.
107. Hoegner, L.; Stilla, U. (2007): Automated Generation of Building Textures from Infrared Image Sequences. In : PIA07, International Archives of Photogrammetry, Remote Sensing and Spatial Information Sciences, vol. 36, pp. 65–70.
108. IAI (2006): Industry Foundation Classes IFC2x Edition 3. Edited by International Alliance for Interoperability (IAI). Available online at [http://iaiweb.lbl.gov/Resources/IFC\\_Releases/R2x3\\_final/](http://iaiweb.lbl.gov/Resources/IFC_Releases/R2x3_final/).
109. IAI (2008-2011): buildingSMART - International Home of openBIM. Edited by International Alliance for Interoperability (IAI). Available online at <http://www.buildingsmart-tech.org/>.
110. IEA-ECBCS (2000 - 2003): Annex 37 "Low Exergy Systems for cooling and Heating of Buildings. International Energy Agency Programme on Energy Conversion in Buildings and Community Systems (ECBCS). Brussels, Belgium. Available online at <http://www.annex49.com>.
111. IEA-ECBCS (2006 - 2010): Annex 49 "Low Exergy Systems for High-Performance Building and Communities". International Energy Agency Programme on Energy Conversion in Buildings and Community Systems (ECBCS). Brussels, Belgium. Available online at <http://www.annex49.com>.
112. IEA-ECBCS (2009): Annex 49 "Low Exergy Systems for High-Performance Building and Communities". Newsletter No. 6. Tools for Exergy Performance Evaluation. ISO 6781. Brussels, Belgium. Available online at <http://www.annex49.com>.
113. DIN EN ISO 14040, Oktober 2006: Environmental Management - Life Cycle Assessment - Principles and framework. Available online at [http://www.iso.org/iso/catalogue\\_detail?csnumber=37456](http://www.iso.org/iso/catalogue_detail?csnumber=37456).
114. DIN EN ISO 14044, Oktober 2006: Environmental Management - Life Cycle Assessment - Requirements and guidelines. Available online at [http://www.iso.org/iso/catalogue\\_detail?csnumber=38498](http://www.iso.org/iso/catalogue_detail?csnumber=38498).
115. Isermann, R.; Münchhof, M. (2010): Identification of dynamical systems. An introduction with applications. Berlin, Heidelberg. Springer-Verlag.
116. ISO 10051, 1996: Thermal insulation – Moisture effects on heat transfer – Determination of thermal transmissivity of a moist material. Available online at [http://www.iso.org/iso/home/store/catalogue\\_tc/catalogue\\_detail.htm?csnumber=18016](http://www.iso.org/iso/home/store/catalogue_tc/catalogue_detail.htm?csnumber=18016).
117. ISO 6781, 1983: Thermal insulation - Qualitative detection of thermal irregularities in building envelopes - Infrared method. Available online at [http://www.iso.org/iso/home/store/catalogue\\_tc/catalogue\\_detail.htm?csnumber=13277](http://www.iso.org/iso/home/store/catalogue_tc/catalogue_detail.htm?csnumber=13277).
118. ISO 9164, 1989: Thermal Insulation - Calculation of Space Heating Requirements for Residential Buildings.
119. Jensen, S.O. (1995): Validation of building energy simulation programs: a methodology. In *Energy and Buildings* 22 (2), pp. 133–144.
120. Jiang, L.; Zhan, W.; Loew, M.H. (2010): Modeling thermography of the tumorous human breast: From forward problem to inverse problem solving. IEEE International Symposium on Biomedical Imaging: From Nano to Macro. Rotterdam, Netherlands, 2010.
121. Jimenez, M.J.; Madsen, H.; Andersen, K.K (2008): Identification of the main thermal characteristics of building components using MATLAB. In *Building and Environment* 43 (2), pp. 170–180.

122. Johnson, K.; Wood, S.; Rynes, P.; Yee, B.; Burroughs, F.; Byrd, T. (1995): A methodology for rapid calculation of computational thermal models. SAE International Congress & Exposition, Underhood Thermal Management Session. Detroit, USA, 1995.
123. Jolliet, O.; et al (2004): The LCIA Midpoint-Damage framework of the UNEP/SETAC Life Cycle Initiative. In *International Journal of LCA* 9 (6), pp. 394–404.
124. Jönsson, A.; Björklund, Th.; Tillman, A.-M. (1998): LCA of Concrete and Steel Building Frames. In *International Journal of LCA* 3 (4), pp. 216–224.
125. Jönsson, A.; Tillman, A.-M.; Svensson, T. (1997): Life Cycle Assessment of Flooring Materials: Case Study. In *Building and Environment* 32, pp. 245–255.
126. Judkoff, R.; Wortman, D.; O’Doherty, B.; Burch, J. (2008): A Methodology for Validating Building Energy Analysis Simulations. Technical Report NREL/TP-550-42059. Available online at <http://purl.access.gpo.gov/GPO/LPS114415>.
127. Klingele, M. (1994): Architektur und Energie. Planungsgrundlagen für Büro- und Verwaltungsbauten: C.F. Müller.
128. Klingele, M.; Lützkendorf, Th. (2007): Informationsmanagement und Stakeholderdialog im Bauwesen. In *Technikfolgenabschätzung – Theorie und Praxis* 16 (3), pp. 46–63.
129. Klocke, W. (1988): Main Haus wird älter - Was tun? Ratgeber mit Checklisten zur Vermeidung von Bauschäden durch preiswerte Pflege und Unterhaltung: Bau-Verlag.
130. Kofoworola, O. F.; Gheewala, Sh. H. (2008): Environmental life cycle assessment of a commercial office building in Thailand. In *International Journal of LCA* 13 (6), pp. 498–511.
131. Kohlhepp, P. (2009): Real-Time Mapping of Rotationally Symmetric Objects for Mobile Inspection. Wiss. Berichte FZKA Nr. 7523. Karlsruher Institut für Technologie (KIT), Institut für Angewandte Informatik (IAI). Available online at <http://opac.fzk.de/oai/fetch-opac.S?titlenr=281044&server=//127.0.0.1>.
132. Kohlhepp, P.; Bretthauer, G.; Walther, M.; Dillmann, R. (2006): Using Orthogonal Surface Directions for Autonomous 3D-Exploration of Indoor Environments. In : 2006 IEEE/RSJ International Conference on Intelligent Robots and Systems: IEEE, pp. 3086–3092. Available online at [http://ieeexplore.ieee.org/xpls/abs\\_all.jsp?arnumber=4058869&tag=1](http://ieeexplore.ieee.org/xpls/abs_all.jsp?arnumber=4058869&tag=1).
133. Kotaji, Sh.; Schuurmans, A.; Edwards, S. (2003): Life cycle assessment in building and construction: A state of the art report. Edited by Society of Environmental Toxicology and Chemistry (SETAC). Brussels, Belgium.
134. Krenzinger, A.; Andrade, A.C. de (2007): Accurate outdoor glass thermographic thermometry applied to solar energy devices. In *Solar Energy* 81 (8), pp. 1025–1034.
135. Langlais, C.; Klarsfeld, S. (1984): Heat and Mass transfer in fibrous insulations. In *Journal of Building Physics* 8 (1), pp. 49–80.
136. Lazzaretto, A.; Tsatsaronis, G. (2006): SPECO: A systematic and general methodology for calculating efficiencies and costs in thermal systems. In *Energy* 31 (8-9), pp. 1257–1289.
137. Li, Q.; Rao, J.; Fazio, P. (2009): Development of HAM tool for building envelope analysis. In *Building and Environment* 44 (5), pp. 1065–1073.
138. Liu, S.; Henze G.P. (2005): Calibration of building models for supervisory control of commercial buildings. Building Simulation '05, 9th Internat. IBPSA Conference. Montréal, Canada, 2005. Available online at [http://www.ibpsa.org/proceedings/BS2005/BS05\\_0641\\_648.pdf](http://www.ibpsa.org/proceedings/BS2005/BS05_0641_648.pdf).
139. Lowe, D.G. (2004): Distinctive Image Features from Scale-Invariant Keypoints 2004. In *Int. Journal of Computer Vision* 60 (2).
140. Lundin, M.; Andersson, S.; Östin, R. (2004): Development and validation of a method aimed at estimating building performance parameters. In *Energy and Buildings* 36, pp. 905–914.
141. Maile, T. (2010): Comparing measured and simulated building energy performance data. Dissertation. Stanford University, Stanford, USA. Available online at <http://purl.stanford.edu/mk432mk7379>.
142. Maile, T.; Fischer, M.; Bazjanac, V. (2007): Building Energy Performance Simulation Tools -a Life-Cycle and Interoperable Perspective. CIFE Working Paper #WP107. Stanford University. Stanford, USA. Available online at <http://cife.stanford.edu/node/169>.



143. Maile, T.; Fischer, M.; Bazjanac, V. (2010a): A Method to Compare Measured and Simulated Data to Assess Building Energy Performance. CIFE Working Paper #127. Stanford University. Stanford, USA. Available online at <http://cife.stanford.edu/sites/default/files/WP127.pdf>.
144. Maile, T.; Fischer, M.; Haymaker, J.; Bazjanac, V. (2010b): Formalizing Approximations, Assumptions, and Simplifications to Document Limitations in Building Energy Performance Simulation. CIFE Working Paper #126. Stanford University. Stanford, USA. Available online at <http://cife.stanford.edu/node/87>.
145. Mayer, H. (2007): 3D Reconstruction and Visualization of Urban Scenes from Uncalibrated Wide-Baseline Image Sequences. In *Photogrammetrie - Fernerkundung - Geoinformation 3*, pp. 167–176.
146. Mazzarella, L.; Pasini, M. (2009): Building energy simulation and object-oriented modelling: review and reflections upon achieved results and further developments. 11th Internat. IBPSA Conference (2009, July 27-30). Glasgow, Scotland, UK, 2009. Available online at [http://www.ibpsa.org/proceedings/BS2009/BS09\\_0638\\_645.pdf](http://www.ibpsa.org/proceedings/BS2009/BS09_0638_645.pdf).
147. Mehra, R. (1974): Optimal input signals for parameter estimation in dynamic systems - Survey and new results. In *IEEE Transactions on Automatic Control* 19 (6), pp. 753–768.
148. Meola, C.; Carlomagno, G. M. (2004): Recent advances in the use of infrared thermography. In *Meas. Science and Technology* 15, pp. 27–58.
149. Meyer, L.; Tsatsaronis, G.; Buchgeister, J.; Schebek, L. (2009): Exergoenvironmental analysis for evaluation of the environmental impact of energy conversion systems. In *Energy* 34 (1), pp. 75–89.
150. Miller, L.E. (2006): Indoor Navigation for First Responders: A Feasibility Study. National Institute of Standards and Technology (NIST).
151. Mirsadeghi, M.; Blocken, B.; Hensen, J.L.M. (2009): Application of externally-coupled BES-CFD in HAM engineering of the indoor environment. In : Eleventh International IBPSA Conference, Glasgow, Scotland, 2009. Available online at [http://www.ibpsa.org/proceedings/BS2009/BS09\\_0324\\_331.pdf](http://www.ibpsa.org/proceedings/BS2009/BS09_0324_331.pdf).
152. Mithraratne, N.; Vale, B. (2004): Life cycle analysis model for New Zealand houses. In *Building and Environment* 39 (4), pp. 483–492.
153. Morosuk, T.; Tsatsaronis, G.: Splitting the exergy destruction into endogenous and exogenous parts - application to refrigeration machines. In : Proceedings of 19th ECOS 2006, Crete, Greece, Vol. 1, pp. 165–172.
154. Nair, N.V.; Das, S.K.; Balasubramaniam, K. (2004): A 2-D Inverse Heat Conduction Formulation for Determination of Heat Source Characteristics from Thermal Images. In *AIP Conference Proceedings* 700 (1), pp. 453–460. Available online at <http://link.aip.org/link/?APC/700/453/1>.
155. Nakhi, A.E. (1995): Adaptive Construction Modeling within whole building dynamic simulation. Dissertation. University of Glasgow, UK. Available online at [www.esru.strath.ac.uk/Documents/PhD/nakhi\\_thesis.pdf](http://www.esru.strath.ac.uk/Documents/PhD/nakhi_thesis.pdf).
156. Nandhakumar, N.; Aggarwal, J.K (1988): Integrated Analysis of Thermal and Visual Images for Scene Interpretation. In *IEEE Trans. PAMI* 10 (4), pp. 469–481.
157. Nebel, B.; Zimmer, B.; Wegener, G. (2006): Life Cycle Assessment of Wood Floor Coverings. A Representative Study for the German Flooring Industry. In *International Journal of LCA* 11 (3), pp. 172–182.
158. Neelamkavil, J. (2009): A Review of Existing Tools and their Applicability to Facility Maintenance Management. Report # RR-285. National Research Council of Canada.
159. Nelsson, C.; Forssell, G.; Hermansson, P.; Nyberg, S.; Persson, A.; Persson, R. et al. (2005): Optical signature modelling - Final report. FOI - Defense Research Agency. Linköping, Sweden (ISSN 1650-1942).
160. Neumann, Ch.; Jacob, D. (Eds.) (2008): Guidelines for the Evaluation of Building Performance. Fraunhofer Institut für Solare Energiesysteme (FHG-ISE). Freiburg, Germany. Available online at [http://www.iee-library.eu/images/all\\_ieelibrary\\_docs/buildingeq\\_guidelines\\_evaluation\\_building\\_performance.pdf](http://www.iee-library.eu/images/all_ieelibrary_docs/buildingeq_guidelines_evaluation_building_performance.pdf).
161. Neumann, Ch.; Jacob, D. (Eds.) (2010): Results of the project Building EQ. Tools and methods for linking EPBD and continuous commissioning. Fraunhofer Institut für Solare Energiesysteme (FHG-ISE). Freiburg, Germany. Available online at [http://www.buildingeq-online.net/fileadmin/user\\_upload/Results/BEQ\\_publishable\\_results\\_report\\_final\\_rev\\_100624.pdf](http://www.buildingeq-online.net/fileadmin/user_upload/Results/BEQ_publishable_results_report_final_rev_100624.pdf).

162. Neymark, J.; Judkoff, R.; Knabe, G.; Le, H.-T.; Dürig, M.; Glass, A.; Zweifel, G. (2002): Applying the building energy simulation test (BESTEST) diagnostic method to verification of space conditioning equipment models used in whole-building energy simulation programs. In *Energy and Buildings* 34, pp. 917–931.
163. Nicodemus, F.E. (1965): Directional reflectance and emissivity of an opaque surface. In *Applied Optics* 4 (7), pp. 767–775. Available online at <http://ao.osa.org/abstract.cfm?id=13818>.
164. Nussbaumer, T.; Wakili, K.G.; Tanner, Ch. (2006): Experimental and numerical investigation of the thermal performance of a protected vacuum insulation system applied to a concrete wall. In *Applied Energy* 83, pp. 841–855.
165. O’Sullivan D.T.J.; Keane, M.M.; Kelliher, D.; Hitchcock R.J. (2004): Improving building operation by tracking performance metrics throughout the building lifecycle (BLC). In *Energy and Buildings* 36, pp. 1075–1090.
166. OGC (2007): CityGML. Exchange and Storage of Virtual 3D City Models. Edited by Open Geospatial Consortium Inc. Available online at <http://www.citygml.org/index.php?id=1533>.
167. OGC 08-007r1, 2008: OpenGIS City Geography Markup Language (CityGML) Encoding Standard, G. Gröger, Th.H. Kolbe, A. Czerwinski, C. Nagel (eds). Available online at <http://www.opengeospatial.org/standards/citygml>.
168. Osman, A.; Ries, R. (2007): Life cycle assessment of electrical and thermal energy systems for commercial buildings. In *International Journal of LCA* 12 (5), pp. 308–316.
169. Ozel, F.; Kohler, N. (2004): Data modeling issues in simulating the dynamic processes in life cycle analysis of buildings. In *Automation in Construction* 13 (2), pp. 167–174. Available online at <http://www.sciencedirect.com/science/article/B6V20-4B4HF7M-1/2/41dc2468017b1afbc2a0929285000426>.
170. Park, C.-S.; Augenbroe, G.; Messadi, T.; Thitisawat, M.; Sadegh, N. (2004): Calibration of a lumped simulation model for double-skin facade systems. In *Energy and Buildings* 36 (11), pp. 1117–1130.
171. Paulsen, J. H. (2003): The Maintenance of Linoleum and PVC Floor Coverings in Sweden. The Significance of the Usage Phase in an LCA. In *International Journal of LCA* 8 (6), pp. 357–364.
172. Peper, S.; Feist W.; Schnieders J. (2003): Wissenschaftliche Begleitung, Qualitätssicherung und Messdatenauswertung beim Projekt "Fabrik als Passivhaus". Endbericht. Passivhaus Institut. Darmstadt, Germany. Available online at [http://www.google.de/url?sa=t&rct=j&q=&esrc=s&source=web&cd=2&ved=0CCcQFjAB&url=http%3A%2F%2Fwww.solarbau.de%2Fmonitor%2Fdoku%2Fproj09%2Fdokuproj%2FPHI\\_Endbericht\\_Surtec.pdf&ei=abFyUJbXNeGp4gS7poCADg&usg=AFQjCNHBXDOjKf0lxz4bk8Ek0xWtjaRvjg&cad=rja](http://www.google.de/url?sa=t&rct=j&q=&esrc=s&source=web&cd=2&ved=0CCcQFjAB&url=http%3A%2F%2Fwww.solarbau.de%2Fmonitor%2Fdoku%2Fproj09%2Fdokuproj%2FPHI_Endbericht_Surtec.pdf&ei=abFyUJbXNeGp4gS7poCADg&usg=AFQjCNHBXDOjKf0lxz4bk8Ek0xWtjaRvjg&cad=rja).
173. Perez-Lombard, L.; Ortiz, J.; Gonzalez, R.; Maestre, I. (2009): A review of benchmarking, rating and labelling concepts within the framework of building energy certification schemes. In *Energy and Buildings* 41 (3), pp. 272–278.
174. Peters, M. S.; Timmerhaus, K. D. (1991): Plant design and economics for chemical engineers. 4th edition. New York, USA: McGraw-Hill.
175. Plagge, R.; Scheffler, G.; Grunewald, J. (2005): Automatic measurement of water uptake coefficient of building materials. 7th Nordic Building Physics Symposium in Reykjavik, 2005, 2005. Available online at [http://web.byv.kth.se/bphys/reykjavik/pdf/art\\_026.pdf](http://web.byv.kth.se/bphys/reykjavik/pdf/art_026.pdf).
176. Platzer, W.J. (Ed.) (2006): Energy Performance Assessment Methodology, IEA Task 27 BUILDING ENVELOPE COMPONENTS. Performance, durability and sustainability of advanced windows and solar components for building envelopes. Report Nr. T27-A1-FRG-WJP-FPR. Freiburg, Germany. Available online at [www.risoe.dk/rispubl/NEI/nei-dk-4718.pdf](http://www.risoe.dk/rispubl/NEI/nei-dk-4718.pdf).
177. Poglio, T.; Mathieu-Marni, S.; Ranchin, T.; Savaria, E.; Wald, L. (2006): OSIRIS: a physically based simulation tool to improve training in thermal infrared remote sensing over urban areas at high spatial resolution. In *Remote Sensing of Environment* 104, pp. 238–246.
178. Poglio, T.; Savaria, E.; Wald, L. (2001): Specifications and conceptual architecture of a thermal infrared simulator of land-scapes. In : Colloquium SPIE (EUROPTO) "Sensors, Systems, and Next Generation Satellites VII". Toulouse, France.
179. Poglio, T.; Savaria, E.; Wald, L. (2003): OSIRIS: A simulator of outdoor scenes in thermal infrared range. In : Wissenschaftliche Begleitung, Qualitätssicherung und Messdatenauswertung beim Projekt "Fabrik als Passivhaus". Endbericht. Passivhaus Institut. Darmstadt, pp. 240–245.
180. Potting, J.; Blok, K. (1995): Life-cycle assessment of four types of floor coverings. In *Journal of Cleaner Production* 3, pp. 201–213.



181. Raftery, P.; Keane, M.M.; O'Donnell, J. (2011): Calibrating whole building energy models: An evidence-based methodology. In *Energy and Buildings* 43 (9), pp. 2356–2364.
182. Rant, Z. (1956): Exergie ein neues Wort für technische Arbeitsfähigkeit. In *Forschung auf dem Gebiet des Ingenieurwesens* 32 (1), pp. 36–37.
183. Reddy, A.; Maor, I. (2006): Procedures for Reconciling Computer-Calculated Results With Measured Energy Data. ASHRAE Research Project 1051-RP (Final Report). Drexel University. Philadelphia, USA.
184. RESNET (2010): Interim Guidelines for Thermographic Inspections of Buildings. Residential Energy Services Network. Available online at [http://www.resnet.us/standards/RESNET\\_IR\\_interim\\_guidelines.pdf](http://www.resnet.us/standards/RESNET_IR_interim_guidelines.pdf).
185. Rivela, B.; Hospido, A.; Moreira, T.; Feijoo, G. (2006): Life Cycle Inventory of Particleboard: A Case Study in the Wood Sector. In *International Journal of LCA* 11 (2), pp. 106–113.
186. Robinson, D.; Stone, A. (2005): A simplified radiosity algorithm for general urban radiation exchange. In *Building Service, Engineering, Research, and Technology* 26 (4), pp. 271–284.
187. Rosen, M. A.; Dincer, I. (2004): Effect of varying dead-state properties on energy and exergy analyses of thermal systems. In *International Journal of Thermal Sciences* 43 (2), pp. 121–133. Available online at <http://www.sciencedirect.com/science/article/pii/S1290072903001418>.
188. Rusinkiewicz, S.; Levoy, M. (2001): Efficient Variants of the ICP Algorithm. In : Proceedings of the Third Intl. Conf. on 3D Digital Imaging and Modeling (2001), pp. 145-152. Available online at <http://citeseerx.ist.psu.edu/viewdoc/summary?doi=10.1.1.23.9388>.
189. Saboktakin, A.; Ibarra-Castanedo, C.; Bendada, A.; Maldague, X. (2010): Finite element analysis of heat generation in ultrasonic thermography. 10th International Conf. on Quantitative Infrared Thermography (QIRT, 2010, July 27-30). Québec, Canada, 2010. Available online at <http://qirt.gel.ulaval.ca/archives/qirt2010/papers/QIRT%202010-117.pdf>.
190. Said, M.N. (2004): Moisture Measurement Guide for Building Envelope Applications. Research Report #190. National Research Council of Canada. Available online at <http://www.scribd.com/doc/100275200/Moisture-Measurement-Guide-for-Building-Envelope-Applications>.
191. Sakulpipatsin, P. (2008): Exergy Efficient Building Design. PhD. University of Delft, Delft. Available online at [http://repository.tudelft.nl/assets/uuid:1bc4962d-4534-44da-81de-9dfa1485eb4b/arc\\_sakulpipatsin\\_20080417.pdf](http://repository.tudelft.nl/assets/uuid:1bc4962d-4534-44da-81de-9dfa1485eb4b/arc_sakulpipatsin_20080417.pdf).
192. Sargent, R.G (2009): Verification and validation of simulation models. In : Winter Simulation Conference. Austin, TX, USA. Available online at [www.informs-sim.org/wsc10papers/016.pdf](http://www.informs-sim.org/wsc10papers/016.pdf).
193. Sargentis, G.F.; Chatzimpiro, A.; Symeonidis N. (2009): Determination method of thermal conductivity of building parts in situ through IR imaging by minimizing the influence of environmental parameters. 11th Internat. Conference on Environmental Science and Technology. Chania, Crete, 2009. Available online at <https://itia.ntua.gr/~fivos/files/Doc/Ref%20no%200542-12-08.pdf>.
194. Schall, G.; Wagner, D.; Reitmayr, G.; Taichmann, E.; Wieser, M.; Schmalstieg, D.; Hofmann-Wellenhof, B. (2009): Global pose estimation using multi-sensor fusion for outdoor Augmented Reality. In : 2009 8th IEEE International Symposium on Mixed and Augmented Reality: IEEE, pp. 153–162.
195. Scherer, R.; Katranuschkov, P.; Suarez, T.; Menzel, K.; Hryshchenko, A. (2010): Lecture Notes on Energy Efficiency in Building Construction. REEB Report D 5.3.2. Available online at [http://tu-dresden.de/die\\_tu\\_dresden/fakultaeten/fakultaet\\_bauingenieurwesen/cib/forschung/reeb/die\\_tu\\_dresden/fakultaeten/fakultaet\\_bauingenieurwesen/cib/forschung/reeb/20110112\\_REEB\\_D532\\_Lecture\\_notes\\_CIB.pdf](http://tu-dresden.de/die_tu_dresden/fakultaeten/fakultaet_bauingenieurwesen/cib/forschung/reeb/die_tu_dresden/fakultaeten/fakultaet_bauingenieurwesen/cib/forschung/reeb/20110112_REEB_D532_Lecture_notes_CIB.pdf).
196. Schickel, C.: Energiengesetze und –verordnungen des Bundes – Aktuelle Einblicke. In : Bundesindustrieverband Heizungstechnik, Klimatechnik, Sanitärtechnik / Technische Gebäudesysteme (BHKS), vol. 2010, pp. 86–90.
197. Schlüter, A. (2010): Model-based, Performance-oriented Building Design Employing Distributed Service Systems. Dissertation. ETH Zürich, Zürich, Switzerland. Institute of Technology in Architecture (ITA). Available online at <http://e-collection.library.ethz.ch/view/eth:2624>.
198. Schlüter, A.; Thesseling, F. (2009): Building information model based energy/exergy performance assessment in early design stages. In *Automation in Construction* 18, pp. 153–163.


199. Schmidt, A.; Jensen, A. A.; Clausen, A.; Kamstrup, O.; Postlethwaite, D. (2004a): A comparative life cycle assessment of building insulation products made of stone wool, paper wool and flax. Part 1: Background, goal and scope, life cycle inventory, impact assessment and interpretation. In *International Journal of LCA* 9 (1), pp. 53–66.
200. Schmidt, A.; Jensen, A. A.; Clausen, A.; Kamstrup, O.; Postlethwaite, D. (2004b): A comparative life cycle assessment of building insulation products made of stone wool, paper wool and flax. Part 2: Comparative assessment. In *International Journal of LCA* 9 (2), pp. 122–129.
201. Schmidt, D.; Sager, Ch.; Schurig, M.; Torio, H.; Kühl, L. (2009): Projektverbund LowEx: Nutzung von regenerativen Energiequellen in Gebäuden durch den Einsatz von Niedrig-Exergiesystemen. IBP-Bericht ES-342. Fraunhofer IBP. Stuttgart. Available online at <http://publica.fraunhofer.de/documents/N-101890.html>.
202. Sciubba, E. (1999): Extended exergy accounting: towards an exergetic theory of value. In : International Conference on Efficiency, Costs, Optimization and Simulation (ECOS 99). Tokyo, Japan, pp. 85–94.
203. Sciubba, E. (2002): Beyond thermodynamics? The concept of extended exergy accounting and its application to the analysis and design of thermal systems. In *International Journal of Exergy* 2, pp. 68–84.
204. Sciubba, E.; Wall, G. (2007): A brief commented history of exergy from the beginnings to 2004. In *International Journal of Thermodynamics* 10 (1), pp. 1–26.
205. See, R.; Haves, P.; Sreekanthan, P.; Basarkar, M.; O'Donnell, J.; Settlemeyre, K. (2011): Development of a user interface for the EnergyPlus whole building energy simulation program. IBPSA Building Simulation 2011 IBPSA. Sydney, Australia, 2011. Available online at [http://www.ibpsa.org/proceedings/BS2011/P\\_1930.pdf](http://www.ibpsa.org/proceedings/BS2011/P_1930.pdf).
206. Sham, J. (2008): Infrared Flash Thermography (FT) for Building Diagnosis - Detection of surface cracks, subsurface defects and water-paths in building concrete structures. Master Thesis. University of Hong Kong, Hong Kong.
207. Shell, J.R. (2004): Bidirectional Reflectance: An Overview with Remote Sensing Applications & Measurement Recommendations. Rochester Institute of Technology. Rochester, USA. Available online at <http://freedownloadb.com/pdf/bidirectional-reflectance-an-overview-with-remote-sensing-17096967.html>.
208. SMSG (2010): Standards and Procedures for Application of Radiometric Sensors. RCC Document 809-10. Edited by Signature Measurement Standards Group (SMSG). U.S. Army White Sands Missile Range. New Mexico, USA. Available online at <http://www.wsmr.army.mil/RCCsite/Documents/Forms/AllItems.aspx?RootFolder=%2fRCCsite%2fDocuments%2f809%2d10%20Standards%20and%20Procedures%20for%20Application%20of%20Radiometric%20Sensors&FolderCTID=&View=%7b48154D10%2d7E75%2d4FA7%2dB6AB%2d652D4F662359%7d>.
209. Snell, J. (2008): Infrared Thermography: (Nearly) A Daily Tool. In *Home Energy Magazine* (March/April), pp. 31–34. Available online at [http://www.affordablecomfort.org/images/Events/32/Courses/1298/DIAG5\\_Snell\\_060109\\_HE\\_Mag\\_IR\\_Building\\_s052008.pdf](http://www.affordablecomfort.org/images/Events/32/Courses/1298/DIAG5_Snell_060109_HE_Mag_IR_Building_s052008.pdf).
210. Snyder, W.C (2004): An In-Scene Parameter Estimation Method for Quantitative Image Analysis. Dissertation. Rochester Institute of Technology, Rochester, USA. Available online at <https://ritdml.rit.edu/handle/1850/11061>.
211. Sodja, A.; Zupančič, B. (2009): Modelling thermal processes in buildings using an object-oriented approach and Modelica. In *Simulation Modeling Practice and Theory* 17, pp. 1143–1159.
212. Sowell, E.F.; Haves, P. (2001): Efficient solution strategies for building energy system simulation. In *Energy and Buildings* 33 (4), pp. 309–317.
213. Srikanthan, R.; McMahon, T.A (2001): Stochastic generation of annual, monthly and daily climate data: A review. In *Hydrology and Earth System Sciences*, 5(4), 653–670 5 (4), pp. 653–670. Available online at [http://scholar.google.de/scholar?cluster=9301231645020951378&hl=de&as\\_sdt=0,5&scioldt=0,5](http://scholar.google.de/scholar?cluster=9301231645020951378&hl=de&as_sdt=0,5&scioldt=0,5).
214. Steeman, M.; Jokisalo, J.; Cameliet, J.; Paepe, M. de (2009): Modelling indoor air and hygrothermal wall interaction in building simulation: Comparison between CFD and a well-mixed zonal model. In *Building and Environment* 44 (3), pp. 572–583.
215. Steskens P. (2009): Modelling of the hygrothermal interactions between the indoor environment and the building envelope. Dissertation. Technical University of Denmark, Lyngby, Denmark. Available online at <http://orbit.dtu.dk/services/downloadRegister/5434320/byg-r216.pdf>.
216. Stilla, U.; Hoegner, L. (2008): IR-Texturierung von 3D-Gebäudemodellen zur thermographischen Inspektion von Stadtquartieren. In *GIS.Science* 4 (12-19).

217. Sun, J. (2004): Methodology for Adapting Rigorous Simulation Programs for Supervisory Control of Building HVAC&R Systems: Simulation, Calibration and Optimization. Dissertation. Drexel University, Philadelphia, USA. Available online at [http://144.118.25.24/bitstream/1860/381/8/Sun\\_Jian.pdf](http://144.118.25.24/bitstream/1860/381/8/Sun_Jian.pdf).
218. Szargut, J. (1978): Minimization of the consumption of natural resources. In : Bulletin of the Polish Academy of Sciences: Technical Sciences 1978, vol. 26, pp. 41–46.
219. Szargut, J. (2004): Optimization of the design parameters aiming at the minimization of the depletion of non-renewable resources. In *Energy* 29, pp. 2161–2169.
220. Szargut, J.; Morris, D. R.; Steward, F. R. (Eds.) (1988): Exergy analysis of thermal, chemical and metallurgical processes. New York (USA): Hemisphere Publishing Corporation.
221. Szargut, J.; Stanek, W. (2005): Thermo-ecological optimization of a solar collector. In S. Kjelstrup, J. E. Hustad, T. Gundersen (Eds.): 18th International Conference on Efficiency, Cost, Optimization, Simulation, and Environmental Impact of Energy Systems (ECOS 2005). Trondheim, Norway, pp. 409–417.
222. Szargut, J.; Ziebig, A.; Stanek, W. (2002): Depletion of the non-renewable natural exergy resources as a measure of the ecological cost. In *Energy Conversion and Management* 43, pp. 1149–1163.
223. Takizawa, H.; Yamada, N.; Sakai, S.; Kobayashi, H. (2006): Radiative Heat Transfer Simulation Using Programmable Graphics Hardware. 5th IEEE/ACIS Internat. Conf. on Computer and Information Science, 2006. Available online at [http://ieeexplore.ieee.org/xpls/abs\\_all.jsp?arnumber=1651966&tag=1](http://ieeexplore.ieee.org/xpls/abs_all.jsp?arnumber=1651966&tag=1).
224. Thiers, St.; Peuportier, B. (2012): Energy and environmental assessment of two high energy performance residential buildings. In *Building and Environment* 51, pp. 276–284.
225. Thormark, C. (2002): A low energy building in a life cycle. Its embodied energy, energy need for operation and recycling potential. In *Building and Environment* 37 (4), pp. 429–435.
226. Thrun, S.; Burgard, W.; Fox, D. (2005): Probabilistic robotics. Cambridge, Mass: MIT Press.
227. Torcellini, P.; Pless, S.; Deru, M.; Griffith, B.T.; Long, N.; Judkoff, R. (2006): Lessons Learned from Case Studies of Six High-Performance Buildings. Technical Report NREL/TP-550-37542. National Renewable Energy Laboratory (NREL). Available online at <http://www.nrel.gov/docs/fy06osti/37542.pdf>.
228. Torio, H.; Angelotti, A.; Schmidt, D. (2009): Exergy analysis of renewable-based climatisation systems for buildings: A critical view. In *Energy and Buildings* 41, pp. 248–271.
229. Torio, H.; Schmidt, D. (2011): Exergy Assessment Guidebook for the Built Environment. Summary report of Annex 49: Low Exergy Systems for High-Performance Building and Communities. Edited by Programme on Energy Conservation in Buildings and Community Systems (ECBCS) of the International Energy Agency. Stuttgart, Germany.
230. Trcka, M.; Hensen, J.L.M.; Wijsman, A.J (2006): Distributed building performance simulation - A novel approach to overcome legacy code limitations. In *HVAC&R* vol.12, pp. 621–640.
231. Tsatsaronis, G.: Application of thermoeconomics to the design and synthesis of energy plants. In: Frangopolous, C. ed., *Encyclopedia of Life Support Systems (EOLSS)*, developed under the auspices of the UNESCO, Eolss Publishers, Oxford, UK, 2007. Available online at <http://www.eolss.net>.
232. Tsatsaronis, G.: Combination of exergetic and economic analysis in energy-conversion processes. In : *Energy Economics and Management European Congress*, Algarve, Portugal, 2.-5. April 1984 Pergamon Press, Oxford, England, Vol. 1, pp. 151–157.
233. Tsatsaronis, G.: Strengths and limitations of exergy analysis. In : Bejan, A. and Mamut, E., *Thermodynamic optimization of complex energy systems*, 1999, pp. 93–100.
234. Tsatsaronis, G.; Czesla, F.: Thermoeconomics. In: *Encyclopedia of Physical Science and Technology*, Third Edition, Volume 16, 2002, pp. 659–680.
235. Tsatsaronis, G.; Czesla, F. (2004-2007): Exergy and Thermodynamic Analysis. Six articles published in topic “Energy”. Edited by *Encyclopedia of Life Support Systems (EOLSS)*. Available online at <http://www.eolss.net>.
236. Tsatsaronis, G.; Morosuk, T.: Advanced exergoeconomic evaluation and its application of compression refrigeration machines. In : *Proceedings of ASME*, Seattle, USA, 2007, CD-ROM, File 2007-41202.
237. Tsatsaronis, G.; Park, M.H (2002): On avoidable and unavoidable exergy destruction and investment costs in thermal systems. In *Energy Conversion and Management* 43, pp. 1259–1270.
238. Tsatsaronis, G.; Winhold, M. (1985a): Exergoeconomic analysis and evaluation of energy conversion plants. Part I - A new general methodology. In *Energy* 10 (1), pp. 69–80.

239. Tsatsaronis, G.; Winhold, M. (1985b): Exergoeconomic Analysis and evaluation of energy conversion plants. Part II - Analysis of a coal-fired steam power plant. In *Energy* 10 (1), pp. 81–94.
240. Türler, D.; Griffith, B.T.; Arasteh D. K. (1997): Laboratory Procedures for Using Infrared Thermography to Validate Heat Transfer Models. In *Insulation Materials: Testing and Applications: Third Volume, ASTM STP 1320*, R. S. Graves and R. R. Zarr, Eds., American Society for Testing and Materials. Available online at <http://gaia.lbl.gov/btech/papers/38925.pdf>.
241. Uciński, D. (2005): Optimal measurement methods for distributed parameter system identification. Habilitation, Boca Raton, Fla. Available online at <http://www.worldcat.org/oclc/55765501>.
242. Uciński, D.; Patan, M. (2007): D-optimal design of a monitoring network for parameter estimation of distributed systems. In *Journal of Global Optimization* 39 (2), pp. 291–322.
243. Udo de Haes, H.A.; et al (2002): Life Cycle Impact Assessment - Striving towards best practice. Society of Environmental Toxicology and Chemistry (SETAC), Pensacola, USA.
244. Uhlmann, J.S.; Csorba, M. (1997): Nondivergent simultaneous map building and localization using covariance intersection. SPIE Conference on Navigation and Control Technologies for Unmanned Systems II, 1997.
245. Urban, B.J. (2007): The MIT Design Advisor: simple and rapid energy simulation of early-stage building designs. Master Thesis. Massachusetts Institute of Technology (MIT). Available online at <http://dspace.mit.edu/handle/1721.1/42032>.
246. Valero, A. (1998): Thermoecconomics as a conceptual basis for energy-ecological analysis. In S. Ulgiati (Ed.): *International Workshops on Advances in Energy Studies*. Siena (Italy), pp. 415–444.
247. Valero, A. (2006): Exergy accounting: Capabilities and drawbacks. In *Energy* 31 (1), pp. 164–180.
248. Valero, A.; Lozano, M. A.; Munoz, M. (1986): A general theory of exergy saving. Part I On the exergetic cost. In R. A. Gaggioli (Ed.): *Computer-Aided Engineering and Energy Systems: Second Law Analysis and Modelling*. New York: ASME Book No. H0341C (Vol. 3).
249. van Belleghem, M.; Steeman, M.; Janssens, A.; De Paepe M. (2011): Validation of a coupled CFD-HAM model with a climate chamber experiment on a small wall sample. In: *Proceedings of the 9th Nordic Symposium on Building Physics, NSB2011*, vol. 1. Available online at <https://biblio.ugent.be/publication/1258552/file/1258559.pdf>.
250. van Schijndel, A. W.M. (2007): Integrated Heat Air and Moisture Modeling and Simulation. Dissertation. University of Eindhoven, Netherlands. Available online at <http://sts.bwk.tue.nl/JosVanSchijndel/AWMvanSchijndelPhDThesis.pdf>.
251. Visier J.C. (Ed.) (2005): Commissioning tools for improved energy performance. Results of IEA ECBCS ANNEX 40. International Energy Agency. Available online at [http://www.ecbcs.org/docs/Annex\\_40\\_Commissioning\\_Tools\\_for\\_Improved\\_Energy\\_Performance.pdf](http://www.ecbcs.org/docs/Annex_40_Commissioning_Tools_for_Improved_Energy_Performance.pdf).
252. Volponi, A. (2008): Enhanced self-tuning on-board real-time model (estorm) for aircraft engine performance health tracking. National Aeronautics and Space Administration (NASA), USA (NASA/CR—2008-215272). Available online at <http://ntrs.nasa.gov/search.jsp?R=20080032604>.
253. Voss, K.; Löhnert, G.; Herkel, S.; Wagner, A.; Wambsganß, M. (2005): Bürogebäude mit Zukunft - Konzepte, Analysen, Erfahrungen. Köln: TÜV-Verlag GmbH.
254. Wagner, A.; Mossmann, C.; Gropp, Th.; Gossauer, E.; Leonhart, R. (2007): Thermal Comfort and Workspace Occupant Satisfaction - Results of Field Studies in German Low Energy Office Buildings. In *Energy and Buildings* 39 (7), pp. 758–769.
255. Wallner, G. (2009): An extended GPU radiosity solver. In *Vis Comput* 25 (5-7), pp. 529–537.
256. Wang, S.; Xu, X. (2006): Simplified building model for transient thermal performance estimation using GA-based parameter identification. In *International Journal of Thermal Sciences* 45 (4), pp. 419–432.
257. Wawrzynek, A.; Bartoszek, M. (2002): Nonlinear Inverse Heat Transfer Analysis with Large Number of Measuring Points – Application in Civil Engineering. 5th World Congress on Computational Mechanics (WCCM). Vienna, Austria, 2002.
258. Weiss, R.A.; Scoggins, R.K.; Meeker, D.L. (1992): Terrain background signature research. Technical Report EL-92-32. USAE Waterways Experiment Station, Environmental Lab. Vicksburg, MS, USA.
259. Westphal, F.S.; Lamberts, R. (2005): Building simulation calibration using sensitivity analysis. Building Simulation '05, 9th Internat. IBPSA Conference. Montréal, Canada, 2005. Available online at

- [http://www.ibpsa.org/proceedings/bs2005/bs05\\_1331\\_1338.pdf](http://www.ibpsa.org/proceedings/bs2005/bs05_1331_1338.pdf).
260. Wetter, M.; Haugstetter, C. (2006): Modelica versus TRNSYS — a comparison between an equation-based and a procedural modeling language for building energy simulation. In : Proceedings of the SimBuild, 2nd National Conference of IBPSA-USA, International Building Performance Simulation Association. Cambridge, MA, USA. Available online at <http://simulationresearch.lbl.gov/wetter/download/WetterHaugstetter-2006.pdf>.
261. Wienold, J. (2009): Daylight Glare in Offices. Dissertation. Fakultät für Architektur, Universität Karlsruhe, Germany. Available online at <http://vg00.met.vgwort.de/na/96ed519747774db3b001f7bafad84a60?l=http://publica.fraunhofer.de/eprints/urn:nbn:de:0011-n-1414579.pdf>.
262. Wilde, P.J. de (2004): Computational Support for the Selection of Energy Saving Building Components. Dissertation. TU Delft, Delft, Netherlands. Available online at [http://repository.tudelft.nl/assets/uuid:96d2ad6f-f13b-48c2-81b2-b88be7751a04/arc\\_wilde\\_20040308.pdf](http://repository.tudelft.nl/assets/uuid:96d2ad6f-f13b-48c2-81b2-b88be7751a04/arc_wilde_20040308.pdf).
263. Wilde, P.J. de; Tian, W. (2009): Identification of key factors for uncertainty in the prediction of the thermal performance of an office building under climate change. In *Building Simulation 2* (3), pp. 157–174.
264. Winter, S. (2002, revised 2008): Grundlagen Holzhäuser - Werthaltigkeit und Lebensdauer. Holzbau Handbuch Reihe 0, Teil 5, Folge 1 Informationsdienst Holz.
265. Wray, C.; Walker, I.; Siegel, J.; Sherman, M. (2002): Practical Diagnostics for Evaluating Residential Commissioning Metrics. LBNL Report 45959. Lawrence Berkeley National Laboratory (LBNL). Berkeley, CA, USA. Available online at <http://escholarship.org/uc/item/5cp523h9.pdf>.
266. Wu, D.; Busse, G. (1998): Lock-in thermography for nondestructive evaluation of materials. In *Revue Generale de Thermique* 37 (8), pp. 693–703.
267. Yoon, S.-H.; Park, C.-S.; Augenbroe, G. (2011): On-line parameter estimation and optimal control strategy of a double-skin system. In *Building and Environment* 46 (5), pp. 1141–1150.
268. Zalewski, L.; Lassue, S.; Rouse, D.; Boukhalfa, K. (2010): Experimental and numerical characterization of thermal bridges in prefabricated building walls. In *Energy Conversion and Management* 51, pp. 2869–2877.
269. Zawada, T. (2005): Simultaneous estimation of heat transfer coefficient and thermal conductivity with application to microelectronic materials. In *Microelectronics Journal* 37 (4), pp. 340–352.
270. Zhong, Z.; Braun, J.E. (2008): Combined heat and moisture transport modeling for residential buildings. Report HL 2008-3. National Institute of Standards and Technology (NIST).





This report substantiates the objectives of subtopic „Technologies for energy efficiency in the Building Sector“ of the Helmholtz Research Program Technology, Innovation, and Society, and develops a detailed work program. A holistic approach rooted in building information models (BIM) and performance simulation models is described for planning and lifelong monitoring of the energy performance of buildings.

The exergoeconomic and exergoenvironmental analysis, well known methods to design cost-effective and environmentally friendly energy conversion systems, are joined and transferred to the building sector. Thereby, the operational efficiency of components is balanced against the materials and energy needed for fabrication. Infrared thermography geo-referenced with respect to the 3D BIM and co-running the thermodynamic simulation is proposed as a novel tool for efficient parameter identification and for improved condition-based maintenance and monitoring of building performance.